Fraunhofer ISI

Fraunhofer Institute for Systems and Innovation Research ISI

Towards climate-neutral district heating in the EU

Enhancing energy system modelling with spatial analysis

Pia Manz

Fraunhofer Verlag

Fraunhofer Institute for
Systems and Innovation Research ISI

Pia Manz

Towards climate-neutral district heating in the EU

Enhancing energy system modelling with spatial analysis

Fraunhofer Verlag

Contact:
Fraunhofer Institute for Systems and Innovation Research ISI
Breslauer Strasse 48
76139 Karlsruhe
Germany
Phone +49 721 6809-0
info@isi.fraunhofer.de
www.isi.fraunhofer.de

Cover illustration: © Pia Manz

Bibliographic information of the German National Library:
The German National Library has listed this publication in its Deutsche Nationalbibliografie; detailed bibliografic data is available in the internet at www.dnb.de

ISBN (print edition): 978-3-8396-2029-8
DOI (free Open Access version): https://doi.org/10.24406/publica-3423

Zugl.: Utrecht, Univ., Diss., 2024

Print and finishing: Fraunhofer-Druckerei, Stuttgart

This book was printed with chlorine- and acid-free paper.

Nobelstrasse 12
70569 Stuttgart
Germany
verlag@fraunhofer.de
www.verlag.fraunhofer.de

als rechtlich nicht selbständige Einheit der

Fraunhofer-Gesellschaft zur Förderung
der angewandten Forschung e.V.
Hansastrasse 27 c
80686 München
Germany
www.fraunhofer.de

Towards climate-neutral district heating in the EU

Enhancing energy system modelling with spatial analysis

Naar klimaatneutrale stadsverwarming in de EU

Het verbeteren van de modellering van energiesystemen met ruimtelijke analyse

(met een samenvatting in het Nederlands)

Proefschrift

ter verkrijging van de graad van doctor aan de
Universiteit Utrecht
op gezag van de
rector magnificus, prof. dr. H.R.B.M. Kummeling,
ingevolge het besluit van het College voor Promoties
in het openbaar te verdedigen op

vrijdag 29 november 2024 des middags te 12.15 uur

door

Pia Susanne Edith Manz

geboren op 26 juli 1990
te Bamberg, Duitsland

Promotoren:

Prof. dr. W.A. Eichhammer

Prof. dr. G.J. Kramer

Copromotor:

Dr. T. Fleiter

Beoordelingscommissie:

Prof. dr. R. Haas

Prof. dr. F. Johnsson

Prof. dr. N. Ozkan

Prof. dr. M. Ragwitz

Prof. dr. E. Worrell

Contents

1 Introduction

1.1 District heating in a climate-neutral energy system

The urgent need to mitigate climate change and thus minimise greenhouse gas (GHG) emissions requires a transformation across all areas and sectors. In 2022, the EU contributed 6.7% to global emissions [1]. The EU has committed itself to reducing GHG emissions by 55% by 2030 [2] and to creating a climate-neutral society and economy by 2050 [3,4]. Climate-neutrality, also known as net-zero emissions, means that the EU will not release more GHG emissions into the atmosphere than are removed by the planet's natural adsorption or through additional measures. Despite a 27% reduction in GHG emissions since 1990 and a 31% reduction per capita, the EU is currently not on track to meet its ambitious targets [5].

Energy use is the largest contributor to GHG emissions, primarily CO_2, with heating (including space heating and hot water), in residential and non-residential[1] buildings accounting for over 30% of energy consumption [5,6]. Currently, more than half of the heat demand of buildings is supplied by natural gas and another 15% by oil [7,8]. About 12% are supplied with district heating (DH) [7,9], which uses fossil fuels to a large extent (68% in 2020) [10]. This underscores the slow past uptake of renewables for buildings and emphasizes the importance of decarbonizing both the heating of buildings and district heating.

The heating transition towards climate-neutrality by 2050 includes the need to improve the efficiency of the building stock. The EU Energy Performance of Buildings Directive (EPBD) [11] drives national legislations in the member states, establishing energy efficiency standards for both new and existing buildings, while the EU Renewable Energy Directive (RED) [12] sets targets for increasing the use of renewables in buildings. These often include heat pumps, which have lower supply temperatures than gas and oil. Potentially renewable energy carriers with higher supply temperatures could be biomass, synthetic gases or hydrogen in boilers in the buildings. However, these options have limited potential and an uncertain cost structure in the future [13,14]. Especially, solutions for densely populated areas are essential, as nearly 40% of EU citizens, a figure that is continually increasing, live in urban areas [15]. These areas typically consist of older multi-family buildings with low refurbishment activity, resulting in limited thermal renovation and insulation of buildings.

DH will be one pillar of an efficient and climate-neutral heating sector, enabling to supply the consumers centrally with climate-neutral energy sources [16–19], including renewable sources, such as biomass, geothermal, solar thermal or heat pumps using

[1] Non-residential buildings are also commonly referred to as tertiary or service buildings.

renewable electricity. Furthermore, it is possible to utilise excess heat (also known as waste heat), a by-product from electricity generation, industrial processes and waste incineration, which is typically released into the environment. The EU Energy Efficiency Directive (EED) [20] promotes the deployment of efficient DH networks, including mandatory heat planning, and sets targets for the member states to increase the renewable share in DH. Figure 1.1 illustrates the principle of a DH area and its various possible climate-neutral sources in the future, as well as the interconnection with the electricity and hydrogen grid via heat pumps and combined heat and power (CHP) plants.

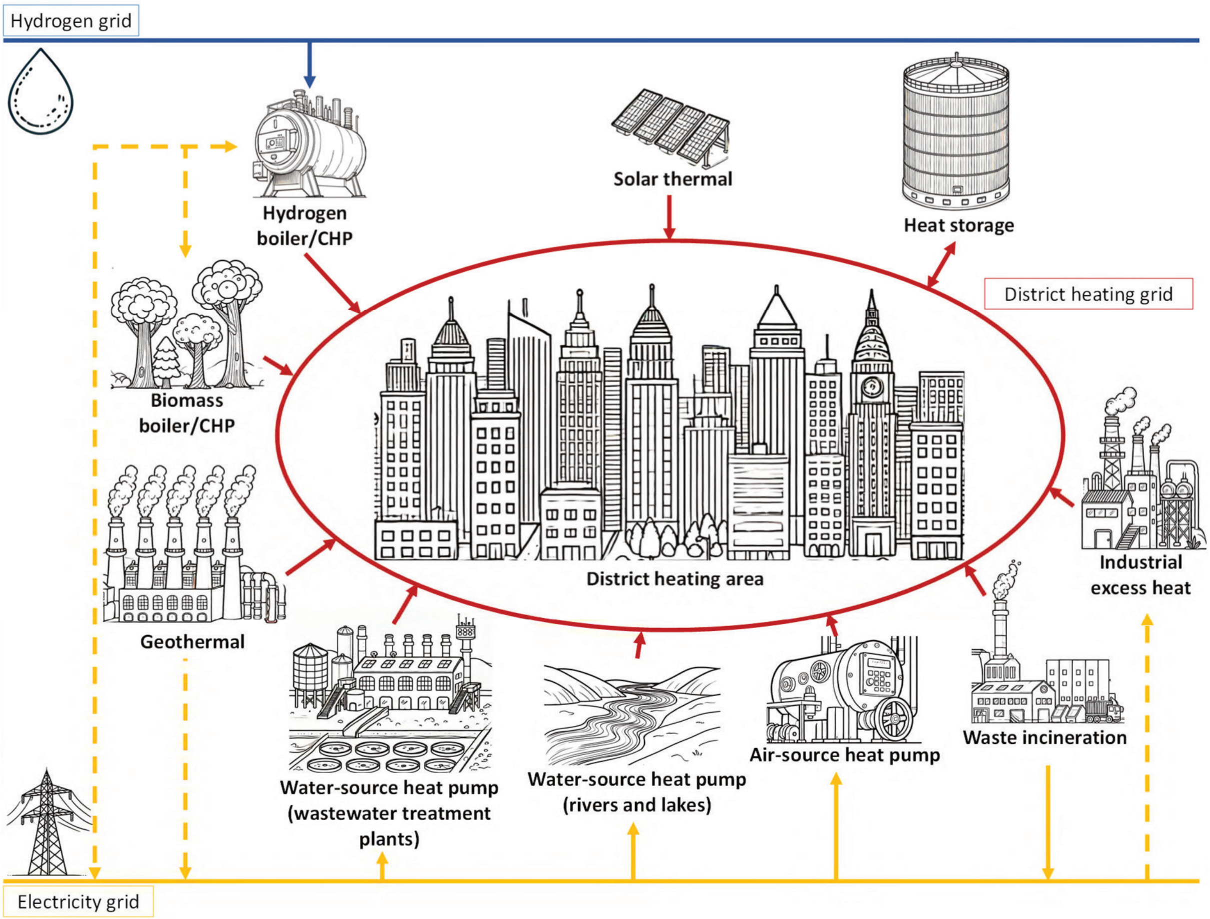

Figure 1.1: Schematic overview of climate-neutral DH and its interconnection with the energy system. Own illustration with the assistance of AI (DALL·E 2)

DH connects multiple buildings, districts, or entire cities with various heat sources via a pipe network, which transports and distributes steam or water to meet the demand for space heating and sanitary hot water in the buildings. This network allows heat to be supplied from any available sources, whether from a central plant or several distributed sources. DH has a long history in the EU and was categorised into four generations by Lund et al., 2014 [21]. According to this publication, the first generation has its beginning in the 1880s in the USA, and has been built until the 1930s in both the USA and the EU, offering higher energy security for heating buildings. This generation typically used steam, resulting in high heat losses, and achieved heat delivery through condensation in the radiators in the buildings. Manhattan (New York) and Paris still use steam in their DH networks. The second generation, from the 1930s until the 1970s, used pressurised hot water with temperatures over 100°C, enabling the utilisation of CHP plants. This technology is still employed in the widespread networks built in the former USSR countries. From the 1980s onward, the third generation was implemented, used for new systems as well as extensions and replacements in existing systems worldwide. This generation is characterised by still using pressurised hot water but with temperatures below 100°C, incorporating components like pre-insulated pipes and plate heat exchangers in substations. These advancements increased efficiency and saved fuel particularly in response to the oil crises. The currently evolving fourth generation uses water with temperatures often below 70°C, allowing for the use of prefabricated polyethylene (PE) pipes, which decreases heat losses and thus increases efficiency. This generation also enables the utilisation of renewable and other low-temperature heat sources.

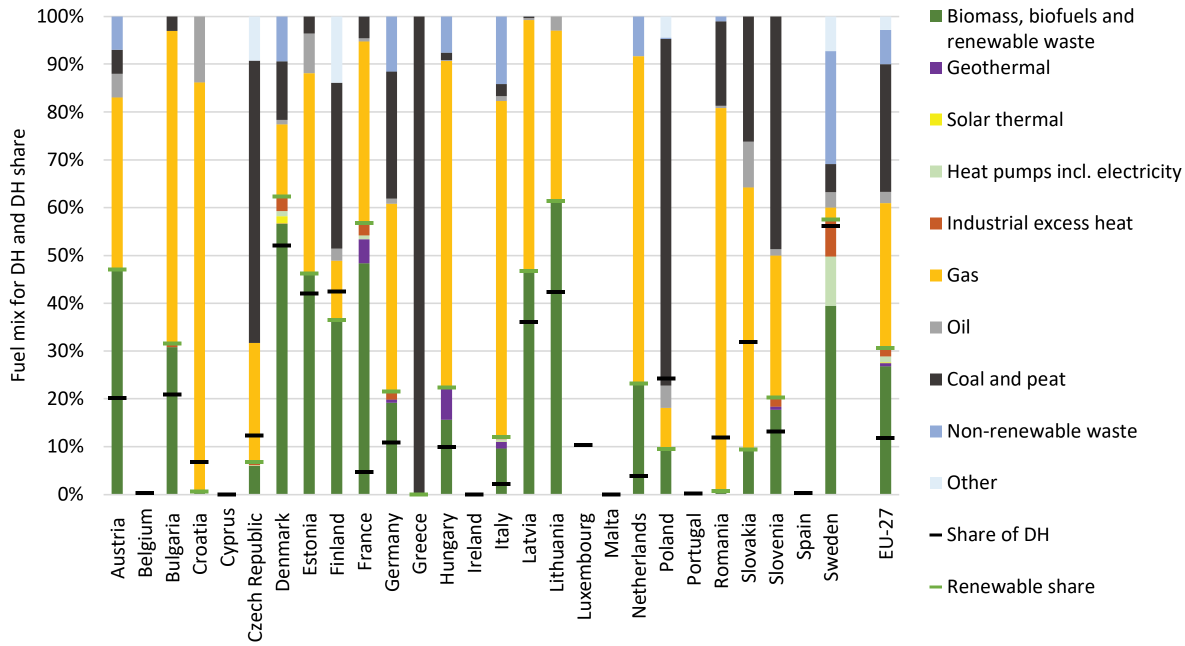

Figure 1.2: **DH market overview in EU member states: Fuel mix and share of renewables in DH as well as the share of DH in heating of residential and non-residential buildings. Own illustration, data source: European Commission, 2022 [9]**

In the EU, the deployment of DH is heterogeneous due to differences in climatic, technical and market conditions, as well as political frameworks and strategies (see Figure 1.2)The Scandinavian and also the Baltic countries, characterised by colder climates, have a long history of DH systems. They represent mature markets with high renewable shares ranging from 40% to 62%. Conversely, most Southern countries, such as Italy, Spain and Portugal, have little to no DH infrastructure. Eastern EU countries have large but often inefficient DH systems, built during the former USSR era, with market shares (of the heating and sanitary hot water demand of residential and non-residential buildings) above the EU average but low renewable contribution. Most of these countries implemented price and third-party access regulations [9]. In contrast, countries like Germany, the Netherlands, Belgium, Italy, Luxembourg as well as Slovakia and Hungary face significant competition from their extensive natural gas network [7]. Notably, Hungary has a high share of geothermal heat in its DH supply, contributing 7%.

DH offers numerous significant benefits. One of the primary advantages of DH is its ability to access a wide variety of energy sources efficiently, such as the currently widespread CHP, based on fossil fuels or biomass, but also possibly based on hydrogen in the future [9]. Renewable sources include air-source heat pumps, water-source heat pumps using either sewage, ground or surface water, or ground-source heat pumps using shallow or also deep geothermal resources, as well as direct solar thermal energy and secondary biomass resources [22]. Additionally, excess heat is a promising source, offering often a large amount of heat that is a by-product from other purposes, either from power generation, industrial processes and waste incineration [23]. This extensive range of sources allows DH to utilise more and diverse energy options that are climate-neutral compared to individual heating systems [17].

Furthermore, DH benefits from scaling effects of generation costs, potentially making it more cost-effective than individual heating. Another key benefit of DH is the possibility to decarbonize the heat source centrally for a large number of buildings, instead of changing the heat generation unit in each building. Additionally, DH interacts increasingly with the electricity system, through CHP plants and the use of large heat pumps. DH incorporates heat storages, enabling to shift the operation of the heat pumps by several hours, providing more flexibility to the energy system than offered by individual heat pumps [24,25]. However, the integration of sector coupling in utilities is still an area with limited experience. Large-scale seasonal storages can possibly store the heat over a large period of time, increasing the utilisation of solar thermal, geothermal or excess heat [26,27]. Low-temperature DH grids of the fourth generation offer efficiency advantages for heat pumps and low-temperature renewable and excess heat sources, possibly reducing costs and being more suitable for decreased heat demand of buildings [28]. Especially, heat from industrial processes with high temperatures such as in the production of iron, cement or glass is often suitable for external use. Furthermore, future DH systems can operate in an integrated, smart energy system based on renewables, which connects the electricity, heat and transport needs in a flexible and efficient way, as shown in Figure 1.1. Moreover, DH systems can be combined with cooling solutions, as suggested by the so-called fifth generation DH systems that function as bidirectional systems or secondary networks [29]. This combination allows for the simultaneous provision of heating and cooling, making DH a comprehensive and future-proof energy solution.

Despite the potential benefits of DH, there are significant challenges and disadvantages that must be considered. As an infrastructure, DH necessitates well-coordinated urban planning and concentrated actions of multiple stakeholders. The complex planning and necessary transformation require DH systems to account for interdependencies between demand, supply sources, and distances between them, as well as long-term projections of these factors. This complicates the identification of the future DH potential. Distribution pipes represent additional costs for infrastructure, such as distribution and transport pipes and transfer stations in buildings, and pose a substantial challenge [30]. For DH systems to be economically viable, there must be a certain level of heat demand from buildings within a potential supply area. In the future, heat demand of buildings may decrease due to thermal renovation and efficiency measures, leading to increased specific distribution costs and decreasing the cost-competitiveness of DH. Heat losses in the distribution infrastructure decrease the efficiency and further increase costs.

Future DH operation will also require more complex and advanced management, with digitalisation serving as a crucial tool for planning and operation. Decarbonizing the heat supply offers several central climate-neutral options for buildings, but it necessitates the use of various renewable sources rather than relying on a single large fossil CHP source. Currently, biomass is almost the only renewable heat source used, representing a share of 30%, together with heat pumps having a share of 1%, in DH generation [10]. However, it has a limited future availability and should primarily come from secondary resources such as agricultural and industrial residues [14,31]. Therefore, ensuring the availability and diversification of climate-neural heat sources is essential. Lowering system temperatures presents an opportunity to address these challenges, enhancing overall system efficiency and decreasing costs. These considerations underscore the need for more fourth generation DH systems and thus the retrofitting of grids, increased digitalisation for operation and integration with other energy infrastructures. Moreover, as a natural monopoly, DH infrastructure requires (price) regulation to ensure fair access and operation [32].

Summarised, considering the future challenges for the building sector such as thermal renovation to reduce heat demand and the transition to climate-neutral energy carriers, DH can facilitate the EU’s shift to a climate-neutral energy system, particularly in cities and densely populated areas. However, DH itself faces several future challenges, including the necessary transition from centrally generated heat in fossil CHP plants to renewable sources, as well as decreased heat demands from buildings. Consequently, solutions involve reducing system temperatures to minimise heat losses and distribution costs, along with implementing suitable planning and operation structures within a smart and sustainable energy system.

While the future of DH is yet uncertain, its potential benefits for a climate-neutral heating system are immense. DH potential could range from supplying a few newly built, densely populated areas to becoming an important technology supplying cities and urban areas, possibly replacing gas infrastructure. Energy system research can enhance the understanding of the role of DH in the EU's climate-neutral energy system. Examples from Nordic countries, including Denmark or Sweden, demonstrate how DH can become a central element in providing heat from renewable sources to buildings.

1.2 Modelling approaches for district heating

Modelling is a tool for simulating complex systems, anticipating future parameters and key drivers, and optimising processes. Energy system models, whether covering the overall system or specific sectors, analyse and optimise energy generation, distribution, and consumption. They evaluate and quantify the impact of technologies, efficiency improvements, and policy changes on energy demand, GHG emissions and costs by modelling various scenarios. This aids in designing efficient and sustainable energy systems, understanding system dynamics as well as identifying necessary political frameworks. These insights can be used to show possible pathways towards climate-neutrality as well as inform policymakers and investment decisions, as demonstrated in numerous studies, e.g. [33–37].

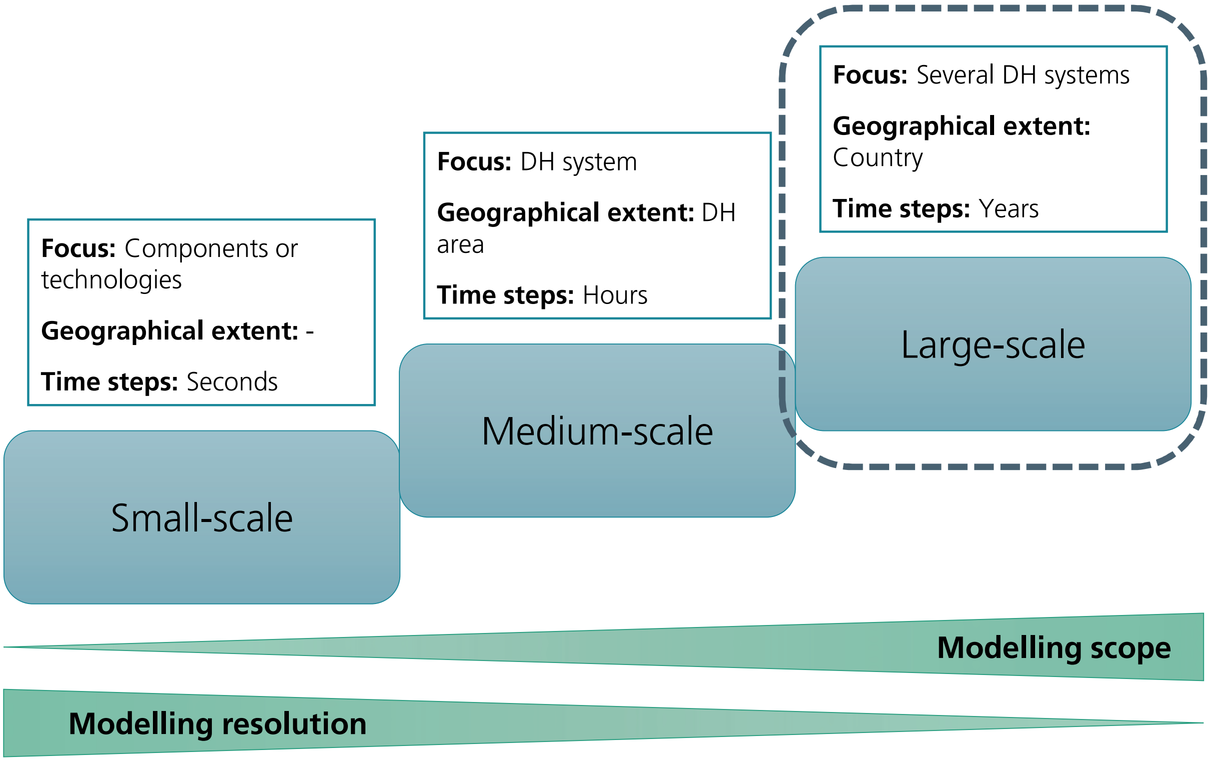

Figure 1.3: Modelling approaches for district heating modelling with typical attributes. Own illustration

Modelling the DH sector includes either completely or partially demand, supply and infrastructure aspects, and can be approached on different levels: small-, medium- and large-scale (see Figure 1.3). Each scale has distinct modelling attributes, primarily regarding geographic scope, technological detail and data requirements, addressing different research questions. Small-scale DH modelling focuses on components such as heat generation plants, heat storages or pumps stations, optimising parameters and providing detailed technological insights. This enables transient modelling, capturing time-dependent system dynamics with time steps of seconds or minutes. Medium-scale models cover an entire DH system by linearising component dynamics, featuring a broader geographical scope and more interacting components, but with lower technical and temporal resolution, typically hourly. Large-scale modelling extends the geographical scope to all DH systems within a country or the EU, further reducing technological as well as temporal and spatial resolution by generalising aspects like flow temperature variations and seasonal dependencies on annual level to simplify the model. Maintaining a sufficiently high spatial resolution in these models is essential to accurately capture how DH infrastructure depends on local supply and demand conditions. Large-scale models can be sector-specific, focussing on DH and simplifying interactions with other parts of the energy system, or integrated energy system models, covering the entire energy system with even less granularity in the DH sector.

In summary, there is a trade-off between scope and resolution, and the choice depends on the focus of the analysis. High-resolution models provide detailed temporal variations and technical specifics but are typically limited in geographic scope. Conversely, large-scale models cover extensive areas but require simplifications, reducing technical, temporal and spatial resolution, as well as the quality of input data. This thesis focuses on quantifying the DH potential at the EU-level, thus employing large-scale sector-specific and energy system models with a large geographical extent, simplifying the temporal dependencies but aiming at increasing the spatial resolution in DH modelling.

In the following, existing large-scale approaches to modelling DH are presented, that cover entire countries or the EU and have thus the same scope as this thesis. These approaches can be categorised into optimisation or simulation models, mainly depending on whether the research focuses on energy demand or supply. Demand modelling often utilises simulation and tools based on Geographic Information Systems (GIS), while supply models typically optimise the energy generation of a given demand with the target of minimising costs. These two approaches are frequently used sequentially, with each step offering different levels of temporal and spatial resolution and technical detail.

A significant series of studies focusing on the heating and cooling sector in 14 member states of the EU is the Heat Roadmap Europe (HRE) projects 1 to 4 from 2012 to 2019 [38,39]. The freeware simulation model EnergyPLAN [40] was used iteratively to find the optimal balance between efficiency gains and renewable energy integration. This model, developed for analysing smart energy systems and DH, incorporates various renewable and excess heat sources. Heat demand is an input, and the supply potential is aggregated on national level. EnergyPLAN can also be applied to individual DH networks, e.g. as implemented for Aalborg [41]. The model was extended in the EU project sEEnergies [42], integrating heat storages and additional renewable and excess heat source such as geothermal, solar thermal, waste incineration and industrial excess heat.

In the HRE projects, the Pan-European Thermal Atlas (Peta) [43,44] was developed as a spatial model and open database for investigating DH demand potential, serving as an input for the model ENERGYPLAN. This approach uses GIS tools to map the heat demand from buildings at the hectare-level. The concept of effective width was developed and applied to calculate distribution costs of a future DH infrastructure, providing a statistical method to anticipate the required length of DH pipes to meet the demand in a given area [30,45]. This approach enables the identification of potential DH areas based on heat density, which is the heat demand in a given area, typically per hectare. The heat density is often the central parameter available for analysing future heat demands, especially when the linear heat density (heat demand per DH trench length) for future grids is unknown. The spatial analysis of Peta assumes maximum feasible distribution costs, resulting in a DH market share in the EU of 45%, with a large plateau of 32 – 68% with minimal cost changes [19]. This represents a substantial increase of DH from the current 12%, to be achieved within 35 years by implementing DH system in all cities and larger towns, even in countries with lower heat demands. The project sEEnergies further developed this approach, indicating a possible DH share of 47% [45,46]. In the GIS tool, renewable and excess heat potential to supply DH areas was additionally allocated. This includes today’s industrial excess heat potential for future energy system and limited data on geothermal heat potential. The demand simulation model FORECAST [47], covering the industry and building sector, was used to determine the future demand for heating and hot water in the buildings on a national level, which was then spatially disaggregated in Peta.

A similar model chain was applied in the Hotmaps project from 2016 to 2020, developing an open-source toolbox for heating and cooling planning [48]. The supply was modelled in GREEN-X [49], which simulates renewable sources for the electricity sector annually at the country level, and Hotmaps DISPATCH/DH GEN Model [50], which identifies the cost-optimal DH generation mix for individual networks. Inputs include demand and aggregated renewable potential. Future heat and DH demand was modelled by INVERT/EE-LAB at the national level, applied in numerous studies [7,51–54], resulting in a 14% DH market share by 2050. The heat demand was spatially disaggregated in a GIS-based approach [55] and used to calculate DH distribution costs on hectare-level by applying the effective width concept [49,56–58]. Compared to the study of HRE, a connection rate within the DH areas below 100% was assumed. However, it also considers an assumed threshold for distribution costs to identify future DH areas. This spatial approach shows that a 31% DH market share is possible, which is comparably higher than current shares, and also higher that the results from models with national resolution, however it is significantly lower than the results found by ENERGYPLAN in the HRE and sEEnergies studies.

In these two projects, similar step-wise approaches were applied to quantify DH potential, analogous to another study focusing on several cities across the EU. The GIS-model NETHEAT was used to disaggregate heat demand at the hectare level [59]. First, demand is modelled at the national level using a simulation model capturing main drivers like thermal renovation. This demand is then disaggregated to the hectare-level using GIS tools, leading to a DH demand potential based on assumed maximum distribution costs. This potential is input for energy system models to optimise generation capacities and dispatch.

Further energy system models are frequently applied to model the energy system and the DH sector. Due to the large modelling scope, they do not utilise a GIS-based approach. The open-source optimisation model BALMOREL [60] covers the energy system and provides a detailed representation of DH grids with high temporal and spatial resolution at the city level and interaction with the electricity sector. It considers industrial excess heat as heat source and optimises the expansion of existing DH grids [61]. However, it does not identify new DH grids, as the heat demand is provided externally. Another optimisation model representing the energy system across all relevant sectors is the model ENERTILE [62], used in several publications and studies [37,51,63–65]. It offers high temporal resolution for the entire EU energy system and beyond [66]. The spatial resolution is national, including DH modelling. It models DH generation in close interaction with the electricity sector, resulting in a high share of heat pumps and biomass CHP, and with a minor role for hydrogen [67]. However, the extension of DH systems and other renewable sources is not part of this model and is an input parameter on national level. The open source optimisation model PYPSA-EU-SEC [68] has a high spatial resolution and can integrate the level of building renovation into the optimisation. However, it does not model possible DH expansion, and has no information on the regionally available renewable sources. Other energy system models like POLES from the EU's Joint Research Centre (JRC) [69], TIMES PANEU [70], PRIMES [71] as well as the International Energy Agency's (IEA) GEC model [72] use DH demand as an input for modelling the energy system and necessary generation capacities at the national level.

These models rely for the DH supply primarily on air-source heat pumps [51,73,74], along with significant shares of biomass [38,51,75] or even hydrogen [33]. This is largely because these studies did not consider other possible renewable sources due to lack of data. Energy system models simplify the DH sector and depend on accurate assumptions and aggregated data for demand and supply potentials, which are often not available. Achieving reliable results necessitates detailed DH models that utilise spatial tools and data, as well as suitable aggregation, which can be accomplished through a step-wise approach.

In the existing stepwise approaches, primarily of the projects HRE, sEEnergies and Hotmaps, spatial analysis allocated renewable and excess heat sources to possible DH areas. However, they lack detailed data on deep geothermal resources and the potential for utilising heat from rivers and lakes. Moreover, the spatial detail of climate-neutral sources identified in these GIS-based approaches is not represented in the energy system models ENERGYPLAN and Hotmaps DH GEN. Estimations of available industrial excess heat require information on the exact location of the sites, along with details on the process or at least sector and the amount produced. While several individual studies quantify industrial excess heat potentials, they base their findings on emissions by sector rather than process-specific production volumes [76–84]. The industrial excess heat potentials considered in Peta and Hotmaps are based on site-specific production data and are a result of this thesis, presented in Chapter 3. However, these results reflect the current industrial structure and do not account for the impact of the transformation within the industrial sector itself.

A comparative literature review on the future DH market share in the EU found a range from 5% to 45%, indicating that higher modelling resolution results in higher DH market shares [85]. Therefore, identifying potential DH areas requires GIS-based approaches with high spatial resolution to map the heat demand at least at the hectare-level. The GIS applications in the Peta and Hotmaps projects utilise thresholds for suitable heat density or distribution costs, demonstrating the suitability of the effective width concept. However, the thresholds used to identify an area as suitable for DH that are based on distribution costs or heat density have not yet been empirically validated.

In summary, existing literature and models vary significantly in their level of detail and representation of DH, regarding modelling approach, focus, extent, spatial and temporal resolution as well as technical details. Modelling approaches necessitate sufficiently high spatial and technological detail to capture important local conditions and accurately represent the DH sector. The two approaches that do incorporate a GIS-based step in the modelling lack a comprehensive dataset on available renewable and excess heat potentials for DH supply, as well as empirical data to validate the identification of DH areas based on maximum distribution costs.

This thesis aims to provide more robust and specific data sets with high spatial resolution, develop GIS tools and models, and aggregate and apply these results while maintaining the necessary granularity in energy system models to quantify the future DH potential.

1.3 Objective and structure of this thesis

In transitioning the heating sector to climate-neutrality, DH can play a key role. DH will require infrastructure investment, utilise various renewable and excess heat sources and increasingly interact with the electricity market while competing with decentralised heating options. Determining the potential extent of DH deployment and climate-neutral supply options is essential for guiding policies. Energy system models are key tools but often oversimplify the DH sector. Detailed and robust spatial data sets and models are needed to accurately quantify the DH potential in a climate-neutral energy system.

This thesis explores the potential of climate-neutral DH systems, quantifying their role in achieving the EU's ambitious climate targets by 2050. Various modelling approaches are established, utilised and refined, supported by the construction of hectare-level data sets. The modelling integrates the supply and the demand perspectives, to assess how and to what extent residential and non-residential buildings in the EU can be supplied by DH using renewable and excess heat sources. Different scenarios are explored to investigate possible developments in DH and the heating sector.

The focus is on GIS-based spatial analyses, quantifying the future DH market share based on empirical data, and assessing the potential supply from industrial excess heat, as well as from geothermal, biomass, wastewater treatment plants, rivers, lakes and waste incineration. The resulting data sets and methods are further applied in sector-specific or energy system models, providing deeper insights into the interactions between DH and the remaining energy system. The results include a detailed analysis of current and future DH areas, the available renewable and excess heat potential and the cost-optimal utilisation of these sources. The identified technical and economic potential enables the derivation of transformation pathways and adequate policies, as well as facilitating public acceptance.

The thesis addresses the following main research question:

What is the potential for a climate-neutral district heating in the EU, taking into account the spatial diversity of heat demand and supply?

The main research question is divided into specific sub-questions to investigate the influencing factors for the future DH potential.

1. How does decreasing heat demand affect the future expansion of DH areas, based on empirical data? (Chapter 2)
2. How much excess heat from energy-intensive industrial processes is technically available for DH at the regional level? (Chapter 3)
3. How does the transformation to a climate-neutral industry affect the excess heat that is available for DH? (Chapter 4)
4. What is the technical potential for renewable and excess heat sources to supply DH demand in a climate-neutral energy system? (Chapter 5)
5. What is the economic potential of climate-neutral DH supply options and what is the impact of the supply temperature in DH grids? (Chapter 6)
6. How do different renewable and excess heat sources for DH interact with the electricity sector? (Chapter 7)

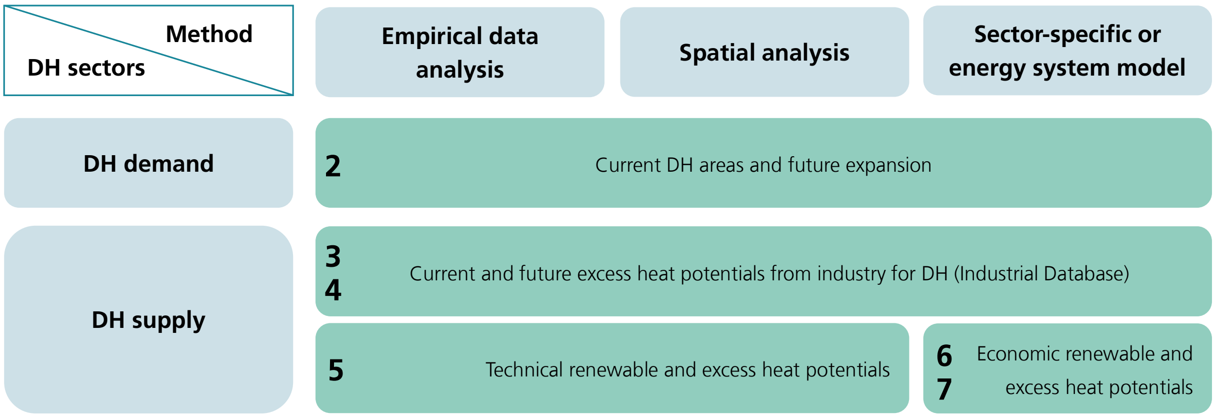

Figure 1.4: Conceptual framework of this thesis

These sub-questions are addressed in separate chapters, each describing the method and data used in detail, presenting results and drawing individual conclusions. The conceptual framework is depicted in Figure 1.4, providing an overview of the scope and the methods of each chapter. Chapter 2 focuses on the DH demand potential and the identification of future DH areas, which serves as a basis for modelling climate-neutral DH supply in subsequent chapters. Most chapters involve constructing data sets based on empirical analyses, forming the foundation for spatial assessment and modelling. The sector-specific model FORECAST was utilised for input data covering the building sector (Chapter 2) and the industry sector (Chapters 3 and 4). In Chapters 6 and 7, optimisation models were employed to optimise the DH supply mix and the overall energy system.

The thesis is structured by individual chapters dedicated to the individual research questions. The final chapter summarises the contributions of each paper, presents the main conclusions regarding the overarching research question and provides an outlook for further research. The following provides a concise overview of the dedicated chapters and their contribution to the thesis.

Chapter 2: Current and future DH extension

DH as an infrastructure is most economical in areas with high heat demands. In areas with lower heat densities, heat transport costs become more significant, reducing the economic efficiency of DH. Future heat demand from residential and non-residential buildings is expected to decrease due to thermal renovations, potentially making DH less feasible. An empirical correlation between heat demand and the existence of DH connections has not yet been evaluated. Therefore, the identification of future DH areas in literature has mainly relied on expert guesses. In this chapter, the current status and future expansion potential of DH in Germany are explored, and a new model DisCo is established. In this model, high-resolution empirical data were collected and processed to assess correlations between heat density, distribution costs and actual DH deployment. Common methods to derive distribution costs were applied and refined. With the empirical data, the threshold values for distribution costs used in literature to identify suitable areas were reviewed. A building stock model was linked with spatial analysis via a common data base and applied in a scenario-based approach. Future DH areas were identified to show the demand potential of DH, based on an integrated modelling approach which could be validated with empirics.

Chapter 3: Excess heat potential from industry available for DH

One possibility for a climate-neutral DH supply is the use of excess heat, a by-product of industrial processes. These can serve as large point sources due to the high temperatures needed in industrial processes. However, estimating excess heat potential often lacks detailed process information for individual sites, leading to the use of average values for entire sectors, which typically overestimate the potential. Additionally, spatial allocation is often conducted in a simplified manner. In this chapter, the excess heat potential from energy-intensive industrial processes was quantified and georeferenced and matched spatially with identified current and future DH areas in the EU. An extensive database of industrial plants was constructed, by matching several data sources. The data set includes coordinates, type of process and annual production, enabling a bottom-up quantification of available excess heat by using specific energy consumption values from the model FORECAST. Uncertainties regarding the future efficiency improvements in industrial processes and the temperature levels in DH grids were addressed by constructing different scenarios. Through spatial analysis, the utilisation potential of excess heat for DH areas was calculated based on the distance between heat source and sink. The resulting EU-wide potential offers a higher level of accuracy not previously available in large-scale analyses.

Chapter 4: Future excess heat potential from low-carbon industrial processes

The transformation to a climate-neutral industry will lead to significant changes at major energy-intensive industrial sites, necessitating efficiency improvements, new processes and changes in energy carriers. This transformation will substantially affect the available excess heat for DH, an effect not yet incorporated in published estimates of industrial excess heat. Applying a similar approach to the previous chapter, the excess heat potential from future industrial processes was estimated, additionally accounting for the necessary shift to low-carbon processes. An extensive review of potential industrial transformation pathways was conducted based on a bottom-up energy model, deriving and applying excess heat factors to the industrial database. The calculated potential was spatially matched with the DH areas identified in Chapter 3, allowing for a conservative assessment of the contribution of industrial excess heat to the future DH supply.

Chapter 5: Technical renewable and excess heat potential for DH

Industrial excess heat is expected to be only a small source for climate-neutral heat supply for DH in the future, especially with potential DH expansion. Therefore, all possible renewable and excess heat sources need to be quantified with high spatial resolution. While extensive literature exists on individual sources, a consistent quantification of climate-neutral heat sources for DH at high spatial resolution across the EU does not yet exist. Particularly, deep geothermal resources have not yet been quantified. In this chapter, the industrial excess potential from Chapter 4 was combined with other heat sources to explore how DH could be supplied in a climate-neutral energy system. Various data sources were collected and processed with high spatial resolution, quantifying the technical heat potential from geothermal, biomass, rivers and lakes, waste incineration, wastewater treatment plants and industrial plants. The spatial matching method was refined to account for smaller future DH areas and prioritise larger networks with a higher DH demand. The resulting DH areas were clustered based on their renewable and excess heat potential to identify homogenous network types. This aggregation enables the integration of the highly detailed data sets into energy system models without losing significant information. The comprehensive data set georeferencing renewable and excess heat potentials expands the possible options for future DH supply in models, allowing for deriving adequate policies targeting sources with high potentials.

Chapter 6: The supply mix of DH in 2050 and the impact of temperatures

The optimal supply mix of available climate-neutral sources for DH depends on the costs of technologies as well as their temporal and spatial availability. DH system temperatures define how efficiently low-temperature heat sources can be utilised, thus influencing the mix of heat supply options and the costs. In this chapter, the economic potential of the identified heat sources from Chapter 5 was identified. An optimisation model for the investment and dispatch of DH supply technologies was applied in different scenarios for the EU, determining the cost-optimal installation capacity for a climate-neutral heat supply in a greenfield approach. Four different DH clusters per country were modelled, each with a distinct share of available climate-neutral heat potential. Technical details, such as the efficiency of the heat pumps depending on the source temperatures, was integrated in this optimisation model. The focus is on the impact of temperature level in DH grids on the optimal DH dispatch and derived costs. The results show the cost-optimal DH capacities and dispatch based on the detailed spatial analysis with high technological detail.

Chapter 7: Cost advantages of renewable and excess heat technologies for DH supply

In the future, DH supply will interact closely with the electricity sector, as large heat pumps for heat generation will play a significant role, by using electricity and offering flexibility. During high renewable electricity generation, heat pumps produce heat which is stored in large heat storages. During lower renewable electricity generation, stored heat can be distributed while heat pumps do operate at lower power or not at all. Depending on the technology mix, cost advantages for the energy system could arise from decreased electricity demand when using renewable resources directly from DH, as well as from the ability of heat pumps to balance peaks in the electricity system. Based on the cluster results and the four DH types identified in Chapter 5, the technical potential for DH areas was integrated into an energy system model to calculate the economic potential in the EU for the year 2050. Unlike in Chapter 6, this analysis examines the interaction with the electricity sector in detail here, by simplifying technical parameters due to linearisation of the model. The costs and assumptions for the available heat sources were integrated into the energy system model on an hourly basis. The cost differences by employing large shares of these sources were compared to a large shares of heat pumps in ten different scenarios, identifying key parameters for a cost-optimal energy system. This approach assesses the impact of the DH generation mix on the electricity sector to achieve lowest costs, capturing the heterogeneous resource availability for DH, by employing an integrated energy system model.

2 Identifying future district heating potentials in Germany: a study using empirical insights and distribution cost analysis

Pia Manz, Tobias Fleiter, Anna Billerbeck, Markus Fritz, Şirin Alibaş, Wolfgang Eichhammer: Identifying future district heating potentials in Germany: a study using empirical insights and distribution cost analysis. In: International Journal of Sustainable Energy Planning and Management 40 131–145, 2024. DOI: 10.54337/ijsepm.8142.

2.1 Introduction

In recent years, the imperative to achieve climate-neutral heating has become a focus of political debate in Germany and the EU. District Heating (DH) could be a decisive factor in this transition, which is at the centre of the discourse on heat planning. DH has numerous advantages, including the utilisation of multiple renewable heat sources, the ability to balance peak demands through heat storage and the cost advantages due to economies of scale [86]. However, the inherent challenge lies in the need for an infrastructure for heat transportation and distribution to the consumers. Distribution capital costs are largely dependent on local conditions and defined as the specific annualised capital costs needed to build the DH distribution grid, per heat quantity delivered. They are an additional cost component on top of the heat generation costs for DH besides further costs for transport and service pipes [30]. Lower distribution costs occur in areas with higher heat densities, i.e. the heating demand per specific area, thus possibly making DH cost-competitive to individual heating solutions. The analysis of potential DH areas on the country-level is therefore intricately linked to local conditions. Existing scenarios of energy system studies present the role of DH as varying in importance by 2050 [85]. This variability implies a broad spectrum of economic possibilities of DH in competition with decentral heating options as well as thermal renovation of buildings. Achieving reliable modelling results for the identification of cost-optimal pathways requires the integration of empirical parameters in the modelling process. Analysing the empirical correlation between heat densities, derived distribution capital costs and their respective DH installations provides valuable insights into the potential DH deployment in the future.

2.1.1 State of research

Empirical analyses for the current state of DH on the country-level have been conducted before, e.g. for Germany, Triebs et al., 2021 [87] analysed the fuel input on the network level, and Weinand et al., 2019 [88] published an open data set on the share of buildings with DH for the municipalities based on the census 2011. However, only a few studies have analysed the current spatial extension of DH on the country- or EU-level, mostly due to lack of data. In the Pan-European Thermal Atlas [89], current DH areas are published as shapefiles in an online map application, together with the heating demand. The data set is derived from a database of DH systems on the city-level based on manual research, with the spatial extension derived from areas with high heat densities [90]. Pelda et al., 2021 [91] developed a district heating atlas comprising 50% of the DH demand of Germany, which is published in an online map [92]. It is based on the census 2011 combined with research on the website of operators, and contains several key indicators about current DH systems on the city scale. In summary, the data sets on existing DH areas with a large geographical extent are available with the spatial resolution of cities. However, higher resolution (i.e. hectare-level) is needed for an empirical analysis of the correlation with distribution capital costs.

Several studies have calculated heat density and derived distribution capital costs for DH with high spatial resolution on a large scale with the aim to identify future DH potential areas. The heat density can be expressed in two different ways. On the one hand as linear heat density which is the ratio between delivered heat and DH grid length. On the other hand as (areal) heat density, which is the delivered heat per hectare of space. This is useful if a grid does not yet exist or data availability on grid lengths is scarce. This approach uses the effective width concept to derive the linear heat density from the heat density analytically based on an empirical correlation. It was first introduced by Persson and Werner, 2011 [30], refined by Persson et al., 2019 and 2021 [18,93], as well as analysed in a parameter study in García et al, 2023 [45]. It was applied with different parameters and compared to a more data-intensive optimisation method on the city-level for Vienna and Brasov, as well as applied for EU-27 in Fallahnejad et al., 2018, 2021 and 2024 [56–58]. In the project Heat Roadmap Europe, the current DH areas from Peta [89] are used to identify possible extensions with an analysis of cost-effective heat densities on the EU-level [94]. Leurent, 2019 [95] analysed the DH potential in France with a spatial approach, by assuming a threshold value for the calculated linear heat density as the upper limit for economical grids. On the local scale, Dochev et al., 2018 [96] used the linear heat densities to assess the DH potential of Hamburg, again with an assumed threshold value as the upper limit. For Germany, Blömer et al., 2019 [97] calculate capital costs in €/m, using a cost threshold value to identify potential areas. In summary, an empirical data analysis considering the correlation between heat density, distribution capital cost threshold and existing DH on the hectare-level is absent in the existing body of research. Instead, assumed thresholds are derived from typical values in highly populated areas and cities to identify potential DH areas in the future, reflecting a normative approach. With empirical data on accepted costs, the economic decisions can be integrated into models.

In energy system studies on the national or EU-level, DH is part of the solution for the heating transition, however often represented with a low modelling resolution. Manz et al., 2022 [85] compare energy system studies with regard to the resulting DH market share. The range for Germany is between 13% and 37%, leaving a broad range for the role of DH in the heating transition. The assumed threshold values for economic future DH areas influence the resulting DH potential and market share and thus, should be proven by empirics. The future role of DH based on empirical cost thresholds has not yet been quantified in models. Therefore, we analyse the empirical DH costs in Germany, and conduct a scenario analysis to improve the accuracy of modelling the possible future role of DH.

2.1.2 Research objective

The objective of this study is to address three main research questions, aiming to fill data gaps in the literature by establishing an empirical correlation between existing DH and accepted distribution capital costs, which facilitates a robust scenario analysis of the potential future of DH in Germany:

- What is the status quo of DH areas and demand?
- What is the empirical correlation between the existing DH infrastructure, heat density and distribution capital costs?
- Where are future DH potentials, considering the existing DH areas and thermal building renovation activity until 2050?

To answer these questions, first, different data sources with a high spatial resolution are combined to analyse the status quo of DH and calculate the heat density, deriving distribution capital costs and analyse the correlation. The influence of the different historical development in West and East Germany in the last century on the correlation is investigated. As a second step, the empirical distribution capital cost threshold is applied to estimate the future potential DH market share in a scenario analysis. The structure of the paper is as follows: In Section 2.2, we describe the data sets used and the methods applied. In Section 2.3, we present the results for the current status of DH, the correlation to distribution capital costs and for DH potentials. We then discuss the results and show the limitations in the approach. Finally, in Section 2.4, we conclude the analysis.

2.2 Data and method

Several data sets on the hectare-level of the building stock and DH were combined in this study. Heat density, commonly in GJ/hectare or kWh/m², includes the annual demand for space heating and sanitary hot water for both residential and tertiary buildings. The DH market share is defined as the share of energy demand for heating and sanitary hot water in the building sector that is covered by DH. The connection rate is defined as the share of connected dwellings to DH compared to the total number of dwellings within a DH area. The empirical analysis of the status quo and current DH distribution capital costs is based on calculated heat density and DH connections in Germany. For the future development, we applied a model-based approach with a soft-coupling of a building stock model (FORECAST) and a spatial model (DisCo). In Figure 2.1, an overview of the data sources and processing as well as the methodological steps is shown, which are described in detail in the following.

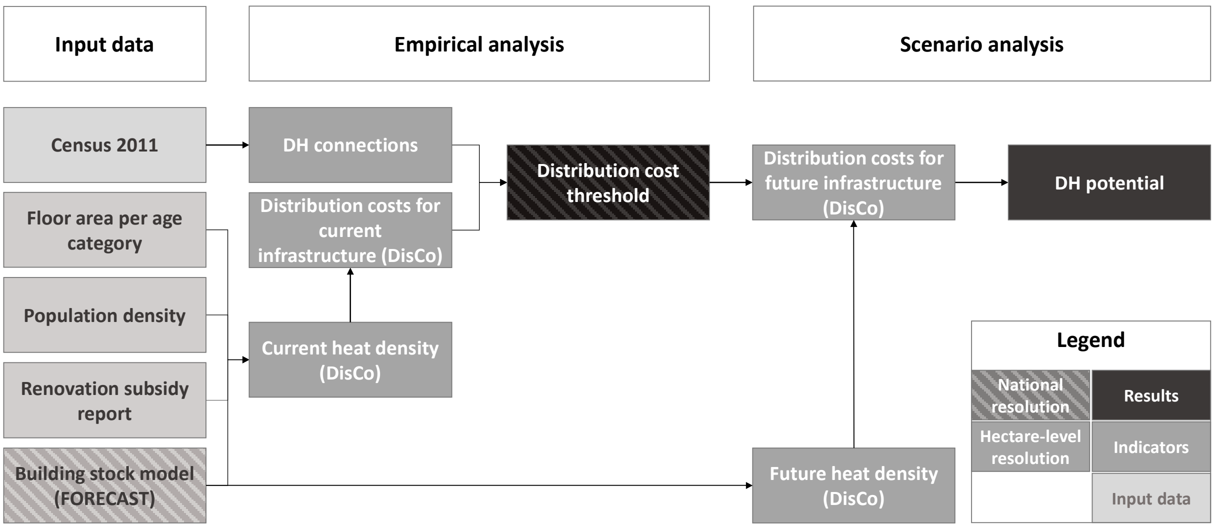

Figure 2.1: Data processing and methodological steps applied in the paper.

2.2.1 Data processing

As shown in Figure 2.1, different data sets were used to derive: (1) the current DH status and (2) the current and future heat density and the distribution capital costs, both on the hectare-level for the geographical scope of Germany. The data source for identifying the current DH extension is the European-wide census, whose results were published for Germany on a 100m x 100m grid (hectare-level) [98]. As the data set is based on the last census, the data are from the year 2011, published in the year 2017. More recent data of the subsequent EU-census 2021 are currently being processed by the statistical offices. Integrating more recent data into the analysis could lead to more accurate thresholds, however, as DH installations are built over a long time horizon, the difference is possibly negligible. In our analysis we used the data set that lists for each hectare the number of dwellings per type of heating (DH and others), totalling to 2.7

million hectare cells in Germany with at least one dwelling. From that, we applied data validation steps as well as neighbour analysis to identify errors in the data set which stem mainly from people who answered incorrectly in the questionnaire about their type of heating. For that, all cells with less than 100 DH connections in a radius of 3 km are filtered out. Another criterion was applied to filter small building networks, so that only networks with more than 10 DH connections of their own and more than 1000 DH connections in a radius of 3 km are considered as DH networks. After the data processing steps, the data set comprises 133,348 cells with DH connections.

The heating demand of buildings and thus the heat density depends mainly on the heated floor area per hectare, the building type (single-/multi-family or non-residential house), the year of construction and the renovation status. The main data source for the calculation of the heat density was the Hotmaps data set, publishing the floor area per building age category on the hectare-level [48]. In this data set, four age categories are used. The age categories needed to be harmonised with statistical values. The base year for this data set is 2012, with no updates available, which aligns with the census data from 2011. Further data needed to estimate the regional heat density is the population density on the hectare-level, to differentiate areas with single-family houses (SFH) and areas with multi-family houses (MFH) that are typically more densely populated. These data were also taken from Hotmaps [48]. Additionally, the regional renovation activity was derived from the subsidy reports on the NUTS 3 level of the German state-owned bank Kreditanstalt für Wiederaufbau (KfW) that gives out loans and subsidies for building renovations [99–104]. The sum of loans for refurbishment from the available years 2015 until 2020 was used to derive regional indicators for the renovation activity and to distribute renovated buildings across the regions.

The energy demand simulation model platform FORECAST [47] was used to model the building stock for the current (2012 and 2020) and future years (2030 and 2050). The model FORECAST-Buildings, which has been applied in several EU-wide analyses, e.g. [105–107], uses an extensive building stock database and models the useful and final energy demand for both residential and tertiary (non-residential) buildings in a high technological resolution. The results were calibrated for statistical years until 2020 and future renovation activity and choice of heating technology is modelled endogenously. The temporal resolution is annual and the spatial resolution is national. The results are disaggregated to the hectare-level in a downstream model DisCo [108], with a soft-coupling via a common SQLite database, where the results of FORECAST are stored and further processed in DisCo. The model DisCo is a Python-based model, which uses the instance of QGIS together with GDAL libraries to perform spatial computations. From FORECAST-Buildings, two input data sets are used as an input for the regional disaggregation in DisCo:

- the total floor area in m² in Germany and
- the specific useful energy demand for heating and hot water in GJ/m².

These parameters are given in the model database per building category, which means:

- per building age class,
- building type (single-/ multi-family or non-residential house) and
- renovation status.

In the model DISCO, first, the floor area per building category is distributed to the hectare-level. For that, the floor area per age class on the hectare-level from Hotmaps is used, and, for residential buildings, split up for each hectare into SFH and MFH depending on the population density. Further, renovated floor areas are distributed to hectare level, with higher shares in regions where the subsidies are comparatively high. As a second step in DISCO, the useful energy demand is calculated on the hectare-level by multiplying the national average of specific useful energy demand in GJ/m^2 with the floor area on hectare level per building category.

2.2.2 Spatial analysis

In this section, the spatial analysis is described as a three-step approach. First, the current heat density is calibrated and matched with the statistical data on DH installations. Second, current distribution capital costs are derived from that matching and an empirical correlation is investigated between the distribution capital costs and the resulting DH installations. Third, a scenario analysis is conducted, based on two different ambition levels of building renovation. Based on the future useful energy demand and thus reduced heat density, future distribution capital costs are derived and DH potential areas are identified. The spatial analysis was conducted in QGIS and the plugin PyQGIS [109] to map and process the raster data sets.

2.2.2.1 Matching DH installations with heat density

The aim of this step is to combine the data sets of the heating demand with DH installations on the hectare-level in QGIS. The resulting raster data set contains the heat density, the number of dwellings and the number of dwellings with a DH installation. The validation of the derived heat density is conducted on the national level for the base year 2012, using the results of FORECAST-Buildings that includes an extensive statistical database. The DH installation numbers are used further to derive average DH connection rates within one DH area.

2.2.2.2 Distribution capital costs

In this step, distribution capital costs are calculated based on the heat density. This is conducted first for the existing DH areas, and later for the possible DH areas in the scenario years. The aim here is to identify parameters from the existing areas that can be projected to the future, with the rational that current accepted costs can be assumed to be accepted in the future. The method to calculate the distribution capital costs $\mathrm{C_d}$

in €/GJ is based on Persson & Werner, 2011 [30], using the updated parameters from Persson et al., 2019 [18] and 2021 [93]. As stated in these sources, these cost parameters can be used as a proxy for future low-temperature grids (4th and 5th generation DH [110]) as well. It represents the annualised investment for the distribution pipes and is dependent on the heat density $\mathrm{q_L}$ [GJ/m²], referring to the sold heat in this case, in the denominator. Further parameters are the average pipe diameter $\mathrm{d_a}$ as a function of the heat density, the effective width w as a function of the plot ratio $\mathrm{pr} = \frac{A_B}{A_L}$ (ratio of building floor area per given land area), the annuity factor a and the cost constants $\mathrm{C_1}$ in €/m and $\mathrm{C_2}$ in €/m²:

$$\mathrm{C_d} = \frac{\mathrm{a \cdot (C_1 + C_2 \cdot d_a)}}{\mathrm{q_L \cdot w}} \ [€/\mathrm{GJ}], \quad \text{with} \qquad (1)$$

$$\mathrm{d_a} = 0.02\ \mathrm{m} \quad \text{for } (\mathrm{q_L \cdot w}) \leq 1.5\ \mathrm{GJ/m};$$

$$\mathrm{d_a} = 0.0486 \cdot \ln(\mathrm{q_L \cdot w}) + 0.0007\ [\mathrm{m}] \quad \text{for } (\mathrm{q_L \cdot w}) > 1.5\ \mathrm{GJ/m}, \qquad (2)$$

and

$$\mathrm{w} = \frac{\mathrm{e}^2}{\mathrm{pr}}\ [\mathrm{m}] \quad \text{for } \mathrm{pr} \leq 0.12;$$

$$\mathrm{w} = 55\ [\mathrm{m}] \quad \text{for } \mathrm{pr} > 0.12. \qquad (3)$$

2.2.2.3 Scenario analysis

The scenario analysis uses the projection of the building stock until the year 2050, with two scenarios differing by their refurbishment ambition levels, called *high-refurb* and *low-refurb*, based on the project Paris Reinforce [111]. With these two scenarios, the influence of a lower heat density on the distribution capital costs can be assessed. The model chain of the national simulation of the building stock in FORECAST-Buildings and the downstream regionalisation of floor area and useful energy demand on the hectare-level in DISCO is applied and analysed for the years 2020, 2030 and 2050. The derived heat density serves as a base for the calculation of future distribution capital costs, depending on renovation and connection rates. It is assumed that the existing infrastructure will not need to be replaced and the current costs are depreciated, thus these costs are subtracted from the future distribution capital costs for each cell. Only for densification, costs are calculated as additional expenditures to add pipes or increase the diameter. The aim is to identify future potential DH areas with comparable distribution capital costs as the current DH structure on the hectare-level. The main parameters in this analysis are the renovation ambition, reflected by two scenarios, and the connection rate and the DH market share that are varied.

The renovation activity of individual building components is triggered by their technical lifetimes. The two scenarios *high-refurb* and *low-refurb* assume different mean values for the distribution of the technical lifetime of building components. This results in an average annual renovation rate (renovated floor area divided by total floor area) of

1.6% and 1.3% between 2020 and 2050 in the *high-refurb* and *low-refurb* scenario, respectively. By 2050, in comparison to 2012, the total useful energy demand decreases by 39% in the *high-refurb*, and by 32% in the *low-refurb* scenario.

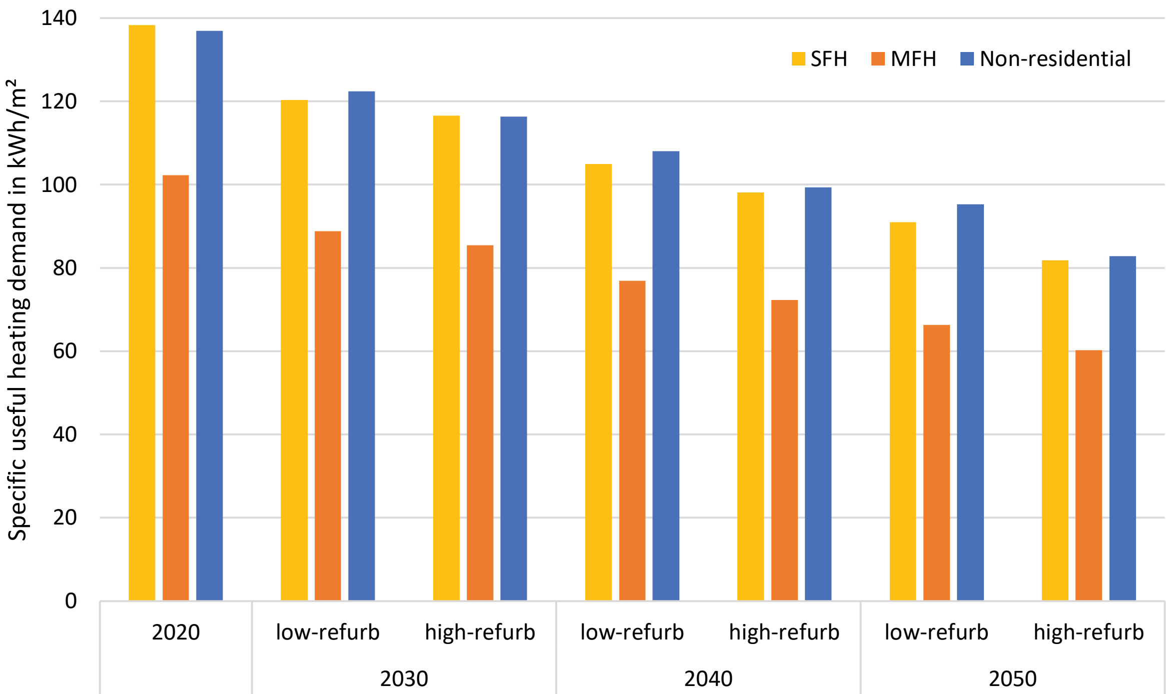

Figure 2.2: Specific useful energy demand per building type as modelling result from FORECAST-Buildings, for the two renovation scenarios

The reduction in the average specific useful heating demand of the different building types is depicted in absolute values in Figure 2.2. It varies from 32% in non-residential buildings to 37% in SFH buildings and 39% in MFH buildings in the *low-refurb* scenario and goes up to 40% in non-residential buildings and to around 43% in residential buildings in the *high-refurb* scenario.

2.3 Results

In the following, the resulting status quo of DH, the correlation with distribution capital costs and the future DH potential for Germany are presented. Each of the results is based on the hectare-level resolution.

2.3.1 Status quo of DH

The census data set indicates that DH is often installed in city centres. In Figure 2.3, the number of connections is shown. The plotted census data have a similar extension as the network from DH operators that publish maps of their grid online (e.g. the city of Karlsruhe), indicating that the filter criteria are sufficient to capture errors and outliers. The connection rate for each DH area can be calculated by dividing the number of dwellings that are connected to DH divided by the total number of dwellings. The highest connection rate is identified to be in Flensburg, with an average value of 91.5%.

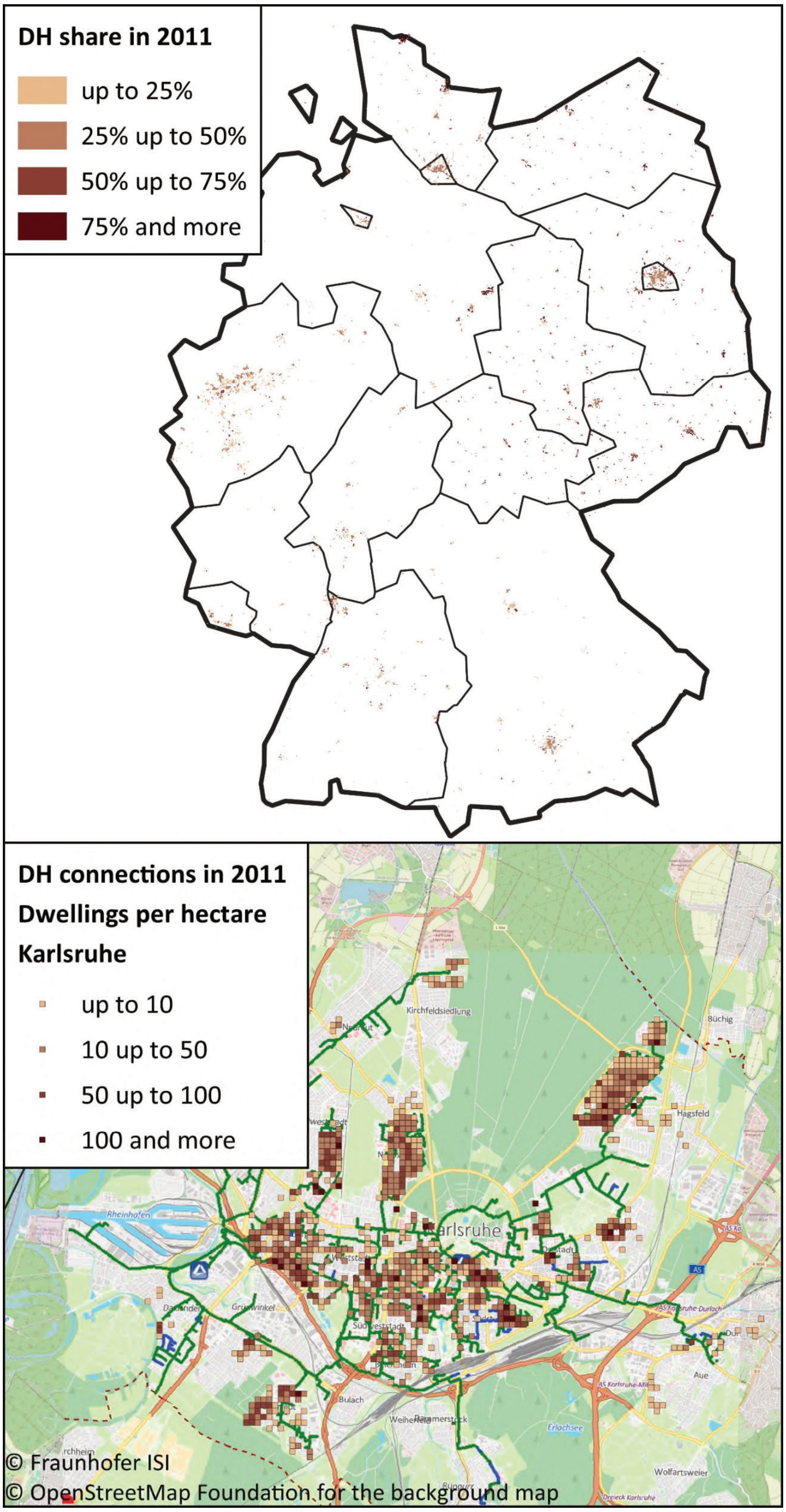

Figure 2.3: **Visualisation of the census 2011 data set after data processing steps, showing the number of DH connections per hectare, visualised overlaid with the DH network map of Karlsruhe in 2021, published in [112]**

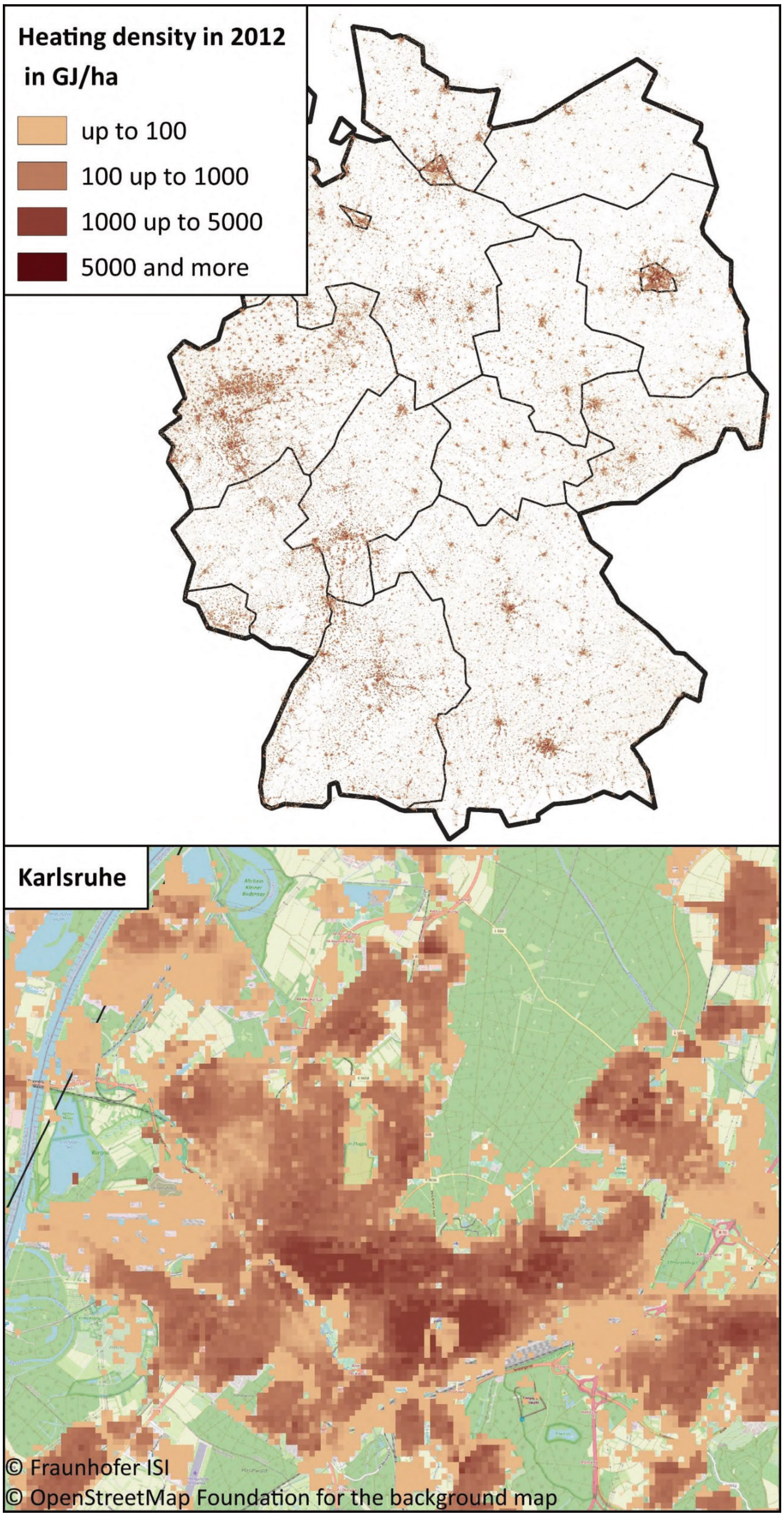

Figure 2.4: Calculated heat density in GJ/hectare in the base year

2.3.2 Correlation of existing DH, heat density and distribution capital costs

The spatial matching of the current DH installations and the heat density aims to derive accepted distribution capital costs. The calculated current heat density is depicted in Figure 2.4. The heating demand covered by district heating was calculated by multiplying the derived connection rate with the respective heating demand of the covered cell. The aggregated annual useful heating demand covered by DH sums up to 199 PJ, in line with the statistics [113].

The resulting raster data set from the spatial matching includes for each hectare cell the heat density, the number of DH connected dwellings and the total number of dwellings. This data set was post-processed in python, to group the cells by the heat density in different classes. For each heat density class, the number of cells in that class as well as the share of cells that have at least one DH connection is calculated (Figure 2.5).

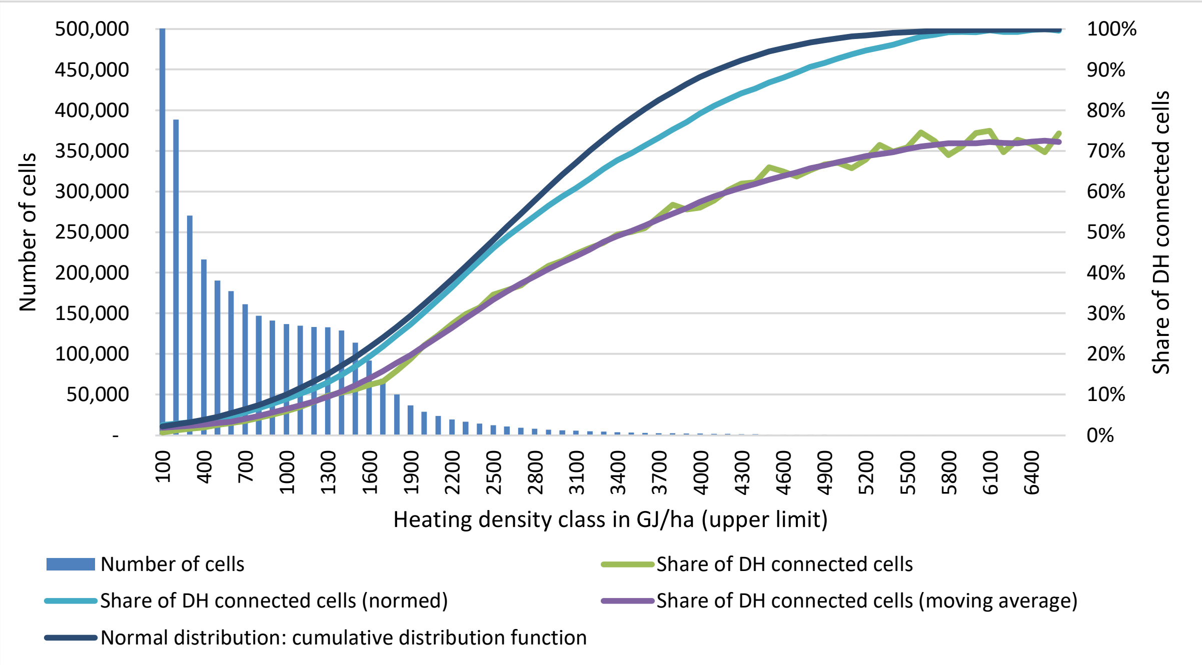

Figure 2.5: Number of cells per heat density class and share of these cells that are connected to DH in Germany in the census 2011 data set, together with a normal distribution fit

In Figure 2.5, it can be observed that with higher heat densities the share of cells that have a DH connection increases. Please note, that the number of cells in the heat density class 100 GJ/ha exceeds the axis limit and adds up to 1.2 million. The range of heat densities between 800 and 1700 GJ/ha includes the centre of villages and also most parts of a city, however without the most densely populated areas. Heat density values above 1700 GJ/ha thus represent mostly city centres. In areas with very high heat densities 70% of the cells have DH access, but there are not many areas with these high heat densities. However, a significant share of cells with low heat densities has DH connection, mainly those that are close to larger cities with an existent DH system. From this comparison, no clear threshold of an economic heat density can be derived. The share of DH connected cells was additionally standardised as 100% (representing the maximum), to enable the fitting to a normal distribution.

Plotting the slope of this function, a normally distributed shape of the share of DH connected cells can be fitted over the heat density (Figure 2.6). The expectation value is 2560 GJ/ha, signifying the value where the probability for a DH connection is 50% of the maximum value. This could be used as the threshold value for an economic value for DH installations. Even though the value of 2560 GJ/ha is in the lower range of possible heat density values, it represents already densely populated cities (compare Figure 2.4). Additionally, the distribution capital costs for the heat density of 2560 GJ/ha are in the range of 8.5 €/GJ, reflecting the accepted costs for DH infrastructure on average. Weighting this value with the amount of heat sold in each cell, the average distribution capital costs decrease to 6.14 €/GJ. The normal distribution shows different values when investigated separately for West and East Germany, which is due to the separation and different situation in the two states of Germany in the last century. This shows the impact of different developments in the heat infrastructure over the last century, when Germany was divided into two countries.

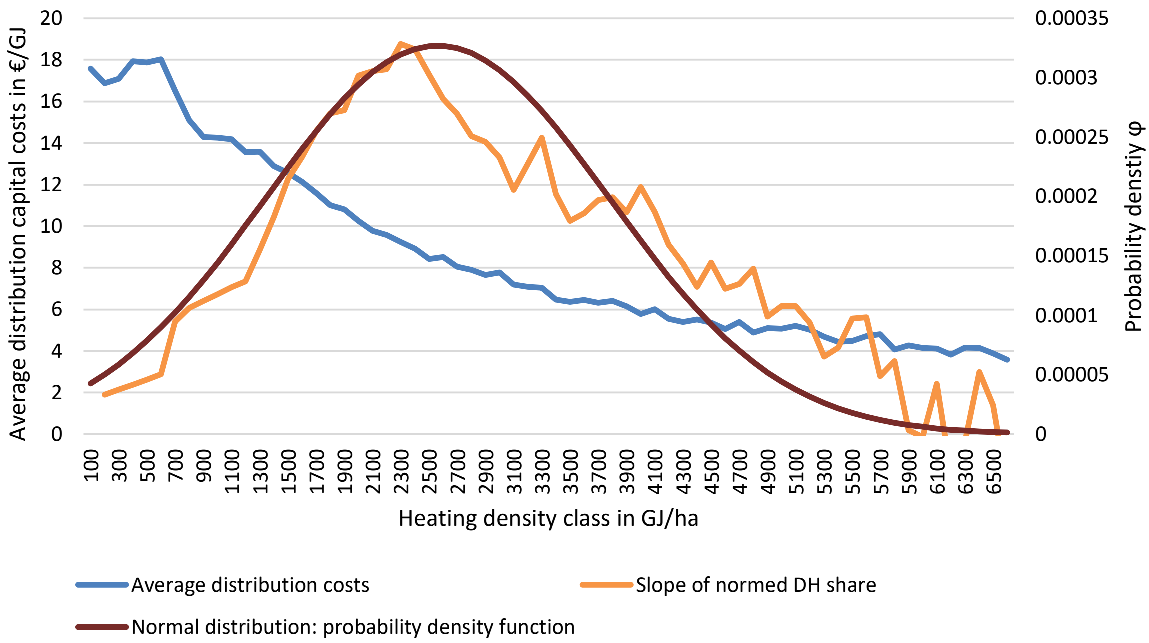

Figure 2.6: Average distribution capital costs for the census data, normal distribution density function and fit to slope of DH share

The statistical values to describe the fit of the normal distribution are listed in Table 2.1 for Germany, and separately for West and East Germany. The expectation value is significantly lower in the Eastern part, with a lower variance and a higher share of DH connected cells, indicates that more DH grids have been built in East Germany while accepting higher distribution costs.

Table 2.1: Parameters derived from the fit of the normal distribution of DH connected cells in census 2011 data set

Statistical value	Germany	West Germany	East Germany
Expectation value μ	2560 GJ/ha	2789 GJ/ha	1685 GJ/ha
Standard deviation σ	1220 GJ/ha	1230 GJ/ha	773 GJ/ha

2.3.3 Future DH potentials

As derived from the results in Section 2.3.2, today's average share of DH in areas with high heat densities is about 70%. The obvious strategy would be to install DH in all city centres. However, the question arises to what extent DH could be expanded and newly built, starting from the current level. The distribution capital costs for future densification of existing networks as well as new construction are calculated based on the future heat density (Figure 2.7). The connection rate and the renovation of buildings are varied. The marginal costs do not change when the existing infrastructure is included in the modelling, however, the average distribution capital costs decrease by about 1 €/GJ.

In general, the lowest distribution capital costs are present in cities and areas with very high heat density where no DH is currently existent, as well as in areas with currently low connection rates within areas with DH. The current average distribution capital costs of 6.14 €/GJ serve as a basis for identifying future DH economic areas. The DH market share in Germany in the year 2021 was 9.2% [114] and the average connection rate was 59% in 2011, which was derived from the census data set. In Figure 2.8, the average distribution capital costs in 2050 for different building thermal renovation ambition levels, connection rates (DH share within DH area) and the DH market share (share of heat supplied by DH) are shown.

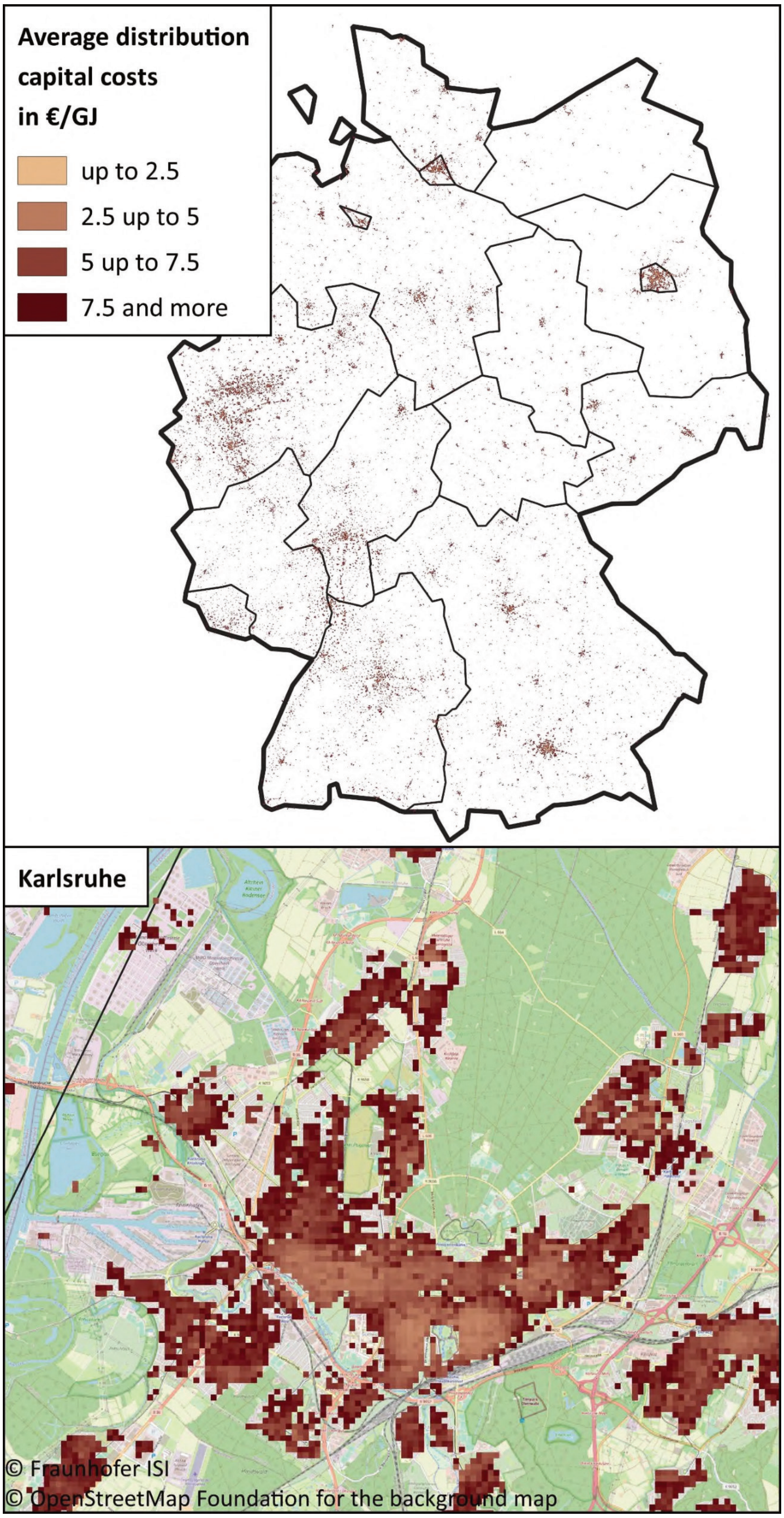

Figure 2.7: **Distribution capital costs in 2050 for DH areas with a connection rate of 75% and a DH market share of 40%, for the *high-refurb* scenario**

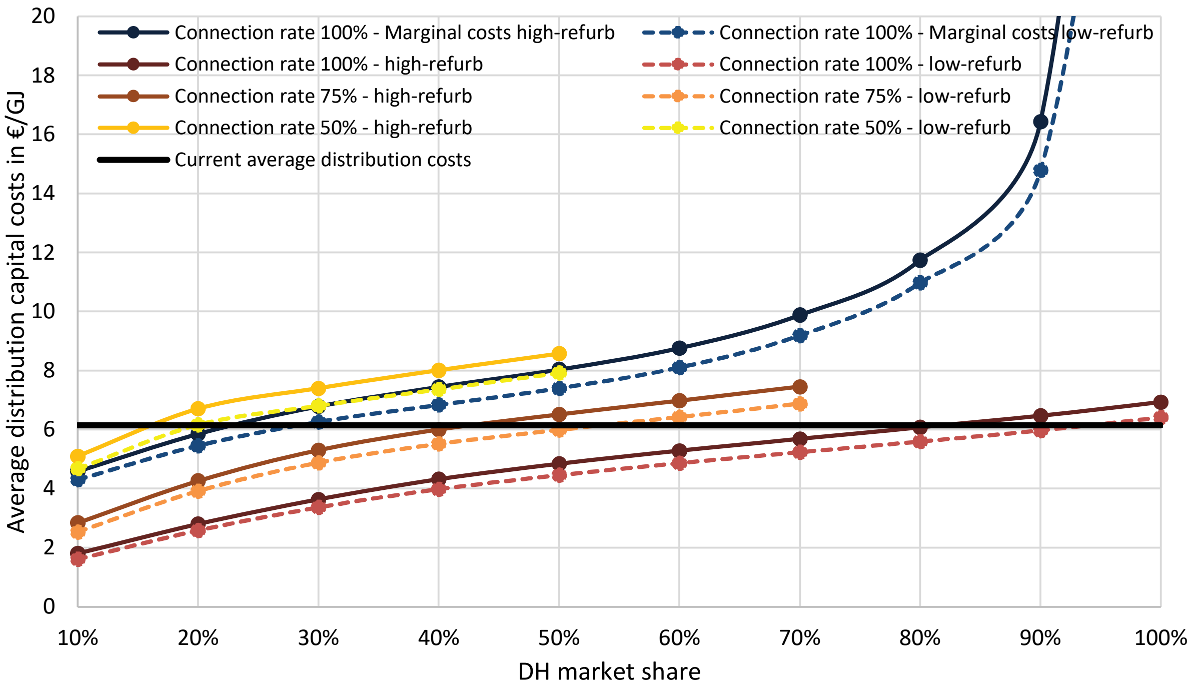

Figure 2.8: **Average distribution capital costs for the connection rates of 100%, 75% and 50% and marginal distribution capital costs for the connection rate of 100% in 2050**

With increasing market shares the average distribution costs increase, as more expensive cells are connected. In general, the distribution capital costs increase by 33-58% from 2020 to 2050, due to the lower heat density achieved by building renovation, depending on the renovation ambition and the DH market share. The connection rate has a significant impact on the resulting average costs, increasing the connection rate from 50% to 75% can lower the cost by up to 46%. Higher resulting market shares can be reached with accepting higher distribution capital costs that show a linear increase. Assuming the current average distribution capital costs as economic in the future, market shares can be derived from the intersection of the curves and lie between 17% and 43% for the *high-refurb* scenario, and between 22% and 52% for the *low-refurb* scenario in 2050, for connection rates between 50% and 75%, respectively. Compared to today's market share and connection rates, this means a possible increase in the DH share by the factor of 2 – 5.

2.3.4 Discussion

The results from the empirical analysis with German data highlight that the existence of DH areas correlates with high heat densities and low distribution costs. However, not all regions with high heat densities have been connected to DH, as not in all cities DH systems have been built in the past. The separate analysis of the correlation in West and East Germany shows that the accepted costs probably depend on the political and social situation. A significant share of regions with low heat densities is connected to

DH, suggesting that suburban regions could also be connected economically to DH. Furthermore, the broad range of the normal distribution shows that there are more parameters that influence the existence of DH systems.

The average accepted distribution capital costs of the status quo can be used as a threshold for cost-effective distribution costs, i.e., competitive to individual heating solutions. Assuming this threshold is valid also in the future, large DH potentials can be derived. However, building thermal renovation and thus lower heat densities decreases the economic advantage of DH. The densification of existing grids (i.e. increasing the connection rate by connecting more buildings within existing DH supply areas) is a main parameter and could significantly decrease the specific distribution capital costs and offset rising costs due to building renovation. In general, the cost threshold is quite close to possible future costs depending on the different parameters, so a wide range of DH market shares could be economical in the future.

The results of this paper are in line with the literature, finding that heat density is an important factor for DH installation and building renovation could lead to higher distribution capital costs [18,30,56,58,93]. Comparing the capital costs to Persson et al, 2021 [93], we observe a similar slope of the cost curves with expectably lower costs of up to 50%, as we do not consider the service pipe infrastructure in the costs. The dependency on the connection rate is comparable to Fallahnejad et al., 2024 [58], who derive possible DH market shares in 2050 of 43% and 29% for average connection rates of 100% and 75%, respectively, for a high-renovation scenario with a demand reduction of 60%. The range of 17% and 52% DH market share is slightly higher than the range of previous studies of Germany (13% to 37%) [85], due to the empirical threshold with a higher accepted cost value and the consideration of several parameters.

The empirical analysis of this paper could be conducted for other EU countries, if the Census data is made available on the hectare-level resolution for all member states. The Census 2021 is planned to be published for all EU member states on a raster with the grid size of 1 km² [115], which could serve as a first approach to an EU-wide empirical analysis.

2.3.4.1 Limitations

It is essential to acknowledge various limitations that have shaped the scope and implications of our study. First, estimating the costs associated with the reinforcement and densification of the DH infrastructure is prone to the uncertainty whether pipe diameters need to be changed. These adaptations are dependent on factors such as increasing connection rates, building renovation efforts and temperature reduction, and were not considered in detail.

Second, the analysis of distribution capital costs neglects components such as supply and transport costs e.g., from heat sources to the distribution grid, losses in the system, and maintenance expenditures. Also, the age structure of existing grids and reinvestment cycles are not available. In the future, the phase-out of fossil fuels will change the heat sources for both DH and individual heating as well as the introduction of 4th and 5th generation DH systems [110] introduce dynamic elements that could alter the configurations and cost dynamics of heating. This will possibly lead to smaller DH networks that were filtered in our data set. All of these factors will change the threshold of acceptable and economic distribution capital costs, thus limiting the results regarding the economic value and limit the accuracy of our conclusions.

Third, our analysis predominantly focused on heat density as a key factor for current DH deployment. However, future research should analyse additional influential factors, such as local stakeholders' involvement, the availability of heat sources, or the presence of an existing gas grid, as all of these factors could significantly impact DH deployment.

In general, the results on the hectare-level are based on statistical approaches and use several assumptions to fill data gaps, most importantly regarding the renovation status. Thus, they do not necessarily reflect the situation on this high level of spatial allocation and cannot replace regional analyses, e.g. local heat planning.

2.3.4.2 Further research

The transferability of the empirical correlation to other countries should be analysed, e.g. with the Census 2021 data once they have been published. The balance between renovation efforts and heating decarbonization has so far been studied mostly in case studies and needs to be analysed on the country-level. Mandel et al., 2023 [52,116] have conducted a thorough economic analysis for a city district, revealing intriguingly close cost economics for renovation, decentralised heating and district heating, showing the necessity of a detailed analysis and including generation costs as well as considering the multiple benefits of energy efficiency. For that, heat generation, transportation and operation and maintenance costs should be included to gain a more comprehensive understanding of the economic competition of DH. Additionally, the cost competition with decentralised heat pumps in buildings as well as 4th and 5th generation DH after the phase-out of decentralised fossil fuels should be analysed. Understanding these changes is crucial for analysing the future economic viability and potential of DH in the evolving energy landscape.

2.4 Conclusion

This paper assesses the current status of DH in Germany on the local level, derives empirical correlations and identifies future DH demand potentials from these results. By combining insights from various data sources, we conducted a comprehensive empirical analysis of accepted distribution costs of DH in Germany at a hectare-level resolution. We coupled a building stock model with a spatial analysis, taking into account the empirical results and various parameters (different connection rates and building thermal renovation ambition) for a scenario-based assessment of future DH potentials.

Our findings show that while current district heating systems in Germany are primarily concentrated in areas with high heat densities and consequently low distribution capital costs, this parameter alone does not capture all factors influencing DH viability. Only 70% of regions with a suitable high heat density currently have DH. This indicates that other factors also play an important role. These could include the historic implementation of a natural gas grid hindering DH deployment, or the availability of heat resources like coal power plants and the role of active local stakeholders supporting the implementation of DH.

The existence of DH systems is normally distributed over the distribution capital costs, having accepted costs on average of 6.14 €/GJ. This is lower than the assumed range of marginal costs in other studies of 10 to 20 €/GJ, but plausible as marginal costs are about twice the average costs [85]. The empirical threshold value could also be used for other countries, as the existing literature assumes comparable threshold values for EU countries. Using the correlation and the empirical threshold for future scenarios, we can show that DH market shares ranging from 17% to 52% are possible in Germany in the future, compared to 9.2% today. The large range reflects the uncertainty regarding the share of buildings that will be connected within a DH area and the ambition of building renovation efforts. The range of a possible DH market share confirms the existing literature with high market shares of up to 40%. The share of buildings that are connected within a DH area is the most important parameter to decrease distribution costs and thus increase the possible DH market share in the future. Reaching 100% DH connection rates in all DH areas in Germany is not realistic and should be considered as an upper theoretical limit. However, in some areas in Germany currently 90% of buildings are connected in certain areas, showing that high connection rates are indeed realistic and could be reached by local heat supply policies. With lower renovation activity, DH has a greater market potential. An integrated local energy planning should focus on renovating buildings that are not feasible for DH and consider the multiple benefits of energy efficiency. With higher renovation activity, the DH potentials are 17-23% lower compared to lower renovation.

As both decentral heat pumps and large-scale heat pumps in DH rely on renewable electricity for heat generation, the effects on the power system need to be considered as well. DH could offer more system integration potentials as large heat storages are in the system that could be loaded in times of low electricity prices. An integrated perceptive is therefore needed in energy planning, e.g. as proposed by the energy efficiency first principle [59] and the smart energy concept [117].

The current revised German heat legislation (Building Energy Act - German: „Gebäudeenergiegesetz", and the Heat Planning Act - German: „Wärmeplanungsgesetz") as well as the EU legislation (Art. 25 and 26 of the revised EED (Energy Efficiency Directive)

(EU) 2023/1791, revised in September 2023) are aiming to reach a climate-neutral heat supply in 2045 and 2050, respectively. In particular, the Heat Planning Act as well as Article 25, EED introduce mandatory communal heat planning. Municipalities need to take action to implement or densify DH grids in areas with high heat densities and increase the connection rate by involving stakeholders and the public. Our study shows that local action and policy support for high connections rates are decisive for low costs, leading to a high cost-effective DH share.

DH can be a competitive source of heating in densely populated areas, possibly replacing the gas grid or individual heating systems. Our study underscores the vast potential of district heating as the DH share could be increased by the factor of 2 to 5 compared to today. Energy system studies with a high modelling resolution can support finding a cost-optimal DH share and can integrate the empirical threshold found by the census analysis. A future comprehensive evaluation of cost competition, as required in the EED and suggested by Hummel et al, 2023 [53] on the EU-level and Mandel et al., 2023 [116] on the district level is needed. The emergence of individual heat pumps and technical progress in 4th and 5th generation DH systems pose intriguing challenges as well as opportunities for the future. Ongoing research will be vital in understanding and navigating the heating transition, particularly in terms of competition and integration of these evolving technologies within the context of DH in Germany and the EU.

Acknowledgments

The authors express their sincere gratitude to Lukas Greif for his valuable contribution to this research, especially in developing the structure of the regional model DISCO and the data preparation in his Master's thesis "Modelling of district heating potentials in Germany".

A.1 Detailed description of input data sets

TableAnnex 1: Overview of input data sets used for empirical analysis

Data set	Census-Data	Hotmaps - Floor area	Hotmaps - Population density	KfW subsidy report
Type	Number of dwellings per heating installation	Floor area and share per age category (gfa_non-res_curr_density, gfa_res_curr_density, ghs_built_1975_100_share, ghs_built_1990_100_share, ghs_built_2000_100_share, ghs_built_2014_100_share)	Population density (pop_tot_curr_density)	Money paid as subsidies for renovation and energy-efficient buildings
Indicators used	Heating type: District heating and total	Floor area before 1975, 1975-1990, 1991-2000, 2011-2014	Population density	Subsidies for renovation measure of buildings
Spatial resolution	100x100m	100x100m	100x100m	NUTS 3
Definition	Permanent construction with at least one dwelling and one access, which are occupied	Heated gross floor area	Population	Funding in € Mio for: energy efficient building, restructuring, individual measures, supplements, subsidies
Number of data	2,737,253 hectare cells	4,436,097 hectare cells	4,436,097 hectare cells	5 different categories for 401 regions
Publication	2017	2019	2019	2016-2021
Year of data	Written survey of homeowners: 2010 - 2011	Statistical approach: 2012	Statistical approach: 2012	2015-2020
Data protection	Raster cells with one data point are classified as 0, with two data points as 3.	-	-	-

3 Decarbonizing district heating in EU-27 + UK: How much excess heat is available from industrial sites?

Pia Manz, Katerina Kermeli, Urban Persson, Marius Neuwirth, Tobias Fleiter, Wina Crijns-Graus: Decarbonizing District Heating in EU-27 + UK: How Much Excess Heat Is Available from Industrial Sites? In: Sustainability 13, 1439, 2021. DOI: 10.3390/su13031439.

3.1 Introduction

Energy-intensive industrial sites (e.g., steel, cement, paper, glass, chemicals and refineries) are spread across the member states in the European Union and UK. The production of basic materials has enormous energy needs driven by economies of scale, and mainly operate at temperatures above 1000 °C. Due to high capital cost, most of these processes are run in 3-shifts operation and only pause for maintenance needs. Thus, they often have uniform energy demands even throughout the year. Together, the energy-intensive industrial subsectors account for about 20% of the final energy consumption in EU-28[2] [118]. The largest share of the energy input is used as process heat for industrial processes like furnaces and steam generation, with 47% of process heat for high-temperature needs above 500 °C [119]. High energy costs of 3–20% of production costs [120,121] led to substantial improvements in energy efficiency in these industries in the past century. However, many industrial sites still release substantial unused energy into the environment. This excess heat from industry, sometimes also referred to as waste heat, should be further decreased as far as possible by energy efficiency measures in the individual industrial sites. Due to technical restrictions, this is only possible to a certain level. The possible use of excess heat at the same industrial site to cover the heat demand at lower temperatures is often limited [122]. Even though industrial processes need to undergo changes towards carbon-neutral fuels and process design, the high-temperature heat demands of the chemical reactions will persist. Excess heat potentials will potentially decrease due to efficiency progress in terms of energy and material use.

[2] Please note, that since February 2020 there are 27 member states of The European Union, however, the geographical extent of the study is the former EU-28, which includes the United Kingdom.

Excess heat from industrial sites can also be fed into a district heating (DH) system to serve as a heat source for buildings reducing the primary energy needs. DH as a way to connect unused heat from industry to buildings heat demand gained importance in the last few years like in the project Heat Roadmap Europe [18,83], or in 2016 by the EU Heating and Cooling Strategy of the Commission [123]. It is a measure towards decarbonizing the heating supply in the future, alongside with renewable-based centralised and individual heat generation where DH is not available. It is and will remain a challenge to decarbonize the mainly decentralised heating until 2050 due to the comparably low prices of fossil fuels, even with national CO_2 taxes implemented, and due to various barriers to retrofitting and switching to renewables for individual building owners.

Heating demand for residential and service buildings including sanitary hot water in the EU-28 accounts for 12,344 PJ (3429 TWh) in 2018, with 64% directly based on fossil fuels [124]. Similarly, the sources for the current energy supply of district heating systems are mainly heat from cogeneration in fossil power plants, direct use of fossil fuels and municipal waste, and a small share of renewables (~5%) [125]. District heating supplied 1315 PJ (11%) in the EU-28 in 2018 to the heating of residential and service buildings, adding up to a total of 1980 PJ with industry's heat consumption [118]. It is estimated that only about 25 PJ of industrial excess heat is recovered in European district heating systems [126]. That corresponds to a share of 2% industrial excess heat in DH for buildings.

An important pillar in the future for decarbonized heating supply is the extension of heating grids for DH and transforming them into low-temperature heating networks with typical temperatures of 30 – 70 °C. Low-temperature grids are described with the term 4th generation DH [21,127,128]. The low temperatures allow the inclusion of renewable sources, together with central and decentral heat pumps that increase the temperature to end-user needs. Excess heat can help transform district heating systems by providing CO_2-neutral heat in large quantities in the medium term and often at comparably low costs [17]. Although in Scandinavian countries DH was ramped up in the last decades with a market share of over 50% in Sweden and Denmark for the heating supply of buildings [118,124,129] its future potential in the EU-28 is largely uncertain. Some energy system studies do not consider industrial excess heat at all [130,131], while others see an enormous potential [18,132]. A quantification of the potentials requires an analysis of the heating demand and available future heat sources like excess heat together with existing and possible future DH infrastructure with a high spatial resolution.

The estimation of industrial excess heat potentials and its utilisation in district heating systems for an extended geographical context covering one or more countries is an emerging research area and the previously proposed methodologies in studies are limited. Only some approaches identify the geolocation of available excess heat. The study by Miró et al. [133] in 2015 reviewed published excess heat estimations and considered ~15% as unreliable, as temperature and system boundaries were missing. A comprehensive overview of the possible classification of methodologies was given by Brückner [77] in 2014: the scale of the study, the method of acquisition of the data (survey or estimation), and the approach (top-down or bottom-up). All of the methodologies presented here are estimations of excess heat from exhaust gases, and most of them are bottom-up, based on the calculation of the fuel input per subsector, process, or sites. One difference is the basis on which the fuel input and excess heat is calculated: emissions, national statistics per sector, or exergy analyses for each process. An overview of the presented approaches is given in Table 3.1. Sophisticated site-specific approaches were introduced by the study of BCS [134] for the U.S. Department of Energy in 2008 and by McKenna and Norman [81] in 2010. The latter approach was further developed by Hammond and Norman [135] in 2014. The methodologies are similar in that they estimate excess heat potentials by comparing the input energy of a process to the energy that is released at the exhaust and estimating the maximum amount of recoverable heat from this exhaust gas. The composition of the exhaust gas is derived from the input fuels and the total enthalpy of the exhaust gas based on this composition is calculated. The fuel input is estimated by production volumes per process. McKenna and Norman [81] used additionally the CO_2 emissions from the European Union Transaction Log (EUTL) for the Emissions Trading System (EU ETS) data [136] and literature values to allocate the energy demand for non-energy intensive industries. A site-specific approach based on fuel input was also used in a study for the project Hotmaps [132] by Manz et al. [137], based on georeferenced annual production from various data sources multiplied by specific energy consumption values (SECs) and taking into account process-specific excess heat recovery potentials from literature. The resulting industrial excess heat was mapped with buildings' demand by Aydemir et al. [138] by network analysis to find 170 PJ from 338 PJ excess heat could be delivered at low costs. Another process-based method presented by studies from Bühler et al. [78,139,140] used emission data per process together with energy and exergy analysis. They determine the annual excess heat potential for 80% of industrial energy demand in Denmark based on several available data sources. The energy analysis was based on the fuel, heat, and electricity demand of industrial processes. The study considered conservative estimates from literature for the fraction of input energy which is released at the exhaust and assume that 50% of this energy is recoverable. The input energy was then calculated at site level from the amount of CO_2-emissions using EUTL data [136]. Brückner et al. [141] used emission reports to the federal states of Germany, that list volume flow rate and temperatures of the exhaust gases allowing a direct estimation of the excess heat which is contained in the exhaust gas streams. In Persson et al. [83] the excess heat estimation was based on subsector-specific values and greenhouse gas (GHG) emission from the European Pollutant Release and Transfer Register (E-PRTR) [142]. Svensson et al. [84] proposed to differentiate unavoidable and avoidable excess heat and calculate an excess heat temperature signature, which relies on site-specific data about the process, age, and technologies. The approaches based on processes and subsector-specific fuel demand are very data-intensive, but enable a very detailed assessment of site-specific characteristics, fuel demand, and efficiencies together with high-resolution spatial analyses for the integration of industrial excess heat into district heating systems.

Table 3.1: Comparison of excess heat estimations in literature

Study	Method	Comments	Temperature Level Considered	Fuel/Heat Demand by Considered Industry in PJ/a	Excess Heat Potential in PJ/a
Brückner et al., 2017 [143]	Emission-based estimates, Germany	Conservative estimates for 80% of companies in Germany	35 °C as a lower boundary value	977	127
Pehnt et al., 2010 [144]	Subsector-based excess heat fraction, Germany	Literature values excess heat per final energy consumption based on [145,146]	140 °C as lower boundary value	2653	316
McKenna & Norman, 2010 [81]; Hammond & Norman, 2014 [135]	Emission based approach by process, UK	Process-specific heat recovery values per process	5 temperature ranges	503	52
Papapetrou et al., 2018 [82]	Subsector based excess heat fractions, EU-28	Literature values from [135]	<200 °C – >1000 °C	6556	1094
I-TheRM, 2016 [80], Panayiotou et al., 2017 [147]	Process-based estimates per subsector, EU-28	Fraction per subsector taken from [79] based on energy consumption statistics	3 temperature ranges <100 °C – >300 °C	10,880	1334
Bianchi et al., 2019 [76]	Theoretical potential by subsector, EU-28	Based on energy consumption statistics	Not considered	3196	279
Manz et al., 2018 [137] and Aydemir et al., 2020 [138]	Specific SECs by process, EU-28	Conservative estimates for energy-intensive industries	3 temperature ranges	4241	338
Miró et al., 2018 [148]	Non-metallic mineral, based on emissions EU-28	Literature values per subsector, based on [81]	Not considered	-	134
Bühler et al., 2017 [78]	Exergy analysis by process, Denmark	22 industrial processes included	40 °C as lower boundary value	64	12.3
Persson et al., 2014 [83]	Emission-based estimates by subsectors, EU-28	Application of estimated emission factors and recovery efficiency.	No	10,880	2924

Excess heat potentials can be quantified as either a theoretical, a technical (accounting for technical constraints) or an economical potential (including cost analysis). Additionally, there is also a realistic potential taking into account the barriers for utilisation of excess heat. The definition of the term excess heat includes latent and sensible heat that is released by a system. The heat is transmitted either by a medium like a flue gas, a solid stream (e.g., hot coke, rolled steel, hot clinker), a liquid stream (e.g., wastewater in paper production), cooling water, or by radiation heat losses (e.g., furnace openings), or conduction heat losses (e.g., heat lost from equipment surfaces) [143,144]. A particularly large source of excess heat are the flue gases resulting from the combustion of fuels in furnaces and boilers. Flue gases, also commonly called exhaust or stack gases, are the combustion gases that emanate from industrial furnaces, ovens, boilers, and steam generators that are conveyed into the atmosphere. They contain the reaction products of the combusted fuel and air and residual substances such as sulphur oxides and particulate matter [149]. In this study, excess heat sources from energy-intensive industrial locations released via flue gases are quantified and the inclusion in district heating systems is estimated. Further excess heat potentials beyond the heat losses from flue gases are not included.

We propose a comprehensive assessment of georeferenced excess heat potentials available in the EU-28, analysing the total potential of excess heat from the energy-intensive industries and assessing the suitability for its use in district heating grids. The quantification is based on current process design, taking into account efficiency progress. However, process change is not considered, e.g., higher share of secondary steel, switch to electrified furnaces and chemical processes based on hydrogen instead of naphtha as feedstock. The quantification is based on the assessment of current yearly energy demands by industry and buildings, therefore neglecting possible mismatch of heat loads. Furthermore, the current heat demand of buildings is used as an indicator of possible future district heating areas. The mapping of district heating areas is based on distance analysis, not on economic parameters. The main contribution of this paper is the introduction of a process-specific approach to estimating excess heat and the mapping of the results with district heating areas. The following research questions are addressed and answered:

- Where are potential sources for industrial excess heat located in the EU?
- How much excess heat from energy-intensive industrial processes is technically available for external use?
- How much excess heat is available for actual and possible DH systems considering efficiency measures in the industrial sector and district heating?

These research questions are answered with an elaborated methodology and based on extensive data sets, including georeferenced industrial sites and DH areas. The excess heat estimations are conducted at a process level. The energy demand of the processes included in this study sums up to 6891 PJ (1914 TWh) in the base year. Obtaining information about the industrial sites at the process level necessitates the collection and consolidation of several industrial data sets. Furthermore, specific energy consumption (SEC) and excess heat factors were calculated for relevant processes. The spatial mapping is conducted in a geographic information system (GIS) combining the data sets from different sources in high resolution. It enables a precise calculation of distances and the identification of the potential contribution of industrial excess heat to district heating areas. The heat sources are matched with heat demand density data and today's DH areas. Furthermore, we analyse the excess heat potentials together with possible DH areas based on a GIS analysis of heat demand densities for all EU-28 countries.

The results presented in this paper are available as an open data set in spreadsheet and shapefiles format from the sEEnergies Open Data Hub [150], are visualised in an online Web-App [151] and are documented in the corresponding report within the EU project sEEnergies [152]. In the sEEnergies project, the presented excess heat potentials with different efficiency measures are integrated in a system analysis and spatial mapping.

3.2 Data and methods

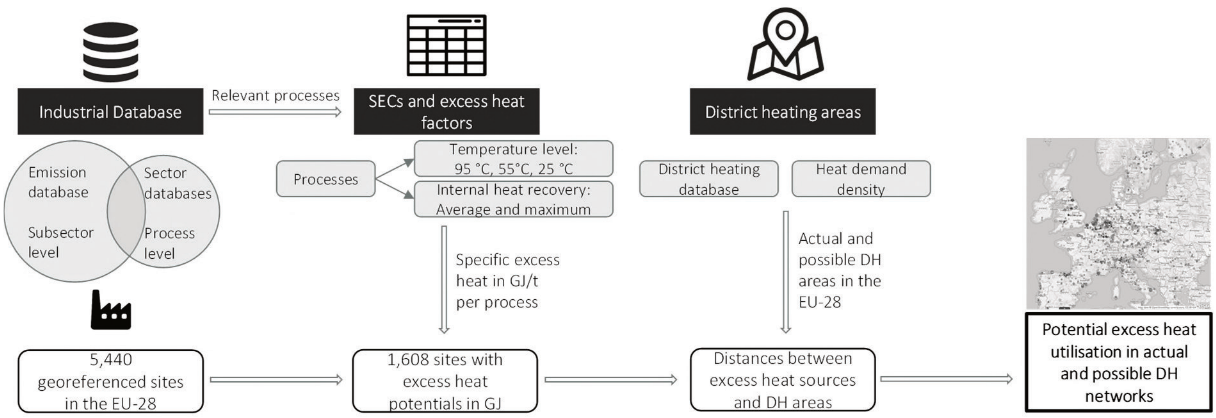

Figure 3.1: **Schematic calculation steps in this analysis**

In the following subsections, the successive steps for considering the georeferenced location of heat sources (industrial sites) and heat sinks (existing and potential future district heating areas) are presented, each with the respective data and method. The analysis consists of three major steps, which are depicted in Figure 3.1:

1. Allocating industrial processes in the EU-28: We first map geographical locations of energy-intensive industrial sites with relevant processes and annual production in Section 3.2.1.
2. Estimation of process-specific excess heat potentials: We estimate specific energy consumption and excess heat on process level regardless of the geographical context in Section 3.2.2. The estimation depends on exhaust gas temperatures.

3. Mapping industrial excess heat to district heating areas: The excess heat potentials are matched with actual and possible DH systems by applying spatial GIS analyses in Section 3.2.3. We calculate six different potentials representing the amount of excess heat that can be supplied to district heating areas depending on the assumptions.

The availability of excess heat for DH depends on how much excess heat from the flue gases can be used internally on the same site, e.g., for preheating materials, and the temperature needs of actual and possible district heating areas. We thereby assess variations in three parameters for this analysis.

The first distinction is based on the level of internal heat recovery:

- Current situation: many industrial processes already utilise excess heat recovery systems. The calculated excess heat potentials represent the excess heat potential available for external use for current average internal use of excess heat. This is estimated individually for each process considered.
- Full internal use of excess heat: we assume a 100% diffusion of main internal excess heat recovery systems (e.g., for preheating materials), thereby reducing the remaining available excess heat for external use. This potential is more future-oriented and assumes that internal excess heat use is always preferable over external heat use.

The second distinction is based on the maximum heat recoverable from exhaust gases when they are cooled down to the following reference temperatures:

- 95 °C: to estimate the maximum excess heat attainable if an exhaust gas is cooled to 95 °C. This can potentially be used directly in typical 3rd generation DH grids, which corresponds to many of the common district heating systems in operation in the EU-28.
- 55 °C: to estimate the maximum excess heat attainable if an exhaust gas is cooled to 55 °C. This is a typical temperature for 4th generation DH grids, which will possibly be operating in the future.
- 25 °C: to estimate the maximum excess heat attainable if an exhaust gas is cooled to ambient temperatures. This can potentially be used as a heat source for large-scale heat pumps feeding into 4th generation DH grids. This value is to be considered as a maximum potential for future heating systems, even though it is quite unlikely that all of the systems can utilise these temperatures.

The last distinction is regarding the DH diffusion, i.e., grid expansion:

- Actual level (DH-A): this represents the DH areas which are currently in operation in the EU-28.

- Possible level (DH-P): this represents the potential extension of DH grids based on today's heating demand density of buildings. These areas can currently have district heating systems already (DH-A). Areas with a current heating demand greater than 500 GJ/ha are assumed to be cost-effective or likely suitable for DH distribution. In this study, the sum of heat demands in all DH-P areas aggregates to a share of ~65% of the total heating demand by the residential and service sector in EU-28. Thus, it represents a very ambitious estimate for the possible DH areas. The reduction of useful energy demand of buildings due to renovation is not considered in the assumptions for the extension of DH systems (DH-P)[3].

In total, we use six different potentials to account for efficiency measures that could be implemented in industrial processes and DH systems. Table 3.2 summarizes the excess heat potential combinations based on the distinctions on the level of internal heat recovery and the DH system diffusion. The status quo is represented by the label Current potential. This potential includes the excess heat for the current average level of internal heat recovery in industrial sites with the exhaust gas cooled down to 95 °C and matched with current district heating areas in EU-28. The term Industrial efficiency describes potential with internal heat recovery measures that are applied to the full extent possible. However, process change to low-carbon processes or increased material efficiency are not considered. DH efficiency considers the transformation of DH to 4th generation systems, without internal efficiency improvements in industry. The maximum excess heat when exhaust gases are cooled down to 55 °C or 25 °C with spatial matching to possible DH areas is analysed. System efficiency takes into account efficiency measures in industrial processes as full internal heat recovery in industry, and transformation to 4th generation district heating systems and is matched with a possible level of DH diffusion.

Table 3.2: Definition of excess heat potentials and labels used throughout the paper

Name of Excess Heat Potential	Level of Internal Heat Recovery		Exhaust Gases Cooled Down to			DH Diffusion	
Distinction	Average	Maximum diffusion	95 °C	55 °C	25 °C	Actual level (DH-A)	Possible level (DH-P)
Current potential	x		x			x	
Industrial efficiency		x	x			x	
DH efficiency (55 °C)	x			x			x
System efficiency (55 °C)		x		x			x
DH efficiency (25 °C)	x				x		x
System efficiency (25 °C)		x			x		x

[3] Please note, that in a previous publication [152] this potential was denominated as "expected" level.

3.2.1 Allocating industrial processes in the EU-28

The objective is to construct a comprehensive database of industrial installations with the geographical area of the EU-28 including information about the annual production per process. The industrial sites are georeferenced by coordinates. A key characteristic of the Industrial Database is the inclusion of detailed information concerning the production processes and annual production of each industrial site. Thus, each data entry of an industrial production site contains the name of the company and site, the geographical location, the industrial sector, annual emission values as well as process-specific data of each associated installation such as manufactured goods and corresponding production process, annual production or production capacity. The Industrial Database covers the basic material industry producing iron and steel, non-ferrous metals (aluminium), non-metallic materials (cement, glass), chemicals (ethylene, chlorine, and ammonia), pulp and paper, and, from the energy and transformation sector, refineries. The industrial subsectors account for about 62% of the total industrial energy demand [118], therefore the database covers the main and largest industrial energy consumers in the EU-28 together with refineries, having high excess heat regarding the temperature and quantity of heat.

For the estimation of georeferenced excess heat potentials from industrial processes the following data are required:

- coordinates or at least the address of the site,
- industrial subsector together with production processes, or in some cases sufficient information on the manufactured goods,
- annual production data or at least production capacity.

As no publicly available database of industrial sites includes all the information needed for process-specific allocation of production data, a new data set based on a combination of several different data sets is created. The Industrial Database is established as a SQL database, which lists the sites as the main table. One important feature of this database is the separate tables of sites and installations. The installations relate to production process and respective annual production.

Table 3.3: Overview of used sectoral data sets and information included

Name of Sectoral Database	Production/Capacity	Location	Processes Included
VDEh Steel Plantfacts	Annual capacity	City	Type of process, age of installations
Global Cement Directory	Annual capacity	City	Clinker: wet/dry and number of kilns
glassglobal Plants	Annual and daily production	Address	Flat, container and tableware glass types together with the type of furnaces

Name of Sectoral Database	Production/Capacity	Location	Processes Included
RISI Pulp and Paper: Fastmarkets RISI	Annual production	Coordinates	Detailed list of paper grades and produced products
Eurochlor Chlorine Industry Review	Annual capacity	City	Chlorine production by membrane, diaphragm, mercury and other processes
Internet research for individual companies in the EU of the sectors ethylene, ammonia, aluminium and petrochemicals	Depending on source; annual capacity/annual production	Depending on source; mostly address	Production processes and type of refinery

Generally, there are two types of industrial data sets: emission reporting covering the whole industrial sector and asset data sets covering single industrial subsectors. The input emission data sets are the European Pollutant Release and Transfer Register (E-PRTR) [142] and the European Union Emissions Trading System (EU ETS) from the EU Transaction Log (EUTL) [136]. The E-PRTR database contains pollutants including GHG emissions for industrial sites and other sources that emit pollutants to air, water, and land above an indicated threshold value in the EU. Most important for our analysis, it contains the coordinates of the listed sites. The industrial activities are classified by four-digit NACE codes[4]. Its objective is to establish uniform and publicly accessible national pollutant release and transfer registers in all Member States of the European Union. The EU ETS is one of the main measures introduced by the EU to achieve cost-efficient reductions of greenhouse gas emissions and reach its targets under the Kyoto Protocol and other commitments. It covers about 45% of the total emissions of CO_2 equivalents in the EU by including major emission sources like power plants, aviation, and most industrial sectors. The data set indicates only addresses of the company headquarters and defines the industrial subsectors by 40 different activities that represent the produced products. Both emission data sets were combined by matching on-site level. If one entry is listed in both data sets, the information is consolidated in one entry. The remaining entries from each data set that are not listed in the respective other data set are appended. The emission data of the EUTL is used if a site is listed in both data sets. Only 20% of the entries of industrial activities in EUTL can be matched with E-PRTR entries, as the threshold values for emissions to be recorded in the emission database differ. However, the matched CO_2 equivalent emission values represent over 70% of all industrial EUTL emissions, because entries with high emissions are likely to be represented in both databases. In EUTL, all CO_2 equivalent emissions for each industrial installation of the covered industrial sector are counted (opt-out exceptions

[4] NACE (Nomenclature statistique des activités économiques dans la Communauté Européenne): Statistical classification system in the EU

for small installations need to be applied for); in E-PRTR threshold values for each pollutant (e.g., 100 kt CO_2 per year) as well as for production for some NACE activities exist. That justifies the high number of unmatched EUTL entries.

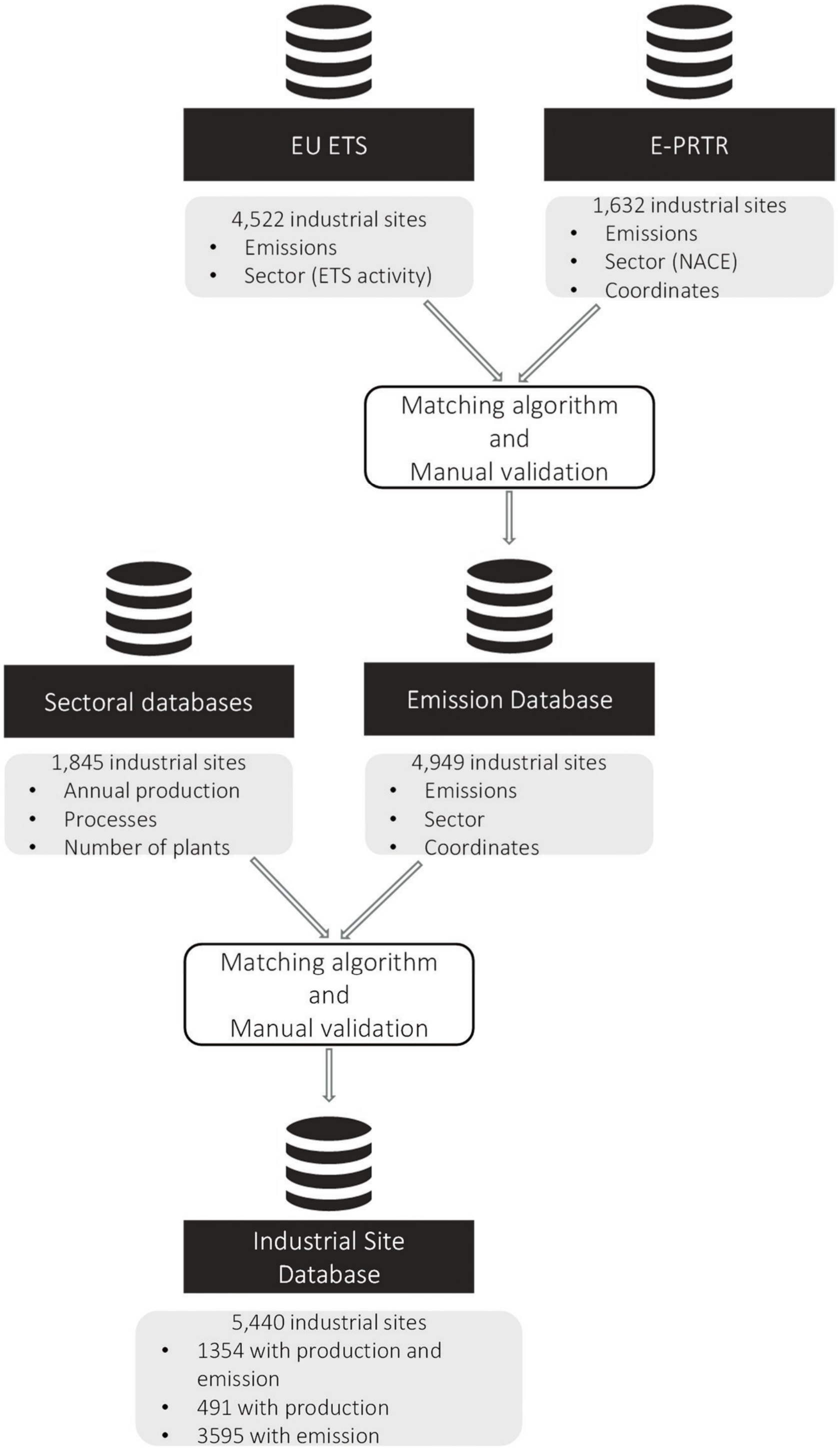

Figure 3.2: Establishing the Industrial Database for the member states of the EU-28

Often the information in the industrial database is sourced from three different input data sets: the EUTL, E-PRTR, and the respective sectoral data set. This leads to difficulties but can also help to fill data gaps. The definition of processes and products differ:

EUTL uses one of thirty defined ETS activities mainly focusing on products, while E-PRTR includes the 4-digit NACE code, which is in some cases not congruent or overlapping with the ETS activities and vice versa. Both input data sets in general contain no information about the production processes of the indicated product. The different product and process definitions can lead to the situation, that e.g., the emissions of one steel site are not totally consistent with the production capacity for steel making, sintering and coking installation, or vice versa. Another issue was addresses and coordinates in the input data sets often being wrong or slightly off from the actual location. Manual crosschecking of matched sites together with internet research is necessary. Entries from input sites that had no match with the E-PRTR do not include the coordinates. When the complete address was known, an automated look-up tool could often gain the coordinates, but otherwise checking with the company's website was unavoidable. Furthermore, another issue is that company names change due to mergers and acquisitions, which are not updated in all data sets.

3.2.2 Estimation of process-specific excess heat potentials

The methodology for quantifying the specific energy demand and the derived excess heat potentials for the processes found in the industrial database is presented in this section. To calculate the unrecovered heat from flue gases in the different industries, we adopt the bottom-up approach based on exergy applied by BCS [134]. The energy lost to exhaust gases E_{ex} is a function of the exhaust gas mass m_{ex} and its enthalpy h. The enthalpy is dependent on the exhaust gas chemical composition and temperature T of the gases:

$$E_{ex} = m_{ex} \bullet h = m_{ex} \bullet \sum (x_i h_i), \tag{4}$$

where x_i is the mass fraction of each component in the exhaust and h_i its enthalpy. By assuming that all gases (except H_2O) are ideal gases, the enthalpy of each gas component can be calculated based on the specific heat capacity of each component ($C_{p,i}$) and temperature T:

$$h_i = \int_{T_r}^{T_{ex}} C_{p,i} \, dT, \tag{5}$$

where T_r is the reference temperature and T_{ex} is the temperature of the exhaust gas (for a list of the assumed exhaust temperatures please refer to A.2).

The enthalpy is not an absolute term and needs to be calculated against a reference state (e.g., room temperature). In this analysis, we calculate the enthalpy of exhaust gas streams at three reference temperatures of 95 °C, 55 °C, and 25 °C, to capture the heat requirements in current and future district heating systems.

In current industrial practices, exhaust gases are typically not cooled below 149 °C in order to avoid condensation of waste streams [134]. In addition, other temperature restrictions, particular to a specific exhaust stream, might apply. For example, in the case of the highly corrosive exhaust gases of glass furnaces, the gases can be cooled to a minimum temperature of 265 °C as at lower temperatures they condensate. In this analysis, we note such restrictions for every stream but do not take them into account for the calculation of excess heat.

The fraction of the excess heat lost in the exhaust (E_{ex}) and the energy input (E_{in}) is equal to:

$$\frac{E_{ex}}{E_{in}} = \frac{m_{ex} \bullet \sum(x_i h_i)}{m_{fuel} \bullet h_c}, \tag{6}$$

where m_{fuel} is the fuel mass and h_c is the heating value of the fuel used. In this analysis, we use the lower heating value (LHV). The mass fraction of each component in the exhaust xi, and the m_{ex}/m_{fuel} ratio are determined from combustion equations assuming full combustion and an air to fuel ratio of 10:1. For a higher air to fuel ratio, the exhaust mass flow rate to the fuel mass flow rate m_{ex}/m_{fuel} increases, thereby increasing the estimated excess heat losses.

With the ratio of E_{ex}/E_{in} the excess heat per tonne of a specific industrial product $m_{Product}$ can be calculated:

$$\frac{E_{ex}}{m_{Product}} = \frac{E_{in}}{m_{Product}} \bullet \frac{E_{ex}}{E_{in}} = \frac{E_{in}}{m_{Product}} \bullet \frac{m_{ex} \bullet \sum(x_i h_i)}{m_{fuel} \bullet h_c}. \tag{7}$$

The enthalpy of each of the exhaust gas components is calculated from the specific heat capacities (see Equation (4)). Because water vapour does not follow ideal gas behaviour at low pressures, the enthalpy change was taken from steam tables for the corresponding partial pressure (by assuming atmospheric pressure, the partial pressure of water vapour is equal to the molar fraction of water in the exhaust gas mixture).

Excess heat potentials can be calculated for entries in the industrial database that include information about production processes and annual production. The production capacity is multiplied with typical sectoral utilisation rates, obtaining the annual production per year $m_{Product,year}$ in t/a. This is needed for the calculation of the annual excess heat potential:

$$E_{ex,year} = \frac{E_{ex}}{m_{Product}} \bullet m_{Product,year}, \tag{8}$$

where $E_{ex}/m_{Product}$ is the specific excess energy per tonne of product (heat in the exhaust). It depends on the temperature of the exhaust of the specific industrial process, the level of internal heat recovery (impact on exhaust gas temperature), the temperature of the exhaust gas is cooled down, and the exhaust gas composition. The total excess heat $E_{ex,year}$ for each of the processes and industrial installation results from multiplication of the production in tonnes $m_{Product,year}$ for the industrial process (with or without internal heat recovery) with $E_{ex}/m_{Product}$, and is added to the Industrial Database.

Table 3.4: Main assumptions made on temperature levels, fuel type, and fuel composition (for more details see [152])

	Temperature Range (°C)	Fuel (Composition)
Coke ovens	200–800	COG (52% H_2; 37% CH_4; 5% C_2H_6; 4% CO; 2% CO_2)
Blast furnaces	130–250	BFG (50% N_2; 26% CO; 21% CO_2; 3% H_2) enriched with COG
Basic oxygen furnaces	250–1700	None (exothermic reaction)
Electric arc furnaces	200–1200	not applicable: furnaces are based on electricity
Cement clinker kilns	250–338	Coal (72% C; 8% H_2O; 4% H_2; 2% S; 12% rest)
Glass furnaces	200–1400	Natural gas (93% CH_4; 4% C_2H_6; 1% C_3H_8; 1% N_2; 1% CO_2)
Pulping	170–260	Black liquor
Lime burning	200–650	Natural gas
Paper making	170–260	Black liquor
Primary aluminium	700	not applicable: furnaces are based on electricity
Chemicals (boilers)	150–260	Natural gas
Refineries (boilers)	170–260	Refinery fuel gas (44% CH_4; 17% H_2; 16% C_4H_{10}; 10% C_3H_8; 9% C_2H_6; 1% CO_2; 2% rest)

In the following paragraphs, the main excess heat flue gas sources are briefly described for each industrial sector. Table 3.4 summarizes the temperature ranges of main gas streams and the assumptions on the composition of the fuels used or of the generated gases (when the gas composition cannot be calculated from the complete combustion of fuels). For the detailed sectoral analysis and the diffusion rates of process and recovery technologies currently employed in each industrial subsector please refer to Fleiter et al. [152].

3.2.2.1 Iron and steel

Coke ovens have two sources of sensible excess heat contained: i) in the coke oven gas (COG) and ii) in the off-gases generated from burning COG [134]. The COG exits the coke oven at a high temperature (650 and 1000 °C). Technologies for excess heat recovery from the highly contaminated COG are available but due to the high capital costs, they are not widely implemented. The sensible heat from the off-gases is commonly recovered with a regenerator and used to preheat the incoming combustion air. The flue gases leave the regenerator at about 200 °C.

Sensible heat in blast furnaces can be recovered from two gas streams: (i) the generated blast furnace gas (BFG) and (ii) the blast stove exhaust. The gases display low temperatures; 200 °C for BFG and 250 °C for the blast stove exhaust. Heat recovery from the off-gases is a common practice [134].

The gases from basic oxygen furnaces (BOF) are very hot, with temperatures typically ranging between 1600 and 1800 °C [153]. An efficient way to utilise both the excess heat and the fuel is the non-combustion heat recovery process [154]. The BOF gas temperature in this case is reduced to about 250 °C [155].

The off-gases from electric arc furnaces (EAFs) are at high temperatures ranging from 1400 – 1900 °C. Scrap preheating reduces the off-gas temperature to about 200 °C. About 20% of the furnace energy input is lost as excess heat, of which in turn 50% is lost in the form of sensible heat [134].

3.2.2.2 Cement

Dry kilns with no heat recovery have an exhaust temperature of about 450 °C. When four preheater stages are used the temperature is lowered to 300–400 °C [156] and when the stages are increased to five or six the temperature decreases to 200–300 °C [134]. If raw material drying is not needed, the medium-low temperature heat in the kiln-off could be used for electricity generation or for supplying hot water [156].

3.2.2.3 Glass

Recuperative furnaces for glass production are in general the least energy-efficient furnaces used with exhaust temperatures at 980 °C. In regenerative furnaces, heat is recovered to heat the combustion air dropping the exhaust gas temperature to about 320 – 540 °C. Oxy-fuel smelters have exhausts with temperatures of about 1400 °C [134]. Batch/cullet preheating can lower the temperature of the flue to about 200 °C. To avoid material agglomeration, the temperature of the flue gases that enter the batch heat exchanger cannot be higher than 550 – 600 °C [157]. If not possible to utilise on-site, excess heat from the cooling of the flue could be potentially available for district heating. This potential could however disappear with the use of advanced batch preheaters that allow higher temperatures. Cullet preheating is currently limited in the container glass industry [157].

3.2.2.4 Pulp and paper

Boilers are the largest fuel consumers generating steam for pulping, evaporation, paper making, and other operations. Exhaust temperatures from industrial boilers vary, but typical temperatures are around 260 °C with no heat recovery and 150 - 200 °C with heat recovery. Lime kilns, used in chemical pulping, are further important fuel consumers. The temperature of the kiln exhaust is lowered under 200 °C when heat exchangers are used [158], as cited in [159].

3.2.2.5 Primary aluminium

The off-gases from aluminium smelting are responsible for only a small part of total heat losses with the most significant part stemming from the electrolytic cell surface. However, in this analysis, we only focus on the exhaust gases. The average off-gas temperature is around 700 °C [134].

3.2.2.6 Chemicals and refineries

The chemical industry is quite complex with many different products generated and many small furnaces in operation for which information is scarce. We have thereby mainly focused on boiler flue gases for the industries for which information on fuel use for steam generation is available.

The hot flue gases (760 – 870 °C) from ethylene furnaces are typically recovered to produce steam, decreasing the flue gas temperature to about 150 °C [160]. In naphtha cracking most of the fuel consumed, about 2/3, is used in the ethylene furnace, while the remaining 1/3 is used in the separation and compression processes usually in the form of steam [161].

In ammonia production, about 40% of the fuel used for energy purposes is for steam generation [162]. In chlorine production, both for the membrane separation and the diaphragm processes the biggest part of fuel use is also for steam generation [163]. Here we assume that 100% of fuel consumption in chlorine production is by boilers. In addition, about 52% of the fuel used in refineries is consumed in boilers [162]. Exhaust temperatures from boiler flue gases are about 260 °C with no heat recovery and 150 °C (natural gas fuel) and 177 °C (refinery fuel gas) with heat recovery.

3.2.3 Mapping industrial excess heat to district heating areas

The objective of this section is to describe the approach and data used to establish the spatial relationship between georeferenced industrial sites and district heating areas on an annual basis. The total annual excess heat potentials identified within the Industrial Database were matched with utilisation possibilities by actual and possible DH areas. This step reduces the total external excess heat potential as only industrial locations that are located nearby a DH area represent exploitable excess heat sources. The underlying data, which was used to determine the geographical locations and areas of currently operational district heating systems in EU-28, was gathered from external data sources. Firstly, and most importantly, information on DH locations, names, and annual heat sales was gathered from the Halmstad University District Heating and Cooling database (HUDHC) [23,83,94,164]. Secondly, heat demand density raster data at hectare level was gathered for residential and service sectors of the EU Member States from the Heat Roadmap Europe project [18,43,94].

A stepwise approach consisting of three main steps was elaborated in this context, as outlined in Figure 3.3. Step one, the extraction of appropriate heat demand density data and converting this raster data into vector features (possible district heating areas (DH-P)), step two, relating this data set to the HUDHC database to establish currently operational systems (actual district heating areas (DH-A), and step three, performing spatial analysis of industrial sites and district heating areas (distance calculations).

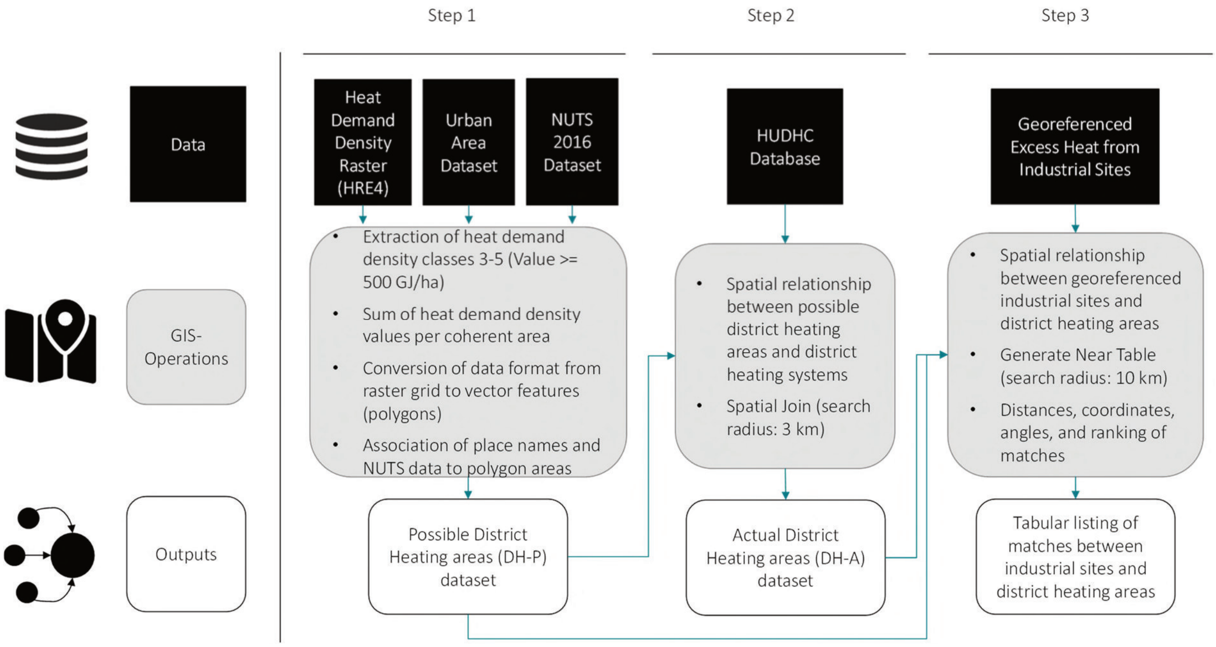

Figure 3.3: **Principal overview of the three main steps used in the spatial mapping of industrial sites and district heating areas. Source for Urban Area Data set: [165]**

In the Heat Roadmap Europe project, heat demand densities were divided into six distinct classes with respect to the corresponding concentration of heat demands. For this study, all heat demand density grid cells with values of 500 GJ/ha and above are considered, corresponding to moderate (next to city centre suburbs and multi-family building residential districts), dense, and very dense (inner urban areas) populated areas. In addition, it was found for these heating densities of the residential and service sector that economic suitability for DH distribution should be prevalent or generally likely [18]. The selected coherent areas of heating densities form the data extract with which representative areas for possible district heating areas (DH-P) can be outlined (Figure 3.4).

In the HUDHC database, the locations of district heating systems are given only by geographical coordinates of each corresponding city centre (point sources) and hence not as spatially extended areas. This is a limitation since district heating grids are spatially distributed and spread out according to their pipe network designs. To allow a spatial analysis based on distance calculations between the georeferenced industrial sites and district heating areas, this work, therefore, includes a transformation of these point-source locations to representative district heating areas. It relies on the assumption of a likely expansion of actual DH grids operating in areas with sufficiently high heat demand densities, and the extraction of heat demand density data from the Heat Roadmap Europe data set as indicative of such areas. The underlying evidence for this assumption consists of published results from several previous studies regarding physical and economic suitability for district heating in Europe [18,30].

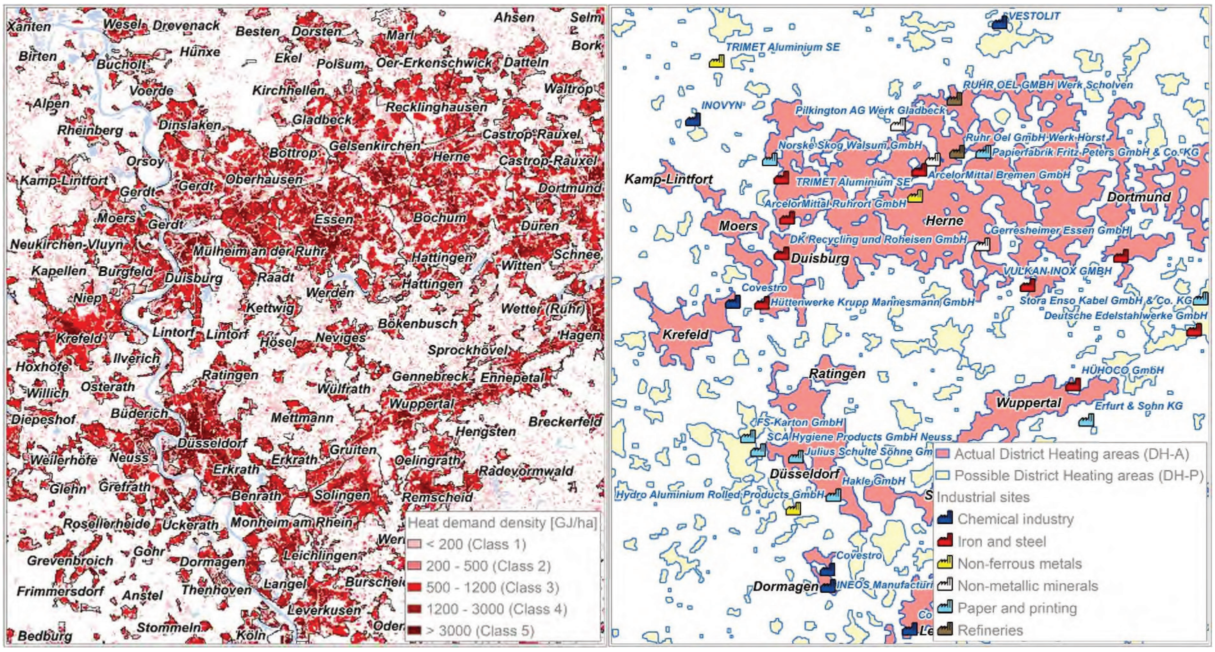

(a) (b)

Figure 3.4: Heat demand density classification by hectare grid cells for residential and service sector building heat demands (a) and the spatial relationship between georeferenced industrial sites to possible district heating areas (DH-P) and actual district heating areas (DH-A) (b), exemplified for Düsseldorf and surroundings in Germany

The final step consisted of calculating Euclidean distances and recording matches between the industrial sites and the possible district heating areas, for which purpose the ArcGIS Proximity tool "Generate Near Table" was used within the context of a spatial model (Model Builder). The distances are measured from one industrial site to the border (spatially closest line segment) of the respective DH area. This GIS operation produces an output table with all identified matches specified by distance (in meters), coordinates, angles, and by rank (inside = 0, next closest = 1, then 2, 3, etc.). The spatial model was run iteratively for a set of different search radii (e.g. 100 km, 25 km, and 10 km) that reflect plausible transition pipe lengths for excess heat recoveries [166]. Their feasibility depends mainly on the capacities and the magnitudes of available excess heat and corresponding heat costs. The shortest and perhaps most realistic distance by which to arrange external excess heat recoveries today, 10 km, was selected to present the potentials and study results.

3.3 Results

In total, 1608 sites including 2567 associated installations with excess heat potentials in EU-28 were identified with the methodology presented. That means about 30% of the 5440 entries in the Industrial Database include processes analysed for excess heat recovery in this study. The geographical locations are depicted in Figure 3.5, indicating the total excess heat potential of 25 °C. Sites of the non-metallic mineral subsector and paper subsector are scattered overall EU-28, having only smaller excess heat potentials. Refineries are mostly located close to the seaside or harbours, having rather high excess heat potentials. Most of the excess heat of the iron and steel production sites and from the chemical subsector is located only in a few countries, like Germany, Sweden, UK, Poland, and France.

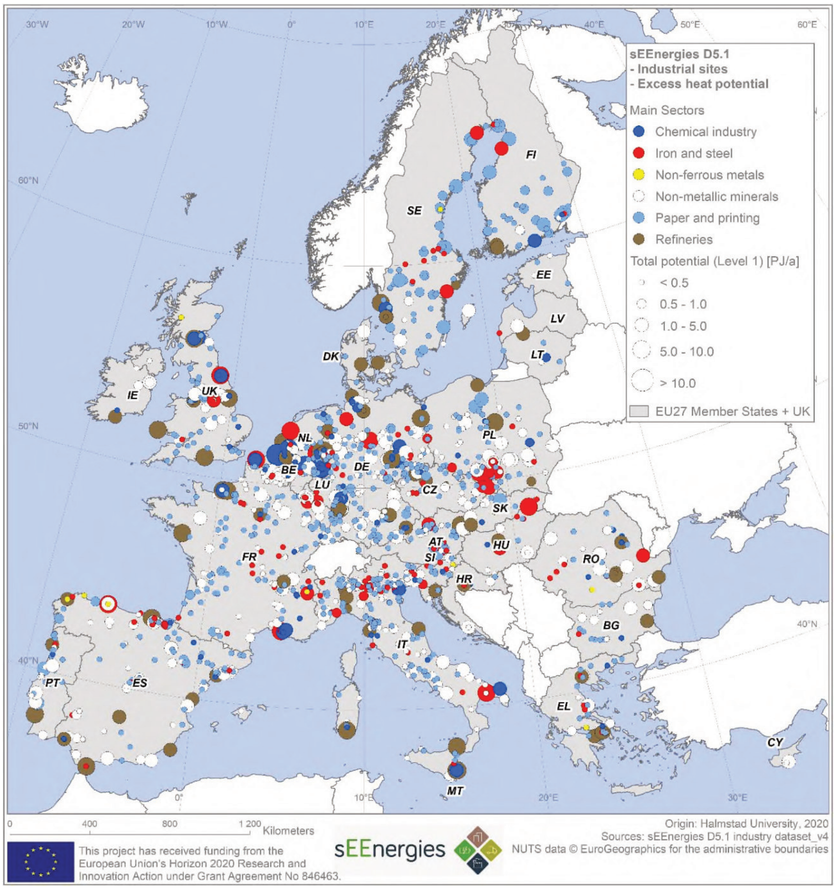

Figure 3.5: Total excess heat potential (25 °C, average internal heat recovery) of the 1608 georeferenced industrial sites by sectors in the EU-28

3.3.1 Excess heat potentials per process

The specific values of excess heat potentials per process based on the physical production are shown in Table 3.5. The scope of this analysis contains the flue gas streams from the 29 energy-intensive industrial processes in the database to capture the most significant high-quality excess heat sources.

Table 3.5: Estimated unrecovered excess heat in GJ/tonne of product from exhaust gases in the different industries depending on efficiency measures

Subsector	Process	Number of Installations	Current Potential	Industrial Efficiency	DH Efficiency (55 °C)	System Efficiency (55 °C)	DH Efficiency (25 °C)	System Efficiency (25 °C)
Iron and Steel	Coke ovens	52	1.06	0.55	1.16	0.65	1.68	1.17
	Blast furnaces	56	0.34	0.30	0.46	0.41	0.56	0.51
	Basic oxygen furnace	32	0.17	0.01	0.18	0.02	0.18	0.02
	Electric arc furnace	186	0.15	0.02	0.16	0.02	0.16	0.03
Non-ferrous metals	Primary aluminium	16	1.00	1.00	1.05	1.05	1.09	1.09
Container glass	Recuperative	165	1.78	0.23	1.88	0.31	2.59	0.89
	Regenerative		0.57	0.19	0.66	0.26	1.25	0.74
	Oxy-fuel	9	0.94	0.08	0.98	0.11	1.22	0.30
Flat glass	Recuperative	61	4.18	0.38	4.35	0.53	5.52	1.52
	Regenerative		1.19	0.31	1.33	0.43	2.28	1.24
	Oxy-fuel	3	1.64	0.10	1.68	0.13	1.97	0.38
Cement Clinker	Wet	28	0.72	0.72	0.83	0.83	1.09	1.09
	Dry	156	0.91	0.29	1.01	0.36	1.23	0.51
	Dry+ph+pc[a] (4 stage PH)	24	0.49	0.29	0.56	0.36	0.73	0.51
	Dry+ph+pc (5–6 stage PH)		0.29	0.29	0.36	0.36	0.51	0.51
Pulp making	Chemical pulping	123	0.48	0.22	0.59	0.32	1.46	1.12
	Mechanical pulping	58	0.04	0.03	0.05	0.04	0.16	0.14
	Recovered fibres	457	0.01	0.01	0.01	0.01	0.04	0.04
Paper making	Board & packaging paper	495	0.09	0.07	0.13	0.10	0.41	0.37
	Graphic paper	175	0.14	0.10	0.19	0.14	0.61	0.55
	Tissue paper	252	0.13	0.09	0.18	0.14	0.59	0.52
Chemicals	Ethylene	31	1.11	0.88	1.77	1.54	6.32	6.02
	Ammonia	26	0.20	0.11	0.28	0.19	0.87	0.75
	Chlorine, diaphragm	4	0.14	0.08	0.20	0.13	0.61	0.53
	Chlorine, membrane	60	0.05	0.03	0.07	0.04	0.20	0.18
	Refinery basic	24	0.09	0.06	0.12	0.09	0.37	0.34

Subsector	Process	Number of Installations	Current Potential	Industrial Efficiency	DH Efficiency (55 °C)	System Efficiency (55 °C)	DH Efficiency (25 °C)	System Efficiency (25 °C)
Refineries	Refinery gasoline focused	13	0.11	0.07	0.14	0.11	0.46	0.41
	Refinery diesel focused	22	0.12	0.09	0.17	0.13	0.54	0.48
	Refinery flexible	39	0.11	0.08	0.15	0.12	0.48	0.43

[a] Dry process with preheater and precalciner

Generally, the highest potential is the *DH efficiency* (25 °C), because it represents the potential with an average internal heat recovery of the industrial processes and the energy that could be used if the exhaust gases are cooled down to 25 °C. The difference to the *Current potential* is only the decrease of the temperature from 95 °C to 25 °C. *Industrial efficiency* and *System efficiency* both take into account the effects of a full internal heat recovery of excess heat, with an exhaust gas temperature of 95 °C, 55 °C, and 25 °C, respectively. The values are therefore lower than the ones with the same temperature but with today's level of internal heat recovery. The significance of this decline varies according to the process. In the sector of non-metallic minerals, the potential for internal heat recovery is the highest and thus decreases the potential for external use significantly. For example, in the recuperative furnaces used in the container glass industry, the excess heat available is estimated at 1.8 GJ/tonne in the Current potential for the reference temperatures of 95 °C. When batch/cullet preheating is used within all plants in EU-28 (*Industrial efficiency*), the excess heat availability is significantly reduced to 0.2 GJ/tonne. Cooling the exhaust gas to 25 °C increases the available excess heat up to 2.6 GJ/tonne, considering preheating of the current level (40% of furnaces). The excess heat available from cooling the gases from 200 °C to 25 °C with preheating implemented in all furnaces is estimated at 0.9 GJ/tonne (*System efficiency* (25 °C)).

Table 3.6: Total excess heat potentials for temperatures of 95 °C, 55 °C, and 25 °C per industrial subsector, without and with internal heat recovery in PJ/a

Industrial Subsector	Number of Sites	Total Current Potential per Site, Average	Total Current Potential	Total Industrial Efficiency	Total DH Efficiency at 55 °C	Total System Efficiency at 55 °C	Total DH Efficiency at 25 °C	Total System Efficiency at 25 °C
Iron and steel	195	0.56	109	54	125	69	157	101
Non-ferrous metals	16	0.14	2	2	2	2	2	2

Industrial Subsector	Number of Sites	Total Current Potential per Site, Average	Total Current Potential	Total Industrial Efficiency	Total DH Efficiency at 55 °C	Total System Efficiency at 55 °C	Total DH Efficiency at 25 °C	Total System Efficiency at 25 °C
Non-metallic minerals	432	0.44	192	51	208	64	262	106
Pulp and paper	760	0.03	26	15	34	22	95	80
Chemicals	107	0.19	20	16	32	27	113	106
Refineries	98	0.77	75	53	103	80	331	297
Total	1608	0.26	425	191	504	264	960	692

The total sectoral excess heat potentials are shown in Table 3.6. The values represent the total available excess heat by the identified industrial processes, without consideration of DH areas. The total potentials sum up to the range of 191 to 960 PJ (53 to 267 TWh) per year in the EU-28 for the 1608 sites that have identified excess heat potentials. Most of the sites (47%) are in the pulp and paper subsector, while relatively numerous, they contribute a much smaller share to the total excess heat (~ 1%). This is because paper production sites are generally smaller both in capacity and specific energy consumption compared to the processes from the energy-intensive industries analysed in the study. The highest potential of a single subsector is identified within the refineries, having a share of excess heat potentials of 18 up to 43%, depending on assumptions, with only 6% of the number of sites. The non-ferrous metals subsector is based solely on the primary aluminium process in this study, having a lower production compared to the other products like steel and cement. The non-metallic mineral subsector includes glass and cement clinker manufacturing, leading to a high number of sites across the EU-28 with high annual production.

3.3.2 Excess heat potentials per district heating area

The EU-28 residential and service sector building heat demands including hot water were assessed at about 10,800 PJ (3000 TWh) for the year 2015 by the Heat Roadmap Europe 4 project [18]. The extraction of areas with a heat density greater than 500 GJ/ha resulted in a total of 47,275 unique polygon areas for the EU-28, with the accumulated heat demands for density classes 3–5 to be at 78% (8410 PJ). The calculated sum of heat demands in possible district heating areas (DH-P) for this study constitute 65% (7018 PJ). The discrepancy is due mainly to outliers and single grid cells being omitted in the extraction process.

The database on current district heating systems (HUDHC_v5) counts a total of 4113 unique systems for the EU-28, which, if grouped by their respective CityIDs, correspond to a total of 3703-point source city coordinate pairs (latitude and longitude). From these, 2763 district heating CityIDs were found to have their city centre coordinates located inside or within the maximum distance of 3 km from a possible district heating area (3025 unique systems). Therefore, they constitute the data sub-set of actual district heating areas (DH-A). Together, the matching systems constitute 98% of recorded statistics on annually sold heat in the HUDHC database (1203 PJ). For a remainder of 940 CityIDs, no matches were established: cities which currently have district heating, but where heat demand densities are below the extraction limit or beyond the maximum distance. After examination, it was found that most of these cities are in countries with high shares of district heating (e.g., Scandinavia, the Baltics, Austria, and the Slovak Republic).

Table 3.7 presents the results of spatial matching at the 10 km default distance of georeferenced industrial sites with respect to district heating areas for the six investigated potentials. For the *Current potential*, 230 PJ (64 TWh) of industrial excess heat could be utilised from 752 industrial sites, corresponding to a share of DH supply of 17% for residential and service buildings. At maximum rates of internal heat recovery, for *Industrial efficiency*, the annual external excess heat potential is reduced to 108 PJ (30 TWh). 1569 industrial sites (98% of the full count) were found to have 1st rank spatial matches with DH-P areas at the 10 km setting. The *DH efficiency* indicates annual external industrial excess heat recovery potential, depending on the exhaust gas temperature, in the range of 493 to 941 PJ (137 to 261 TWh) per year in the EU-28. This is only marginally lower than the total potentials of 504 to 960 PJ per year for the respective temperature. Even for the *System efficiency*, 258 to 679 PJ (72 to 189 TWh) per year are available for external heat recoveries at the 10 km distance setting.

Table 3.7: Spatial matching of industrial sites with 1st rank matches inside or within 10 km of DH areas in different configurations and resulting excess heat utilisation potential per country in the EU-28

Member State	Number of Industrial Sites	Number of Industrial Sites—1st Rank Match to DH-A	Current Potential in PJ/a	Industrial Efficiency in PJ/a	Number of Industrial Sites—1st Rank Match to DH-P	DH Efficiency (55 °C) in PJ/a	System Efficiency (55 °C) in PJ/a	DH Efficiency (25 °C) in PJ/a	System Efficiency (25 °C) in PJ/a
AT	44	40	10.7	5.1	44	13.1	7.2	24.3	17.7
BE	34	26	14.4	7.7	34	18.3	10.9	37.7	29.4
BG	19	10	1.9	0.7	18	4.1	2.0	7.6	5.2
CY	2	0	0	0	0	0	0	0	0
CZ	39	38	11.2	4.6	39	13.1	6.1	20.5	12.8
DE	310	142	52.8	26.2	310	99.3	53.0	184.1	132.8
DK	5	4	2.3	0.8	5	3.2	1.5	5.9	4.0
EE	4	3	0.4	0.3	4	0.5	0.4	0.7	0.5
EL	36	1	0.0003	0.0002	31	8.0	4.5	15.7	11.7

Member State	Number of Industrial Sites	Number of Industrial Sites—1st Rank Match to DH-A	Current Potential in PJ/a	Industrial Efficiency in PJ/a	Number of Industrial Sites—1st Rank Match to DH-P	DH Efficiency (55 °C) in PJ/a	System Efficiency (55 °C) in PJ/a	DH Efficiency (25 °C) in PJ/a	System Efficiency (25 °C) in PJ/a
ES	143	21	3.9	0.9	138	43.3	21.4	81.5	57.1
FI	47	38	8.8	4.5	44	11.4	6.8	25.9	20.4
FR	197	102	24.3	10.7	193	53.4	27.9	101.1	72.7
HR	12	6	2.1	1.0	10	3.8	1.9	7.6	5.3
HU	14	12	4.1	2.0	14	6.0	2.9	10.2	6.9
IE	4	0	0	0	3	1.5	0.6	1.8	0.9
IT	275	47	6.5	1.6	274	54.2	25.0	102.4	70.0
LT	8	8	2.1	1.5	8	2.7	2.0	6.6	5.8
LU	5	2	1.8	0.2	5	2.9	0.5	3.6	1.1
LV	2	2	0.9	0.3	2	1.0	0.3	1.2	0.4
MT	0	0	0	0	0	0	0	0	0
NL	41	10	8.1	5.3	41	25.2	17.4	65.8	56.6
PL	98	76	27.6	12.5	97	40.5	19.8	63.8	41.6
PT	38	3	0.3	0.04	33	10.8	5.0	20.1	13.4
RO	36	18	6.5	2.4	35	12.5	5.5	20.6	12.8
SE	70	54	12.6	6.5	62	17.9	10.6	41.3	32.5
SI	15	14	1.0	0.4	15	1.1	0.5	1.6	0.8
SK	16	16	7.2	3.5	16	8.3	4.5	13.2	9.1
UK	94	59	17.9	9.3	94	36.4	20.3	76.0	57.8
EU-28	1608	752	230	108	1569	493	258	941	679

The full distribution of 1st rank spatial matches between all 1608 industrial sites and all actual and possible district heating areas are depicted in Figure 3.6 for four distance settings: unlimited search radius, 100 km, 25 km, and 10 km. As can be seen at the unlimited setting, a few sites (located on Atlantic islands) constitute study population outliers at distances above 1000 km. It is clear that the main bulk of spatial matches occur within the 25 km distance for both actual and possible DH areas, while this tendency is less pronounced for actual DH areas as the distance decreases. At the 10 km default, 98% of all industrial sites (1569) have a 1st rank match to one of 11,389 DH-P areas, while 752 sites (47%) have a 1st rank match to one of 684 DH-A areas, as also detailed in TableAnnex 9. The total count of spatial matches at the 10 km setting amounts to 18,575 matches.

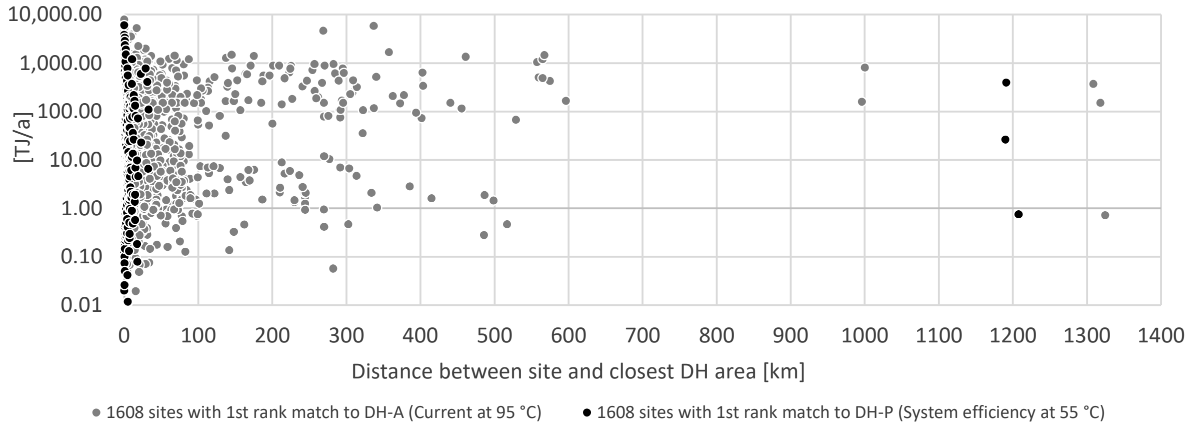
10,000.00
1,000.00
100.00
10.00
1.00
0.10
0.01
[TJ/a]
0
100
200
300
400
500
600
700
800
900
1000
1100
1200
1300
1400
Distance between site and closest DH area [km]
1608 sites with 1st rank match to DH-A (Current at 95 °C)
1608 sites with 1st rank match to DH-P (System efficiency at 55 °C)

(a)

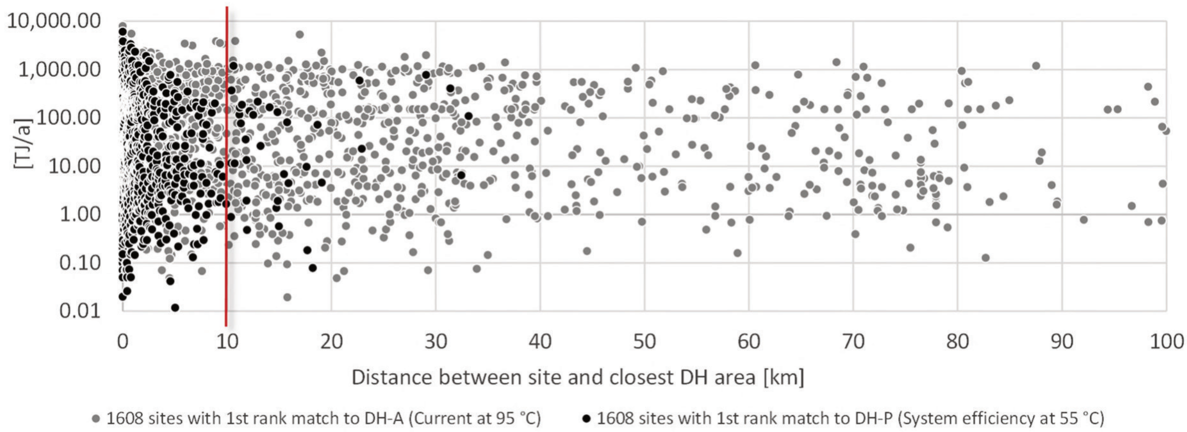
10,000.00
1,000.00
100.00
10.00
1.00
0.10
0.01
[TJ/a]
0
10
20
30
40
50
60
70
80
90
100
Distance between site and closest DH area [km]
1608 sites with 1st rank match to DH-A (Current at 95 °C)
1608 sites with 1st rank match to DH-P (System efficiency at 55 °C)

(b)

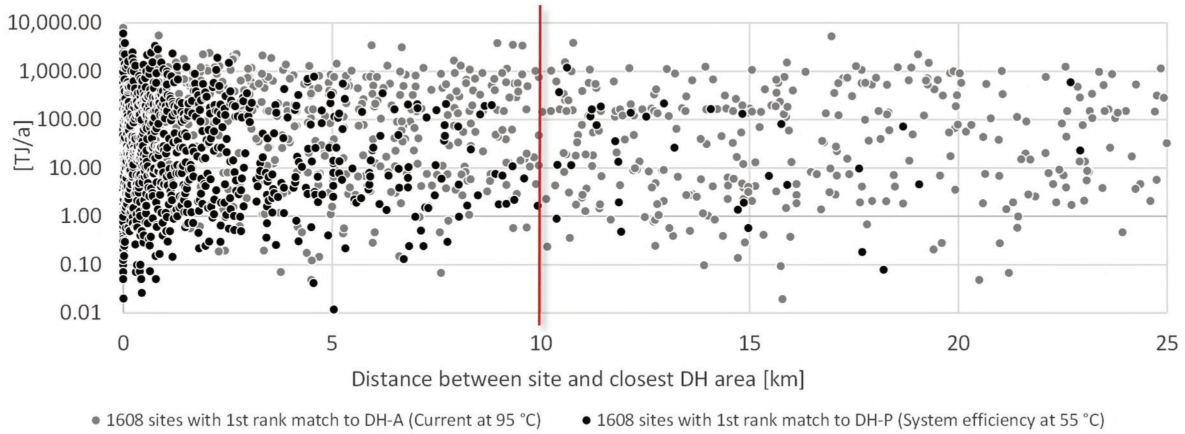
10,000.00
1,000.00
100.00
10.00
1.00
0.10
0.01
[TJ/a]
0
5
10
15
20
25
Distance between site and closest DH area [km]
1608 sites with 1st rank match to DH-A (Current at 95 °C)
1608 sites with 1st rank match to DH-P (System efficiency at 55 °C)

(c)

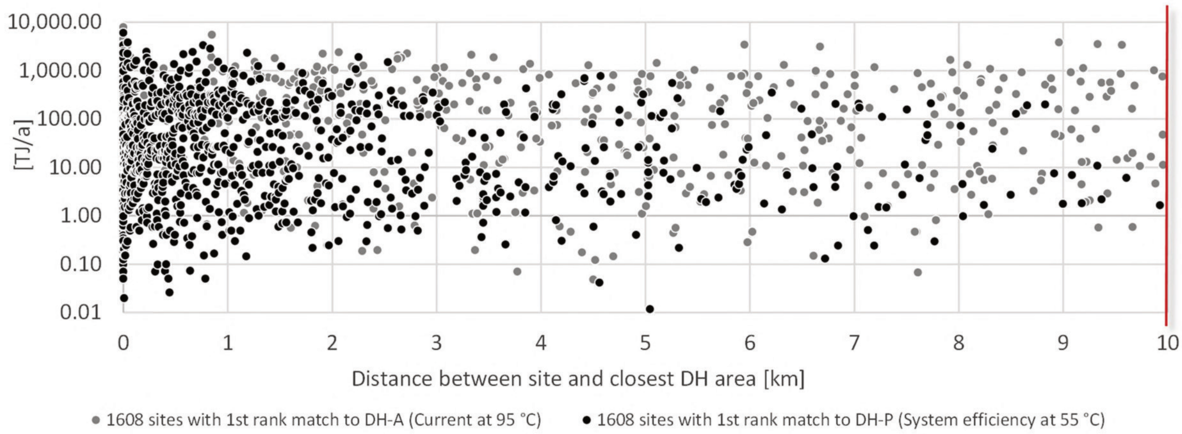

(d)

Figure 3.6: Distribution of 1st rank spatial matches between industrial sites and district heating areas by distance for Current potential (relative DH-A, grey dots) and System Efficiency (55 °C) (relative DH-P, black dots), with annual excess heat volumes per site in TJ/a for all distances (a), within 100 km (b), within 25 km (c), and within the study default 10 km limit (d)

Most 1st rank spatial matches between industrial sites and possible DH areas are indeed happening inside or within only a few kilometres from these areas, as illustrated in Figure 3.6d. For the *Current potential* (analogous in terms of counts with the *Industrial efficiency* and thus relating to actual DH areas), a total of 206 sites are located inside (13%) such areas. In terms of annual energy magnitudes, the total *Current potential* amounts to 425 PJ of which 230 PJ per year (54%) is available in the direct vicinity of DH-A areas (within ten kilometres). Similarly, if focusing on the *System efficiency* (analogous in terms of counts with the *DH efficiency*), we find that 44% (702 sites) are located inside, 40% (639 sites) within two kilometres, and another 9% (149 sites) are located between two and five kilometres from the borders of these areas. Excess heat for external utilisation originating from sites located inside or within only two kilometres from DH-P areas adds up to 90% (238 PJ per year) of the total *System efficiency* (55 °C) and to 91% (632 PJ per year) of the total *System efficiency* (25 °C).

3.4 Discussion

This study presents a process-specific approach that estimates bottom-up excess heat for 29 processes from energy-intensive industrial subsectors with a spatial matching to actual and possible DH areas in the EU-28. The assessment of different temperatures and levels of internal heat recovery in the industrial processes enables taking into account efficiency measures in the important industrial sectors that decrease the available excess heat. Information concerning industrial locations was collected from various sources, stored, and georeferenced in the Industrial Database, enabling a systematic calculation of energy demand and excess heat based on the production process and annual production. The main sources of excess heat from exhaust gases for the production processes were identified and analysed based on the temperature level and flue gas composition. In a subsequent step, the excess heat potentials were matched with the district heating database HUDHC and possible district heating systems based on heating densities with high resolution.

3.4.1 Data validation

The excess heat potentials calculated based on physical production for each production process were benchmarked with excess heat estimations found in other studies (see Table 3.1). The deviations are shown in Figure 3.7. Please note, that for this validation the spatial analysis is omitted, and the total excess heat potentials are used. Depending on the assumptions in the other publications, the best fitting value depending on temperature and internal heat recovery was chosen for comparison. The calculation method of the literature values differs in many cases from the one presented here. Furthermore, the input data regarding the inclusion of industrial processes and the assumed temperature levels can differ greatly. Compared to Brückner et al. [143], the value for Germany is comparable with −5%. It should be noted, that for similar temperatures comparable values are found even though our approach is based on production data instead of emissions. This holds true for the values that were found for a full internal heat recovery which corresponds best to the conservative assumptions. Compared to Pehnt et al. [167], there is a deviation of +219% for Germany, originating from a different methodology. The deviation for EU-28 of +205% to Persson et al. [83] can be explained by a different methodology of excess heat calculation using average estimates per sector. This comparison can hint at the fact that sectoral values are prone to overestimate the potentials compared to a process-specific approach. The approach from Manz et al. [137] is similar to the one presented in this study, without the chemical sector and refineries. When the respective value is compared, there is a deviation of +2% remaining. Regarding the values for Denmark from the study of Bühler et al. [78], there is a deviation of +311%, as it covers most sites of the industrial sector in Denmark (80% of industrial final energy consumption). As Denmark has only a few industrial sites from the energy-intensive industry, a lot of processes are from non-energy intensive subsectors that are not included in our study. As a summary, our values are within the range of other studies presented before. With our approach, process-specific efficiency measures and even change of process can be considered in contrast to subsector-based values. It should be emphasised that our bottom-up approach for the EU-28 inherently underestimates the available potentials because it focuses on the largest point sources, major processes, and flue gases as the most attractive excess heat streams. Although the analysis covers the most attractive potentials, including additional excess heat sources would increase the potentials available, particularly at lower temperatures.

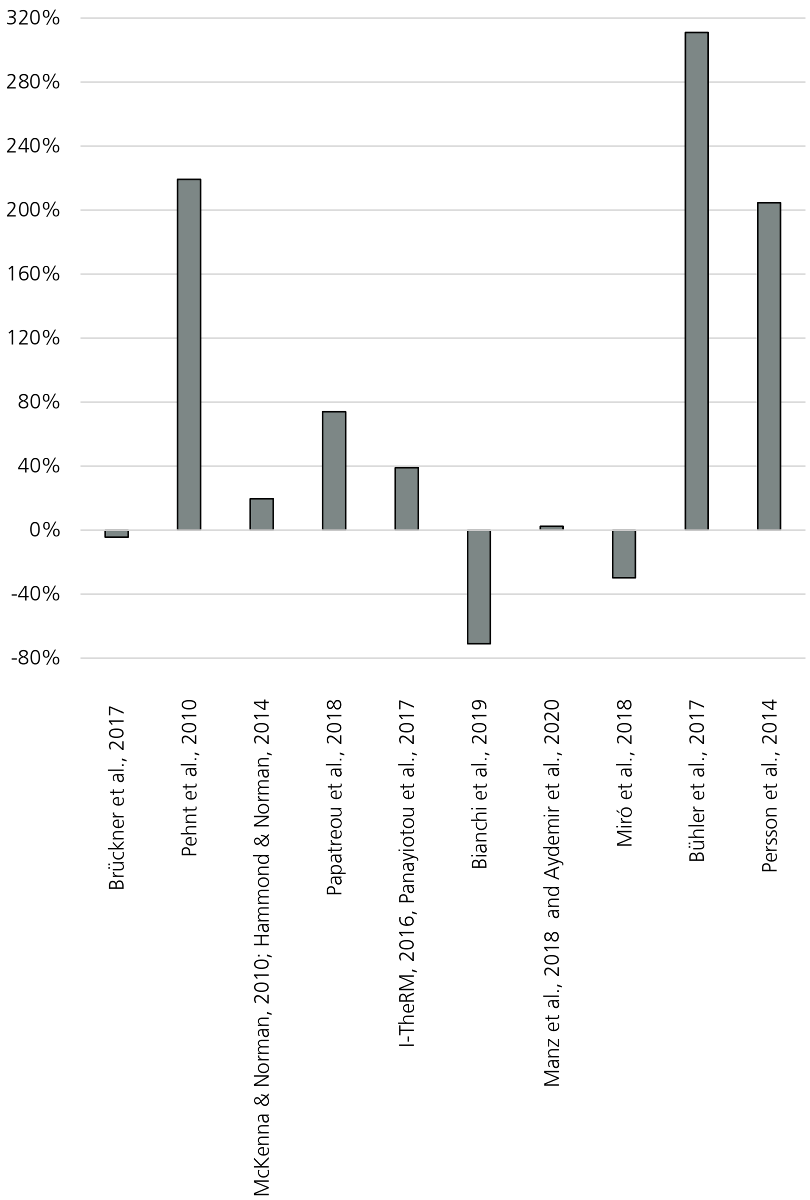

Figure 3.7: Deviations of excess heat potentials found in this study

The data quality of the Industry Database regarding the annual production and annual fuel consumption is validated with EU statistics for each country and process. In Figure 3.8, a comparison of the production data is validated with national production data on country level. The national data is taken from sectoral associations with gaps filled with data from PRODCOM [168], as presented in [119]. It is based on the year 2015. The national values indicate that most of the processes are covered completely by the Industrial Database, but for some processes, there is a deviation up to 20%. This can have several reasons: the most important factor is a remaining uncertainty regarding annual utilisation factors where only production capacity is given to calculate the annual production. When the statistical production is greater than what can be found in the database, it also indicates that some smaller installation could be missing. In general, the comparison shows that the database has a sufficient quality to estimate process-specific excess heat potentials, even though it can be refined and checked persistently.

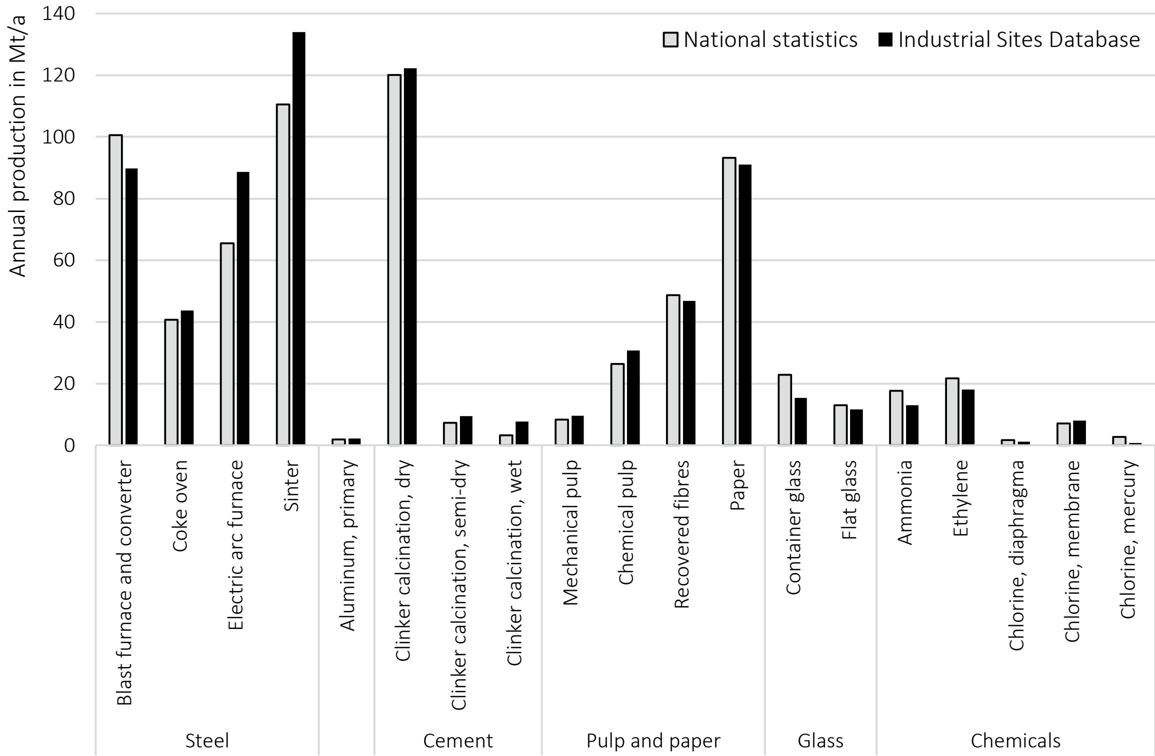

Figure 3.8: Production per process as stated in statistics of sectoral associations on national level (label: National) and included in industrial database (label: Process specific). Data source: [168]

3.4.2 Limitations

Even though various efficiency measures both in industry and DH are considered in this study to capture future developments, it is not a scenario-based analysis and important expectable structural changes are therefore not integrated. In general, energy-intensive processes are currently mainly based on fossil fuels and additionally often have process-related CO_2 emissions. A transformation to carbon-neutral processes, such as the replacement of blast furnaces by hydrogen (direct reduction, plasma) and electricity-based (electric arc furnace) processes, and the electrification of furnaces and steam generation might lead to different excess heat potentials. Consequent circular economy and material efficiency will lead to less primary production of these energy-intensive materials. Refineries especially will face structural change until 2050, producing for example synthetic fuels. In addition, future excess heat potentials for use in DH must be evaluated under the assumption that industrial locations are likely to be situated where they are now and there is no or little shift of production to other countries outside the EU-28. Furthermore, district heating systems are expected to face a decreasing heating demand due to higher building standards and renovation of buildings. The heating demand in this study neglects the influence of a decreasing heating demand or communal initiatives promoting the installation or extension of DH, instead calculating the possible DH areas with today's heat density where competitiveness was already proven [18].

Moreover, the data basis for all calculation steps can be improved continuously. The deviation of national production data from the georeferenced data implies that sites are missing, that the calculation of annual production from capacity among individual sites varies significantly and not all closure of sites are recorded. The inclusion of further industrial processes, cross-cutting technologies like machines, less energy-intensive, heterogeneous sectors, and even other low-temperature excess heat sources like data centres or wastewater treatment plants is limited with the methodology presented. The HUDHC database [164] lists 4113 DH systems in the EU-28, a number that captures the largest DH city systems, but probably misses some minor DH systems as nobody knows exactly how many district heating systems are currently in operation in the EU-28. However, regarding the data used, most large-size district heating systems operated over long time periods are included, while those missing mainly refer to smaller systems and more recent developments. The data displays a 68% coverage rate regarding statistics on annual heat sales, which is improvable. The possible DH areas are based on today's heating densities by buildings that will be reduced in the future due to refurbishments and thus lowering the feasibility for DH.

For the calculation of excess heat potentials, exhaust gas temperature and quality restrictions due to condensation and corrosive materials are not taken into account. Although the heat could still be recovered at lower temperatures, it would require more advanced technologies and different materials [149,169]. We therefore emphasise the need to intensify R&D activities for technical solutions (e.g., heat exchangers for corrosive gases or filters for chemicals). Heat sources other than flue gases are neglected. This leads to a rather conservative estimate as other significant sources of excess heat such as from solid and liquid streams, cooling water, radiation, and conduction heat losses are not considered. However, the excess heat potential within the scope of this study comprises the most relevant potentials, being large major point sources and often providing heat at high-temperature levels. Thus, exploiting sources beyond our system boundary would probably involve higher specific costs, as smaller excess heat streams would need to be addressed. Still, further research should also include such excess heat sources that probably will also become more attractive with the diffusion of heat pumps and technical learning of these systems.

In this study, we quantified the possible contribution of industrial excess heat to DH areas based on annual values, which is justified due to the work being organised mostly in three shifts in energy-intensive industries. However, this neglects the fact that some industries do not produce throughout the entire year e.g., the cement industry mostly closes in the winter months due to a decreased demand in the construction sector. Higher time resolutions of the excess heat availability and the match with demand was not considered in our study. In Bühler et al. [140], it can be seen that these factors could reduce the potential by 30%.

Furthermore, the economic potential is not evaluated. As a next step, costs for pipes and DH extension could be included [18,140]. Instead, we base our assumptions on the findings of Heat Roadmap Europe [18] and on a focus on the 10 km default distance range. Our findings emphasise that the pipe length is most probably not the limiting factor. A cost analysis is needed to prioritise the measure that will be cost-efficient at a system level: applying best available technologies and efficiency measures in processes, using the excess heat internally at the site, or feeding the heat into DH systems. But it should be noted, that especially for DH networks, costs are not the only factor defining the realisation of such long-term projects, the framework conditions and communal strategies are also very important.

As a summary, the limitation shows that there are uncertainties in excess heat estimations, that can be overcome or decreased with further research, but some will persist, as excess heat utilisation is dependent on local parameters. In the end, there are factors that could increase the estimated potential, others could limit it further.

3.4.3 Conclusions

The results show that there are at least 1608 large point sources of industrial excess heat available, across different subsectors. Refineries have the largest potentials with a total excess heat potential of 331 PJ/a at status quo, allocated to only about 100 sites. The production of chemicals and steel have high average excess heat potentials per site, each with only around 100 sites in the EU-28. The sites that produce paper, cement, and glass are more distributed, having lower average excess heating potentials per site. The amount of heat that is available depends mainly on two factors: the heat recovery measures that use the excess heat internally, and the temperature at which the exhaust gas is cooled down. These factors should always be included in excess heat estimations, as we found total excess heat potentials from all 1608 industrial sites ranging from 191 to 960 PJ/a depending on the assumptions.

The excess heat currently available from industrial flue gases for use in district heating is significant: About 230 PJ can be recovered and used in current DH systems (95 °C), which corresponds to 17% of today's DH demand of buildings for space heating and hot water. This share can be significantly higher for single DH areas and regions, where industrial sites can deliver high amounts of excess heat. Compared to the 25 PJ of industrial excess heat recovery in European district heating systems [126], a rough estimate on this basis would suggest that current industrial excess heat volumes inside or within 10 km of actual district heating areas are nine times higher. The main sources would be the energy-intensive processes in the refineries, cement kilns, and blast furnaces.

The wide implementation of heat recovery in industries limits the excess heat available for district heating: The wide adoption of main internal heat recovery can reduce the currently available excess heat potential by 53% to 108 PJ/a, which, however, is still more than four times the current external recovery level. The industrial subsectors where we assume that there is still a great potential for efficiency measures such as increasing the internal heat recovery, contribute most to the reduction of the overall potential. That is predominantly the non-metallic minerals subsector (−73%) with cement and glass manufacturing.

The utilisation of excess heat at 55 °C doubles the excess heat potentials available for district heating: If DH systems are extended and all are transformed to 4th generation by reducing the operating temperature, the number of sites that are in a 10 km radius of DH areas increases from 752 to 1569 (98% of all sites), with about 83% of these within 2 km. With that, the excess potentials at 55 °C compared to the temperature of 95 °C increase from 230 to 493 PJ/a for average internal heat recovery, and from 108 to 258 PJ/a for maximum heat recovery.

The implementation of 4th generation DH networks with large-scale heat pumps substantially increases the heat recovery potentials: The further reduction of exhaust gas temperature to 25 °C increases the excess heat potential at a 10 km distance up to 941 PJ/a at average rate of an internal heat recovery. If the maximum potential of efficiency measures in industrial sites is applied, this potential is reduced by 28% to 679 PJ/a. In this analysis, 25 °C are shown as a lower estimate to depict the maximum potential for the supply of 4th generation DH networks with large-scale heat pumps or of cold DH networks where the heat is supplied to the end-consumer with a heat pump (decentral or central at substations).

Industrial sites are located often within 2 km to district heating areas: Considering that 83% of all industrial sites analysed and 91% of the total annual excess heat potential at 692 PJ (25 °C, with internal heat recovery for industry) are located inside or within 2 kilometres from possible DH areas, we expect a high economic feasibility for the connection of most industrial sites recovering excess heat in the EU-28. Combining excess heat sources and the deployment of district heating systems should therefore be a central element in the transition towards a sustainable and CO_2-neutral heating and cooling sector. However, the analysis also shows that industrial excess heat alone will not be sufficient, and the major heat source for district heating will need to come from renewable energy sources.

A.2 Detailed industry specific fuel demand, exhaust temperatures and excess heat estimates

In the following, the assumptions used for the calculation of the excess heat per process are presented per subsector. It includes the temperatures of the exhaust gas, the SEC per tonne of respective product, the calculated percentage of available excess heat of the fuel input or the absolute values in GJ/tonne of the product and the diffusion rate of processes within the sites that produce the specific product. The assumed future diffusion rate accounts for the implementation of more efficient process design in the future.

TableAnnex 2: Iron and Steel Industry. Assumptions: SEC values from [106]. For more details see [152].

	Exhaust Gas Temperature (°C)	Fuel SEC (GJ/t)	Unit	% of Fuel Input as Excess Heat			Current Diffusion Rate (%)	Assumed Future Diffusion Rate (%)
				25 °C	55 °C	95 °C		
Coke ovens								
Sensible heat in COG	816	-	GJ/tonne coke	0.98	0.95	0.91	100%	0%
Sensible heat in COG; with HR	449	-	GJ/tonne coke	0.47	0.44	0.40	0%	100%
Excess heat in off-gases	200	1.6	% of fuel input	44%	13%	9%	100%	100%
Blast furnaces								
Sensible heat in BFG	221	-	GJ/tonne steel	0.42	0.36	0.27	100%	100%
Blast stove exhaust	250	1.5	% of fuel input	13%	10%	8%	50%	0%
Blast stove exhaust; with HR	130	1.4	% of fuel input	6%	4%	2%	50%	100%
Basic oxygen furnace								
Sensible heat in BOF off-gases	1704	-	GJ/tonne steel	0.56	0.55	0.54	30%	0%
Sensible heat in BOF off-gases; with HR	250	-	GJ/tonne steel	0.02	0.02	0.01	70%	100%
Electric arc furnace								

Electric arc furnace	1204	1.8	% of fuel input	12%	12%	12%	70%	0%
Electric arc furnace; with HR	204	1.5	% of fuel input	2%	1%	1%	30%	100%

TableAnnex 3: Non-ferrous Metals Industry. Source: [106] for electricity demand and [134] for excess heat estimation

	Exhaust Gas Temperature (°C)	Electricity SEC (GJ/t))	Unit	% of Fuel Input as Excess Heat			Current Diffusion Rate (%)	Assumed Future Diffusion Rate (%)
				25 °C	55 °C	95 °C		
Primary aluminium	700	54	GJ/tonne aluminium	1.09	1.05	1.00	100%	100%

TableAnnex 4: Glass Industry: Specific values based on produced glass in tonne. Assumptions: To estimate the SECs per technology with and without batch/cullet preheating, we used the fuel use reported in [106] as an average, and we assumed that for 40% of the production it is 15% lower and for 60% of the production 15% higher. The typical energy savings from batch/cullet preheating are around 10–20% [157]. For more details see [152].

	Exhaust Gas Temperature (°C)	Fuel SEC (GJ/t)	Unit	% of Fuel Input as Excess Heat			Current Diffusion Rate (%)	Assumed Future Diffusion Rate (%)
				25 °C	55 °C	95 °C		
Container glass								
Recuperative	982	6.2	% of fuel input	60%	47%	45%	60%	0%
Recuperative; with HR	200	4.6	% of fuel input	19%	7%	5%	40%	100%
Regenerative	427	5.2	% of fuel input	30%	18%	16%	60%	0%
Regenerative; with HR	200	3.8	% of fuel input	19%	7%	5%	40%	100%
Oxy-fuel	1427	5.2	% of fuel input	35%	30%	29%	60%	0%
Oxy-fuel; with HR	200	3.8	% of fuel input	8%	3%	2%	40%	100%
Flat glass								
Recuperative	982	9.2	% of fuel input	60%	47%	45%	100%	0%
Recuperative; with HR	200	7.8	% of fuel input	19%	7%	5%	0%	100%
Regenerative	427	7.5	% of fuel input	30%	18%	16%	100%	0%
Regenerative; with HR	200	6.4	% of fuel input	19%	7%	5%	0%	100%

Oxy-fuel	1427	5.6	% of fuel input	35%	30%	29%	100%	0%
Oxy-fuel; with HR	200	4.8	% of fuel input	8%	3%	2%	0%	100%

TableAnnex 5: Cement Industry: Specific values based on produced clinker in tonne. Assumptions: SEC from [106]. Current diffusion rate not applicable as production volumes are known for each kiln technology. For more detail see [152].

	Exhaust Gas Temperature (°C)	Fuel SEC (GJ/t)	Unit	% of Fuel Input as Excess Heat			Current Diffusion Rate (%)	Assumed Future Diffusion Rate (%)
				25 °C	55 °C	95 °C		
Wet	338	5.5	% of fuel input	20%	15%	13%	not needed	not needed
Dry	449	4.5	% of fuel input	27%	22%	20%	not needed	not needed
Dry, with preheating and precalciner (4 stage preheating)	338	3.3	% of fuel input	22%	17%	15%	not needed	not needed
Dry with preheating and precalciner (5-6 stage preheating)	250	3.0	% of fuel input	17%	12%	10%	not needed	not needed

TableAnnex 6: Pulp and Paper Industry: Specific values based on produced pulp (pulp making) or paper (paper making) in tonne. For more details see [152].

	Exhaust Gas Temperature (°C)	Fuel SEC (GJ/t)	Unit	% of Fuel Input as Excess Heat			Current Diffusion Rate (%)	Assumed Future Diffusion Rate (%)
				25 °C	55 °C	95 °C		
Pulp making								
Chemical pulping	260	12.3	% of fuel input	9%	3%	3%	30%	0%
Chemical pulping; with HR	177	10.3	% of fuel input	8%	2%	1%	70%	100%
Lime burning	650	2.2	% of fuel input	52%	36%	34%	30%	0%
Lime burning; with HR	200	1.4	% of fuel input	24%	8%	6%	70%	100%
Mechanical pulping	260	2.2	% of fuel input	9%	3%	3%	30%	0%
Mechanical pulping; with HR	177	1.9	% of fuel input	8%	2%	1%	70%	100%

	Exhaust Gas Temperature (°C)	Fuel SEC (GJ/t)	Unit	% of Fuel Input as Excess Heat			Current Diffusion Rate (%)	Assumed Future Diffusion Rate (%)
				25 °C	55 °C	95 °C		
Recovered fibres	260	0.6	% of fuel input	9%	3%	3%	30%	0%
Recovered fibres, with HR	177	0.5	% of fuel input	8%	2%	1%	70%	100%
Paper making								
Board & packaging paper	260	5.7	% of fuel input	9%	3%	3%	30%	0%
Graphic paper	260	8.4	% of fuel input	9%	3%	3%	30%	0%
Tissue paper	260	8.1	% of fuel input	9%	3%	3%	30%	0%
Board & packaging paper; with boiler HR	177	4.9	% of fuel input	8%	2%	1%	70%	100%
Graphic paper; with boiler HR	177	7.2	% of fuel input	8%	2%	1%	70%	100%
Tissue paper; with boiler HR	177	6.9	% of fuel input	8%	2%	1%	70%	100%

TableAnnex 7: Chemical Industry: Specific values based on produced product in tonne. Assumptions: SEC estimated from the fuel use reported in [170], while also accounting for the share of production that uses boiler economizers and the share that does not. When economizers are used, 5–10% of the fuel use can be saved [170]. For more details see [152].

	Exhaust Gas Temperature (°C)	Fuel SEC (GJ/t)	Unit	% of Fuel Input as Excess Heat			Current Diffusion Rate (%)	Assumed Future Diffusion Rate (%)
				25 °C	55 °C	95 °C		
Ethylene								
Furnace	149	23.9	% of fuel input	17%	4%	3%	100%	100%
Boiler	260	13.3	% of fuel input	22%	10%	8%	30%	0%
Boiler, with HR	149	11.4	% of fuel input	17%	4%	3%	70%	100%
Ammonia								
Boiler	260	5.1	% of fuel input	22%	10%	8%	30%	0%
Boiler, with HR	149	4.4	% of fuel input	17%	4%	3%	70%	100%

	Exhaust Gas Temperature (°C)	Fuel SEC (GJ/t)	Unit	% of Fuel Input as Excess Heat			Current Diffusion Rate (%)	Assumed Future Diffusion Rate (%)
				25 °C	55 °C	95 °C		
Chlorine diaphragm								
Boiler	260	3.6	% of fuel input	22%	10%	8%	30%	0%
Boiler; with HR	149	3.1	% of fuel input	17%	4%	3%	70%	100%
Chlorine membrane								
Boiler	260	1.2	% of fuel input	22%	10%	8%	30%	0%
Boiler, with HR	149	1.0	% of fuel input	17%	4%	3%	70%	100%

TableAnnex 8: Refineries: Specific values based on produced product in tonne. Assumptions: SEC estimated from the fuel use reported in [106], while also accounting for the share of production that uses boiler economizers and the share that does not. When economizers are used, 5–10% of the fuel use can be saved [170]. In boilers fired with by-product fuels, such as refinery fuel gas, the minimum final exhaust temperature after waste heat recovery is more likely to be higher compared to when conventional fuels are used [134]. For more details see [152].

	Exhaust Gas Temperature (°C)	Fuel SEC (GJ/t)	Unit	% of Fuel Input as Excess Heat			Current Diffusion Rate (%)	Assumed Future Diffusion Rate (%)
				25 °C	55 °C	95 °C		
Boiler, no HR								
Refinery basic	260	1.60	% of fuel input	29%	11%	9%	30%	0%
Refinery gasoline focused	260	2.00	% of fuel input	29%	11%	9%	30%	0%
Refinery diesel focused	260	2.30	% of fuel input	29%	11%	9%	30%	0%
Refinery flexible;	260	2.10	% of fuel input	29%	11%	9%	30%	0%
Boiler, with HR								
Refinery basic	177	1.40	% of fuel input	24%	6%	4%	70%	100%
Refinery gasoline focused	177	1.70	% of fuel input	24%	6%	4%	70%	100%
Refinery diesel focused	177	2.00	% of fuel input	24%	6%	4%	70%	100%
Refinery flexible	177	1.80	% of fuel input	24%	6%	4%	70%	100%

A.3 Spatial matches of industrial sites and district heating areas by distance classes

TableAnnex 9: Summary table for 1st rank spatial matches with reference to the Current potential and System efficiency at 55 °C and 25 °C by distance classes

Scenario	Dimension	Inside (0 km)	Up to <2 km	2 up to <5 km	5 up to < 10 km	10 up to < 25 km	25 up to < 100 km	> 100 km	Total
Current potential	Matches DH-A (n)	206	187	163	196	324	383	149	1608
	Share (%)	13%	12%	10%	12%	20%	24%	9%	100%
	Matches (Acc.) (n)	206	393	556	752	1076	1459	149	1608
	Share (Acc.) (%)	13%	24%	35%	47%	67%	91%	9%	100%
Current potential (95 °C)	Heat (PJ/a)	54	60	52	64	77	66	53	425
	Share (%)	13%	14%	12%	15%	18%	16%	12%	100%
	Heat (Acc.) (n)	54	114	166	230	306	373	53	425
	Share (Acc.) (%)	13%	27%	39%	54%	72%	88%	12%	100%
System efficiency	Matches DH-P (n)	702	639	149	79	32	4	3	1608
	Share (%)	44%	40%	9%	5%	2%	0.25%	0.19%	100%
	Matches (Acc.) (n)	702	1341	1490	1569	1601	1605	3	1608
	Share (Acc.) (%)	44%	83%	93%	98%	99.6%	99.8%	0.2%	100%
System efficiency (55 °C)	Heat (PJ/a)	132	106	17	4	4	1	0.4	264
	Share (%)	50%	40%	6%	2%	1%	0.5%	0.2%	100%
	Heat (Acc.) (n)	132	238	254	258	262	263	0.4	264
	Share (Acc.) (%)	50%	90%	96%	98%	99%	99.8%	0.2%	100%
System efficiency (25 °C)	Heat (PJ/a)	384	248	39	9	10	2	1.5	692
	Share ()	55%	36%	6%	1%	1%	0%	0%	100%
	Heat (Acc.) (n)	384	632	671	679	689	691	2	692
	Share (Acc.) (%)	55%	91%	97%	98%	100%	100%	0%	100%

4 The effect of low-carbon processes on industrial excess heat potentials for district heating in the EU: A GIS-based analysis

Pia Manz, Tobias Fleiter, Wolfgang Eichhammer: The effect of low-carbon processes on industrial excess heat potentials for district heating in the EU: A GIS-based analysis. In: Smart Energy 10 100103, 2023. DOI: 10.1016/j.segy.2023.100103.

4.1 Introduction

The European Union (EU) has committed itself to becoming a climate-neutral society and economy, i.e. net-zero emissions by 2050. This is demonstrated in its Green Deal from 2019 to 2020 [3,171,172], the scenarios developed in 2020 [71], and the set of proposals in its 'Fit for 55' package in 2021 to bring EU legislation in line with the climate targets [2]. In 2020, the industrial and building sector accounted for 34%, and energy supply for 24% of GHG emissions in the EU [173]. Even though these sectors have reduced their emissions by 20% over the last decade, a fundamental transformation is needed to achieve net-zero emissions, i.e. climate-neutrality. These terms signify that a future energy system and society does not emit more GHG to the atmosphere than are removed by the planet's natural adsorption or additional measures. About 50% of the final energy demand is used for heating, mainly for buildings and process heat in industry [6]. Thus, strategies for climate-neutral heating are essential. Strategies include the use of CO_2-neutral energy carriers and improving energy efficiency, but also reducing the primary heat demand for district heating (DH) by using heat that is available from industrial processes, i.e. excess heat[5].

To achieve carbon-neutrality in the industrial sector, all subsectors need to undergo transformation and the following steps are crucial: First, process heat will need to be supplied by renewable energy sources [174,175]; second, process emissions stemming from chemical reactions (e.g. iron ore reduction using coal leads to CO_2 emissions in steel production) should be avoided or reduced as much as possible [175,176]; and third, material demand will change if material circularity is promoted [177]. It is ex-

[5] The term *waste heat* is frequently used as a synonym for *excess heat*.

pected that many industrial processes will continue to produce excess heat, which cannot be used in the process or on-site for other purposes [122,178–180]. However, this fundamental transformation will affect the excess heat available from industrial processes and could reduce it.

There are two main strategies to become climate-neutral in the building sector: increasing the insulation level of the building stock and changing the energy source for heating buildings [181]. There are national legislations in effect in the member states driven by the Energy Performance of Buildings Directive[6] [183], which sets energy efficiency standards, for both newly built and existing buildings. District heating can be an efficient source of climate-neutral heating [16–18,21], if the provided heat is generated by climate-neutral sources. In 2020, however, 68 % of DH in the EU was still based on fossil fuels [184]. Industrial excess heat could be one option for a climate-neutral DH supply.

4.2 Background

Several studies have quantified the possible utilisation of industrial excess heat in the EU, identifying potentials ranging from 80 up to 800 TWh per year [76,82,83,90] (compared to the current DH demand of residential and non-residential buildings in 2020 of 336 TWh [118]). This identified potential could contribute to the transformation of DH generation [83,90,138,140,185]. These studies are based on different methods for estimating excess heat, which were described in a previous publication [90]. However, these studies did not systematically consider the transformation of the energy system and of the industrial sector to low-carbon processes. To the best of our knowledge, to date, no study assessing industrial excess heat potentials in the EU-27 has also considered the transformation of industrial production towards climate-neutral processes. This paper aims to fill this gap by matching excess heat potentials spatially to district heating areas in a climate-neutral energy system.

Spatial matching is commonly used to analyse the techno-economic potential for utilising heat in DH systems and has been applied in national and EU-wide potential analyses that included industrial excess heat [83,138,140,185,186]. Spatial matching considers the locations of both the heat sources and the DH systems, as well as the quantity of heat that could actually be provided and utilised in the respective areas. Several studies have pointed out that the most economic DH areas are those with the highest heat demand and thus the lowest specific distribution costs for DH [18,30,55–57,85,94,128,132,187,188]. However, only a few studies have included the effect of building renovation and its impact on future demand when determining economic DH areas, especially at EU level, e.g. [48,189–191]. In this paper, we use open data for the

[6] Negotiations are underway for a recast of the EPBD [182] as part of the "Fit for55" package [2].

spatial extent of current and possible DH areas for the EU from the Pan-European Thermal Atlas (Peta) 5.2 [89,90], and assume an efficiency improvement of the buildings within the identified areas.

In the future, district heating systems can have temperatures below 50 °C, often called 4th generation DH [21], which increases the possibility to utilise excess heat and renewables more efficiently, while reducing heat losses [23,192]. In a previous analysis, we found that decreasing the temperature at which the industrial excess heat is recovered from 95 °C to 55 °C increases the potentials by about 20% [90]. However, this did not take the future transformation of industry into account. Thus, we now aim to quantify the effect of a reduced system temperature when matching of industrial locations with future excess heat potentials to DH areas.

This paper quantifies the potential contribution of industrial excess heat in DH grids in a future climate-neutral energy system for the EU. We particularly aim to understand how the transformation to low-carbon industrial processes will affect the excess heat available that can be used to supply DH to the building sector.

To account for the transition of the industry sector, we integrate future industrial production quantities and low-carbon processes, as the transformation of process and material demands will substantially change the available excess heat. We estimate the process-specific excess heat potentials per industrial plant and then spatially match the georeferenced available excess heat from climate-neutral industry in a Geographic Information System (GIS) to a data set of "Current DH areas" and "Possible DH areas". To deal with uncertainties, we construct several scenarios and variations to show a range of possible outcomes. This analysis contributes to the discussion of the future potential of industrial excess heat for supplying DH and the impact of industrial transformation.

4.3 Method and data

The method consists of three steps (Figure 4.1). The year 2015 is used as a status quo reference due to data availability for industrial sites and DH areas, 2050 is the year of reference for a climate-neutral energy system and the geographical reference is the EU-27.

1. *Estimation of industrial excess heat potentials:* We estimated georeferenced future excess heat potentials from energy-intensive industrial sites. The specific excess heat potential per process was based on a broad literature review. In particular, we considered future low-carbon production processes like electrified and hydrogen-based process heating and distinguished a transformation and an import scenario.
2. *Matching of DH areas and demand:* We took the two data sets available from Peta 5.2 [89] and mapped the DH coverage of Current and Possible DH areas, together with the associated heat demand. We estimated DH demand based on assumptions concerning the connection rate and improved energy efficiency of

the building stock, which consequently lowered the demand for heat. We distinguished in particular system temperature levels of 25, 55 and 95 °C.

3. *Spatial matching to calculate the utilisation potential:* We matched the excess heat potentials with the data set of Current and Possible DH areas to estimate the range of potential utilisation in district heating supply.

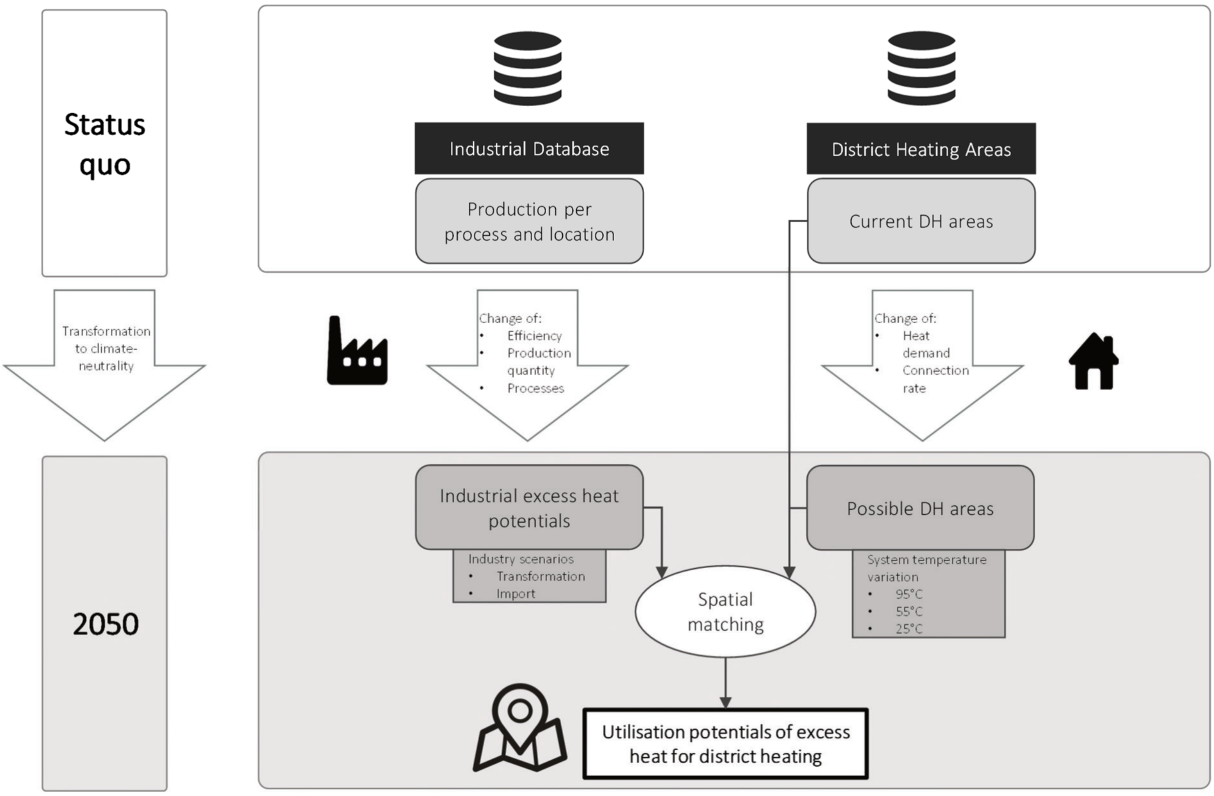

Figure 4.1: Methodology applied in the study to estimate the future excess heat utilisation for DH

The industrial excess heat potential (based on the respective industry scenario) is combined with the Current and Possible DH areas (with different system temperatures), i.e. matched separately to these DH areas. In total, 12 combinations were calculated, showing the range of possible future developments and their influence on the results.

4.3.1 Estimating industrial excess heat potentials

This section describes the methodology and databases used to estimate the potential excess heat at industrial sites available for external utilisation in a climate-neutral energy system. The analysis focuses on energy-intensive industries producing steel, aluminium, cement, glass, paper, chemicals and refinery products. For these processes, data on site-specific annual production are available in several databases and stored in the Industrial Database (see Section 4.3.1.2). The excess heat available at industrial sites depends on several factors that will change in the future. Important factors considered here include the future production volumes, the locations of industrial sites and the switch from mostly fossil-based to low-carbon processes.

4.3.1.1 Industrial production volumes and processes

The assumptions concerning future production volumes and possible technology switch to replace the carbon-intensive processes were based on the study "Industrial Innovation: Pathways to deep decarbonization of Industry", 2018 for DG Clima [175,193]. We used the production volumes of the scenario 4b "Mix95" with a 95% reduction of GHG emissions, as this describes an almost carbon-neutral EU industry sector with a strong role of new low-carbon processes. There are several central assumptions of the scenario that influence material demand and process design. The gross value added of all industrial sectors will grow, but energy-intensive industrial subsectors will grow at a slower rate than the other subsectors. Circular economy approaches (recycling and material efficiency) will reduce the demand for primary materials like steel or chemicals. New low-carbon processes will completely replace today's fossil-based and emission-intensive processes. Examples include hydrogen-based steelmaking and electrified furnaces. CCS will be used to capture any remaining process emissions in lime and cement production. In the Mix95 scenario, electricity is the most important energy carrier, with hydrogen for high-temperature processes and as a feedstock in chemical processes. FORECAST, which is the bottom-up industry sector model used, provides a high level of technological detail [47], which makes a process-specific estimation of excess heat potentials possible.

In addition to the production volumes at national level and the general technological pathways described above, we further assumed that energy efficiency potentials and internal excess heat recovery in all plants are exploited to the technical limits. This is a normative approach that prioritizes energy efficiency and internal excess heat use over the external use of excess heat. Furthermore, there is still substantial uncertainty about how process heat will be supplied in the future. While the DG Clima study [175] assumes widespread electrification in process heating, hydrogen is also a feasible and frequently discussed alternative for high-temperature processes [194]. Additionally, the import of basic materials could move outside the EU to locations with greater availability of renewable energy resources. Two possible scenarios are calculated in order to cope with these uncertainties:

- Transformation scenario: Industrial furnaces will be electrified where deemed feasible, based on the Mix95 scenario in Ref. [175], with the difference that hydrogen will be used in glass and cement production [194].
- Import scenario: The production output of industry will decrease as the energy-intensive basic materials ammonia, ethylene and iron sponge will be imported to the EU. Everything else is the same as in the transformation scenario.

Excess heat from electrolysers on site was not considered in this study. While there might be certain industrial sites that will produce hydrogen locally, this is very unlikely for large industrial plants due to enormous hydrogen demands and the need to store it locally.

4.3.1.2 Locations of industrial sites

The location of all the major energy-intensive industrial sites in the EU today are listed in the Fraunhofer ISI Industrial Database, which includes information about industrial production sites, their locations and associated processes together with annual production output from emission and sectoral databases, as described in previous publications [90,137]. The sites listed in the database represent 62% of the EU's total industrial energy demand[7]. These industrial sites were published together with the estimated excess heat potentials for current processes as open data in Hotmaps [48] and Peta 5.2 [89]. In this analysis, we assumed that the current locations will remain and all sites with similar processes will undergo the same transformation to low-carbon processes. The production volumes for 2050 at national level from the Mix95 scenario were distributed to the individual sites based on current production capacities. In the import scenario, it was assumed that the respective production plants will be shut down.

Table 4.1 shows the current and future production volumes, number of georeferenced installations and assumed process development for each energy-intensive product considered. For example, direct reduction of iron ore with hydrogen (H-DR) was assumed for steel production in the transformation scenario. This means that all current blast furnaces will be replaced by hydrogen shaft furnaces together with electric arc furnaces (EAF). Each of these installations will have about a third of the current capacity in the future, as overall production of primary steel will decrease. Coke ovens and basic oxygen furnaces will be phased out together with the blast furnaces and will not be replaced. In the import scenario, only EAFs were assumed at these sites, since iron sponge is imported.

[7] The listed sites cover almost all of the processes needing high temperatures above 500 °C and most processes with temperatures between 200 and 500 °C. Excess heat from other industrial processes was not quantified using the bottom-up methodology due to the lack of site-specific production data. These sites could contribute a smaller share of excess heat in the future, especially for low-temperature DH (missing processes with significant demand for process heat above 200 °C are gypsum, lime burning, brick, carbon black, bread and bakery, soda ash) [119].

Table 4.1: Current status and future transformation of processes with excess heat. Technology data and production from [175], hydrogen processes based on [194], number of sites based on [90]

Product	Annual production in Mt in EU		No. installations in EU, 2015	Process 2015	Process 2050	
	2015	2050			Transformation scenario	Import scenario
Steel, primary	92	33	52	Coke ovens	Phased out	
			56	Blast furnaces/Direct reduction natural gas	H-DR + EAF	Import of iron sponge, EAF
			32	Basic oxygen furnace	Phased out	
Steel, secondary	63	112	186	Electric arc furnace	Increase of secondary steel (~77%)	
Aluminium, primary	2	1	16	Bayer & Hall–Héroult process	Process 2015 remains	
Aluminium, secondary	3	3	154	Melting furnace	Increase of secondary aluminium (~70%)	
Container glass	20	18	165	Recuperative / Regenerative	Hydrogen melting	
			9	Oxy-fuel		
Flat glass	12	14	61	Recuperative/Regenerative	Hydrogen melting	
			3	Oxy-fuel		
Clinker	123	98	28	Wet	Hydrogen furnaces	
			156	Dry		
			24	Dry and preheating		
Pulp	26	18	123	Chemical pulping	Electrification	
	8	5	58	Mechanical pulping	Process 2015 remains	
	45	66	457	Recovered fibres	Electrification	
Paper	89	97	922	Paper making	Electricity for process heat and heat pumps	
Ammonia	18	14	26	Haber-Bosch	Feedstock H2	Phased out
Chlorine	11	10	9	Diaphragm/Mercury	Replaced by membrane process	
			60	Membrane	Process 2015 remains	
Ethylene and Olefins	19	20	98	Steam cracker (Refineries)	Synthesis of methanol and olefins	Phased out

4.3.1.3 Excess heat factors of low-carbon processes

This section describes the approach used to calculate the excess heat potential per process, presents the data used per subsector and summarizes the resulting indicators. We calculated the specific excess heat potentials per process according to the method presented in Ref. [90], which was based on [134], where applicable. We used the excess heat factors from our previous publication [90] for the current processes. The excess heat potentials for the low-carbon processes were calculated for three different temperature levels, at which the heat will be recovered externally: 25 °C as a lower limit, 55 °C, and 95 °C as the upper limit. We assumed that internal heat utilisation potentials will be exploited with priority in the future when new processes are installed and the pressure for efficient heat utilisation increases due to higher energy costs. For hydrogen processes, the estimation was based on a combustion calculation considering temperatures, energy carrier composition and mass flow of the exhaust gases. It calculates the enthalpy in the exhaust gases at a certain temperature based on the gas composition, which is mainly water vapour. For electrical furnaces, there is no exhaust gas from fuel combustion, so the excess heat factors were based on the energy efficiency values of the process. There is a lack of data for some of these processes, as they are not yet in industrial operation, although there may be larger demonstration plants. Therefore, parameters based on thermodynamic models and estimates of efficiency were taken into account, and data gaps were closed by comparisons with similar processes. These are discussed in the following paragraph on a process level. For all processes, the maximum level of internal heat recovery was assumed. The resulting specific excess heat factors for each process are summarised in Table 4.2.

To calculate the total available excess heat per process at one site, the annual production per process $m_{Product, year}$ in tonne was multiplied with the specific excess heat factor $\frac{E_{ex}}{m_{Product}}$ in GJ/tonne:

$$E_{ex,year} = \frac{E_{ex}}{m_{Product}} \bullet m_{Product,year} \tag{9}$$

Table 4.2: Estimated specific excess heat factors for processes in a carbon-neutral energy system

Product	Process technology 2050	Exhaust gas temperature (°C)	Excess Heat 25 °C (GJ/t)	Excess Heat 55 °C (GJ/t)	Excess Heat 95 °C (GJ/t)	Calculation based on	Calculation method
Steel, primary	Hydrogen direct reduction shaft furnace	250	0.19	0.04	0.03	Bhaskar et al. 2020 [195]	Exhaust gas composition based on Manz et al. 2021 [90]
	Electric arc furnace	200	0.03	0.02	0.02	Manz et al. 2021 [90]	Directly taken from source
Container glass	Electric furnace	200	0.26	0.09	0.07	Stormont 2010 [196], Ireson et al. 2019 [197]	Estimation of process efficiency
	Hydrogen furnace	200	0.37	0.13	0.09	Neuwirth et al. 2022 [194]	Exhaust gas composition based on Manz et al. 2021 [90]

Product	Process technology 2050	Exhaust gas temperature (°C)	Excess Heat 25 °C (GJ/t)	Excess Heat 55 °C (GJ/t)	Excess Heat 95 °C (GJ/t)	Calculation based on	Calculation method
Flat glass	Electric furnace	200	0.43	0.15	0.11	Stormont 2010 [196]	Estimation of process efficiency
	Hydrogen furnace	200	0.62	0.22	0.16	Neuwirth et al. 2022 [194]	Exhaust gas composition based on Manz et al. 2021 [90]
Cement clinker	Electric furnace	250	0.45	0.32	0.24	Antunes et al. 2021 [198]	Estimation of process efficiency
	Hydrogen furnace	250	0.54	0.38	0.32	Neuwirth et al. 2022 [194]	Exhaust gas composition based on Manz et al. 2021 [90]
Ammonia	Haber-Bosch with hydrogen as input	150	2.15	1.51	1.25	Smith et al. 2020 [199]	Thermodynamic analysis of process
Ethylene/Olefins	Methanol synthesis and MtO	-	3.80	0.97	0.56	Thonemann et al. 2019 [200]; Fritz et al. 2020 [201]	Thermodynamic analysis of process
Steel rolling/forming	No fundamental changes	-	0.01	0.01	0.01	Manz et al. 2021 [90]	Directly taken from source
Aluminium, primary	No fundamental changes	700	1.09	1.05	1.00	Manz et al. 2021 [90]	Aluminium, primary
Aluminium, secondary	No fundamental changes	538	1.09	0.71	0.65	Manz et al. 2021 [90]	Directly taken from source
Chlorine, membrane	No fundamental changes	149	0.18	0.04	0.03	Manz et al. 2021 [90]	Directly taken from source

Steel. Hydrogen-based steel production offers the possibility of a carbon-free reduction of iron ore to iron, in contrast to the conventional blast furnace and converter route based on coke [202–206]. Several pilot projects for direct reduction in shaft furnaces began in Sweden, Germany and China in 2020 [207–213].[8] In this paper, the ex-

[8] One pilot plant for the direct reduction of iron ore with hydrogen in a shaft furnace was built in Sweden in 2020. In addition, the partial replacement of coke with hydrogen in the blast furnace route is currently being tested by Dillinger/Saarstahl and Thyssenkrupp Steel in Germany. Direct reduction plants with (partial) hydrogen usage are announced by the HBIS Group to be in operation in China, and were started in 2022 by SALCOS/Salzgitter AG in Germany, and in 2023 by ArcelorMittal in Germany, Liberty in Romania and H2GS in Sweden.

cess heat estimation was based on the hydrogen direct reduction and electric arc furnace route in all scenarios.[9] The production sites of blast furnaces will be converted into H-DR shaft furnaces and EAF. The import scenario assumes that the first production stage of reducing iron ore to iron sponge is relocated to areas outside the EU where green hydrogen can be produced at lower costs, as vast amounts of hydrogen will be needed.

The temperature in the shaft furnace was assumed to be 800 – 900 °C [214,215]. The exhaust gas contains water and excess hydrogen, which is separated from the water in a condenser and then reintroduced to the shaft furnace after preheating. The energy from cooling in the condenser can be used to preheat the hydrogen [215]. We used the modelling results of Bhaskar et al., 2020 [195] with a calculated exhaust gas temperature at 250 °C. Based on that, we calculated the energy of the exhaust gas to assess the specific excess heat factor. We assumed that 50% of this heat is available for utilisation in DH, in order to account for technical limitations, other internal heat utilisation possibilities and utilisation efficiencies.

Aluminium. Primary aluminium production was assumed to remain basically the same process, mainly based on electricity, so excess heat will only change due to efficiency gains and shifts towards more secondary production, which will reduce the total primary production by 30% by 2050. The excess heat values for the Hall-Héroult-process were based on [90], with a limited potential for hydrogen replacing natural gas for process heat [194]. For secondary production, typical losses for electric melting furnaces (e.g. immersion heaters) with heat recovery were based on Brough et al., 2020 [169].

Glass. In glass production, all-electric melting furnaces are already in operation, albeit with smaller capacities than gas-fired furnaces, and for special glass types [216]. More common are electric boosters, which are co-fired furnaces for quality improvements [196,217]. The study of Zier et al., 2021 [216] gives an overview of the decarbonization options for glass production, and regards hydrogen-fired furnaces as well as electrified furnaces as options. Electric furnaces heat the glass melt using several electrodes; microwaves or plasma could be future alternatives. Since there is no exhaust gas present, electric furnaces have an efficiency of up to 90% [197]. As no plants exist with comparable capacities to gas-fired furnaces nor detailed models of energy losses, the electricity scenario assumes that 2% of the energy input can be utilised for external use, with most of the losses being radiant losses from the furnace's walls. Hydrogen-fired furnaces require changes to the process design and future research [218,219]. For these, we used the excess heat factors from our previous study of gas-fired furnaces [90], assuming that natural gas will be completely replaced by hydrogen.

[9] There has been recent progress in using electrolysis for iron making and this could potentially be more energy-efficient than the H-DR process [193].

Cement clinker. Clinker calcination emits large amounts of CO_2, mainly from the chemical reaction. However, about one third of these emissions are from burning fuels and waste in the process. Hydrogen co-fired or electric plasma furnaces could be possibilities, but have not yet been constructed [198,220], and future research is needed for large-scale plants. There are no published data available on demand and efficiency of low-carbon processes for clinker production. The specific energy demand of electric kilns was assumed to be slightly lower than of the conventional process, with estimations about energy efficiency from Ref. [198]. For hydrogen, the specific energy demand values were taken from Ref. [194], and the excess heat factors are similar to those for the conventional process.

Pulp and paper. In general, most process heat in the pulp and paper subsector is used for drying processes and chemical pulp production with temperatures between 100 °C and 200 °C. It is common to use biomass in paper production, using residues like the black liquor from the processes themselves. At a paper production site, usually more low-temperature than high-temperature heat is required. The process steps using higher temperatures could be electrified or use hydrogen, and process heat on lower temperature levels offers huge potential for exploiting the excess heat [193]. Based on this, we assumed on-site utilisation of this excess heat in drying processes using heat pumps with temperatures up to 150 °C, so that no excess heat remains for external use. This was also shown in the study by Rogers, 2018 [221].

Ammonia. Ammonia is conventionally produced using the Haber-Bosch process, with synthesis gas of hydrogen and nitrogen as an input. The hydrogen for the synthesis gas is currently based on steam reforming using natural gas [199]. In the transformation scenario, green hydrogen is used instead. Thus, we assumed that the energy losses from the Haber-Bosch process will remain the same in the future. The process itself is exothermic, and needs electricity for compression, auxiliary aggregates and air separation, depending on the process design. The heat from the reaction generates 2.7 GJ/t with no possible heat utilisation on site [199]. After accounting for conversion losses, we assumed that any remaining heat can be utilised for district heating, depending on the temperature level.

Ethylene and high value chemicals (HVC). Refineries produce oil-based fuels for transport and feedstock for the chemical industry, mainly ethylene and high value chemicals (HVCs or olefins). Thonemann et al., 2019 [200] assumed in one scenario that the total production of ethylene and HVCs is converted to the Methanol-to-Olefines (MtO) route. This route synthesises methanol using hydrogen and carbon dioxide to produce long-chained chemicals like ethylene and other HVCs. We assumed that locations of refineries will remain and produce synthetic HVCs from hydrogen in the MtO route, as the infrastructure already exists for different materials (located close to harbours or rivers, access to pipelines for ethylene). In total, 0.43 t hydrogen is needed for 1 t of HVC. The energy input is 5 GJ/t for MtO and 12 GJ/t for methanol synthesis. This is comparable to the value of 18 GJ/t in Ref. [201]. The methanol synthesis itself is an exothermic reaction [222], resulting in excess heat potentials.

4.3.2 Spatial analysis and matching algorithm

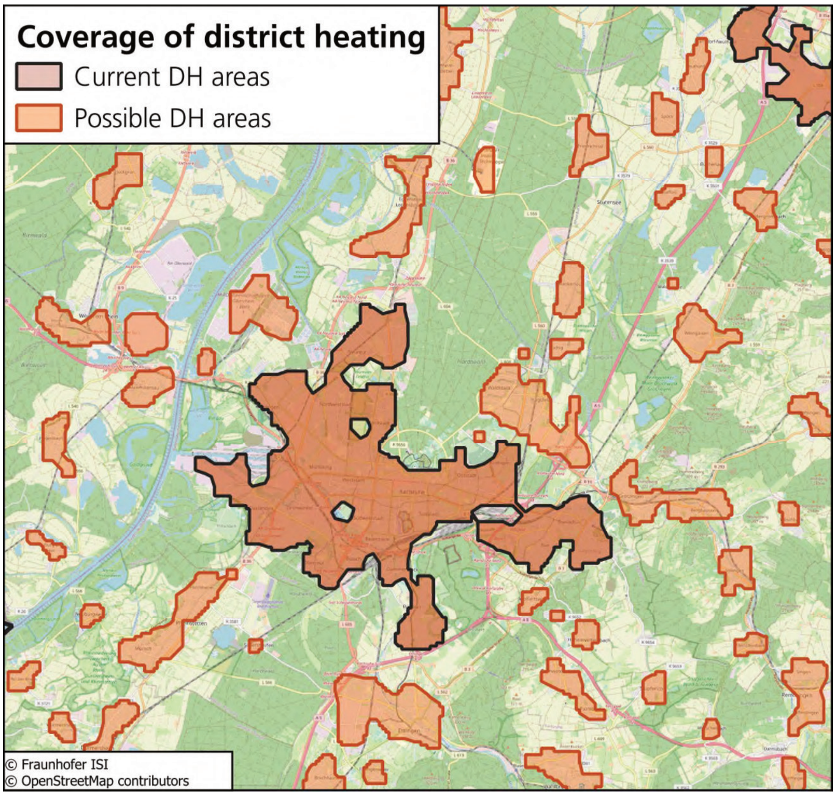

Figure 4.2: **Current and Possible DH areas based on the example of Karlsruhe, Germany. Own illustration based on [89]**

The excess heat potentials from industrial sites identified as point sources were mapped and matched to DH areas to quantify the future utilisation of this excess heat for DH. This section presents the data sources for the DH demand and areas, the data processing as well as the matching method used. We considered different possible future DH coverages, using the open data repository from Peta 5.2 [89]. Two data sets were used from the project report sEEnergies D5.1 [152]: Current District Heating areas and Possible District Heating areas. These data sets can be downloaded as shapefiles with the corresponding heat demand in these areas in the attribute tables, and visualised and processed in a GIS software. Current DH areas represent the locations where DH networks currently exist, originating from the Halmstad University District Heating and Cooling database [164], with further boundary assumptions based on Heat Roadmap Europe data [94]. Possible DH areas represent areas with regional heat demand densities per hectare above 500 GJ per year, determined using the useful heat demand of buildings in the respective area [17,30]. Current DH areas can be seen as the lower limit of DH coverage in the EU. In contrast, Possible DH areas represent a DH market share of 45%, if all the buildings in these areas are connected in the EU in 2050. This can be seen as a very ambitious expansion of DH to include all areas with sufficient heat density (Figure 4.2). This scenario is used to show the upper limit of industrial excess heat that could be utilised in the future. The initial data sets do not include a decrease in heat demands due to building renovation

Two adaptations were made to consider efficiency improvements to the buildings stock and thus the reduced heating demand, and possible developments in the connection rate, i.e. the share of buildings that are connected within the DH area. Similar to building sector analyses, an average reduction of the heating demand to 70% of the current status was assumed for both Current and Possible DH areas, which is stated as necessary in an efficient energy system in Refs. [16,52,223]. The connection rate was assumed to be 46% for Current DH areas, which is the implicitly assumed connection rate in the Current DH area data set, to show the lower limit [85,90], and 100% for Possible DH areas to show the upper limit.

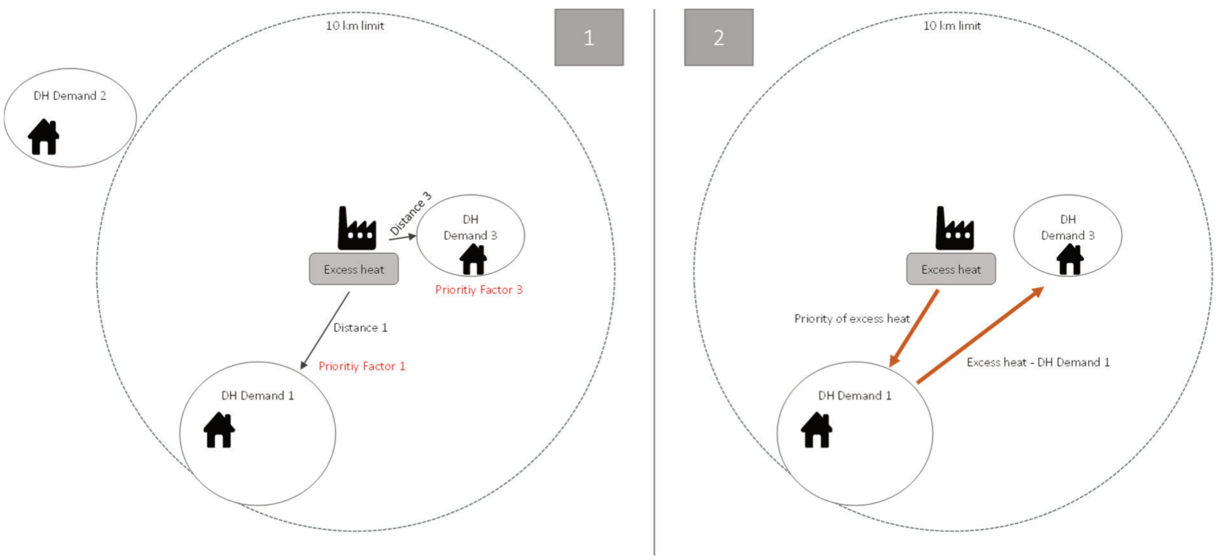

Figure 4.3: Schematic overview of spatial matching algorithm. Step 1 on the left with distance calculations within a 10 km limit and step 2 on the right with prioritised sequential excess heat allocation

The regional analysis and spatial matching to the industrial excess heat sources was conducted in the software QGIS with the PyQGIS plugin [109] with a customised matching algorithm. Industrial locations with excess heat were matched to the most suitable DH areas, within a defined maximum distance. The PyQGIS plugin allows automated processing of regional data. The required inputs include the identified DH areas as polygons, and the excess heat sources as point layers. The matching algorithm consists of two steps (Figure 4.3). First, the industrial sites with excess heat in the transformation and import scenarios were allocated to the Current and Possible DH area polygon data sets, limited by the maximum distance of 10 km from the excess heat source to the boundary of a DH area. This distance is used as a conservative break-even point of cost-effectiveness for connection pipes [90,224]. For this, a spatial grid was created to presort the heat sources to the DH areas. Otherwise, the distances from all industrial excess heat point sources to all DH areas would have been calculated. As a result of this first step, excess heat sources were allocated to all DH areas which do not exceed the maximum distance of 10 km, and for each DH area a prioritisation factor was calculated based on the annual DH demand and distance from the excess heat source. In the second step, the prioritisation factor was used to allocate each excess heat source to a single or to several suitable DH areas sequentially if there is more than one area within the 10 km, to prevent the closest but very small DH area being connected to an industrial site with large amounts of excess heat. This approach is quite similar to the one presented by Möller et al., 2019 [17], but our approach does not consider maximum transmission costs based on delivered heat, as we assumed a conservative maximum distance of 10 km that includes most of the industrial excess heat sources.

The algorithm calculates the supply potential, irrespective of how much of the heat could actually be consumed by the DH areas within the 10 km limit after the prioritisation. The utilisation potential was calculated subsequently, with the annual DH demand in the suitable DH areas as a limit of the supply potential.

4.4 Results

This section describes the results obtained from each methodological step. First, the evolution of industrial excess heat potentials, and second, the results of matching them to DH areas. Finally, we discuss and analyse the implications of industrial transformation for the possible utilisation of industrial excess heat in DH systems. The results are depicted for the three possible system temperatures regarded: 95 °C, 55 °C and 25 °C.

4.4.1 Future industrial excess heat potentials in the EU

The annual industrial excess heat in a climate-neutral energy system ranges from 9.2 TWh (import scenario, 95 °C) up to 50.2 TWh (transformation scenario, 25 °C). These figures indicate the total potential for external use after internal heat utilisation, e.g. for preheating and drying. The import scenario has lower excess heat potentials (37 - 48% of the transformation scenario, depending on the temperature level considered), as basic materials like iron and ethanol are imported, so there is no excess heat available from the production processes involved.

There is a general decrease in the excess heat from industrial sites for all subsectors in a climate-neutral energy system, compared to the status quo (see Figure 4.4 for the results for the temperature level of 55 °C). For the results of all temperature levels, the reader is referred to TableAnnex 10. The figure illustrates the different effects considered when quantifying the excess heat from low-carbon processes separately, starting from current production process and volumes, and average levels of efficiency and internal heat utilisation. The effects are separated to identify the main influencing factors. One major effect on excess heat potentials is the increased energy efficiency of current processes (i.e. using BAT per process and fully exploiting the potential of internal heat utilisation). Thus, energy efficiency was incorporated using the specific excess heat factors from Ref. [90]. We first added these efficiency improvements of today's processes; second, the change in production volumes due to higher material efficiency and circularity; and third, the process transformation assumed in the transformation and import scenarios. Compared to current potentials, the future potentials decrease by 78% - 80% for the transformation scenario and by 90 - 92% for the import scenario, depending on the assumed temperature level of heat utilisation.

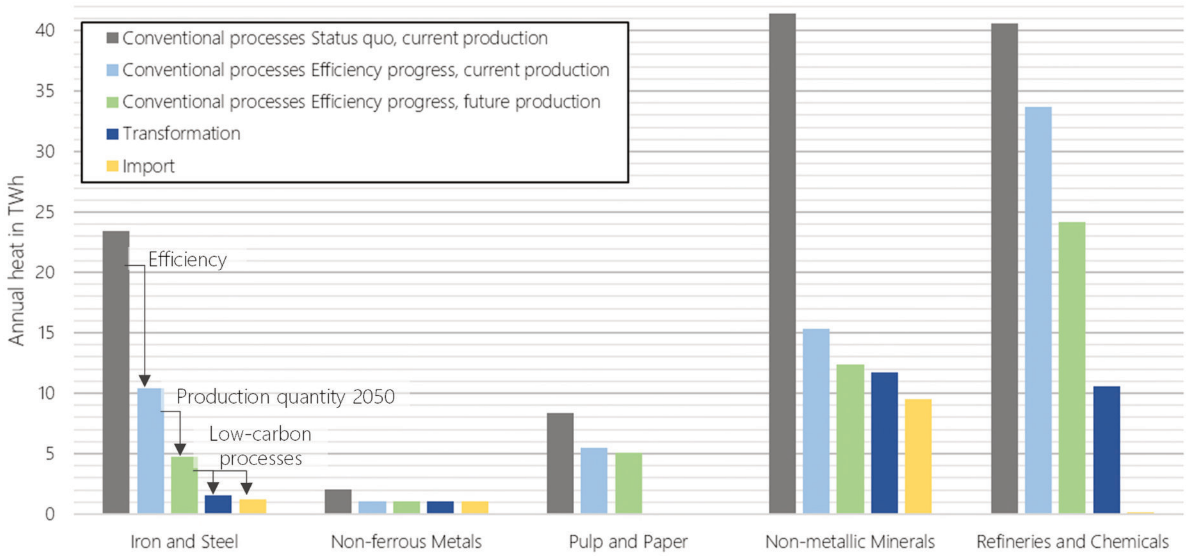

Figure 4.4: **Industrial excess heat potentials available per subsector in the EU for 55 °C, showing the separate effects of future developments: status quo, efficiency progress, production volumes and for the two scenarios of process transformation to low-carbon processes**

Efficiency progress lowers the excess heat potentials by around 40%, with the most significant decrease in the non-metallic subsector. The assumed future production volumes further decrease the potentials by around 16%, compared to the status quo. This is due to a circular economy and a higher share of secondary production routes in steel, aluminium and paper as well as a lower demand for oil-based products. The implementation of low-carbon processes in the transformation scenario reduces the available excess heat potentials even further by another 20%. There is no excess heat from the pulp and paper subsector, because all excess heat is assumed to be utilised internally with heat pumps. The chemical industry and refineries have lower potentials as oil refining will be phased out in a climate-neutral energy system, with a remaining demand for petrochemicals that will be produced synthetically. The synthesis of methanol, ethylene and ammonia could be a potential new source for excess heat. The excess heat potentials in the import scenario are 11% lower than in the transformation scenario. If basic materials are imported, there will be a substantial decrease in the potential excess heat from the chemical and refinery sites as well as from iron and steel sites.

The spatial distribution of industrial plants and corresponding excess heat potentials across the EU is mapped in Figure 4.5 for 55 °C in the case of the transformation scenario. The map reveals industrial cluster in coastal areas or industrial regions, e.g. in the Netherlands/Belgium/North-West Germany. Few sites show high excess heat potentials above 200 GWh per year and more.

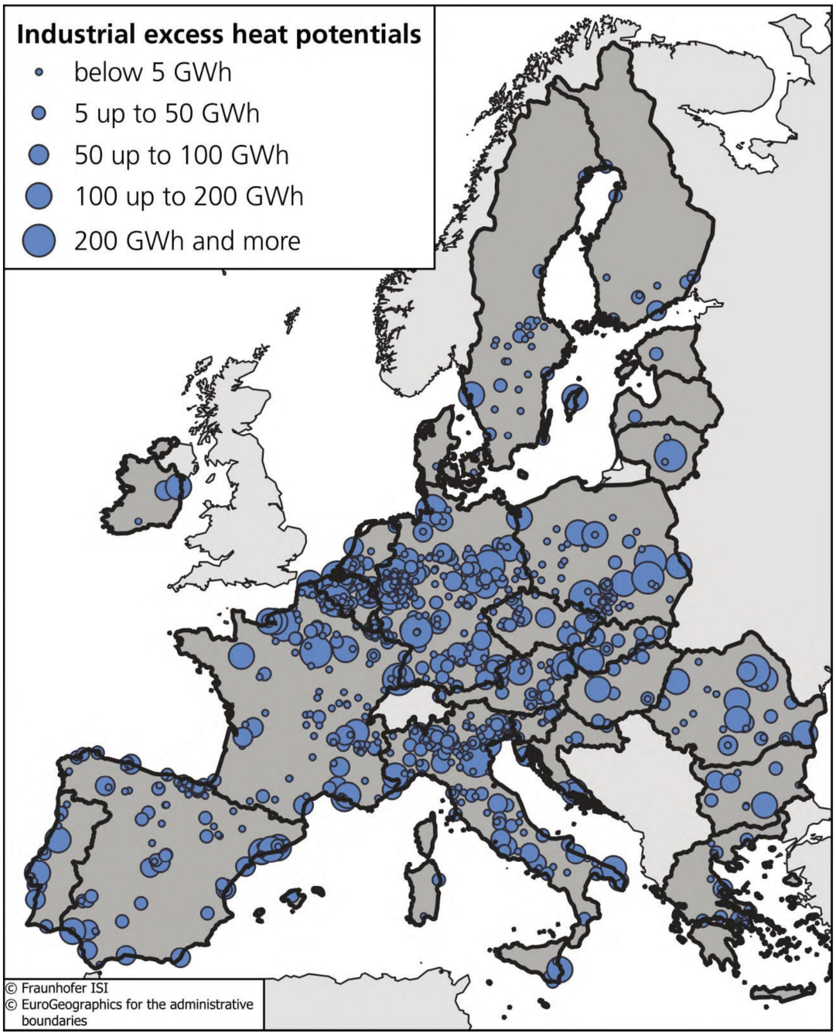

Figure 4.5: Annual industrial excess heat for external use in the EU for 55 °C in the transformation scenario

4.4.2 Utilisation potential of excess heat for DH in the EU

The spatial matching of the industrial excess heat sources with the Current and Possible DH areas for the two industry scenarios and the different temperature levels results in utilisation potentials taking into account the annual heat demand from the matched DH areas (Figure 4.6). The available industrial excess heat for district heating ranges from 3 - 36 TWh per year. The value of the first bar (grey) depicts the total potential of industrial excess heat, before matching with the DH areas. Given the DH demand of

165 TWh in Current DH areas, and 1155 TWh in Possible DH areas, this results in a potential share of industrial excess heat in DH of 1 - 8% (transformation scenario, 55 °C: 3.7%). This figure depends on the assumed DH coverage, temperature level and industry scenario. Industrial excess heat can be utilised by 316 Current DH areas, and by 885 Possible DH areas.

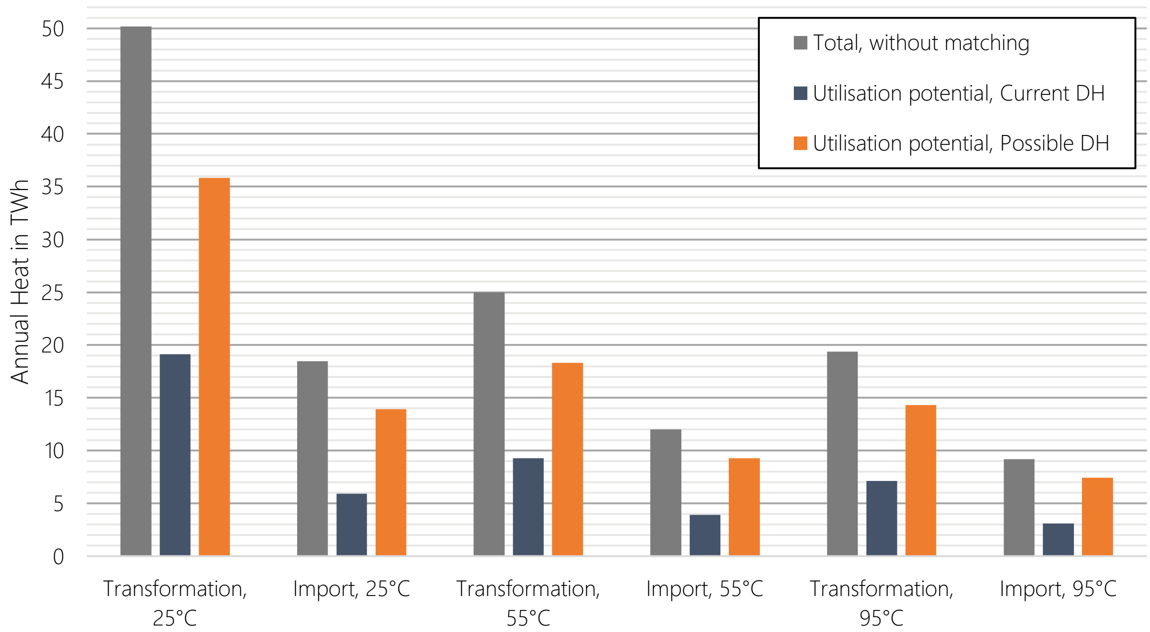

Figure 4.6: **Total excess heat potential from low-carbon processes available for external use and utilisation potentials spatially matched with Current and Possible DH areas from Ref. [89], distinguished by temperature level in a climate-neutral energy system**

Two factors limit the excess heat utilisation potential: the distance to suitable DH areas from an industrial site and the DH demand in the specific DH area. For all temperature levels, about 35% of the total excess heat potential can be utilised for Current DH areas, and about 75% for Possible DH areas. Thus, DH demand is a main limiting factor (see also TableAnnex 11, where supply potentials are included). This means that the excess heat available from industrial sites is often larger than the demand for DH within 10 km. The utilisation potentials in the import scenario are 31 - 52% lower than in the transformation scenario. Country-specific values for 55 °C in the transformation scenario are listed in TableAnnex 12.

Comparing the utilisation potentials of a climate-neutral industry to the status quo shows a reduction of 63 - 90%, depending on temperature and DH coverage (Figure 4.7). Even though the utilisation potentials are substantially lower, temperature level has a strong influence and could partially compensate the reduction due to industrial transformation.

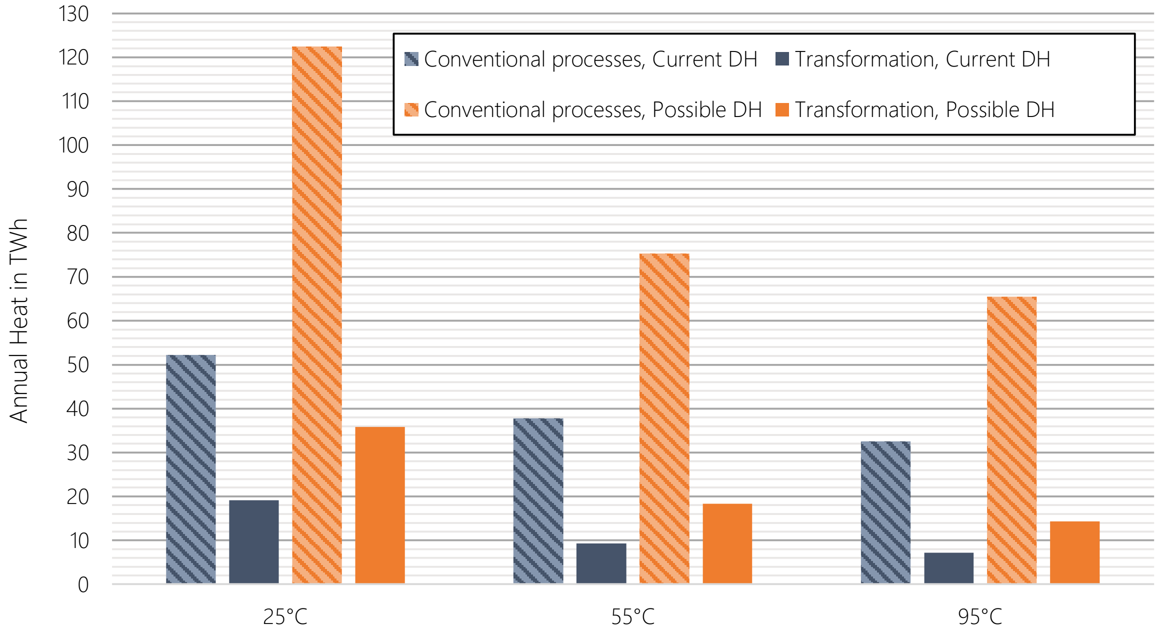

Figure 4.7: Comparison of utilisation potentials of excess heat for conventional and low-carbon processes, each matched with Current and Possible DH areas

A regional analysis for the transformation scenario and the temperature level of 55 °C reveals that even though the utilisation potentials make a rather small contribution to overall DH demand, in specific regions, this share could exceed 30% and even amount to 100% (Figure 4.8). For illustration purposes, the DH demand and the utilisation potential were aggregated for each NUTS 3 region and shaded by the share of excess heat in DH demand. There is a general decrease in the share of excess heat when comparing Possible DH areas with Current DH areas, as they have a higher demand for DH. On the other hand, Possible DH areas are more widespread than Current DH areas, thus utilising additional excess heat from sources that are too far from Current DH areas.

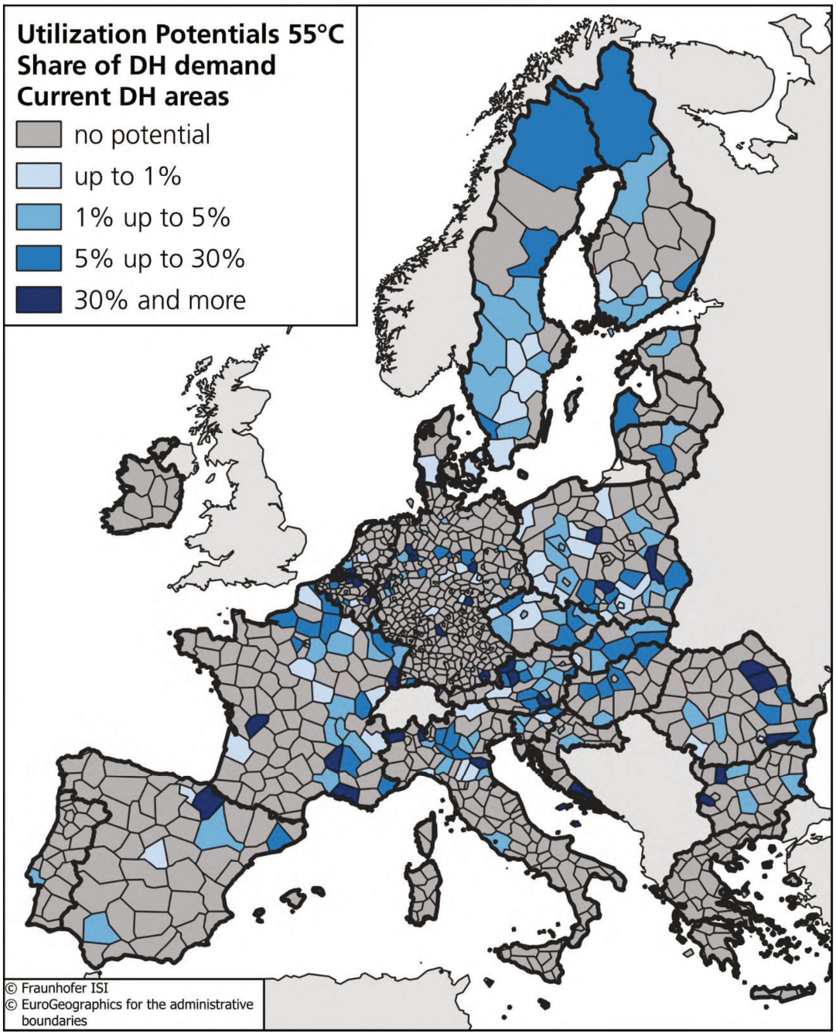

Figure 4.8: Share of excess heat for DH demand per NUTS 3 region. Depicted for the transformation scenario, the temperature of 55 °C and matched with Current DH areas (left) and Possible DH areas (right)

At the level of individual suitable DH areas, excess heat could supply more than 90% of the demand for heat in 22% of Current DH areas and 26% of Possible DH areas. These are generally small and medium-sized DH areas. In other words, the excess heat utilisation potentials are distributed unevenly across regions. In total, the 16 regions with the highest utilisation potential account for 25% of the total utilisation potential of industrial excess heat (Figure 4.9).

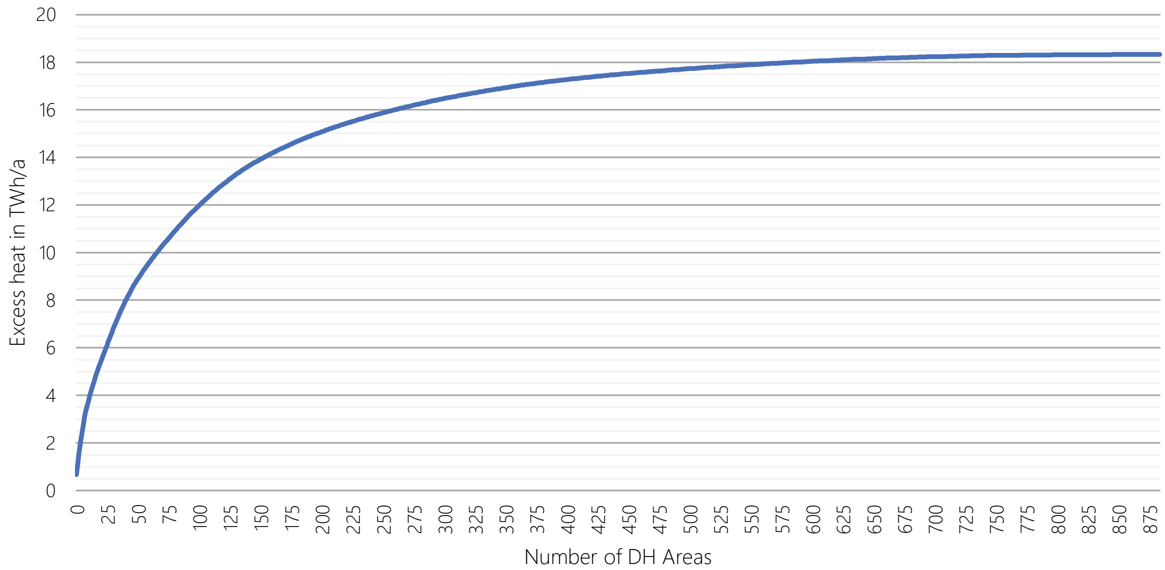

Figure 4.9: **Utilisation potential aggregated over DH areas. Transformation scenario, 55 °C, spatially matched with Possible DH areas**

4.5 Discussion

Our findings suggest that there will be a significant reduction in the industrial excess heat available in a climate-neutral energy system compared to current levels. The contribution to a climate-neutral heating sector by utilising excess heat in DH systems is limited, even though locally this may cover a large share of DH demand. We used the process-specific method of excess heat factors multiplied with production volumes to calculate the georeferenced excess heat potential, and a spatial matching algorithm to estimate its utilisation in DH areas. The excess heat potentials of low-carbon industrial processes add up to 9 - 50 TWh per year, which is 78% - 92% lower than current levels and also lower than the figures in other studies quantifying industrial excess heat, which range from 80 to 800 TWh per year [76,82,83,90]. Process changes in industry and the exploitation of efficiency potentials are the main influencing factors, but also the general decrease in the production of basic primary materials in the EU (driven by an assumed shift towards a circular economy and secondary production routes). The excess heat available is based on ambitious assumptions regarding efficiency, internal heat utilisation and the diffusion of low-carbon processes, and therefore indicates a lower limit. Matching the excess heat sources to DH areas shows that excess heat can supply up to 4% of the DH demand for a system temperature of 55 °C, which is lower than the estimations of other studies based on current industry processes [83,90,138]. Decreasing the system temperatures increases the amount of heat that can be recovered and can partially compensate the reduction of industrial excess heat potentials.

In absolute terms, the excess heat potential from energy-intensive processes that could be utilised in DH systems in a climate-neutral system in the EU is in the range of 3 - 36

TWh per year. Regionally, the utilisation potential could be substantially higher, generally in small and medium-sized DH areas. Expanding DH from current levels to ambitious market shares could roughly double the utilisation of industrial excess heat. Limiting factors not only include spatial availability, but also that the demand is too low in nearby areas. The coverage of DH systems depends on policies and regional action, as well as on the economic competitiveness of district heating. This emphasizes the need for communal heat strategies and integrated infrastructure planning [225], that take regional characteristics into account.

In general, we deal with great uncertainties in this analysis. The transformation to a climate-neutral energy system depends - among other things - on the regulatory and economic framework, available technologies and energy carriers. Regarding the transformation of the industry sector, it is only possible to estimate the excess heat of climate-neutral processes that are not yet in operation based on assumptions about their process design. We chose rather values that result in conservative numbers of future excess heat potentials. If other processes became established e.g. using hydrogen for steam generation in the pulp and paper industry instead of heat pumps or electric steam crackers instead of methanol synthesis, this could increase our quantified potentials, potentially close to current levels. The future volume of produced materials is based on the decarbonization scenario Mix95 from the European study [175], and strongly influences the excess heat potentials. Furthermore, the future production routes of refineries are quite uncertain, especially regarding the choice of feedstock and production locations. Shifts from current locations to more favourable locations with better availability of renewable energy like electricity and hydrogen could be a factor in the future when processes are transformed. These considerations were covered in the import scenario. In this study, we assumed that all internal heat utilisation potentials are exploited as a priority, as energy efficiency in industry is a key element in the transition towards climate-neutrality. We also assumed highly efficient process technologies. This is reasoned by the fact that energy prices will increase if electrified or hydrogen-fuelled processes are established, and that newly built processes will be more efficient than already existing ones that could be more than 40 years old. Alternatively, the total excess heat from a process could be used externally, which would increase the utilisation potentials for DH possibly by 40% up to 100%, depending on the temperature level [90].

Regarding the development of district heating, we considered the Current and Possible DH areas to illustrate the lower and upper limit. The 10 km maximum distance of industrial sites from DH areas is a rather generic assumption. What constitutes a suitable connection distance in the future depends mainly on the heat quantity transported, but also other factors like geographic aspects and local stakeholders. Increasing the maximum distances could increase the number of matched excess heat sources. Increasing the maximum distance from 10 km to 30 km would connect almost all excess heat sources and increase the utilisation potentials by 10 to 50%, depending on the temperature level and DH coverage. Furthermore, the utilisation potential was estimated based on annual values. As the demand for DH in winter is by several factors higher in summer, the contribution could be lower and utilisation potentials could be further reduced by around 20-30%, depending on seasonal thermal storages [140]. Increasing the capacity of seasonal thermal storages could address the mismatch of supply and demand, but might increase the overall system costs. An additional factor that is not considered in the methodology of spatial matching is that the existence of excess heat could be a factor in establishing a new DH system to utilise the heat, even in areas with higher distribution costs. The Possible DH areas represent a high share of DH (45%) in the EU and include regions at the lower limit of economic suitability for DH, which are close to industrial excess heat sources.

A possible additional excess heat source not considered in this study are electrolysers to produce hydrogen. Currently, these are used on small scale in the EU, but there are ambitious EU goals for domestic hydrogen production for 2030 (RePowerEU [226]). In the near future, individual electrolysers could be larger than 100 MW capacity and studies indicate significant excess heat potentials. As a rough estimate, and given the strategic goal of establishing 40 GW electrolysis capacity in the EU by 2030 [227,228], about 150 GW of PEM-electrolysers could be installed by 2050. With an efficiency of 92% and a temperature level of 80 °C [229], this could lead to annual excess heat potentials of 210 TWh in the EU. This value is in line with the results of EU-wide studies on the capacity and excess heat potential of electrolysers [230,231]. These electrolysers would be large point sources of excess heat, concentrated at several locations in the EU with high renewable potentials, which could provide heat for DH areas in their vicinity. In the future, the excess heat from electrolysis could exceed the potentials from energy-intensive industrial processes by several factors. We decided to disregard the potentials of electrolysers for covering DH demand, as too little is known about their possible locations. Electrolysers and their potential contribution to DH are a topic for future research.

4.6 Conclusion

Industrial excess heat potentials for providing heat to district heating will decrease substantially in a climate-neutral energy system. The transformation of industrial production towards low-carbon and efficient processes with internal heat utilisation and a lower share of energy-intensive primary materials will reduce the amount of excess heat in the future by 78-92% compared to current levels. The possible utilisation in district heating decreases accordingly by 50% compared to current levels and could supply up to 8% of the future district heating demand. The industrial excess heat potentials decrease further if energy-intensive materials are imported rather than produced at current locations. Reducing the system temperature in district heating grids and expanding the supply area could partially compensate for the decrease in industrial excess heat in the future.

In the future, the supply of heat in district heating grids needs to be based on technologies like heat pumps utilising renewable sources like ambient heat, water resources (ground or surface) or low-temperature excess heat (e.g. waste water treatment, server cooling), as well as deep geothermal heat. Excess heat from energy-intensive industries may only cover a small share of the district heating supply. At the local level, however, industrial sites are large point sources of excess heat and can provide a considerable share of the heat for district heating. The contribution of industrial excess heat depends on the future costs of the competing heat sources. District heating expansion and densification will increase the possible utilisation of industrial excess heat.

These results indicate that policies and regional action in the form of regional heat strategies are essential to increase the competitiveness of district heating even with a decreasing heating demand, as well as to identify and utilise regional excess heat potentials that could have a great contribution. The planning of district heating and the utilisation of excess heat should take into account that latter could decrease in the future, depending on which transformation pathways are taken by industry. Local heat strategies should include such uncertainties.

Several processes analysed here are still being developed or are not yet being operated on an industrial scale. Further research is needed about the process design of electrified or hydrogen-fuelled processes in order to refine the excess heat factors applied in this paper. Other research should investigate the excess heat potentials from new products needed for a climate-neutral energy system, especially the excess heat from electrolysers. We have made conservative estimates of the available excess heat of future low-carbon processes to show the minimum contribution of industrial potentials.

Acknowledgments

This work was supported by the Reiner-Lemoine-Stiftung through a PhD-scholarship for Pia Manz and by the Fraunhofer Cluster of Excellence "Integrated Energy Systems" (CINES).

A.4 Detailed process- and country-specific results

TableAnnex 10: Available excess heat potentials from industrial sites for external use for all scenarios and temperature levels in TWh per year

Temperature	Scenario	Iron and Steel	Non-ferrous Metals	Pulp and Paper	Non-metallic Minerals	Refineries and Chemicals	Total for external use
25 °C	Status quo, current production	29.5	2.4	23.9	55.2	120.7	231.8
	Efficiency progress, current production	16.5	1.4	20.1	26.0	110.8	174.8
	Efficiency progress, future production	5.9	1.4	18.8	21.4	80.2	127.7
	Transformation scenario	3.2	1.4	-	18.7	26.8	50.2
	Import scenario	1.5	1.4	-	15.0	0.6	18.5
55 °C	Status quo, current production	23.4	2.0	8.4	41.4	40.6	115.8
	Efficiency progress, current production	10.5	1.1	5.5	15.4	33.6	66.1
	Efficiency progress, future production	4.7	1.1	5.1	12.3	24.2	47.4
	Transformation scenario	1.6	1.1	-	11.7	10.6	25.0
	Import scenario	1.2	1.1	-	9.5	0.2	12.0
95 °C	Status quo, current production	21.3	1.9	6.5	37.3	29.4	96.5
	Efficiency progress, current production	8.4	1.0	3.8	12.1	22.9	48.2
	Efficiency progress, future production	3.5	1.0	3.5	9.7	15.4	33.0
	Transformation scenario	1.2	1.0	-	9.7	7.6	19.4
	Import scenario	0.9	1.0	-	7.2	0.1	9.2

TableAnnex 11: Industrial excess heat potentials for the industry scenarios and temperature levels matched with Current and Possible DH areas from Ref. [89] in TWh per year.

Scenarios	Total for external use (without matching)	Supply potential with Current DH	Supply potential with Possible DH	Utilisation potential with Current DH	Utilisation potential with Possible DH
Transformation 25 °C	50.2	25.6	50.1	19.1	35.8
Transformation 55 °C	25.0	12.7	24.9	9.3	18.3
Transformation 95 °C	19.4	9.8	19.3	7.1	14.3
Import 25 °C	18.5	8.4	18.4	5.9	13.9

Scenarios	Total for external use (without matching)	Supply potential with Current DH	Supply potential with Possible DH	Utilisation potential with Current DH	Utilisation potential with Possible DH
Import 55 °C	12.0	5.4	11.9	3.9	9.3
Import 95 °C	9.2	4.2	9.1	3.1	7.4

TableAnnex 12: District heating demand and industrial excess heat supply and utilisation potentials for the transformation scenario for DH, 55 °C, per member state, in GWh per year

Country	Current DH Demand	Possible DH Demand	Supply potential with Current DH	Supply potential with Possible DH	Utilisation potential with Current DH	Utilisation potential with Possible DH
AT	9,229	25,220	695	614	304	504
BE	4,888	41,007	1,655	1,693	1,233	1,605
BG	1,773	6,264	81	195	41	106
CY	-	146	-	-	-	-
CZ	10,174	26,936	398	394	316	354
DE	67,018	344,781	2,984	5,434	2,795	4,751
DK	7,454	19,946	8	8	7	8
EE	1,588	3,829	2	3	2	3
EL	129	12,791	-	245	-	215
ES	7,545	63,998	208	2,114	208	1,716
FI	9,636	25,631	195	188	160	169
FR	48,514	177,533	1,765	3,445	1,754	2,698
HR	1,429	4,679	195	253	167	220
HU	4,629	16,319	250	270	101	183
IE	1,695	8,187	-	249	-	74
IT	22,167	171,225	691	3,666	689	2,664
LT	1,455	4,458	327	319	30	68
LU	585	3,189	22	115	22	115
LV	2,176	5,923	16	16	10	16
MT	-	332	-	-	-	-
NL	6,973	66,093	243	1,305	237	644
PL	22,242	60,318	1,697	2,128	661	1,012
PT	581	4,508	15	491	15	258
RO	4,957	14,641	384	869	174	423
SE	12,194	34,564	281	274	156	176
SI	1,139	3,150	76	79	36	41
SK	3,564	9,407	480	525	153	297
EU-27	253,734	1,155,078	12,668	24,891	9,272	18,319

5 Spatial analysis of renewable and excess heat potentials for climate-neutral district heating in Europe

Pia Manz, Anna Billerbeck, Ali Kök, Mostafa Fallahnejad, Tobias Fleiter, Lukas Kranzl, Sibylle Braungardt, Wolfgang Eichhammer: Spatial analysis of renewable and excess heat potentials for climate-neutral district heating in Europe. In: Renewable Energy 224 120111, 2024. DOI: 10.1016/j.renene.2024.120111.

5.1 Introduction and background

Decarbonized District Heating (DH) can be an important pillar for an efficient and climate-neutral heat supply for buildings, as various renewable and excess heat sources can be utilised, which was investigated by the Heat Roadmap Europe study [39], and can be cost-competitive, which was shown in an EU study [73]. Energy system analyses have modelled DH with different temporal and spatial resolutions, resulting in possible future DH market shares in the EU from 5% to 45% [85]. Especially in regions with high heat demand, DH are cost-competitive compared to individual heating systems.

In the future, there will be several challenges that need to be addressed in the field of DH. First, ambitious standards for the building stock are set by the EU legislative of the Energy Performance of Buildings Directive (EPBD) [183], leading to a reduced heat demand and, thus, possibly to a decreased competitiveness of DH due to lower heat sales. The competitiveness of DH depends not only on the supply costs but rather on the distribution costs, which decrease with increasing heat density, i.e. the heat demand per defined area. Several studies use empirical parameters to define the distribution costs and thus identify economic DH areas based on the heat density and effective width [18,30,45,56,57,95,232]. Second, renewable and excess heat should be the source for DH in a climate-neutral energy system. DH today mainly depends on heat from fossil-fuelled combined heat and power plants (CHP) [9], with fossil fuels contributing about 67% to the DH supply in the last years [10]. Consequently, the DH system itself needs to be transformed. One important measure is to decrease the supply temperatures of DH below 50 – 70 °C, into modern 4^{th} and 5^{th} generation DH networks, as investigated by several studies [21,29,110,233,234]. Many studies state the increased efficient utilisation of renewable or excess heat sources in low-temperature DH systems, especially in combination with heat pumps [235–239], as well as less heat losses and thus lower costs [86,192,224,240,241].

In general, several renewable and excess heat sources can be used for DH generation. Possible options are the direct use of renewable or excess heat sources and the use of low-temperature heat sources combined with heat pumps. Most of the potentials are limited by their spatial proximity to the DH demand, e.g. secondary biomass resources, geothermal, excess heat from industries (Industrial EH) and waste-to-energy plants (WtE), heat from surface water of rivers and lakes or wastewater treatment plants (WWTP). The suitability and high potential of renewable sources for heating has been proven in studies, e.g. shallow geothermal in the Canary Islands [242], Western Switzerland [243] and Vienna [244], deep geothermal in Geneva [245], the Himalaya region [246], biomass in rural areas in Spain [247], sea and river water heat pump in case studies in Norway [248] and Korea [249,250] as well as solar thermal in case studies in Northern EU [251] and Denmark [252]. However, all of these studies do not quantify potentials on a larger geographical scale. A high resolution of the input data sets is needed to quantify these potentials for DH, ideally georeferenced with coordinates. In some studies, potentials for renewable and excess heat sources for heating have already been allocated and quantified in a high resolution at the country- or EU-level, and several data sets are available, mainly focusing on technical potentials. Several studies have focused on the potentials for one individual country, e.g., for Italy [185], Germany [253,254] and Switzerland [255], while other country-level or EU-level studies have focused on individual technologies, considering potentials from e.g. geothermal [256–260], biomass [14,31], rivers and lakes [261,262], WWTP [23,263–265], industrial EH [76,82,83,266] and excess heat from WtE potentials [267–269]. Several open data sets are available for excess heat sources with the geographical extent of the EU, the Pan-European Thermal Atlas 5.2 (Peta 5.2) [44]], Hotmaps toolbox [48]] and the Waste Heat Map [270].

Furthermore, DH supply potentials need to be analysed for each DH area (e.g. city or region with DH) to consider the local renewable and excess heat potentials. The method of allocating the demand and supply of heat with high spatial resolution is called spatial matching. Several studies analyse the spatial proximity of DH supply and demand, often focusing on one technology in one country. The matching algorithms use geographic information systems (GIS), either on proximity analysis enabling cost calculations [23,90,93,94,140,190,191] or spatial clustering with optimisation [271–274]. Several studies [23,259,264–266] introduced the terms supply or available potential in contrast to utilisation or accessible potential, to differentiate the potentials of heat sources before and after spatial matching to the demand. Only one study matched the available renewable and excess heat potentials for DH in the geographical context of the EU with a high spatial resolution in the EU project sEEnergies [93]. However, it lacks a quantification of the renewable potentials on the country-level as well as potentials from rivers and lakes. Thus, there exists not yet a quantification of the technical renewable and excess heat potentials available for DH with high spatial resolution in the future. With this paper, we aim to fill this literature gap.

The quantification of heat generation potentials for DH on a regional level and the identification of DH types can be used to assess the future DH generation mix on EU-level, e.g. in district heating or energy system models and thus the economic potential of each source. In order to reduce the complexity of the results and analyse DH areas by their main potentials, the DH areas are clustered. With that, detailed results can be generalised, structured and understood, as well as serve as a basis for stronger conclusions for policy-making [87].

The objective of this paper is the quantification of the spatially limited renewable and excess heat potentials for DH by developing a spatial matching algorithm and clustering method. More specifically, we aim to answer the following research questions:

- How much can technical renewable and excess heat potentials in the EU contribute to supply the buildings' DH demand in a climate-neutral energy system?
- What is the potential role of the individual renewable and excess heat sources?
- What is the effect of transitioning towards low-temperature DH on the utilisation of renewable and excess heat potentials?
- Which clusters of DH areas represent the respective renewable and excess heat potentials?

In this study, we focus on the geographical context of the EU-27 and assume a climate-neutral energy system. Our analysis is conducted based on annual values. Using GIS, we identify and match renewable and excess heat sources to future DH areas with high spatial resolution. Additionally, a hierarchical clustering algorithm categorizes the DH areas into distinct DH types based on their possible utilisation of renewable and excess heat sources.

The structure of the paper is as follows: Section 5.2 describes the data used for quantifying renewable and excess heat potentials, along with a detailed description of the spatial matching and cluster algorithm method. In Section 5.3, the results of the potentials as well as the resulting DH types are presented. Section 5.4 and 5.5 are dedicated to discuss the results and draw conclusions based on the obtained results.

5.2 Data and method

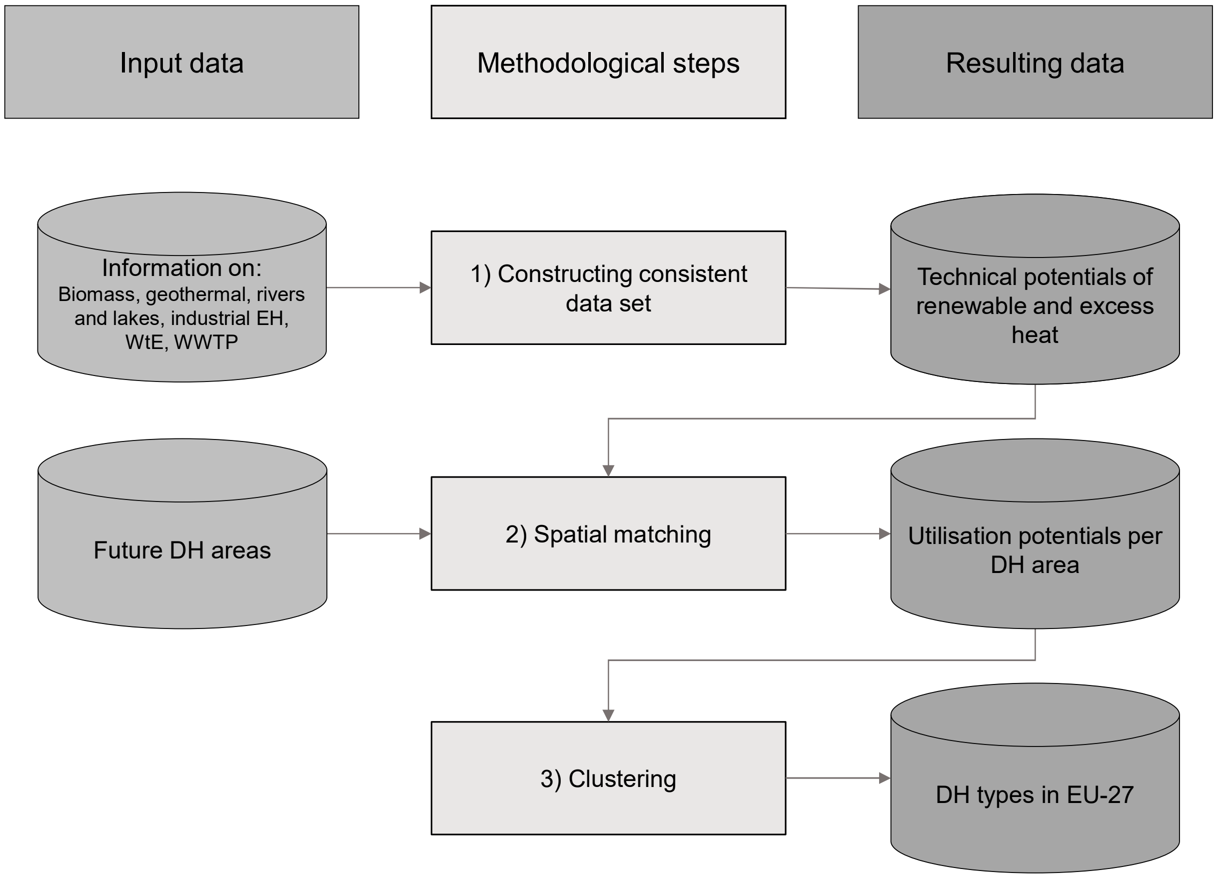

Figure 5.1: Schematic overview of data input, methodology and results in this study

Figure 5.1 shows a schematic overview of the workflow. Two main data sets were used: (1) renewable and excess heat potentials for DH, and (2) identified future DH areas. Both data sets have high spatial resolution and include mainly annual energy values. The data sets were constructed and processed in three methodological steps: step 1, the estimation of the renewable and excess heat technical potentials; step 2, the spatial matching with future DH areas; and step 3, the clustering based on the potentials resulting in DH types for EU. The identified data and results are discussed in the context of a climate-neutral energy system in 2050. The methodology and data were partly established within the EU project "Renewable Heating and Cooling Pathways, Measures and Milestones for the implementation of the recast Renewable Energy Directive and full decarbonisation by 2050 (N° ENER C1 2019-482)" [7]. Preliminary results were previously presented as a case study for Germany in a conference paper [253]. The data set of the DH areas is a shapefile, containing the future DH demand for each of the 5815 DH areas. In the scenario, an ambitious DH expansion and connection rates are assumed, increasing the DH demand from 506 to 631 TWh, even though the buildings demand decreases significantly due to renovation. Details of the methodology, assumptions and results for the future DH areas are described in Annex A.5.

5.2.1 Definition of scenarios

We analysed two scenarios in this study that differed by the assumed DH system temperature level: (1) high-temperature scenario and (2) low-temperature scenario. The two different DH system temperature levels were used to show the influence of temperature on the utilisation of low-temperature heat sources and comprised the current level of 3rd generation DH (flow temperature 90 °C - 70 °C) and a lower temperature of 4th generation DH (flow temperature 60 °C - 70 °C). The DH demand in the DH areas is constant, with lower heat losses in the low-temperature scenario.

5.2.2 Definition of potentials

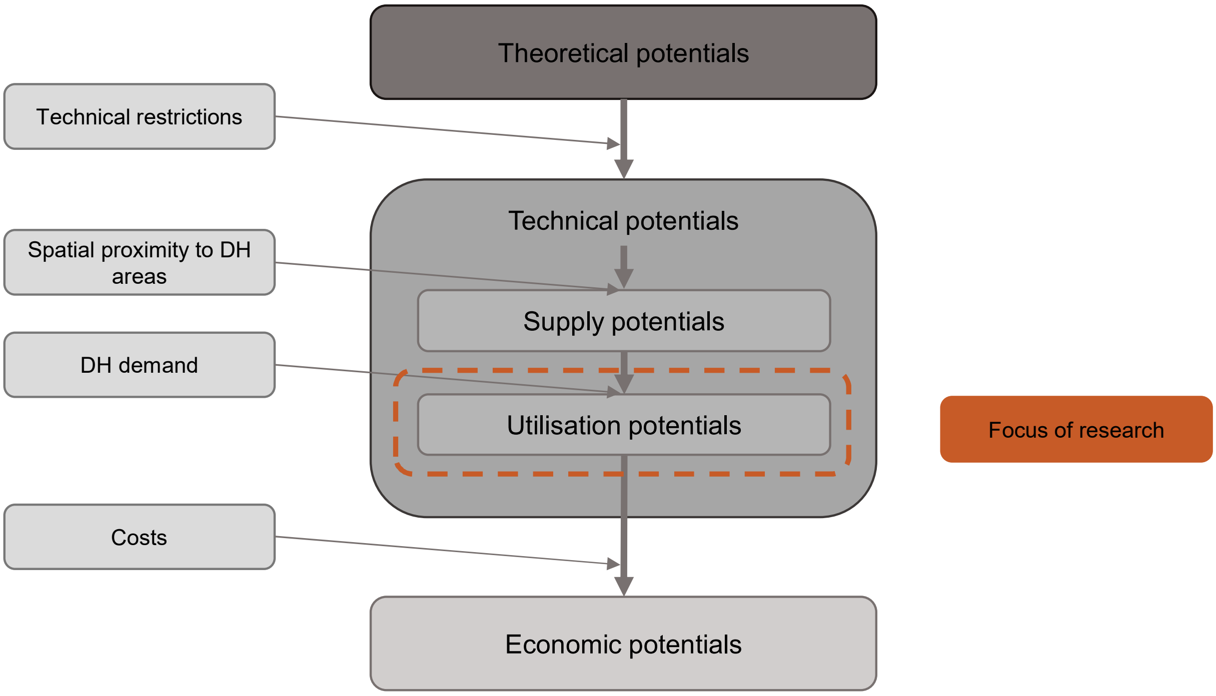

Figure 5.2: Overview of type of potentials and each considered limiting factor

Generally, this study considers technical potentials and differentiates between supply and utilisation potentials (see Figure 5.2). In contrast, theoretical potentials represent the total heat that one resource could provide (e.g. the total amount of heat stored underground amounts to theoretical geothermal potentials). The technical potentials are limited by technical restrictions (e.g., the amount of heat that geothermal plants could extract). The supply potentials represent technical potentials limited by the geographical proximity to future DH areas (e.g. the geothermal plants that could be built close to a specific DH area). The method of spatial matching is used to identify the supply potentials. The utilisation potentials represent technical potentials that are additionally limited by the DH demand in the DH areas that could utilise the potential (e.g. only the geothermal plants needed to serve the demand in the DH area are accounted for). For the technical potentials of rivers and lakes, additional economic limitations were considered in this study by assuming typical project sizes. The supply potentials and the DH demand are compared on an annual basis, and if the potential exceeds the demand, it is limited to the value of the annual DH demand. Thus, the seasonal match of heat demand and source load curves was only partly considered, mainly by assuming typical full-load hours for wastewater treatment and geothermal plants. The focus of this paper lies in the analysis of spatial proximity by spatial matching and identifying the utilisation potentials.

5.2.3 Renewable and excess heat potentials

This section presents the data on the spatial availability of technical potentials suitable for DH generation and the assumptions and processing conducted to construct a consistent data set. We analysed the following heat supply potentials: (1) Renewable sources, including deep geothermal, biomass and ambient heat from surface water and wastewater together with a heat pump as well as biogas from sewage sludge; (2) Excess heat from large industrial facilities and the thermal treatment of waste (WtE).

The data collection and processing steps depend on the technology and the available data. The technologies considered are summarised in Table 5.1, and the processing steps as well as assumptions are presented in the following subsections. The potential heat quantified in this paper always refers to the heat delivered to the DH area, i.e. after a heat pump for the heat from rivers and lakes and wastewater treatment plants (WWTP). An efficiency increase was assumed when system temperatures are decreased, especially for heat pumps or CHP plants. The assumptions are also listed in the Table 5.1, showing the increase between the two temperature scenarios.

Table 5.1: Overview of the renewable and excess heat potentials considered

Heat source	Spatial resolution (grid size)	Temporal resolution	Considered source temperature	Maximum distance from source, based on [90,224]	Source	Efficiency increase for low-temperature compared to high-temperature scenario, based on [275]
Biomass	NUTS 2	Annual	Direct combustion/Biogas	Within NUTS 2	ENSPRESO - Biomass (JRC) [276]	Efficiency increases from 53% to 55% for biomass CHP
Geothermal (petro- and hydrothermal)	1000 x 1000m	Annual, full-load hours considered	>60 °C	15 km	Geothermal Atlas [277], GeoDH [278]	No additional assumptions
Rivers and lakes	5000 x 5000m	Annual, full-load hours considered	2 – 8 °C	5 km	Copernicus [279]	35% efficiency increase for heat pumps

Industrial excess heat	Coordinates	Annual, monthly profile considered	> 55 °C	20 km	ISI Industrial Database [90]	Reduced recovery temperature
Waste-to-energy plants	Coordinates	Annual	100 °C	20 km	Peta 5.2 [44]	Efficiency increases from 66% to 76% for heat utilisation
Wastewater treatment plants (heat and sludge)	Coordinates	Annual	10 – 25 °C	2 km	Peta 5.2 [44], Hotmaps [48]	33% efficiency increase for heat pumps. Efficiency increases from 50% to 55% for heat utilisation of biogas CHP

5.2.3.1 Biomass

In line with the EU ambitions on sustainable biomass, we assume a structural shift from primary biomass resources (e.g. round wood) to secondary sources for energy use [14,31]. The potentials for secondary sources will be shared for energy use in industry and the heating and DH sectors.

The biomass potentials were taken from the ENSPRESO data set provided by JRC [276,280]. The data set is downloadable in tabular format, differentiated by commodity and at NUTS 2[10] level. We chose the annual values from the medium scenario (ENS_Med) for 2050 and selected residues from agriculture and forestry together with fast-growing energy crops[11]. With the additional assumption that 50% of these residues are available for DH, they represent an annual potential of 734 TWh for the EU. This biomass potential at NUTS 2 level was distributed to all DH areas in the respective NUTS 2 region, relative to the DH demand. This limitation implicitly assumes a short possible transport distance for secondary biomass.

5.2.3.2 Geothermal (hydro- and petrothermal)

In the EU, there were 2161 MW of geothermal plants for DH installed in 2020 [281], producing about 7.1 TWh of heat [282]. Geothermal plants consist of two (or more) boreholes, typically separated by a distance of around 1 km, one for extraction and one for injection of the fluid. In general, a distinction is made between petrothermal (i.e. hot dry rock, enhanced geothermal system) and hydrothermal (i.e. hot fluid) projects. Almost all the currently operating geothermal projects are hydrothermal plants that extract heat from thermal water in hot water basins and reservoirs at typical depths of 2000 to 4000 m. Petrothermal plants use the heat stored in underground rocks and extract it by injecting water as the extraction fluid. Generally, the petrothermal potential

[10] NUTS (Nomenclature of Territorial Units for Statistics) regions is a hierarchical system used by the European Union (EU) for dividing up the territory of its member states for statistical purposes.

[11] The following codes represent the selected commodities: MINBIOAGRW1, MINBIOCRP31, MINBIOCRP41, MINBIOCRP41a, MINBIOFRSR1, MINBIOFRSR1a, MINBIOWOOW1, MINBIOWOOW1a

is by several factors higher than the hydrothermal potential, as the probability for the occurrence of water basins in the underground decreases with larger depths. Petrothermal projects have lower flow rates and thus lower economic competitiveness [283], despite recent advances in increasing the technical exploitation possibilities [284]. Competition for geothermal resources is not expected from individual heating systems, as these use near-surface geothermal energy. For geothermal projects, we assumed exploitation at depths between 2000 and 3000 m, with an underground temperature gradient of 30 K/1000 m [283]. In areas with hydrothermal potentials where high temperatures are available, geothermal plants can also operate as cogeneration units to produce heat and electricity. While this improves overall system efficiency, it also reduces the potential for DH supply. There may be other competing interests from land use (e.g. national parks, cities [285]]) or mining activities (e.g. radioactive waste storage or carbon capture and storage [286]). Moreover, geothermal projects face high upfront costs and risks, as on-site test drillings are needed, which can reveal insufficient suitability (exploration risks).

We estimate the technical geothermal potentials based on two data sources: First, the Atlas of Geothermal Resources in Europe [277] provides maps for temperature contours at a depth of 2000 m. The data were extracted from the maps as raster files with a resolution of 1000 m x 1000 m. Each raster was assigned the respective temperature at 2000 m depth. This temperature was increased by 15 K, representing heat extraction between 2000 m and 3000 m. Second, the maps from the GeoDH project [278] were used to identify possible hydrothermal projects. From these, the areas classified as "hot sedimentary aquifer" and "other potential reservoirs" were extracted as vector layers for the 14 member states available. Other countries may also have hydrothermal potentials, however, no data is available. The temperature data were clipped to the vector layers, assuming that the temperature of the thermal fluid in the water basins is similar to the temperature of the rock. National parks and regions higher than 500 m above NN were excluded, as were water bodies. The geothermal potentials were quantified using the following formula, based on [283]:

$$P = Q \cdot \rho \cdot c \cdot (T_1 - T_2), \tag{10}$$

where T_1 is the underground temperature, and T_2 is the temperature of the injected water. As a volumetric flow rate Q was assumed, the density ρ and heat capacity c of water were used. Typical values were used for the flow rates with 0.0194 m^3/s for petrothermal projects [259,283] and 0.06 m^3/s for hydrothermal projects [260,283]. Potential areas were identified using a minimum temperature spread between T_1 and T_2 of 15K, depending on the temperature scenario. For the extraction temperature, 85 °C was assumed for the high-temperature scenario and 65 °C for the low-temperature scenario. A risk factor was also included by assuming that 25% of hydrothermal and 50% of petrothermal projects are not successful [283]. Furthermore, 6.93 km^2 was assumed to be the area needed for one geothermal project with two boreholes. The potential *P* in MW was calculated for each raster in the map. Conservative values regarding the full load hours were assumed, 3000 and 4000 full-load hours for petrothermal and hydrothermal projects [282,287], respectively, and were used to calculate the annual heat provided.

5.2.3.3 Rivers and lakes

Ambient heat from surface water like rivers and lakes can be a source for DH supply when combined with large-scale heat pumps [261,262,288]. Using water from rivers or lakes has implications for local ecosystems, such as a decrease in water temperature. However, this impact is marginal compared to conventional power plants that extract vast volumes of water for cooling and raise the temperature of rivers. Furthermore, heat pumps do not reduce the amount of water in rivers and lakes as it is returned after the heat has been extracted.

Detailed data on temperatures, flow rates and location in high temporal resolution is necessary to estimate the heat that could be extracted from rivers and lakes in the EU. A detailed and consistent data set is unavailable and has to be constructed. The data for river and lakes locations and monthly average flow rates were taken from Copernicus Climate Change Service Information [279]. Thereby, only rivers with a minimum average flow rate of at least 20 m^3/s in winter months were defined as suitable regarding temperatures, as lower flow rates lead to unsuitable temperatures [261]. The rivers and lakes were classified into three groups based on their average winter flow rate: (1) rivers with flow rates between 20 and 50 m^3/s were defined as small, (2) rivers with flow rates between 50 and 100 m^3/s as medium, and (3) rivers above 100 m^3/s as large. The temperatures were taken from hourly measurements from a data set published by the Federal State of Bavaria [289], grouped by the flow rates, and assigned to rivers throughout the EU. Typical project sizes were defined for each group (30 MW for small, 80 MW for medium and 150 MW for large projects, in combination with a heat pump) based on [261,290]. Full-load hours of 2000 h were assumed for smaller projects and 3000 h for medium and large projects so that we could estimate the annual amount of energy extracted from rivers and lakes using heat pumps. To estimate the electricity needed for DH supply, we assumed a seasonal performance factor for the heat pumps of 2.4 and 3.2 for the high-temperature and the low-temperature scenario, respectively. The minimum distance between two extraction points in the rivers was assumed to be 10 km [291].

5.2.3.4 Industrial excess heat (Industrial EH)

Energy-intensive industries use large amounts of process heat, often at high temperature levels above 500 °C. Thus, excess heat potentials from large industrial plants are a promising source for DH. In the future, the amount of industrial excess heat available may decrease due to efficiency improvements in industrial processes and internal on-site heat utilisation. We, therefore, assumed a reduction in industrial excess heat compared to today's potential based on [266]. In [266], excess heat from steel, cement, glass, paper, chlorine, ammonia, and methanol production was georeferenced in the ISI Industrial Database [137], and the effect of industrial transformation was estimated. The available industrial excess heat in 2050 was determined by considering the transformation of industry in terms of production volumes and low-carbon processes. This approach results in lower potentials, as improved energy and material efficiency lead to reduced production volumes. Electrified furnaces are often more efficient than conventional fossil fuel-based processes, which reduces not only energy demand but also excess heat potentials. The locations of industrial sites are assumed to remain unchanged. The methodology for estimating excess heat potentials based on production is described in Refs. [90,266] and has been adapted to include climate-neutral processes such as hydrogen-based steelmaking and petrochemical products. The flow temperature of DH systems also affects the energy available at industrial sites and is varied from 95 °C to 55 °C depending on the scenario.

5.2.3.5 Waste-to-Energy (WtE)

Municipal solid waste is treated either by recycling, incineration or landfilling. Waste incineration plants (Waste-to-Energy, WtE) recover the energy that is contained in the treated waste, mainly by CHP [269]. The future potential of WtE is uncertain as it could be higher or lower than today's level, depending on the development of landfilling and circular economy approaches. There are implicit incentives for burning waste instead of reducing it once a WtE plant is built, as waste burning requires certain temperatures that are only reached at full capacity. This could lead to a stable amount of incinerated waste.

The sites and amount of the theoretically available excess heat (60% of energy input) from WtE plants were taken from the Pan-European Thermal Atlas 5.2 (Peta 5.2) [44] as shapefiles, developed in the project Heat Roadmap Europe 4 [94]. From this, the heat recovery efficiency in CHP plants was assumed to reach 66% and 76% for the two temperatures respectively [268,292]. Further, we assumed that the locations and the amount of incinerated waste remain constant until 2050.

5.2.3.6 Wastewater treatment plants (WWTP)

Wastewater treatment plants (WWTP) are distributed all over the EU, often close to settlements. There is a regular inflow of sewage water and precipitation. The temperature remains relatively stable between 8 and 15 °C [263,265] and the heat contained could be used for DH when combined with a heat pump. There are a number of existing projects, e.g. in Budapest and Kalundborg, as well as the biggest project so far currently being built in Vienna.

We combined two data sources: Hotmaps [48,132] provides calculated power of the plants, derived from the volume of sewage water and the temperature difference of 5 K. In Peta 5.2 data and locations of annual excess heat from WWTP is published [44], taken from ReUseHeat [23]. As the Hotmaps data set includes more plants, the locations and power values were taken from Hotmaps. The ReUseHeat data set was used to derive typical full-load hours of 4421 by calculating average values for each plant where both power and annual excess heat were available. The seasonal performance factor of the heat pumps was assumed to be 2.7 and 3.6 for the high-temperature and the low-temperature scenario, respectively.

Additionally, sewage sludge can be fermented in an anaerobic digester to produce biogas (as is the case, for example, in Innsbruck and Amsterdam), often combined with solid waste. We used the sludge values from the ENSPRESO data set [276] and assigned them to the WWTP locations relative to size. Sewage sludge is often used in clinker production (kilns), and this may increase in the future, reducing the potential for DH generation.

5.2.3.7 Other potentials

We did not integrate any solar thermal potentials, as it was assumed that the technical potentials are not limited by the spatial proximity but rather the economic potentials limited by their costs. Technically, solar thermal can be utilised (almost) everywhere, as radiation is high enough in the EU [293]. Other types of heat pumps, e.g. air-source heat pumps, were not considered for similar reasons. Furthermore, seasonal storage and peak load plants like hydrogen boilers, electric boilers or CHP plants were not considered, as they were not relevant to the research question of this paper.

5.2.4 Spatial matching

The regional analysis and spatial matching to the heat sources were conducted using a customised matching algorithm in the software QGIS with the PyQGIS plugin [109] mainly based on distance analyses. The renewable and excess heat potentials were matched to the most suitable DH areas identified within a defined maximum distance. The PyQGIS plugin allows the creation of Python scripts for automatised spatial data processing. Input data included future DH areas as polygons (see Annex A.5) and the excess heat sources as point layers. The potential of geothermal and rivers and lakes had to be converted from raster to point sources, each point representing the potential of one geothermal project or river extraction point, with a minimum distance between each of them.

In the matching algorithm, which has previously been described in [266], the heat sources are allocated to the DH areas that are no further away than the assumed maximum distance. First, a spatial grid is created to pre-sort the heat sources to the DH areas, in order to reduce the calculation time by several factors. The DH areas within the distance limit are identified for each heat source. For industrial excess heat and WtE plants, the available energy is prioritised and sequenced by a calculated factor for each DH area within the maximum distance, based on its annual DH demand and the respective distance. This prioritisation factor is used to allocate each excess heat source to one or several most suitable DH areas and prevents the connection of an industrial site with large amounts of excess heat to the closest but very small DH area. The prioritisation factor also enables one individual large point source to supply multiple DH areas, e.g., multiple DH areas could be supplied by one WtE plant if the DH demand of one DH area is lower than the heat potential. Likewise, the prioritisation factor is used to determine the order of multiple heat sources that could supply DH areas, with the source with the highest factor given priority, ensuring that large DH areas are supplied first. With that, a stepwise matching is conducted, with the largest DH areas being connected first until their demand could be supplied.

The output of the matching algorithm is a table with the matched potentials for each DH area, i.e. the supply potentials. These potentials are then used to calculate the utilisation potentials by limiting the supply potentials to the magnitude of the annual DH demand in the matched DH area, which then forms the input for the clustering algorithm.

5.2.5 Clustering

A clustering analysis is performed as the final step to derive DH types, which we define as a set of DH areas with similar renewable and excess heat potential patterns. In line with this definition, input data for the clustering are the 5815 DH areas and their matched renewable and excess heat utilisation potentials. In order to minimise the effect of different orders of magnitude, the potentials are expressed as a percentage of demand. This results in figures between 0 and 1, i.e. 0% - 100% coverage of the demand by a potential heat source.

Clustering was performed using an agglomerative clustering algorithm provided by the Python package SciPy[12] . In agglomerative clustering, the algorithm calculates the dissimilarity between all elements and gradually combines two elements with the least dissimilarity to form a cluster. This cluster is then reused in the next iteration. There are different algorithms varying in how they calculate the dissimilarity between the original elements and how the clusters are formed. In this paper, we use ward's minimum variance method and the Euclidean distance (similar to the analysis in [87]), as this best fits our data and objective. Further details on the clustering analysis, including a sensitivity analysis and the reasoning for our choice of algorithm, are provided in Annex A.6.

[12] https://docs.scipy.org/doc/scipy/index.html

5.3 Results

This section presents and analyses the renewable and excess heat potentials (first as technical potentials, then as supply and utilisation potentials) in the EU. The final section presents the DH types identified by clustering the results for individual future DH areas.

5.3.1 Technical potentials

This section presents the technical potentials for renewable and excess heat sources in the EU with high spatial resolution. The identified geothermal potentials are classified into hydro- and petrothermal potentials for the two DH system temperatures assumed (Figure 5.3). This means that the minimum underground temperature needs to be at least 85 °C for the high-temperature scenario and 65 °C for the low-temperature scenario. Petrothermal potentials are available across most countries in the EU but with lower heat extraction. This is mainly due to the lower flow rates assumed for petrothermal projects. Hydrothermal potentials, on the other hand, are more limited as they depend on the existence of aquifers but offer high local potentials. The DH system temperature and thus the return temperature strongly influence the availability and amount of the technical geothermal potentials.

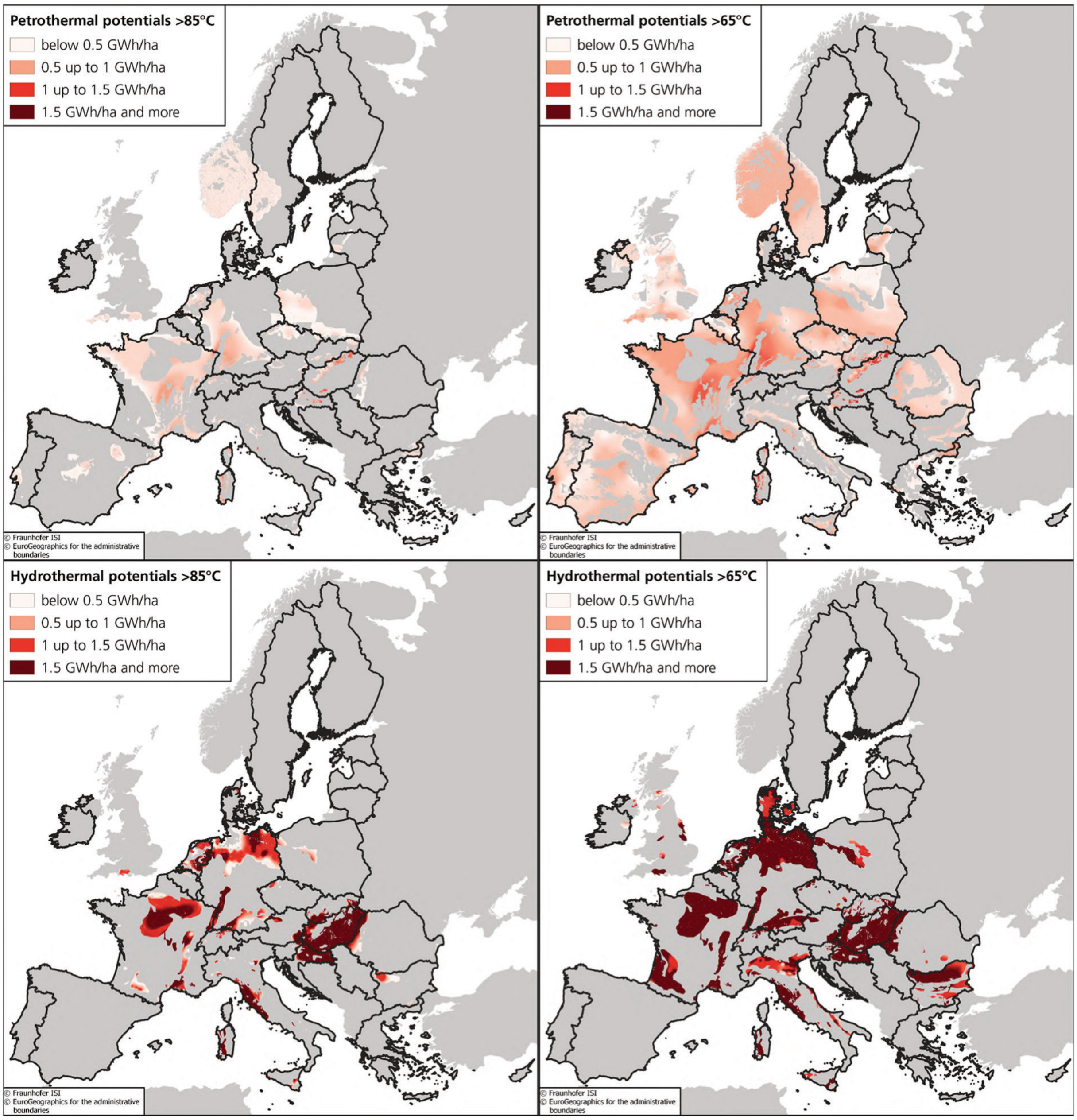

Figure 5.3: Visualisation of the calculated annual technical geothermal potentials in the EU for petrothermal (top) and hydrothermal (bottom) in GWh per hectare. Possible areas with minimum temperatures for the high-temperature scenario (left) and the low-temperature scenario (right)

The other potentials are more scattered over the countries with different spatial patterns (Figure 5.4). Waste-to-Energy and industrial excess heat potentials comprise relatively large sources at fewer sites across the EU. In contrast to this, WWTPs are more widespread but with lower potentials. Potentials from rivers and lakes are limited to rivers with sufficient flow rates, which are generally larger rivers closer to the sea.

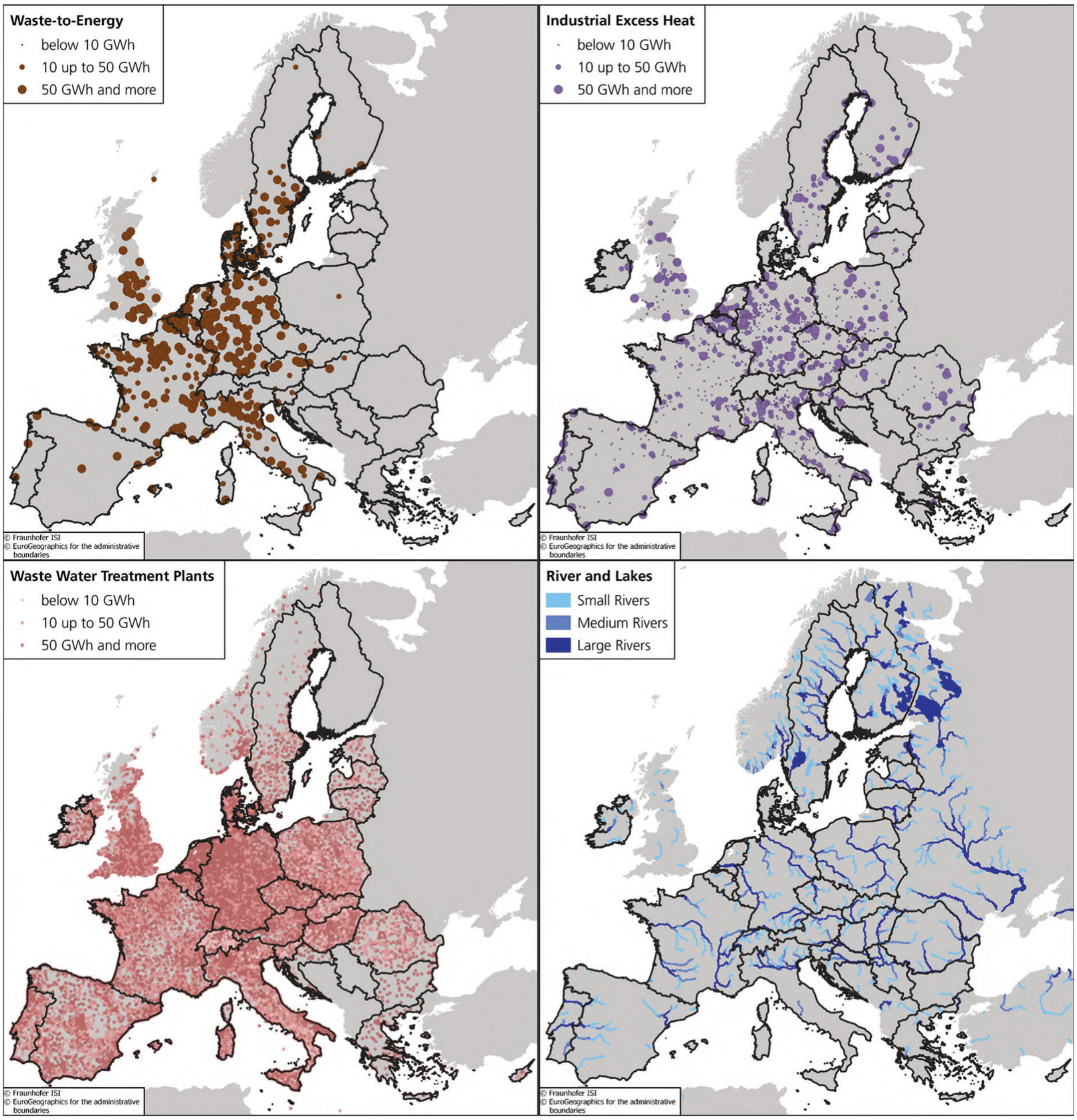

Figure 5.4: **Visualisation of the calculated annual technical potentials for renewable and excess heat potentials in the EU**

5.3.2 Supply and utilisation potentials

The supply potentials are matched to future DH areas within the maximum distance, while the utilisation potential comprises the demand that actually exists within the assumed distance. As this is calculated for each individual heat source, the sum of all source types can still exceed the DH demand in the DH areas. Table 5.2 lists the technical, supply and utilisation potentials, which are published per DH area in the online data repository [294]. The analysis includes the electricity demand for the heat pumps used in WWTP and rivers and lakes and is listed separately in Table 5.2. As the potentials can supply a considerable share of DH demand, the corresponding electricity demand is relatively high, even higher than some of the other potentials themselves. As a lower system temperature increases the efficiency of a heat pump, the electricity demand decreases in the low-temperature scenario, i.e., the same amount of heat could be provided to the DH area by using less electrical energy.

Table 5.2: Annual supply and utilisation potentials for DH in a climate-neutral energy system in the EU, in TWh

Heat source	High-temperature scenario			Low-temperature scenario		
	Technical potential	Supply potential	Utilisation potential	Technical potential	Supply potential	Utilisation potential
DH demand	732.13			694.26		
Biomass	727.86	727.86	385.30	742.41	742.41	377.16
Geothermal (hydrothermal)	814.94	422.89	80.12	2097.71	1201.36	173.84
Geothermal (petrothermal)	84.56	48.37	27.31	554.37	272.61	120.18
Rivers and lakes	1155.86	582.16	143.05	1553.48	782.42	153.58
of which electricity for heat pump	428.10	215.62	52.98	427.83	215.48	42.30
Industrial excess heat	19.91	19.52	16.19	32.48	31.96	29.88
Waste-to-Energy	97.91	97.14	88.16	110.63	106.85	95.49
Wastewater treatment plants	373.35	214.39	185.90	455.87	261.77	217.60
of which electricity for heat pump	155.56	89.33	77.46	142.46	81.81	68.00
Sludge	7.72	4.01	4.01	8.10	4.21	4.21
Total	3282.11	2116.34	930.04	5555.05	3403.61	1171.94

In general, the highest supply potentials are found in hydrothermal, biomass and wastewater treatment plants, depending on the assumed temperature level. The total utilisation potential is several factors smaller than the supply potentials. This is mainly due to the high hydrothermal supply potentials in the EU, especially for the low-temperature scenario, greatly exceeding the DH demand. The heat from rivers and lakes shows a similar pattern to hydrothermal potentials but with a smaller increase due to lower system temperatures. In contrast to this, almost the entire potential from WWTP can be utilised, as these are often smaller plants close to larger cities with high DH demand. About 50% of the biomass supply potentials can be utilised if no transport across NUTS 2 regions is assumed. Overall, the calculated potentials are sufficient to supply the heat for DH demand in both scenarios at EU-level, with a higher potential in the low-temperature scenario. The aggregated utilisation potentials at country level are sufficient to meet the DH demand in most countries (Figure 5.5). At the level of individual DH areas, 128 TWh (17% of the total DH demand) in the high-temperature scenario and 66 TWh (9% of the total DH demand) in the low-temperature scenario cannot be covered annually. These figures do not include potential heat generation from solar thermal plants, air-source heat pumps, or peak load boilers. Thus, overall there are enough renewable and excess heat potentials to reach a climate-neutral DH supply in 2050.

Reducing the system temperature from the high-temperature scenario to the low-temperature scenario can increase the potentials by 26%, mainly due to the broader availability of hydrothermal and petrothermal resources, as well as the improved efficiency of heat pumps using rivers and lakes and wastewater treatment plants as source. There is only a minor effect of the increased efficiency of heat utilisation from WtE, industrial EH and biomass.

Where available, hydrothermal potentials could cover the main share of the DH supply. Furthermore, the dependency on biomass as a resource for DH generation could be reduced by lowering the DH system temperature. The other renewable and excess heat potentials could also cover a large share of the demand.

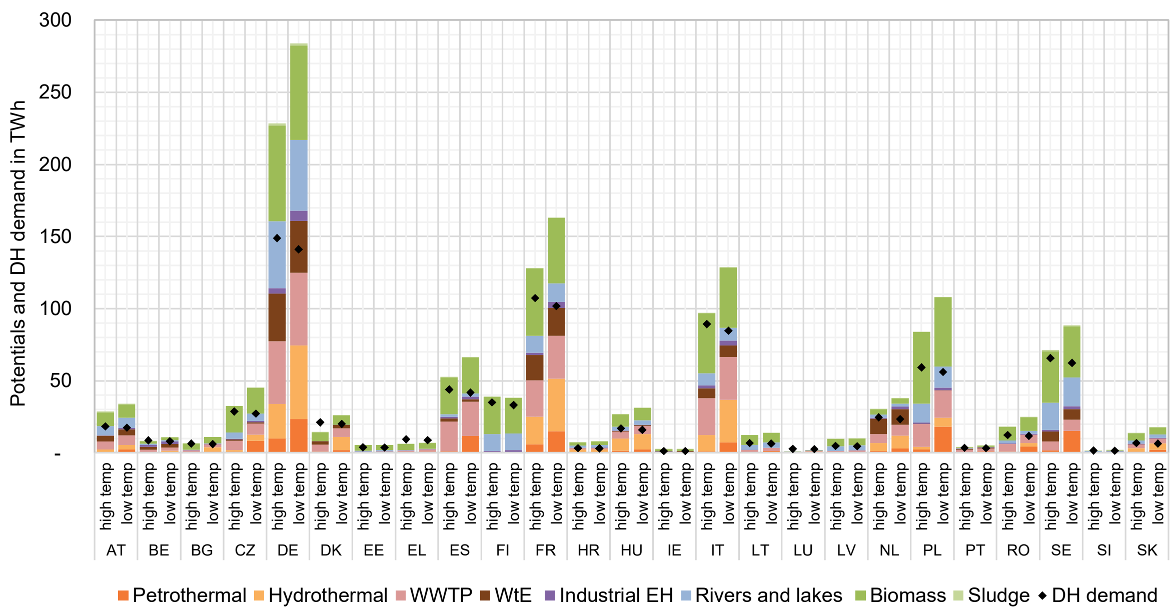

Figure 5.5: **Aggregated utilisation potentials of renewables and excess heat for DH areas and DH demand in 2050 per country for the two scenarios**

5.3.3 DH types

After quantifying the potentials, a clustering approach is used to define DH types. The DH types represent future DH areas with similar patterns of the available renewable and excess heat potentials (compare Section 5.2.5 and Annex A.6). In both scenarios, four different DH types were identified, although not all countries necessarily feature all four types. The dendrograms of the hierarchical clustering can be found in Annex A.6.

Table 5.3 gives an overview of the four DH types with the average contribution of the potentials. Hence, beside the total and average DH demand per cluster, the average contribution of the different heat sources in percentage is shown, e.g. in cluster 1 in the high temperature scenario, 14% of the DH demand could be covered by petrothermal energy. In both scenarios and all DH types, biomass potentials are relatively high, and sludge potentials are relatively low as well as several renewable and excess heat sources can be used to cover the demand, i.e., all DH types represent multivalent networks

Table 5.3: Overview of DH types for both scenarios with average share of the potentials to cover the demand (Note: Distinct patterns are shown in bold)

DH type	Total demand in TWh	Average demand in GWh	Number of DH areas	Petrothermal	Hydrothermal	WWTP	WtE	Industrial EH	Rivers and lakes	Biomass	Sludge
High-temperature scenario											
1	115	84	1364	14%	26%	31%	6%	2%	99%	74%	1%
2	32	44	714	24%	98%	34%	4%	5%	0%	72%	1%
3	542	198	2745	4%	2%	18%	5%	6%	4%	70%	0%
4	43	44	992	38%	1%	73%	0%	2%	0%	74%	1%
Low-temperature scenario*											
1	131	97	1346	40%	41%	35%	1%	3%	98%	77%	1%
2	87	60	1454	38%	88%	38%	1%	16%	5%	74%	1%
3	435	263	1652	17%	8%	31%	16%	1%	6%	67%	1%
4	42	31	1363	98%	1%	44%	0%	1%	0%	78%	1%

* When clustering the DH areas in the low-temperature scenario, the order of the clusters was changed, i.e. cluster 3 and cluster 4 were swapped. This was done in order to have the same sequence in both scenarios. This does not change the results but only the form of presentation.

The clusters show distinct patterns in both temperature scenarios. Cluster 1 can be supplied almost completely with heat from rivers and lakes, while representing quite low geothermal potentials. Cluster 2 shows the highest hydrothermal potentials, supplemented with high WWTP potentials. Cluster 3 has overall quite low potentials, except biomass potentials. Cluster 4 shows an overall more mixed pattern with dominant sources from petrothermal, WWTP and biomass, with a lower contribution of petrothermal in the high-temperature scenario. Even though the absolute contribution of the individual heat sources differs, from a qualitative point of view, the DH types in the two scenarios show several similarities, hence the clusters are given the same name (compare Table 5.4).

Table 5.4: Qualitative description of the DH types for both scenarios

DH type	Name	Description
1	Rivers and lakes	DH areas with high rivers and lakes potentials, supplemented by higher WWTP and hydrothermal potentials
2	Hydrothermal and WWTP	DH areas with high hydrothermal potentials, supplemented by higher WWTP and petrothermal potentials
3	Biomass	DH areas with overall lower (matched) potentials, except biomass
4	Mixed	DH areas with mixed potentials, especially petrothermal, WWTP and biomass

Figure 5.6 further illustrates the DH types by showing the stacked potentials for all DH areas ordered by type, i.e., the DH areas are arranged on the x-axis and the potentials to cover demand are stacked on the y-axis. These figures further highlight the differences between the two scenarios. In the high-temperature scenario, a high number of areas are clustered in the biomass type, while the low-temperature scenario shows a more even distribution. Furthermore, in the low-temperature scenario, almost all areas can rely on a greater variety of sources. The reason for both these differences is that sources other than biomass are available to meet demand in the low-temperature scenario.

Not every country has all four DH types. For example, in the high-temperature scenario, Finland only has types 1 and 3: the rivers and lakes and the biomass type. These types represent the primary heat sources, but not the only ones. Thus, more sources are available in Finland than biomass and heat from rivers and lakes. More country-specific results are presented in Annex A.7 and in the online data repository [294].

The geographical allocation of the DH types mainly follows the available potentials (compare Figure 5.7), especially for hydrothermal and rivers and lakes. The biomass and mixed types are mostly found in regions without hydrothermal or river and lake potentials, more distributed in the high-temperature scenario. For the low-temperature scenario, the geothermal areas are much more prominent due to the greater availability of geothermal energy for lower temperatures. However, the overall pattern is similar to the high-temperature scenario.

The results of the cluster analysis have significant implications for assessing transformation pathways in countries and the EU regarding DH by providing valuable insights into the most important renewable and excess heat sources. Moreover, the results offer a streamlined approach as an input for modelling DH supply mixes, in the way that they enable the reduction of the complexity of integrated energy system models while retaining essential technological and spatial details. Specific transformation pathways can be modelled with the cluster results as an input by considering different DH types as representatives of numerous DH areas across the EU, enabling a more focused analysis within energy system models.

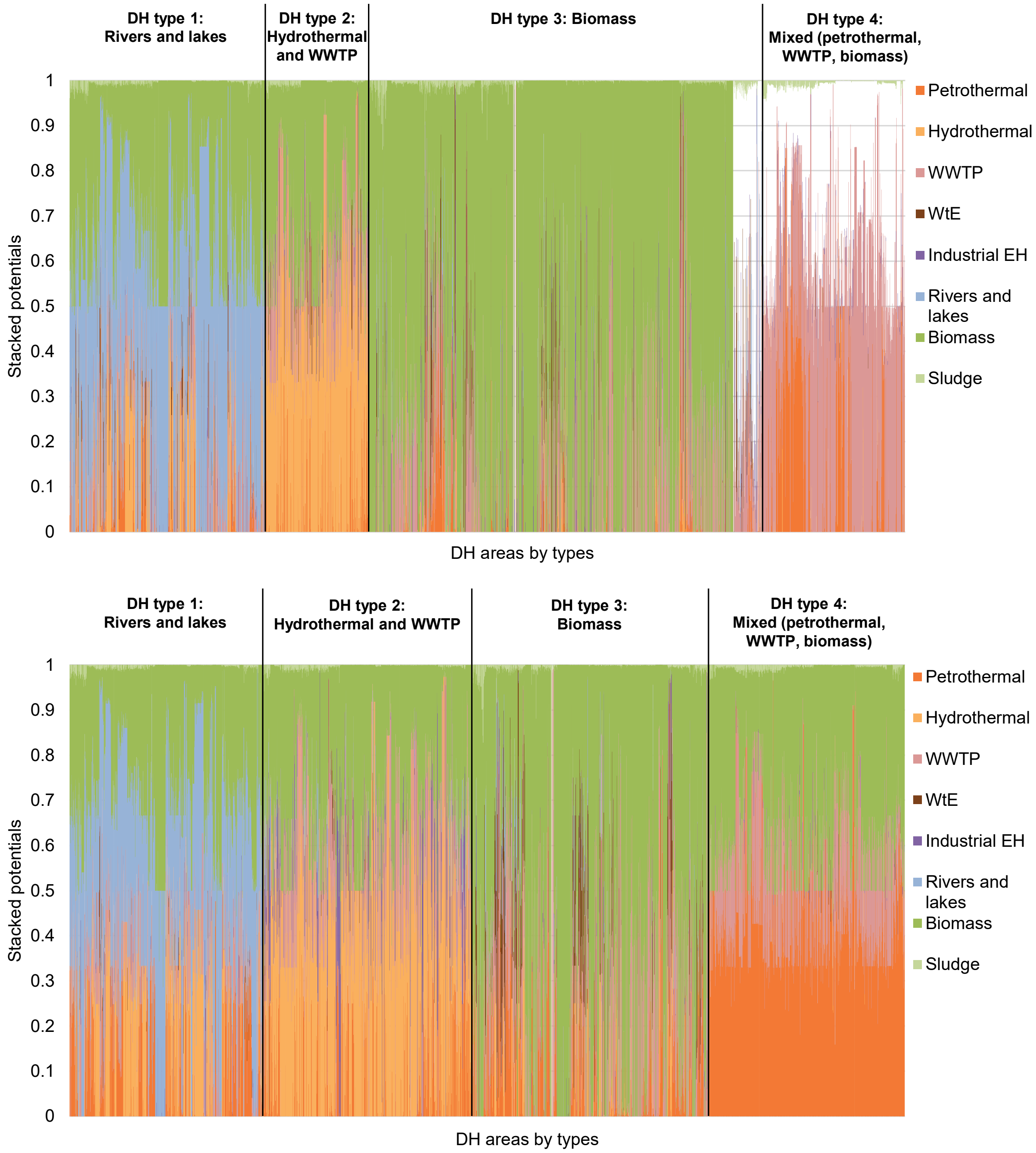

Figure 5.6: Visualisation of the DH types in the high-temperature (top) and low-temperature (bottom) scenario

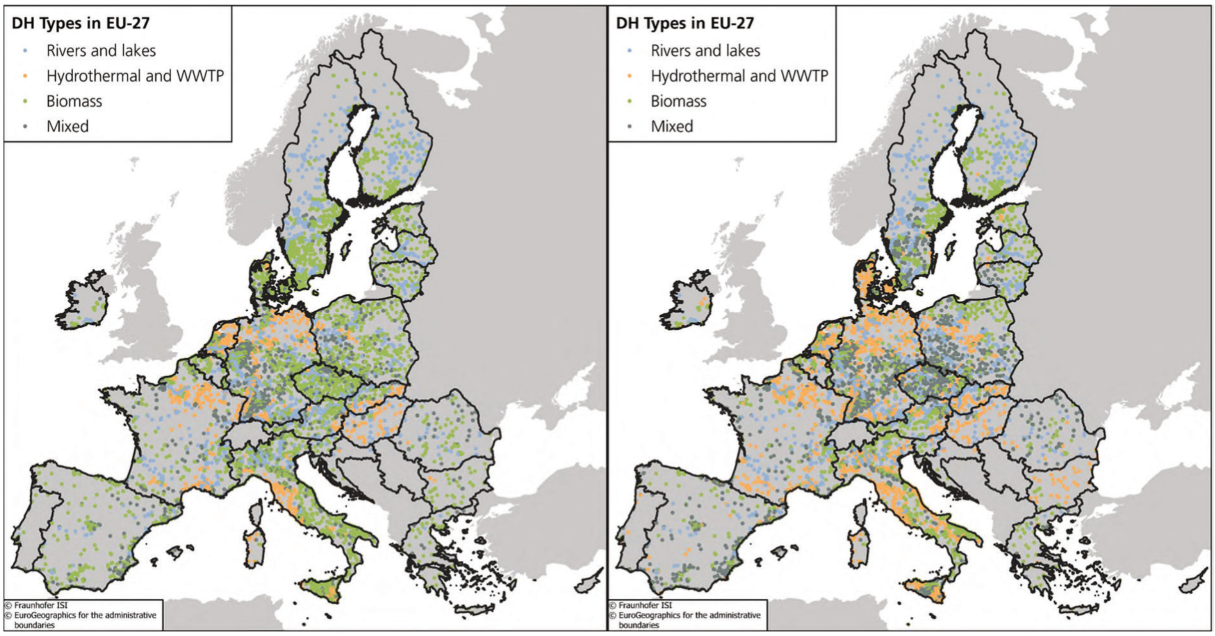

Figure 5.7: DH areas in the EU identified by type in the high-temperature (left) and low-temperature (right) scenarios

5.4 Discussion

In this paper, we quantified the available potential for the heat supply of future climate-neutral DH in the EU. The results show that biomass and geothermal energy could contribute large shares, covering up to 40-50% of future ambitious DH demand. Other large sources include heat from rivers and lakes and WWTP that could be exploited using heat pumps. If locally available, there is a high potential of excess heat from industrial plants and waste incineration. Thereby, the DH system temperature strongly influences the geothermal potential, as a lower temperature can double the hydrothermal potential where available and increases the scope of petrothermal potentials. The matched potentials serve 83% - 91% of the total DH demand locally, depending on the temperature level. The gap could be filled by air-source heat pumps, solar thermal or peak load boilers as sources for DH that were not considered in this paper. Overall, we show that climate-neutral DH in the EU is technically possible. If the DH demand is even more widespread in the future than assumed, the supply and utilisation potentials also increase as more potentials are in spatial proximity of the demand.

The method of spatial matching yielded the utilisation potentials concerning the local annual demand and supply as well as the maximum distances depending on the heat quantity of the source. The subsequent clustering reveals that most future DH areas include several different renewable and excess heat sources with different load profiles (i.e. multivalent DH systems).

Comparing the quantified potentials in this study to other analyses shows that our results are mostly in the range of existing literature (compare Table 5.5). The table also shows the large range of literature values. For industrial excess heat, the validation is published in previous papers [90,266].

Table 5.5: Comparison of annual quantified potentials in literature with values identified in this study

Heat source	Type of potential*	Geographical focus	Literature value in TWh	Value quantified in this study in TWh	Source
Biomass	Technical	EU	2300 (for all sectors)	734 (for DH)	Imperial College London [31]
Petrothermal	Supply	EU, 2050	1000 for buildings	273 (suitable with heat pump)	Dalla Longa et al., 2020 [258], based on [257]
Petrothermal	Technical	Germany	214 - 478	171 - 377	German Environment Agency [283]
Hydro- and petrothermal	Utilisation	Germany	99 (of that mostly petrothermal)	34	TAB, 2003 [259]
Hydro- and petrothermal	Utilisation	Austria, 2050	2-3	2	Könighofer et al., 2014 [260]
Hydrothermal	Utilisation	Germany	300	24	Bracke et al., 2021 [256]
Rivers and lakes	Supply/Utilisation	Switzerland	44	Out of scope of the study	Gaudard et al., 2018 [262]
Waste-to-Energy (WtE)	Technical	EU, 2030	51	97	Persson & Münster, 2016 [268]
Waste-to-Energy (WtE)	Technical	Germany	30	35	Weber et al., 2020 [269]
Wastewater treatment plants (WWTP)	Supply	Hungary	0.2	5	Somogyi et al., 2020 [263]
Wastewater treatment plants (WWTP)	Utilisation	Germany, 2050	37	43	Nielsen et al., 2020 [265]
Wastewater treatment plants (WWTP)	Utilisation	Austria, 2050	0.5	6	Nielsen et al., 2020 [265]
Wastewater treatment plants (WWTP)	Utilisation	Spain, 2050	16	21	Nielsen et al., 2020 [265]
Wastewater treatment plants (WWTP)	Utilisation	France, 2050	18	25	Nielsen et al., 2020 [265]
Wastewater treatment plants (WWTP)	Utilisation	BW in Germany, 2030	4	6	Münch et al., 2022 [264]

*The types of potential are defined in Section 5.2.2

There may be barriers to the exploitation of technical potentials. Exploiting geothermal energy involves risks due to drilling, high upfront costs, low public acceptance and complex permit processes. Limited data availability requires on-site exploration by project developers. Policy support and regulations, such as guarantee funds, are possibly required to manage such risks. Utilising the heat from WWTPs and rivers and lakes could be challenging regarding regulations and market maturity, and WWTP operators may have varying rules regarding the return temperature. Utilising industrial excess heat requires bilateral contracts between DH operators and companies. Long-term availability, downtimes, decreased production capacities, and changes in plant efficiency or closures add uncertainties. Installing backup technologies can reduce competitiveness. Data availability, especially for non-energy-intensive industries, is low, and integration into local heat planning may be challenging. Obligations for companies to assess and publish their excess heat potentials could help to identify potentials. Competition for biomass as a resource is likely to increase in the future, so the future availability for DH is uncertain. Furthermore, in this modelling approach, it was assumed that future DH areas are defined only by the distribution costs, as these were used as input data. However, DH areas could also be installed in regions with higher distribution costs where suitable renewable and excess heat potentials are located, e.g. geothermal, industrial excess heat, data centres or electrolysers. Furthermore, the implementation of climate-neutral DH systems has positive system effects, e.g. on flexibility and the market value of renewables in the electricity system [24,64,295–297], and reducing the necessary grid expansion [298].

This paper made several assumptions regarding the EU-wide potentials, the most important of which are discussed in the following. The potential of Waste-to-Energy was quantified without assuming any structural changes regarding waste. The amount could increase (as landfilling needs to be phased out in eastern EU member states) or decrease (due to a more circular economy). The composition could be more bio-based (if petrochemicals are substituted), or locations could shift to other EU countries. Furthermore, the amount of sewage water could change in the future and affect the potential from WWTP. Only general assumptions were possible concerning geothermal potentials. Field drilling is essential and could lead to entirely different results regarding underground temperatures, the existence of aquifers for hydrothermal use, and actual flow rates. The geothermal potentials quantified in this study were made without a heat pump. Including heat pumps could increase potentials in size and availability, and lower depths would be necessary. Hydrothermal also offers potential for electricity generation in CHP plants (Kalina and ORC) if sources above 100 °C are available [260]. Generally, if electricity is generated with 10% efficiency [299,300], the hydrothermal potential could decrease by 5-8%. Additionally, the assumption of a maximum transportation distance for biomass within a NUTS 2 area is inconsistent, as the NUTS 2 areas vary widely in size across different countries. This represents a conservative approach, particularly in DH types with high biomass potentials, as biomass could be transported over a larger distance. Generally, the distance assumptions based on typical sizes of the different sources do not strongly influence the results in a certain range of assumptions. However, the results of spatial matching of supply and demand depend on the method used [272]. The seasonal variability of DH demand and some sources could decrease the technical potentials and require cost-effective seasonal storage solutions.

For excess heat, the reduction of the potential of 30% by seasonal mismatch was quantified by Bühler et al., 2018 [140], and the increase by utilising seasonal storages by 12% was quantified by Chambers et al., 2020 [301]. The costs of such storage systems are uncertain and may decrease substantially in the future. Other excess heat sources like non-energy-intensive industries, data centres, hospitals, metro stations or cooling of office buildings, were not considered due to missing data but could provide excess heat on a low-temperature level and could increase the efficiency of heat pumps compared to air-source heat pumps [265,302].

5.5 Conclusions

To reach climate-neutrality in 2050, DH must be based on renewables and excess heat. This paper quantifies the technical potentials of renewable and excess heat sources for future DH systems in 2050 for the geographical extent of the EU-27 and high spatial resolution.

The findings indicate that there is sufficient potential of renewable and excess heat sources to supply DH in the future even when DH is expanded to an ambitious market share of 33%. Both types of geothermal energy, hydrothermal and petrothermal, show large potentials in many countries. Hydrothermal energy is unevenly distributed across the EU and shows vast potentials in locations where it is available, particularly in Germany, Denmark, Hungary, Romania, and Slovakia. The supply potentials are several times higher than the DH demand close by. Petrothermal sources are available in many regions but come with inherent risks and low technological maturity. Furthermore, biomass from secondary sources such as residues has a high potential. Heat from Waste-to-Energy shows a high potential to supply DH. Industrial excess heat from large individual point sources represents a possibility for utilisation, whereby the number und thus the amount of heat is smaller than of other sources. Heat pumps can utilise heat from wastewater treatment plants and rivers and lakes, having a potential distributed all over the EU. Furthermore, the results highlight that decreased system temperatures can increase the available technical potentials for DH by 26%. This is particularly relevant for geothermal potentials, which increase by a factor of three. This can substantially reduce the dependency on biomass. The exploitation of the available utilisation potentials requires a paradigm shift, which involves a transition from large-scale CHP units to a greater variety of smaller sources at lower temperatures, often combined with heat pumps.

Further research is needed to identify the economic potentials and thus hint to the future cost-optimal DH supply mix. Our study provides the basis to identify the local renewable and excess heat potentials that are spatially limited. The DH types defined here are published as open data set and can be used to model DH supply mixes and dispatch. Possible transformation paths can be modelled for the different representative DH types and thus reduce the complexity of energy system modelling.

Finally, this article provides combined and harmonised potentials for renewable and excess heat sources for district heating supply in 2050 for more than 5000 areas in Europe. This paper is the first to present potentials in high resolution for the future supply of DH, thus contributing significantly to improving the data situation, which can be used in future research. Finally, it emphasises the need for strategic policies, coordination, and collaboration among various stakeholders to effectively exploit the potentials and drive the paradigm change towards sustainable DH systems.

Acknowledgements

The analysis is based on work conducted within the project "Renewable Heating and Cooling Pathways, Measures and Milestones for the Implementation of the Recast Renewable Energy Directive and Full Decarbonisation by 2050" with the project reference number N° ENER C1 2019-482. The authors would like to thank all the project members, namely Oeko Institute, TU Vienna, e-think, Halmstad University and Fraunhofer ISI. Furthermore, we want to thank our student assistant Friedrich Graaf for his excellent work in developing the matching algorithm. The publication was supported by the Fraunhofer Cluster of Excellence "Integrated Energy Systems" (CINES).

A.5 DH areas

This annex provides a description of how the DH areas are modelled and where more information about the approach is published. To model the future location and extent of DH areas in the EU-27, the parameters of heat demand, gross floor area, a distribution cost ceiling and a DH market share within DH areas (connection rate) are set exogenously as input parameters to the calculation. The annual useful heat demand for residential and tertiary buildings in the EU is modelled to decrease from 3,129 TWh in 2020 to 1,900 TWh in 2050. This significant decrease of the heat demand leads to a decreased economic competitiveness of DH, which could be compensated with high connection rates. Therefore, it was assumed that in all countries, a connection rate between 70% and 90% within DH areas should be maintained or achieved till 2050. TableAnnex 13 shows the assumed DH connection rate and cost ceiling per country in 2020 and 2050. For the identification of the DH areas, two conditions should be fulfilled:

- The annual heat demand supplied in a DH area should be greater than 5 GWh/a;
- The average distribution cost may not exceed the pre-defined distribution cost ceiling.

A depreciation time of 40 years is considered for the DH grid. More about the modelling approach, assumptions and results can be found in the project report [7] as well as in Ref. [58] and a python implementation of the approach is provided on Github [303].

TableAnnex 13: Country-specific DH connection rate in 2020 and 2050 and distribution cost ceiling as input parameter

Country*	DH connection rate, 2020	DH connection rate, 2050	Distribution cost ceiling, 2050 in €/MWh
AT	55%	80%	36
BE	15%	70%	34
BG	64%	75%	38
CZ	44%	80%	35
DE	32%	75%	36
DK	88%	90%	40
EE	58%	80%	36
EL	29%	70%	31
ES	3%	70%	36
FI	63%	90%	37
FR	15%	75%	41
HR	37%	80%	32
HU	33%	80%	30
IE	0%	70%	36

Country*	DH connection rate, 2020	DH connection rate, 2050	Distribution cost ceiling, 2050 in €/MWh
IT	17%	70%	36
LT	78%	90%	32
LU	29%	80%	32
LV	57%	80%	32
NL	26%	75%	38
PL	51%	80%	31
PT	33%	70%	41
RO	43%	75%	32
SE	86%	90%	42
SI	52%	80%	31
SK	74%	90%	32

* Please note, that Malta and Cyprus have no DH installed until 2050.

Two or more identified coherent DH grids are considered as one connected DH area, if their focal points lie in the same LAU 2[13] region. Distribution losses occur when the heat is transported through the pipe system, from the heat generation to the heat demand. Thus, 10% and 16% of the demand for the low- and high-temperature scenario respectively was added, before matching to possible heat sources.

The DH demand and connection rate change in the time horizon until 2050. The DH potential is obtained by multiplication of the heat demand in the identified DH areas with the country-specific connection rate. Based on the investment made for the DH distribution grid and delivered heat by DH from 2020 to 2050, the average cost of DH distribution per unit of delivered heat in each country is calculated.

The resulting DH demand increases by 31.6%, from 506 TWh in 2020 to 631 TWh in the EU in 2050, with 5815 identified DH areas (FigureAnnex 1). An overview of the results of DH potentials per country in 2020 and 2050 is provided in TableAnnex 14. Average distribution costs of 31.4 €/MWh can be expected for EU. The average distribution costs in Netherlands and Portugal are relatively higher than in other countries. This is due to the fact that these countries have a low starting connection rate, leading to lower heat supply over the period of 2020 to 2050 and therefore, higher average distribution costs. Three countries, namely Estonia, Latvia and Lithuania, have relatively low average distribution cost as the heat density within DH areas in these countries is very high and the DH connection rate remains high through the study horizon.

[13] LAU (Local Administrative Units) is a territorial classification system used by the European Union for statistical purposes. LAU divisions provide a more detailed breakdown of regions compared to the NUTS classification within member states.

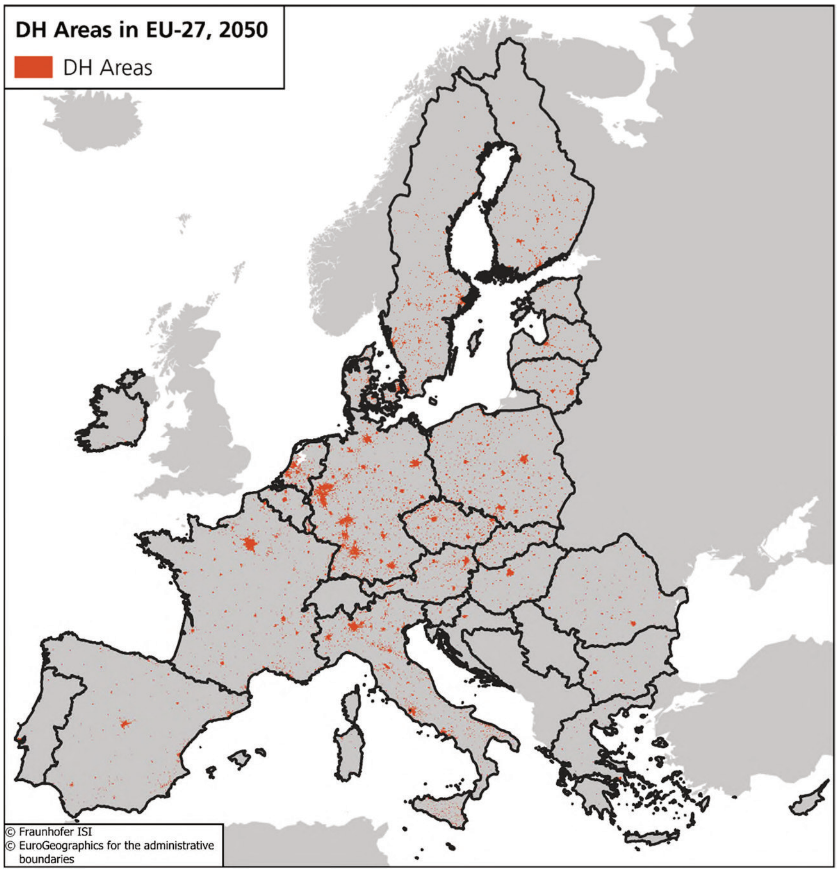

FigureAnnex 1: DH areas in the EU in 2050

TableAnnex 14: DH demand in DH areas modelled for 2020 and 2050 as well as key indicators comparing to total heat demand for buildings

Country	Demand in DH areas in GWh		Heat demand covered by DH in %		Heat demand covered by DH in GWh		Average distribution costs in €/MWh
	2020	2050	2020	2050	2020	2050	
AT	38,763	19,890	25.3%	33.2%	21,319	15,912	28.1
BE	26,027	10,636	3.4%	14.1%	3904	7445	32.8
BG	10,160	7382	26.7%	34.9%	6503	5536	28.7
CZ	51,729	30,994	24.7%	43.0%	22,761	24,795	28.1
DE	375,321	171,208	14.9%	32.4%	120,103	128,406	33.0
DK	35,273	20,287	52.8%	46.7%	31,040	18,259	32.6
EE	9105	4293	42.1%	52.2%	5281	3434	14.3
EL	14,346	11,582	10.8%	24.8%	4160	8107	29.4
ES	65,881	54,311	1.4%	30.8%	1976	38,018	33.3
FI	57,870	33,453	47.6%	63.0%	36,458	30,108	30.5
FR	203,160	123,460	6.3%	27.5%	30,474	92,595	33.7
HR	7702	3614	11.3%	25.7%	2850	2892	31.9
HU	32,249	18,281	13.3%	32.5%	10,642	14,625	28.2

Country	Demand in DH areas in GWh		Heat demand covered by DH in %		Heat demand covered by DH in GWh		Average distribution costs in €/MWh
	2020	2050	2020	2050	2020	2050	
IE	1760	1630	0.0%	4.7%	0	1141	33.1
IT	178,312	109,970	7.9%	31.0%	30,313	76,979	33.8
LT	10,987	6625	49.2%	59.2%	8570	5962	15.9
LU	5266	3066	19.5%	51.7%	1527	2453	29.0
LV	11,195	5253	41.5%	59.9%	6381	4203	15.9
NL	46,759	28,372	9.0%	26.5%	12,157	21,279	35.7
PL	130,002	63,942	27.2%	38.0%	66,301	51,153	29.6
PT	5437	4390	6.4%	13.9%	1794	3073	40.5
RO	29,236	14,314	15.0%	26.0%	12,571	10,735	29.8
SE	66,416	62,989	66.3%	65.5%	57,118	56,690	30.7
SI	3192	1809	13.6%	19.2%	1660	1447	30.7
SK	13,582	6614	32.7%	36.9%	10,051	5952	29.4
EU	1,429,732	818,367	16.2%	33.2%	505,916	631,202	31.4

A.6 Cluster analysis

This annex provides additional details on the cluster analysis, including a sensitivity analysis with different clustering algorithms. Clustering or cluster analyses is a collective term for statistical procedures that make it possible to structure a data set by group assignments. Cluster analyses are based on the consideration of the similarity or distance of the objects to each other. There are a variety of different algorithms that use different distance measures to assign objects to clusters. In general, partitioning (including k-means), hierarchical, density-based, grid-based and combined methods are distinguished (compare [304]).

In this paper, we performed hierarchical clustering as well as k-means clustering. In hierarchical clustering, the algorithm calculates the dissimilarity between all elements and gradually combines two elements with the least dissimilarity into a cluster. This formed cluster is then used again in the next iteration. In k-means clustering, clusters are represented by a central vector. When the number of clusters is fixed to k, k-means clustering gives a formal definition as an optimisation problem: find the k cluster centres and assign the objects to the nearest cluster centre, such that the squared distances from the cluster are minimised. The hierarchical clustering was performed using algorithms provided by the Python package SciPy[14]. The k-means clustering was computed using the k-means++ algorithm provided by the Python package Scikit-learn[15].

Input data for the clustering are the DH areas with their matched renewable and excess heat potentials. In order to minimise the effect of different orders of magnitudes, the potentials are expressed as a percentage of demand, resulting in figures between 0 and 1, i.e. 0% to 100% coverage.

Thus, the following input figures are used in the clustering:

- Petrothermal potentials as a percentage of demand coverage [%],
- Hydrothermal potentials as a percentage of demand coverage [%],
- Potentials form WWTP a percentage of demand coverage [%],
- Potentials from WtE as a percentage of demand coverage [%],
- Industrial EH potentials as a percentage of demand coverage [%],
- Rivers and lakes potentials as a percentage of demand coverage [%],
- Biomass potentials as a percentage of demand coverage [%],

[14] See https://docs.scipy.org/doc/scipy/reference/generated/scipy.cluster.hierarchy.linkage.html#scipy.-cluster.hierarchy.-linkage and https://docs.scipy.org/doc/scipy/reference/generated/scipy.spatial.distance.pdist.html#scipy.spatial.distance.pdist

[15] See https://scikit-learn.org/stable/modules/generated/sklearn.cluster.KMeans.html and https://scikit-learn.org/stable/modules/clustering.html#k-means

- Sludge potentials as a percentage of demand coverage [%].

TableAnnex 15 provides the maximum, the minimum and the mean of the input data per scenario.

TableAnnex 15: Overview of input data for the cluster algorithm

Scenario	High temperatures			Low temperatures		
	Maximum	Minimum	Mean	Maximum	Minimum	Mean
Petrothermal	100%	0%	14.6%	100%	0%	46.5%
Hydrothermal	100%	0%	19.3%	100%	0%	34.0%
WWTP	100%	0%	32.5%	100%	0%	36.8%
WtE	100%	0%	4.6%	100%	0%	5.2%
Industrial EH	100%	0%	4.4%	100%	0%	5.3%
Rivers and lakes	100%	0%	25.2%	100%	0%	25.7%
Biomass	100%	0%	71.7%	100%	0%	73.5%
Sludge	8.5%	0%	0.8%	9.4%	0%	0.9%

A.6.1 High-temperature scenario

For the hierarchical clustering algorithms, we use the cophenetic correlation coefficient[16] to compare different linkage types and dissimilarity calculations (TableAnnex 16). This coefficient calculates the cophenetic distances between each observation in the hierarchical clustering defined by the linkage. It measures the height of the dendrogram at the point where two branches merge. The magnitude of this value should be close to one for a high-quality solution.

TableAnnex 16: Cophenetic correlation coefficient for different hierarchical clustering (S1)

method / metric	ward*	centroid*	single	complete	average	weighted
euclidean	0.705	0.826	0.590	0.787	0.842	0.797
cityblock (Manhattan distance)	-	-	0.524	0.604	0.826	0.759
mahalanobis	-	-	0.509	0.583	0.655	0.543
chebyshev	-	-	0.624	0.628	0.807	0.681

Note: Numbers in bold indicate which clustering methods are selected for further analysis.

* Ward and centroid require Euclidean distance.

For further analysis, we choose three hierarchical clusterings with a high cophenetic correlation coefficient. We also computed k-means clustering as an additional sensitivity. Thus, the following clusterings are analysed:

- S1.1: hierarchical clustering with average linkage and Euclidean distance,

[16] See https://docs.scipy.org/doc/scipy/reference/generated/scipy.cluster.hierarchy.cophenet.html

- S1.2: hierarchical clustering with centroid linkage and Euclidean distance,
- S1.3: hierarchical clustering with ward linkage and Euclidean distance,
- S1.4: k-means clustering.

In hierarchical clustering, dendrograms, which show the pairwise combination of elements over dissimilarity, are used to select a terminus, i.e. the number of clusters. FigureAnnex 2 shows the dendrograms of the hierarchical clusterings.

S1.1: hierarchical clustering with average linkage and Euclidean distance

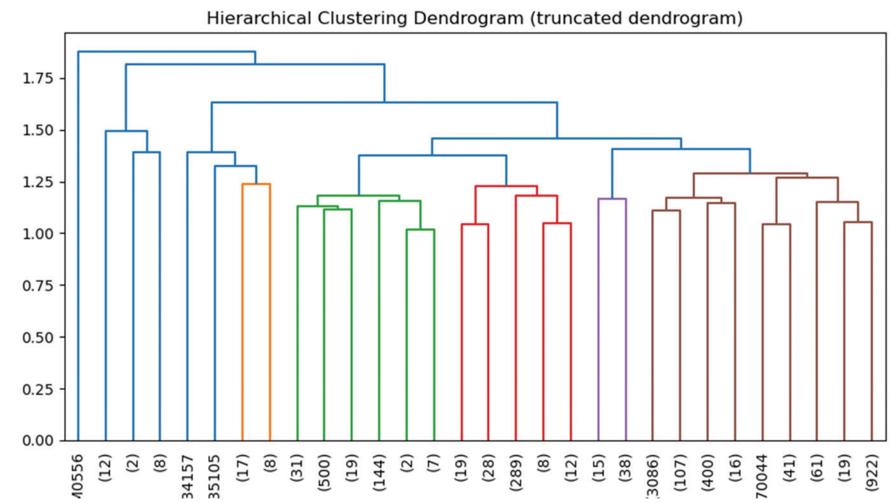

S1.2: hierarchical clustering with centroid linkage and Euclidean distance

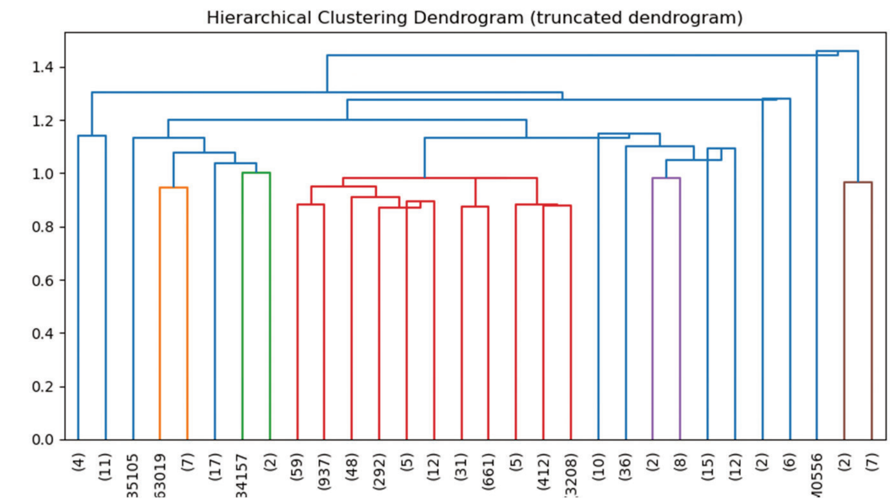

S1.3: hierarchical clustering with ward linkage and Euclidean distance

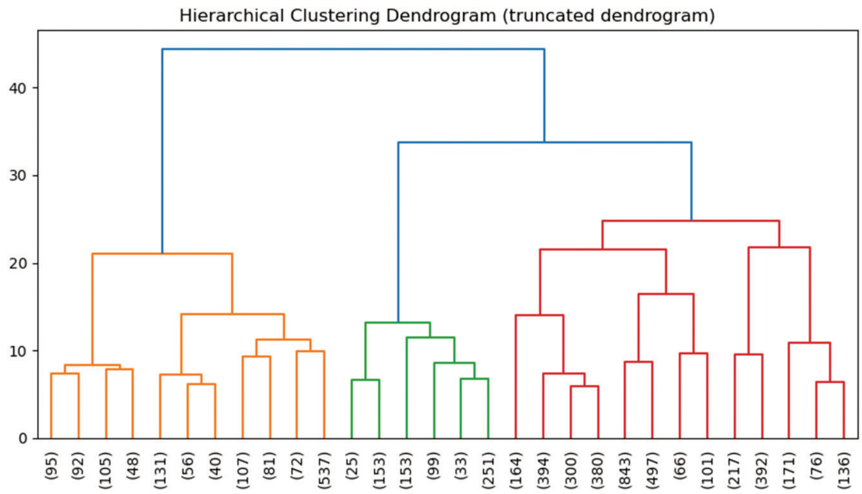

FigureAnnex 2: Dendrograms of the different hierarchical clusterings (S1)

Choosing for example four clusters leads to the following results (compare TableAnnex 17).

TableAnnex 17: Overview of results of different clusterings (S1)

Cluster	Total demand in GWh	Average demand in GWh	Number of DH areas	Petrothermal	Hydrothermal	WWTP	WtE	Industrial EH	Rivers and lakes	Biomass	Sludge	Highest potential
S1.1: hierarchical clustering with average linkage and Euclidean distance												
1	115,084	84	1364	14%	26%	31%	6%	2%	99%	74%	1%	Rivers and lakes
2	31,584	44	714	24%	98%	34%	4%	5%	0%	72%	1%	Hydrothermal
3	2,374	36	66	26%	33%	48%	5%	85%	100%	84%	1%	Rivers and lakes
4	583,086	159	3671	13%	1%	32%	4%	4%	1%	71%	1%	Biomass
S1.2: hierarchical clustering with centroid linkage and Euclidean distance												
1	1,383	92	15	1%	30%	98%	85%	0%	100%	54%	2%	Rivers and lakes
2	730,605	126	5790	14%	19%	32%	4%	4%	25%	72%	1%	Biomass
3	77	9	9	98%	100%	19%	0%	92%	0%	69%	1%	Hydrothermal

Cluster	Total demand in GWh	Average demand in GWh	Number of DH areas	Petrothermal	Hydrothermal	WWTP	WtE	Industrial EH	Rivers and lakes	Biomass	Sludge	Highest potential
4	64	64	1	1%	100%	14%	86%	100%	0%	3%	0%	Hydrothermal
S1.3: hierarchical clustering with ward linkage and Euclidean distance												
1	115,084	84	1364	14%	26%	31%	6%	2%	99%	74%	1%	Rivers and lakes
2	31,584	44	714	24%	98%	34%	4%	5%	0%	72%	1%	Hydrothermal
3	542,304	198	2745	4%	2%	18%	5%	6%	4%	70%	0%	Biomass
4	43,156	44	992	38%	1%	73%	0%	2%	0%	74%	1%	Biomass, WWTP
S1.4: k-means clustering												
1	103,854	93	1116	13%	3%	29%	6%	5%	98%	75%	1%	Rivers and lakes
2	506,273	193	2618	9%	1%	12%	4%	3%	1%	70%	0%	Biomass
3	59,652	59	1017	22%	1%	85%	5%	5%	0%	72%	1%	WWTP
4	62,350	59	1064	23%	98%	36%	5%	6%	32%	72%	1%	Hydrothermal

Comparing the output for five clusters shows that the clusterings lead to very different results. However, on a quantitative level, similarities can be observed: (i) There are several clusters where (at least) one source could cover (almost) all the demand. (ii) In all clusters, different renewable and waste heat sources can be used to cover the demand, i.e. all DH types represent multivalent networks.

A.6.2 Low-temperature scenario

As in the high-temperature scenario, we use the cophenetic correlation coefficient to compare different linkage types and dissimilarity calculations for hierarchical clusterings (TableAnnex 18).

TableAnnex 18: Cophenetic correlation coefficient for different hierarchical clusterings (S2)

metric \ method	ward*	centroid*	single	complete	average	weighted
euclidean	0.649	0.747	0.571	0.733	0.777	0.668
cityblock (Manhattan distance)	-	-	0.522	0.654	0.755	0.687
mahalanobis	-	-	0.407	0.373	0.564	0.434
chebyshev	-	-	0.593	0.526	0.728	0.710

Note: Numbers in bold indicate which clustering methods are selected for further analysis.

* Ward and centroid require Euclidean distance.

Again, we choose three hierarchical clusterings with a high cophenetic correlation coefficient and the k-means clustering for further analysis:

- S2.1: hierarchical clustering with average linkage and Euclidean distance,
- S2.2: hierarchical clustering with average linkage and Manhattan distance,
- S2.3: hierarchical clustering with ward linkage and Euclidean distance,
- S2.4: k-means clustering.

FigureAnnex 3 shows the dendrograms of the hierarchical clusterings.

S2.1: hierarchical clustering with average linkage and Euclidean distance

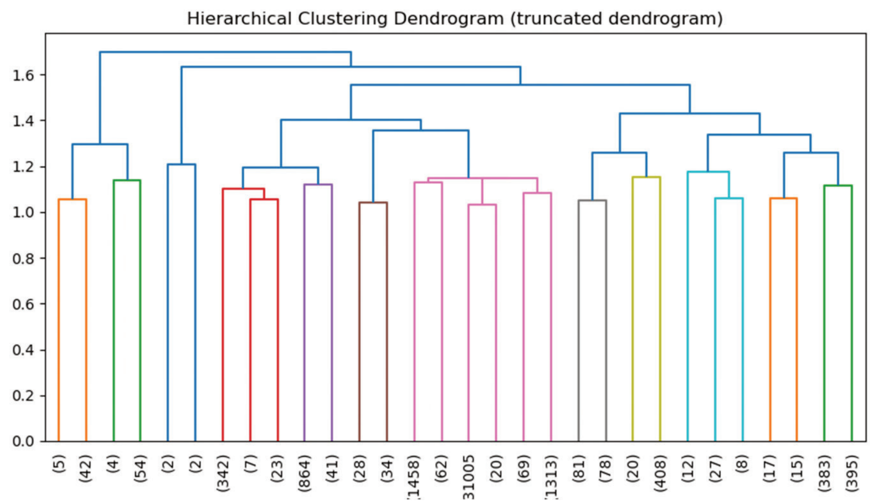

S2.2: hierarchical clustering with average linkage and Manhattan distance

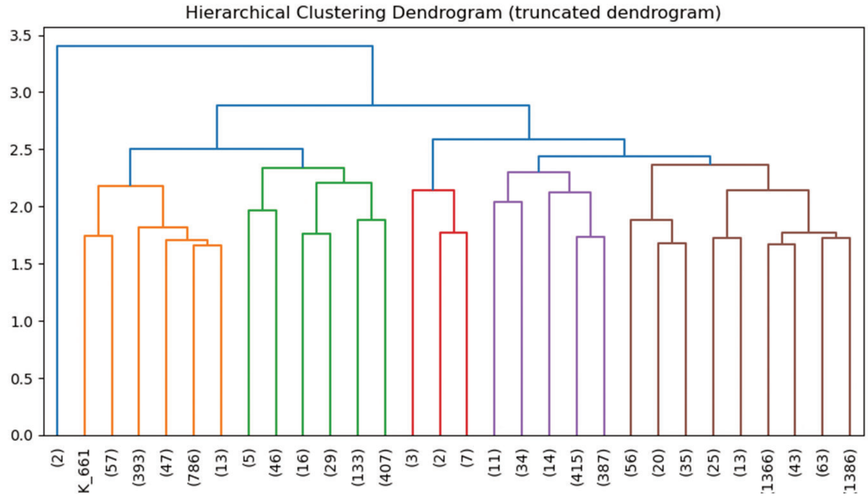

S2.3: hierarchical clustering with ward linkage and Euclidean distance

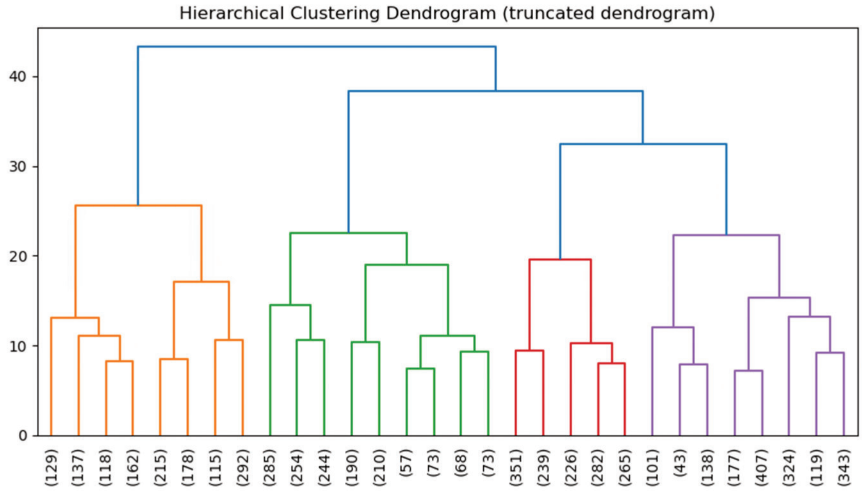

FigureAnnex 3: Dendrograms of the different hierarchical clusterings (S2)

Choosing again four clusters leads to the results shown in TableAnnex 19. As in the scenario with high temperatures, the clusterings lead to very different results. On a qualitative level, there is again the similarity that in several clusters (at least) one source could cover (almost) all of the demand and all types are multivalent networks.

TableAnnex 19: Overview of results of different clusterings (S2)

Cluster	Total demand in GWh	Average demand in GWh	Number of DH areas	Petrothermal	Hydrothermal	WWTP	WtE	Industrial EH	Rivers and lakes	Biomass	Sludge	Highest potential
S2.1: hierarchical clustering with average linkage and Euclidean distance												
1	177,87	169	105	12%	97%	38%	95%	1%	45%	66%	1%	Hydrothermal
2	728	182	4	5%	27%	13%	0%	91%	50%	10%	0%	Industrial EH
3	547,705	129	4262	49%	30%	37%	3%	5%	0%	73%	1%	Biomass
4	128,039	89	1444	43%	41%	36%	4%	7%	99%	77%	1%	Rivers and lakes
S2.2: hierarchical clustering with average linkage and Manhattan distance												
1	227	114	2	10%	0%	26%	0%	91%	100%	18%	1%	Rivers and lakes
2	133,527	69	1933	31%	99%	39%	6%	6%	33%	72%	1%	Hydrothermal
3	6,394	533	12	9%	21%	35%	56%	29%	25%	88%	1%	Biomass
4	554,112	143	3868	54%	2%	36%	5%	5%	22%	74%	1%	Biomass
S2.3: hierarchical clustering with ward linkage and Euclidean distance												
1	130,986	97	1346	40%	41%	35%	1%	3%	98%	77%	1%	Rivers and lakes
2	86,628	60	1454	38%	88%	38%	1%	16%	5%	74%	1%	Hydrothermal
3	42,118	31	1363	98%	1%	44%	0%	1%	0%	78%	1%	Petrothermal
4	434,528	263	1652	17%	8%	31%	16%	1%	6%	67%	1%	Biomass
S2.4: k-means clustering												
1	61,396	39	1590	96%	1%	45%	4%	5%	1%	79%	1%	Hydrothermal
2	87,501	66	1321	32%	99%	38%	5%	6%	1%	73%	1%	Petrothermal
3	133,172	91	1470	41%	43%	35%	7%	7%	99%	76%	1%	Rivers and lakes
4	412,191	287	1434	11%	2%	28%	5%	4%	1%	65%	1%	Biomass

Looking at both scenarios, the clusterings with average linkage type lead to groupings with only a few DH areas; i.e. only two or four areas in one cluster. These results are not in line with our objective to find representative DH types. In contrast, the clustering with ward linkage and the k-means clustering lead to a more equal distribution of areas into clusters. They also show several similarities, cross-validating the results. For example, in the low-temperature scenario (compare TableAnnex 19), both algorithms lead to (ii) one cluster with high average coverage of petrothermal, (ii) one cluster with high average coverage of hydrothermal, (iii) one cluster with high average coverage of rivers and lakes and (iv) one cluster with overall lower potentials, where only biomass can cover a larger share of the demand. Against this background, it seems reasonable to choose one of these clusterings for the analysis in this paper. For hierarchical clustering, it is not necessary to pre-specify the number of clusters. Because of this advantage, we decide to use hierarchical clustering with ward linkage and Euclidian distance and conduct further analyses to find a suitable number of clusters.

To decide on a reasonable number of clusters, we calculate the Silhouette score[17] and the Calinski-Harabasz score[18] for four, five and six clusters (compare TableAnnex 20). The silhouette coefficient measures how well an observation is clustered and it estimates the average distance between clusters. The best value is one and the worst value is minus one. The Calinski-Harabasz score is a variance ratio measurement, which measures the ratio between within-cluster dispersion and between-cluster dispersion. A higher Calinski-Harabasz score relates to a model with better-defined clusters.

TableAnnex 20: Silhouette and Calinski-Harabasz score

Scenario	High temperatures		Low temperatures	
	Silhouette score	Calinski-Harabasz score	Silhouette score	Calinski-Harabasz score
4 clusters	0.285	1468	0.223	1278
5 clusters	0.276	1373	0.256	1223
6 clusters	0.290	1363	0.273	1175

Note: Numbers in bold indicate high values.

The comparison of the Silhouette score and the Calinski-Harabasz score shows that four clusters seem suitable as it reaches (rather) high values in both scenarios. Against this background, we choose to use hierarchical clustering with ward linkage and Euclidian distance with four clusters.

[17] Based on the package SciKit; https://scikit-learn.org/stable/modules/generated/sklearn.metrics.silhouette_score.html

[18] Based on the package SciKit; https://scikit-learn.org/stable/modules/generated/sklearn.metrics.calinski_harabasz_score.html

The following box shows the formulas for the Euclidean distance and the wards minimum variance.[19]

The Euclidean distance between the two figures $p = (p_1, \ldots, p_n)$ and $q = (q_1, \ldots, q_n)$ is calculated as follows:

$d(p,q) = \sqrt{\sum_{i=1}^{n} (q_i - p_i)^2}$.

The wards minimum variance is computed as follows:

$d(u,v) = \sqrt{\frac{|v|+|s|}{T} \cdot d(v,s)^2 + \frac{|v|+|t|}{T} \cdot d(v,s)^2 - \frac{|v|}{T} \cdot d(v,s)^2}$.

Thereby, u is the newly joined cluster consisting of the clusters s and t. The value v is an unused cluster and $T = |v| + |s| + |t|$. The operator $|\square|$ calculates the cardinality of its argument.

[19] Compare https://docs.scipy.org/doc/scipy/reference/generated/scipy.spatial.distance.pdist.html#scipy.spatial.-distance.pdist and https://docs.scipy.org/doc/scipy/reference/generated/scipy.cluster.hierarchy.linkage.html#scipy.cluster.-hierarchy.linkage

A.7 Country-specific results (output of clustering)

In the following tables, the results of the clustering for the DH types are listed. The average potentials per country and cluster can be calculated by dividing the sum of the respective potentials by the number of DH areas, i.e. sum potential = average potential • number of DH areas. The numbers are also published in the data repository as supplementary material to this publication [294].

A.7.1 High-temperature scenario

TableAnnex 21: Country-specific annual DH demand, number of DH areas and annual renewable and excess heat potentials per DH type (high-temperature)

Country	DH Type	Total DH demand in GWh	Average DH Demand in GWh	Number of DH areas	Sum of potentials in GWh							
					Petrothermal	Hydrothermal	WWTP	WtE	Industrial EH	Rivers and lakes	Biomass	Sludge
AT	1	4888	41	119	186	1090	1397	1432	134	4054	4536	141
	2	371	20	19	123	371	114	0	3	0	371	11
	3	12712	122	104	34	429	3697	2388	360	2255	4215	385
	4	482	16	30	50	3	433	0	2	0	471	35
BE	1	534	44	12	0	2	160	324	19	534	513	10
	2	33	17	2	0	28	17	7	0	0	22	1
	3	8050	278	29	1	169	1564	1859	1183	323	1434	142
	4	26	9	3	11	0	26	0	2	0	18	2
BG	1	202	101	2	0	0	47	0	0	202	202	0
	2	60	30	2	6	60	0	0	12	0	60	0
	3	5885	218	27	1	19	1372	0	186	13	3953	0
	4	275	92	3	0	0	228	0	0	0	275	0
CZ	1	2085	39	53	297	297	693	0	15	2029	1675	15
	2	397	79	5	5	381	65	0	1	0	235	2
	3	25228	138	183	308	444	4919	869	395	2447	15305	119
	4	1053	24	43	217	0	761	0	1	0	1019	16
DE	1	37655	97	389	1886	9285	12208	8433	1364	35803	16778	402

Country	DH Type	Total DH demand in GWh	Average DH Demand in GWh	Number of DH areas	Sum of potentials in GWh							
					Petrothermal	Hydrothermal	WWTP	WtE	Industrial EH	Rivers and lakes	Biomass	Sludge
	2	8351	39	216	810	8012	3211	1230	151	0	6801	118
	3	95391	283	337	3129	6617	22691	23481	1953	10579	37572	873
	4	7547	26	286	4051	211	5227	9	224	0	5253	170
DK	2	137	46	3	37	137	72	10	0	0	97	1
	3	19588	306	64	71	482	3846	2252	24	0	5407	62
	4	1455	104	14	63	2	971	130	17	0	731	9
EE	1	237	47	5	0	0	91	0	0	237	237	0
	3	3531	82	43	0	0	535	0	20	440	3531	0
	4	216	43	5	0	0	213	0	0	0	216	0
EL	1	147	73	2	0	0	0	0	0	106	45	1
	3	8729	178	49	13	0	980	0	197	0	3661	114
	4	529	38	14	226	0	295	0	1	60	516	9
ES	1	1352	38	36	80	0	444	0	8	1351	1044	5
	3	29559	120	246	472	0	9923	1520	991	523	15113	138
	4	13190	118	112	383	0	10520	355	136	0	9495	100
FI	1	10745	160	67	0	0	13	42	494	10745	10745	1
	3	24181	255	95	0	0	0	264	359	1060	15135	0
FR	1	8547	52	163	844	5969	2211	2523	148	7686	6065	0
	2	7125	40	180	1442	6556	1975	914	216	180	6123	0
	3	88255	446	198	1713	6531	19042	14025	1328	3478	31804	1
	4	3416	31	110	2012	63	1865	83	50	220	2922	0
HR	1	2092	523	4	79	2086	684	0	16	1381	1158	6
	2	30	30	1	0	30	20	0	30	0	17	0
	3	942	118	8	7	14	219	0	28	14	885	2
	4	290	290	1	0	0	290	0	21	0	274	2
HU	1	1834	71	26	258	1666	691	0	32	1590	1660	11

Country	DH Type	Total DH demand in GWh	Average DH Demand in GWh	Number of DH areas	Sum of potentials in GWh							
					Petrothermal	Hydrothermal	WWTP	WtE	Industrial EH	Rivers and lakes	Biomass	Sludge
	2	3625	95	38	975	3559	1706	8	33	60	3552	25
	3	11276	3759	3	210	3146	2233	457	180	900	3329	27
	4	229	76	3	154	0	187	0	0	0	229	2
IE	1	209	23	9	0	0	30	0	0	209	209	0
	3	1101	36	31	0	0	428	469	110	0	1101	0
	4	13	7	2	0	0	10	0	0	0	13	0
IT	1	6369	42	153	4	446	2163	1152	134	6203	3530	4
	2	5384	40	133	479	5225	1638	295	293	0	3324	4
	3	73129	115	636	311	5707	17543	5616	1548	2199	32289	38
	4	4414	29	152	144	123	3921	14	63	0	2486	7
LT	1	1686	130	13	53	0	510	0	15	1686	1686	0
	3	4885	136	36	28	0	1087	0	43	1660	4885	0
	4	346	43	8	56	0	255	0	0	0	346	0
LU	1	94	13	7	0	0	1	0	0	94	9	0
	3	2683	60	45	0	20	280	195	52	0	245	0
	4	82	20	4	0	0	82	0	0	0	7	0
LV	1	3569	99	36	0	0	886	0	0	3414	3569	0
	3	1233	39	32	0	0	226	0	10	120	1233	0
	4	73	12	6	0	0	58	0	0	0	73	0
NL	1	2042	79	26	151	1372	800	390	59	2042	1061	7
	2	3357	45	75	502	3316	963	1131	122	0	1577	12
	3	17954	321	56	359	848	3432	8848	651	100	660	40
	4	1324	74	18	204	93	1125	0	0	0	643	8
PL	1	7969	97	82	604	971	2401	0	98	7713	7561	39
	2	806	50	16	144	747	316	0	3	60	806	4
	3	46426	179	259	531	127	10396	16	661	5408	37701	173

Country	DH Type	Total DH demand in GWh	Average DH Demand in GWh	Number of DH areas	Sum of potentials in GWh							
					Petrothermal	Hydrothermal	WWTP	WtE	Industrial EH	Rivers and lakes	Biomass	Sludge
	4	4137	37	112	913	12	3005	0	38	0	3521	37
PT	1	150	19	8	52	0	106	0	4	150	102	3
	3	2900	223	13	139	0	1294	636	133	48	543	39
	4	515	57	9	51	0	486	0	3	0	246	11
RO	1	1669	64	26	55	428	855	0	33	1589	1656	1
	2	24	24	1	2	16	0	0	0	0	24	0
	3	8277	176	47	0	0	2333	0	350	386	5532	3
	4	2483	89	28	4	334	2040	0	21	0	2483	2
SE	1	19318	217	89	829	0	2339	1672	426	17376	13494	205
	3	45919	285	161	534	0	3846	5052	636	1573	21971	382
	4	523	40	13	248	0	224	0	27	0	338	19
SI	1	370	46	8	9	218	95	0	11	356	234	2
	3	1249	89	14	11	11	54	12	33	203	228	7
	4	59	20	3	0	0	59	0	0	0	0	1
SK	1	1322	46	29	148	313	520	0	52	1288	1188	0
	2	1883	82	23	435	1804	507	0	38	60	1826	0
	3	3221	111	29	67	286	1432	47	190	843	1730	0
	4	478	37	13	84	40	300	0	0	0	470	0

A.7.2 Low-temperature scenario

TableAnnex 22: Country-specific annual DH demand, number of DH areas and annual renewable and excess heat potentials per DH type (low-temperature)

Country	DH Type	Total DH demand in GWh	Average DH Demand in GWh	Number of DH areas	Sum of potentials in GWh							
					Petrothermal	Hydrothermal	WWTP	WtE	Industrial EH	Rivers and lakes	Biomass	Sludge
AT	1	3341	30	111	797	386	1616	68	138	3274	2963	152
	2	1914	50	38	501	1727	302	0	364	523	1914	32
	3	488	12	42	478	0	139	0	0	0	488	13
	4	11755	145	81	673	1002	4531	4040	416	3351	3836	404
BE	1	101	14	7	63	0	22	0	0	101	84	5
	2	1618	116	14	155	1140	444	772	826	289	835	34
	3	31	8	4	31	2	25	0	3	0	24	2
	4	6447	307	21	135	4	1634	1637	1005	541	1010	122
BG	1	192	96	2	23	192	57	0	0	192	192	0
	2	2433	90	27	668	2205	628	0	323	12	2378	0
	4	3465	693	5	24	857	1303	0	17	0	1819	0
CZ	1	2941	49	60	1714	1338	1180	0	6	2639	2619	25
	2	2943	75	39	930	2576	770	0	629	324	2337	18
	3	3181	24	134	3081	11	1587	0	8	0	3095	33
	4	18211	357	51	2510	334	4169	956	286	2231	9728	84
DE	1	44232	121	366	4841	19657	15535	10684	2570	38198	16463	447
	2	17325	51	338	2616	15185	6102	1771	2483	2384	14568	227
	3	7394	22	329	7070	67	4262	0	203	0	5000	153
	4	72290	371	195	8924	16102	24463	23633	1682	8581	29391	814
DK	2	6770	130	52	703	6751	2712	797	71	0	3387	35
	3	807	81	10	745	70	430	35	0	0	456	6
	4	12507	658	19	441	2400	2700	1774	0	0	2516	35
EE	1	913	130	7	0	0	268	0	0	816	913	0

Country	DH Type	Total DH demand in GWh	Average DH Demand in GWh	Number of DH areas	Sum of potentials in GWh							
					Petrothermal	Hydrothermal	WWTP	WtE	Industrial EH	Rivers and lakes	Biomass	Sludge
	2	46	15	3	0	0	15	0	27	0	46	0
	4	2819	66	43	0	0	685	0	17	0	2819	0
EL	1	258	86	3	151	0	0	0	1	205	164	3
	2	79	26	3	17	0	5	0	55	0	73	2
	3	424	28	15	412	0	236	0	3	0	369	6
	4	8157	185	44	218	0	1291	0	218	0	3469	119
ES	1	1855	46	40	1371	0	466	12	13	1601	1529	6
	2	901	38	24	496	0	246	0	739	31	686	6
	3	5817	30	195	5427	0	2919	0	202	0	4948	35
	4	33247	246	135	4400	0	20015	1950	832	323	18102	209
FI	1	12328	174	71	0	0	16	38	961	11310	12328	1
	2	221	74	3	0	0	0	0	109	0	221	0
	4	20570	234	88	0	0	0	298	381	303	12163	0
FR	1	11021	74	148	2449	6980	4369	1801	1423	8471	9627	0
	2	13493	56	241	3780	11115	4100	2181	755	512	11811	0
	3	4922	38	128	4696	17	2263	563	92	81	4406	0
	4	72355	540	134	4072	18295	19166	14734	1666	3856	19923	1
HR	1	1981	495	4	180	1976	835	0	30	1842	1180	6
	2	45	22	2	0	45	24	0	40	16	27	0
	4	1155	144	8	0	0	543	0	55	0	1155	4
HU	1	1709	68	25	341	1550	723	0	44	1551	1570	11
	2	3505	88	40	1316	3486	2021	9	80	110	3418	27
	3	203	51	4	203	0	179	0	0	0	196	2
	4	10670	10670	1	480	5662	2726	503	304	1210	3378	29
IE	1	198	22	9	0	0	31	0	0	198	198	0
	2	256	37	7	10	142	9	77	131	0	256	0

Country	DH Type	Total DH demand in GWh	Average DH Demand in GWh	Number of DH areas	Sum of potentials in GWh							
					Petrothermal	Hydrothermal	WWTP	WtE	Industrial EH	Rivers and lakes	Biomass	Sludge
	4	801	31	26	0	11	416	379	0	0	801	0
IT	1	5774	40	144	391	4059	2305	604	209	5388	3566	4
	2	21310	56	380	2856	19548	7361	628	1816	1343	10519	14
	3	2257	18	122	1922	93	916	8	80	0	1317	2
	4	55336	129	428	2114	5800	19202	6515	1413	2229	26328	35
LT	1	3835	256	15	90	0	1164	0	33	3821	3835	0
	2	130	130	1	10	0	42	0	64	0	130	0
	3	634	37	17	625	0	213	0	0	0	634	0
	4	1960	82	24	358	0	803	0	7	0	1960	0
LU	1	89	13	7	83	0	2	0	0	89	9	0
	2	216	31	7	61	113	0	0	68	0	21	0
	3	120	9	13	116	0	9	0	0	0	12	0
	4	2286	79	29	219	208	410	215	41	0	224	0
LV	1	3628	95	38	203	0	1209	0	0	3546	3628	0
	2	43	22	2	0	0	17	0	23	0	43	0
	3	56	19	3	52	0	18	0	0	0	56	0
	4	896	29	31	20	0	178	0	1	0	896	0
NL	1	1366	62	22	289	1276	573	0	35	1366	814	5
	2	4647	46	100	1288	4069	2050	38	1098	240	1712	18
	3	351	25	14	321	4	207	0	0	0	213	1
	4	17036	437	39	1114	3732	4517	10737	668	425	1243	46
PL	1	11657	124	94	5032	2203	4040	0	781	10780	11279	67
	2	4085	64	64	1711	3316	1600	0	501	471	3878	20
	3	7411	37	199	7132	145	3383	0	84	0	6943	47
	4	33116	296	112	4171	584	10111	18	394	3454	25905	132
PT	1	135	17	8	101	0	83	0	35	135	96	3

Country	DH Type	Total DH demand in GWh	Average DH Demand in GWh	Number of DH areas	Sum of potentials in GWh							
					Petrothermal	Hydrothermal	WWTP	WtE	Industrial EH	Rivers and lakes	Biomass	Sludge
	2	175	35	5	175	0	103	0	125	30	70	3
	3	257	26	10	253	0	172	0	8	0	177	5
	4	2814	402	7	396	0	1794	695	15	24	534	45
RO	1	2180	75	29	1434	722	1169	0	162	1807	2168	1
	2	1001	111	9	277	710	425	0	295	82	993	0
	3	1816	42	43	1773	0	1166	0	21	0	1816	1
	4	6812	324	21	777	1143	2985	0	298	161	4331	3
SE	1	18935	204	93	5263	0	2956	1403	880	17959	14236	232
	2	787	79	10	648	0	101	10	426	135	510	9
	3	5680	84	68	4848	0	693	90	61	81	3435	62
	4	36957	402	92	4584	0	3938	5749	525	1911	17351	334
SI	1	444	40	11	130	294	121	13	28	444	309	4
	2	105	35	3	23	77	0	0	17	6	77	0
	3	23	23	1	23	0	0	0	1	0	23	0
	4	1019	102	10	2	4	106	0	20	161	29	6
SK	1	1875	59	32	736	993	869	0	147	1663	1749	0
	2	2578	61	42	1047	2509	1003	0	132	148	2474	0
	3	246	21	12	242	18	96	0	1	0	238	0
	4	1848	231	8	128	932	1313	52	159	605	500	0

6 Achieving climate-neutrality in district heating: The impact of system temperature levels on the supply mix of EU-27 in 2050

Ali Kök, Anna Billerbeck, Pia Manz, Lukas Kranzl: Achieving climate-neutrality in district heating: the impact of system temperature levels on the supply mix of EU-27 in 2050. Under review in: Energy.

6.1 Introduction

The European Union's Climate Law and Green Deal have set an ambitious target to achieve carbon neutrality by 2050, placing the spotlight on the heating and cooling sector, which accounts for nearly half of the EU's total energy consumption [305]. District heating (DH) could play a significant role in integrating low-carbon energy sources into the heating energy mix on a large scale [306]. However, two-thirds of the DH fuel supply mix in the EU-27 consists of fossil fuels, indicating an urgent need for systemic changes [9].

DH systems traditionally operate at high-temperature levels to ensure efficient heat transfer and distribution. However, recent advancements and environmental considerations have spotlighted the significance of reducing these temperature levels. Historically, DH systems have evolved through various generations: the 1st generation, which used steam as the heat carrier; the 2nd generation, which utilised high-temperature water; the 3rd generation, which introduced medium-temperature water systems; and now, the 4th generation, focused on low-temperature systems that enhance energy efficiency and integrate renewable energy sources [21]. Emerging now is the 5th generation (5GDH), which integrates district heating and cooling (DHC) systems, enabling even greater flexibility and efficiency by using ultra-low temperature networks and leveraging synergies between heating and cooling demands.

Ref. [21] gives an overview of the historical development of the past generations of DH and defines 4th generation of DH (4GDH), following the 3rd generation of DH (3GDH).The DH generations differ in terms of system temperatures, heat carriers (steam, pressurised hot water, low-temperature water), type of pipes used (in situ/pre-insulated, steel/flexible), integration with smart energy systems, digitalisation, and many other aspects [21]. Even though the system temperature level is not the only characteristic of the different DH generations, it is one of the most fundamental differences among them.

The benefits of lowering system temperatures in DH are multifaceted. Reduced system temperatures increase efficiency on the heat production and network sides. Lower supply temperatures can increase the efficiency of not only heat pumps and solar thermal but also conventional heat generation technologies such as combined heat and power (CHP) plants [28]. Lower operating temperatures inherently reduce heat loss during heat transportation and distribution. One of the most significant benefits of reduced system temperatures is unleashing the potential of low-temperature renewable energy sources (RES) and excess heat (EH) [192]. For instance, geothermal energy sources are available at different temperature levels depending on the geographical location. Similarly, EH is available at varying temperatures based on the process. Reduced DH supply temperatures enable exploiting low-temperature geothermal and EH sources, which cannot be utilised within the DH system with high supply temperatures.

In the quest to decarbonize the heating sector, policy direction plays a pivotal role, originating from the highest echelons of European governance. Through directives, the European Commission and Council chart the course for this transition. Key among these are the recently revised Energy Efficiency Directive EU/2023/1791 (EED III) [20] and the Renewable Energy Directive EU/2023/2413 (RED III) [12].

The EED III, with specific articles emphasising high-efficiency DH, and the RED III, set an indicative target of an annual 2.2 ppt increase in RES and waste heat and cold share from 2021 to 2030 in Article 24. Even though the target for DH is indicative, it gives a signal to the Member States (MS) that it might become binding in future amendments. Similarly, RED III Article 23 is amended to make the target of increasing the share of RES in heating and cooling by 1.1 ppt annually binding, which also puts the spotlight on DH collectively driving the agenda towards a more sustainable and efficient heating sector with an increasing focus on DH. These directives set a top-down framework that member states (MS) must adopt into their national laws. In this context, adopting a European-level perspective becomes crucial for comprehensively understanding and aligning with these overarching policy goals. Modelling at this level not only aids in assessing the collective impact of Individual MS actions but also ensures that the strategic direction for decarbonisation is coherent, efficient, and aligned with the broader EU objectives. Such an approach enables a unified assessment of progress, challenges, and opportunities, guiding policy design and implementation across the EU for a harmonised transition towards sustainable heating.

Against this backdrop of policy-driven initiatives and the urgent need for a sustainable heating sector, our paper addresses the research questions:

- What is the impact of system temperature levels on the cost-minimal decarbonized DH supply mix in the EU-27 by 2050, considering the expansion of DH grids and the availability of RES and EH potentials?

- To what extent does the levelised cost of heat generation (LCOHG) decrease on the EU level by reducing DH system temperature levels?

These questions aim to contribute to understanding how DH system temperatures can influence DH systems' efficiency, sustainability, and alignment with EU climate objectives. By exploring this question, our research aims to provide a deeper insight into the dynamics of DH systems under varying temperature levels, assess the feasibility and implications of integrating diverse energy sources, and gauge the potential economic and environmental impacts.

Our work relates to two streams of studies in the literature: studies analysing the reduction of DH system temperatures and studies modelling the DH sector on a European level. In the former stream of studies, numerous studies focus on the different dimensions of the DH system temperature reduction as it is a complex topic requiring improvements on supply, building, and grid sides. Studies such as Refs. [12,20] show the monetary benefits of reducing DH system temperatures by calculating the cost reduction gradient for selected heat supply technologies and storage. Ref. [307] reviews DH business models with a particular focus on business models encouraging the reduction of return temperatures and provides suggestions for Austrian utilities. Ref. [308] investigates the effects of lower operational temperatures on a CHP-supplied DH system's overall energetic and exergetic efficiencies and costs. Ref. [309] evaluates the variable costs of DH plants under different supply temperatures. Ref. [310] analyses the network configurations implemented in low-temperature DH systems and discusses their suitability. Ref. [311] proposes a methodology to model the optimal retrofitting of DH distribution networks to lower the supply temperatures and implements it in a case study. Ref. [312] presents a method to estimate the potential temperature reduction in the existing DH substations. The implementation of the method in a case study shows that the supply temperatures on existing substations can be reduced significantly without any modifications. Ref. [313] compares low temperature and ultra-low temperature with electric boosting and heat pump boosting concepts for DH with a long-term energy system perspective. Through scenario analysis, the authors show that the low-temperature DH concept has the lowest costs. Ref. [314] provides a comprehensive review of benefits, challenges, required actions, and current practices of supply temperature reduction in existing DH networks. It is also essential to note that there are many studies in the literature focusing on 5GDH such as Refs. [233,315,316], however, 5GDH is out of the scope of this study.

A limited number of studies in the literature model the DH on a European level, mainly in the grey literature. Heat Roadmap Europe (HRE) project series provides local heat planning strategies to reach carbon neutrality by 2050 for selected MS, the highest 14 selected MS in the last series of the project [38]. The project series significantly contributes to understanding the decarbonization of the heating sector from a European-level perspective. The sEEnergies project presents pathways for EU-27 and each MS separately to reach carbon neutrality by 2050 with a focus on energy efficiency measures. Both studies employ the ENERGYPLAN tool to simulate hourly energy systems with a whole energy system perspective [40]. Ref. [64] analyses the market value of renewable energy sources for EU-27, where DH is modelled as one of the flexibility options. Ref. [317] investigates the role of hydrogen and heat pumps in space and water heating for EU-27 in 2050, concluding that the heat pumps are more favourable over the hydrogen in both decentral and central heating systems. Both Refs. [64,317] employ the ENERTILE optimisation tool to model DH as a part of the European energy system. However, these studies do not consider the use of excess heat, and geothermal and solar generation are fixed, not optimised. Ref. [7] provides decarbonization pathways for heating and cooling sectors of EU-27 by 2050. Our work builds on the modelling framework developed by Ref. [7]. However, our work still significantly differs from Ref. [7], as we design our primary scenarios based on temperature levels and provide a variety of sensitivity analyses.

This paper contributes to the existing literature in the following ways:

- We model the DH sector for the EU-27 by designing the scenarios around the system temperatures, highlighting the explicit impact of temperature levels. This approach provides a unique insight into the operational efficiencies and potential of renewable energy integration under different system temperature levels.
- Our modelling considers a comprehensive range of DH supply technologies. To the best of our knowledge, our paper provides the future DH supply mix of EU-27 with the most detailed technological level by optimising their investments and operations.
- To the best of our knowledge, this study is the first to explicitly model the impact of supply temperature levels on the LCOHG of DH on the European level.

The structure of this paper is organised as follows: the next section describes the methodology employed in our study, including the data sources, key assumptions, and scenario design. Section 6.3 presents the findings, including the DH generation mix, installed capacities, LCOHG, and exploitation of RES potentials. Section 6.4 addresses the discussion and limitations of our study. Finally, Section 6.5 concludes the paper, synthesising the results and their policy implications.

6.2 Methodology

In this paper, we employ the Hotmaps DH GEN model [50] to model the future DH supply across EU MS. Our analytical framework focuses on two core system temperature scenarios: high-temperature and low-temperature DH, corresponding to 3GDH and 4GDH, respectively. We further investigate the sensitivity of specific variables like energy prices for biomass and hydrogen and the economic impact of implementing a carbon price on waste incineration.

6.2.1 Overview of modelling framework

DH, by its nature, shows heterogeneous characteristics within different regions. One of the factors creating this heterogeneity is the building stock. Depending on the current status and future evolution of the building stock, the feasibility of decentral heating or different DH generations and expansion of DH might change. Another critical factor leading to heterogeneity is the locally available heat sources. DH utilises locally available heat sources efficiently and effectively while helping secure the heat supply. Depending on the available heat sources, the dominant heat sources in DH supply vary in different regions. Both building stock characteristics and availability of local heat sources differ among and even within the MS. Thus, it is essential to consider these heterogeneous characteristics.

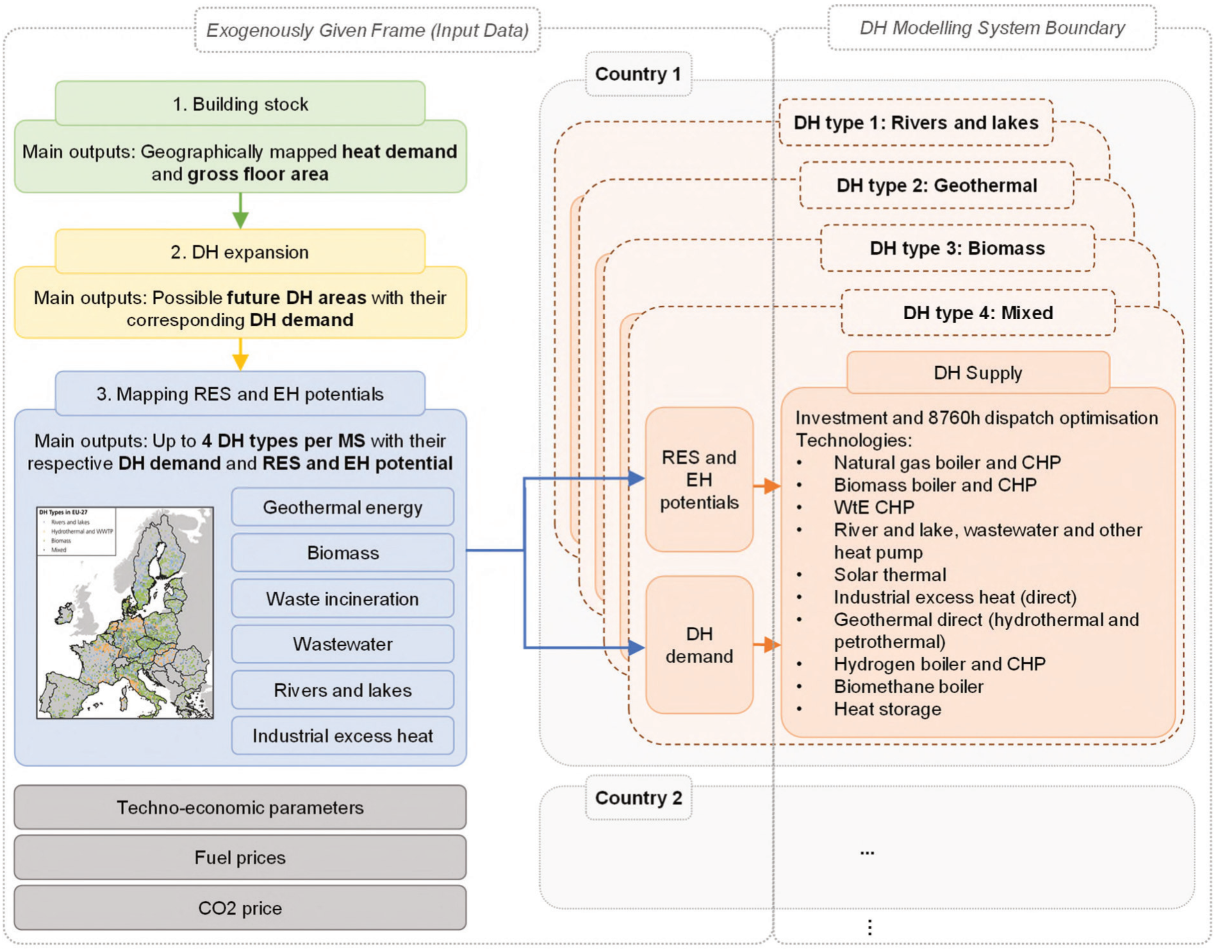

Figure 6.1: Schematic overview of the modelling system boundaries and input data

In our work, we reflect the heterogeneity of DH in the primary input data: DH demand and RES and EH potentials. This input data is prepared in three steps, where each factor creating heterogeneity is modelled in three steps via soft-linking three models. This framework is developed by the project Renewable Heating and Cooling Pathways – Towards full decarbonisation by 2050 (ENER C1 2019-482) [7] to model the DH ecosystem comprehensively. Figure 6.1 provides an overview of the modelling framework, depicting data flow between models (in bold) and the DH system boundary. This paper primarily focuses on DH generation modelling, which is the DH Modelling System Boundary in Figure 6.1. As it is essential to understand the broader context provided by the preceding phases of the modelling framework (steps 1 – 3), they are described briefly in the following paragraphs. The remainder of this section explains the preliminary work done to create data used in this paper that is already published in the respective papers and reports and allows us to capture the heterogeneity of DH systems. The last step of the modelling framework, DH modelling, is explained in the following subsection.

In the initial step, the INVERT/EE-LAB [318] model is employed by Ref. [7] to characterise the building stock. INVERT/EE-LAB is a dynamic bottom-up simulation tool considering technological and socio-economic factors. It assesses how various policy combinations influence key aspects such as overall energy consumption, energy carrier mix, reductions in CO_2 emissions, and expenses associated with heating, cooling, hot water supply, and lighting in buildings. The primary outputs from INVERT/EE-LAB, which are utilised by the DH expansion model, are heat demand and gross floor area. These outputs are initially generated at the NUTS 0 geographical level and further disaggregated to the hectare level for utilisation by the DH expansion model. A comprehensive description of the model setup and the results of the building stock modelling can be found in Ref. [7].

In the second step, the DH expansion model of Ref. [58] is employed by Ref. [7] to calculate potential future DH areas based on DH connection rates and grid costs through geospatial modelling. A DH region is designated as a potential DH area if its grid cost falls below a specified threshold (cost ceiling). These cost thresholds are assumed to be country-specific and the same within a country. Details about the grid cost ceilings and DH connection rates for each MS are available in Ref. [7]. The identified hectare-level DH areas are assumed to be connected if they lie in the same local administrative unit (LAU) regions. A total of 5815 prospective DH areas are identified. While temperature levels influence heat losses in DH areas, the regions and useful energy demand remain constant across the two temperature scenarios. Further information about model parameters and results can be found in Ref. [7].

In the third step, Ref. [319] builds upon the first two steps, establishes spatially high-resolution datasets covering RES, including biomass, deep geothermal, heat from rivers and lakes, heat from wastewater treatment plants (WWTP), both from sewage water and biogas from sludge, and EH sources including industrial excess heat (IEH) and waste-to-energy (WtE) to quantify technical potentials for supplying the DH areas. The geothermal potentials are split up into hydrothermal (based on aquifers) and petrothermal (heat from the rock) potentials. We refer to the term geothermal as the sum of two types of geothermal energy unless one of them is explicitly stated. A detailed description of the methodology can be found in Ref. [319], and the open-source datasets are accessible through Ref. [294]. Assumptions regarding technical parameters and restrictions for each potential heat source to reflect the technical potential at two different temperature levels are established. Lower DH system temperatures enhance the efficiency and availability of heat sources, particularly geothermal energy. These supply potential datasets have spatial resolutions of point coordinates (WtE, WWTP) to 5000m x 5000m (rivers and lakes), varying depending on the heat source, with an annual temporal resolution. The possible utilisation over the year is represented in terms of full load hours.

These supply potential datasets are spatially matched using a geographic information systems (GIS)-based approach, accounting for maximum distances for each heat source. The maximum distances are chosen for each source based on the heat that is typically available. The matching algorithm prioritises areas with higher demand [319]. Thus, a single large point source could supply multiple DH areas, e.g., the WtE plant can supply multiple DH areas if one DH area's demand is lower than the heat potential. More details on maximum distances for heat sources and assumptions can be found in Ref. [319]. As a result, for each DH area, the technical potentials that are available to supply the DH areas from each heat source are listed as tabular data and spatial data in Ref. [294]. The DH demand and RES potentials for each MS are available in Annex A.8.

A clustering analysis by Ref. [319] concludes the third step to identify so-called "DH types", defined as sets of DH areas with similar RES and EH potentials. Input data for clustering consists of the DH areas with their corresponding RES and EH potentials, normalised as percentages of demand to mitigate variations in magnitude (ranging from 0% to 100%) for each temperature scenario considered. DH areas are grouped into up to 4 clusters (DH types) for each MS using an agglomerative clustering algorithm [319]. Figure 6.2 shows the geographical distribution of the DH types, named after the dominant heat source in each cluster, namely, Rivers and lakes, Hydrothermal and WWTP, Biomass, and Mixed.

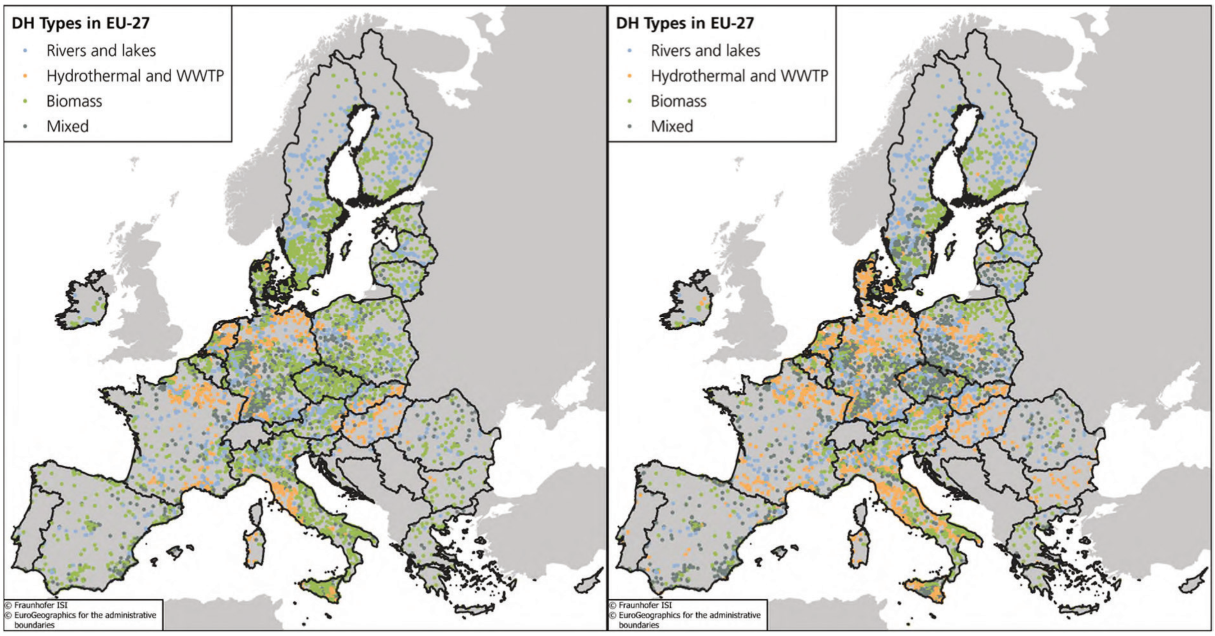

Figure 6.2: DH areas in the EU identified by type in the high-temperature (left) and low-temperature (right) scenarios [319]

6.2.2 DH generation model

Hotmaps DH GEN model is an open-source mixed-integer linear programming tool (available at Ref. [320]) that minimises the total cost of DH generation. The model optimises both investments and the operation of technologies on an hourly level. The model incorporates various input parameters including, but not limited to, hourly data related to district heating demand, electricity price, solar radiation, and source temperatures for heat pumps (river, wastewater, et cetera), as well as investment and operational costs. Each technology incorporated into the model is defined by its nominal heat production capacity and associated thermal and electrical efficiencies. The main outputs of the model are the levelised cost of heat production, associated investment, operational and fuel expenses, the distribution of heat production across different generators, CO_2 emissions, and full-load hours.

The objective function of the optimisation model and the primary constraint to meet the DH demand are presented below. The model's complete mathematical formulation, which consists of numerous constraints, is available in Ref. [50].

$$\min(c_{total} - rev_{total}) \tag{11}$$

The objective function (11) of the model minimises the difference between the total cost of DH generation, c_{total}, and revenues from the electricity production, rev_{total}.

$$rev_{total} = \sum_{j,t} x_{el_{j,t}} \cdot p_{s,el_{j,t}} \tag{12}$$

The revenues from the electricity production (12) are defined as the sum of the electricity generated, $x_{el_{j,t}}$, by each plant j at hour t times the electricity sale price, $p_{s.el_{j,t}}$, for the plant j at hour t. Hence, it is assumed that all the electricity produced by the CHP plants is sold for the given electricity price.

$$c_{total} = OPEX_{fix} + OPEX_{var} + c_{cold} + c_{ramp} + IC \quad (13)$$

Equation (13) defines the total cost of heat production as the sum of fixed operational expenses, $OPEX_{fix}$, variable operational expenses, $OPEX_{var}$, cold start costs, c_{cold}, ramping costs, c_{ramp}, and investment costs, IC. The investment costs are annualised based on the interest rate and the lifetime of the heating plants (depreciation time).

$$\sum_{j,t} x_{th_{j,t}} + \sum_{hs,t} (x_{unload_{hs,t}} - x_{load_{hs,t}}) = demand_{th_t} \quad (14)$$

The demand constraint (14) ensures that the DH demand is met at all time steps, where $x_{th_{j,t}}$ is the thermal generation by each plant j at hour *t*; $x_{unload_{hs,t}}$ is the amount of thermal energy extracted from each heat storage hs while $x_{load_{hs,t}}$ is the thermal energy loaded in each heat storage hs at hour t. The sum of thermal generation by each plant and the thermal energy loaded and unloaded to/from heat storage must be equal to the thermal demand, $demand_{th_t}$, at the corresponding time step t.

One of the most critical parameters of the optimisation model is the efficiency of the DH plants. Among the technologies considered in this study, only heat pumps have a variable coefficient of performance (COP) value, while all the remaining technologies, including solar thermal, have a fixed nominal efficiency. Therefore, changes in the system temperature levels have a direct impact only on the heat pumps through their COPs. The COPs of the heat pumps are calculated as a function of the source, flow, and return temperatures.

$$n_{th_t} = COP_{nom_j} + s_{COP,source} \cdot \left(v_{s_{j,t}} - v_{s_{nom,j}}\right) + s_{COP,flow} \cdot \left(v_{f_{j,t}} - v_{f_{nom,j}}\right) + s_{COP,return} \cdot \left(v_{r_{j,t}} - v_{r_{nom,j}}\right) \quad (15)$$

Equation (15) defines the efficiency of heat pumps, n_{th_t}, at each time step t. Nominal values for COP, COP_{nom_j}, source temperature, $v_{s_{nom,j}}$, flow temperature, $v_{f_{nom,j}}$, and return temperature, $v_{r_{nom,j}}$, are used as reference values. The nominal temperature values are subtracted from the actual source, flow, and return temperatures at each time step, represented as $v_{s_{j,t}}$, $v_{f_{j,t}}$, $v_{r_{j,t}}$, respectively, and multiplied by the source, flow, and return temperature sensitivities, represented as $s_{COP,source}$, $s_{COP,flow}$, $s_{COP,return}$, respectively. In this way, the COPs of the heat pumps are pre-calculated and given the optimisation as a parameter. Similarly, the flow and return temperatures are also calculated as a function of the outside ambient temperature.

6.2.3 Data and assumptions

In our work, we model the target year 2050 by doing a so-called greenfield investment optimisation, meaning no plants exist at the beginning. The main reason for using a greenfield approach is that even though spatially high-resolution data is available for identifying prospective DH areas and local heat sources, data with similar granularity is lacking for current installed capacities and the remaining lifetimes of DH plants, which is required to model the evolution of existing DH systems. We implement this approach with one exception: pre-installing capacities for WtE plants. This reflects the policy decisions as landfilling of municipal waste is forbidden in the EU, and incineration is the most favourable way of getting rid of the waste that cannot be recycled.

The projected DH demand for 2050 and the RES and EH potentials to meet this demand are foundational to our modelling study. Projections for 2050's heat demand are derived from Ref. [319]. Ref. [319] implements stringent minimum energy performance standards for the worst-performing 25% of buildings, mandating renovations within ten years starting 2025. By 2035, these standards are tightened to improve energy performance to levels between A and B. Subsidies cover 15% for standard renovations and 35% for high-efficiency renovations, although pre-1945 buildings face barriers to achieving class A performance (see Ref. [58] for the details on policies implemented on building stock). The energy efficiency measures reduce the useful heat demand of the buildings from 3129 TWh in 2020 to 12900 TWh in 2050. DH final energy demand rises to 631 TWh compared to 446 TWh of DH final energy consumption in 2018 [9]. The DH shares of each MS as a result of the DH expansion modelling are available in Annex A.9. We assume grid losses of 10% in the low system temperature scenario and 16% in the high system temperature scenario, which results in a DH demand of 695 TWh and 732 TWh, respectively. The difference in DH demand between the two system temperature scenarios comes from the higher grid losses due to the higher system temperatures. The RES and EH potentials are used as constraints on how much heat can be produced by the corresponding DH plants.

The techno-economic data used for DH plants is primarily based on Ref. [73], which provides a country- and size-specific dataset for the future cost of DH supply technologies. The authors use a construction cost index to scale the investment cost data within countries. However, they scale the investment cost as a whole even though the shares of equipment and installation costs in the investment cost are provided. This leads to big dispensaries within the countries. Thus, we adapt the investment cost data by keeping the equipment costs constant within countries and using the construction cost index only for installation costs, as proposed by Ref. [321]. The techno-economic data of Ref. [73] does not provide variable COP values for heat pumps but only seasonal coefficient of performance (SCOP) values. Hence, we use temperature sensitivity values from Ref. [25] following the methodology presented in the Section 6.2.2. Similarly, Ref.

[73] does not cover the direct use of geothermal energy. Therefore, we use the techno-economic data for direct geothermal energy of Ref. [321].

Our analysis covers all relevant DH generation technologies, three of which are large-scale heat pumps. A complete list of technologies and how they are affected by system temperatures is available in Annex A.10. We explicitly model wastewater and river and lake heat pumps. On the other hand, we model all other kinds of heat pumps, namely air-source, low-temperature geothermal and excess heat, and data centre heat pumps, aggregated into a single technology due to the lack of data on geographically dispersed low-temperature heat sources used by these heat pumps. We call this type of heat pump "other heat pumps" and model them as air-source heat pumps.

The energy carrier prices (including taxes and fees) and emission factors used in this paper are mainly based on Ref. [51]. The prices in Ref. [51], in particular electricity prices, are hourly prices for each MS. Ref. [51] uses a multisectoral energy supply model to model future electricity prices for a climate-neutral energy system, so that, among other things, interdependencies between sectors and the impact of high variability of RES are taken into account in the input data. Table 6.1 shows the overview of the energy carrier prices. Finally, we assume a high CO_2 price of 500 €/tCO_2 to ensure a decarbonized DH sector.

Table 6.1: Overview of the energy carrier prices

Energy Carrier	Price (average) [€/MWh]	Country-specific	Time resolution	Source
Electricity	127	Yes	Hourly	[51]
Hydrogen	148	Yes	Annual	[51]
Biomethane	108	Yes	Annual	[51]
Biomass	35	No	Annual	Own assumption
Industrial excess heat	10	No	Annual	Own assumption
Waste	0	No	Annual	Own assumption

6.2.4 Scenario design

We frame our main scenarios based on the system temperature levels: high- and low-temperature DH systems, representing the 3GDH and 4GDH, respectively. In our scenario design, the only difference between the 3GDH and 4GDH comes from the system temperature differences, even though the 4GDH covers more than only lower temperature levels, i.e., diversified heat sources, seasonal thermal storages, digitalisation, etc. [322]. This makes modelling entire European DH systems computationally possible, and it also still aligns with the original definition of the 4GDH by Ref. [21]. The system temperatures affect the DH GEN model directly through the heat pumps and indirectly through the RES potentials. Table 6.2 gives an overview of the main scenarios and their temperature levels, which are in line with the temperature levels used in the calculation of RES and EH potentials.

Table 6.2: System temperature levels used in the scenario design

Scenario	Abbreviation	Flow temperature	Return temperature
High system temperature (baseline)	HighTemp	95-85°C	60°C
Low system temperature (baseline)	LowTemp	65-55°C	30°C

In addition to the main scenarios, we calculate four sensitivities for each temperature scenario. We investigate the sensitivities of energy carrier prices for hydrogen and biomass and the investment cost of geothermal energy plants to reflect their uncertainties and assess the robustness of the results. The biomass price sensitivity reflects the uncertainty regarding its limited availability and competition with food production and other sectors as highlighted by Ref. [323]. This scarcity, coupled with its use in various renewable energy systems, makes biomass a sensitive and crucial factor in determining the economic feasibility of DH systems. Hydrogen prices were included due to the uncertainty surrounding its future role and evolving market conditions, which could significantly affect its competitiveness as an energy source. Geothermal investment costs were analysed due to the high initial capital required, influencing its adoption in low-temperature DH systems. Additionally, the increase in geothermal investment costs reflects the exploration risk, as deep geothermal projects typically involve multiple drillings, some of which may fail, resulting in higher overall investment costs. In our main scenario, we do not apply a CO_2 price to the WtE plants. Thus, in the last sensitivity scenario, we implement a CO_2 price for WtE plants to reflect the impact of corresponding policy decisions regarding monitoring WtE plants' emissions and evaluation of their inclusion into the emission trading system in the Revised Emission Trading Directive (EU 2023/959) [324]. Table 6.3 provides an overview of sensitivity scenarios.

Table 6.3: Overview of the sensitivity scenarios

Sensitivity scenario	Abbreviation	Difference to the baseline scenarios
High geothermal investment cost	Geo	100% increase in geothermal investment costs
Low biomass price	Bio	Reduction of biomass price to €25/MWh
Low hydrogen price	H2	50% decrease in hydrogen price
Carbon price for WtE	WtE	Implementation of a CO_2 price for WtE plants

6.3 Results

The presentation of our results is divided into three steps. Initially, we provide an overview of the DH generation mix for all scenarios with the corresponding LCOHG values, which cover only the heat generation costs (without grid costs). Subsequently, we present the installed capacities for each scenario. Finally, we present the exploitation of RES and EH potentials in each scenario.

6.3.1 DH generation mix and LCOHG

This section analyses the DH generation mix by comparing the high and low system temperature scenarios and their corresponding sensitivities. Figure 6.3 shows the DH supply mix of EU-27 in 2050 for all scenarios. The left y-axis shows the thermal generation in TWh, represented by the bars. The right y-axis shows the LCOHG in €/MWh, represented by the white and red squares. A more detailed figure on the DH supply mix of MS for the two main system temperature scenarios is available in Annex A.11.

The *HighTemp* scenario primarily comprises heat pumps, accounting for nearly 50% of the thermal generation (18% from wastewater heat pumps and 31% from other heat pumps). This is followed by 18% from biomass (of which 16% CHP), 12% from WtE CHPs, and 13% from direct geothermal energy sources (both hydrothermal and petrothermal). In the *LowTemp* scenario, the geothermal energy share significantly increases to 34% and becomes the most dominant heat source together with heat pumps. Almost the entire DH production from wastewater heat pumps shifts to geothermal technologies, as well as half of the biomass share. One would expect an increase in the share of heat pumps in case of lower temperature levels; however, the results show that this is not necessarily the case due to the increased availability of alternative heat sources, such as low-temperature geothermal and excess heat, which become more feasible under reduced temperature levels.

Sensitivity scenarios were explored to better understand the cost effects, each offering its own set of key insights (cf. Table 6.3). In the *LowTempGeo* scenario, the share of direct geothermal energy use sharply declines to 16%, and its share shifts to the heat pumps. There is no other significant change in the remaining technologies. This indicates a strong competition between heat pumps and the direct use of geothermal energy. However, in the *HighTempGeo* scenario, there is a minor change in the share of geothermal technologies. The limited availability of heat sources to supply high temperatures makes direct geothermal still an economically viable option even in case of high investment costs.

In low biomass price sensitivity, where biomass price drops from 35 €/MWh to 25 €/MWh, the contribution of biomass rises significantly in both temperature scenarios. In both scenarios, the increase in biomass shares originates from the drop in the heat pump shares. This implies a competition between heat pumps and biomass technologies.

In the case of the low hydrogen price scenario, the share of hydrogen increases significantly in both temperature scenarios compared to the baseline scenarios. However, the share of hydrogen in the overall DH supply mix remains low. It makes the highest contribution of 6% in the *HighTempH2* scenario.

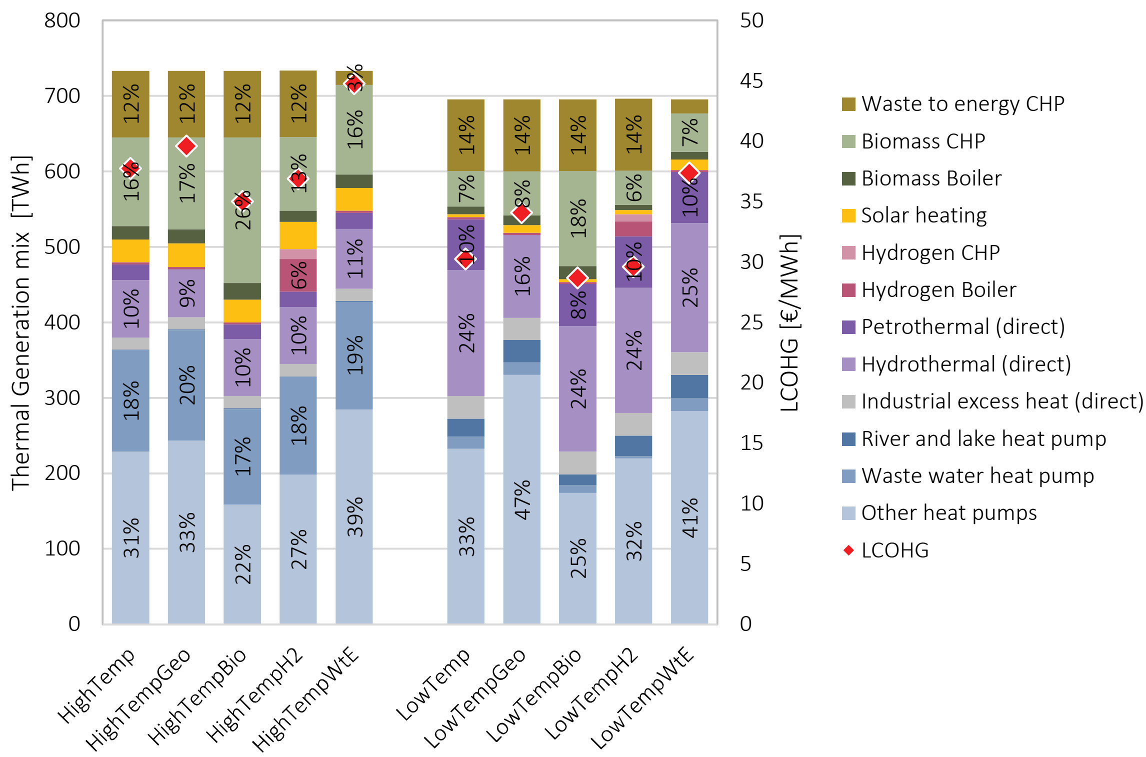

Figure 6.3: **DH thermal generation mix in the EU in 2050**

In the last sensitivity scenario, the implementation of a CO_2 price for the WtE plants makes the share of waste incineration in the DH supply decline sharply in both temperature scenarios. Recall that the WtE capacities are pre-installed in our modelling (as explained in Section 6.2.3), which means that investment is already made into the WtE plants. This shows the strong impact of the high carbon price on the economic viability of waste incineration.

Wastewater heat pumps significantly contribute to DH supply across all high-temperature scenarios due to their relatively stable and high source temperature. However, their contribution plummets in all low-temperature scenarios as the availability of other heat sources, such as geothermal energy and IEH, increases, and river and lake and other heat pumps can also reach higher COPs.

Table 6.4 shows the LCOHG values for all high- and low-temperature scenario variants, the reduction in LCOHG in each scenario pair, and the total monetary savings. In terms of LCOHG, all low-temperature scenarios consistently demonstrate lower costs when compared to their high-temperature equivalents and a cost reduction of up to 20%. This underscores the cost-effectiveness of transitioning to lower system temperature levels. In both temperature scenarios, the highest LCOHG occurs in case of a CO_2 price for waste incineration, and the lowest occurs in low biomass price scenarios. The results also show that reduction of system temperature can lead to annual savings of up to 6.83 billion Euros, which can be invested into measures required for temperature reduction.

Table 6.4: LCOHG reduction and total annual savings across all the scenarios

Scenario	LCOHG [€/MWh]		LCOHG Reduction	Total annual savings [bn EUR]
	HighTemp	LowTemp		
Baseline	37.75	30.24	20%	6.64
Geo	39.62	34.07	14%	5.35
Bio	35.05	28.69	18%	5.74
H2	36.92	29.63	20%	6.46
WtE	44.78	37.38	17%	6.83

6.3.2 Installed capacities in DH

Figure 6.4 shows the DH installed capacities of EU-27 in 2050 across all scenarios. The installed capacities follow a similar pattern to the DH generation mix, with one notable exception: hydrogen boilers. While hydrogen boilers are among the highest installed capacities in all the scenarios, their contribution to the thermal generation mix is among the lowest. This high capacity and low generation pattern underlines their role as backup technologies in peak demand hours.

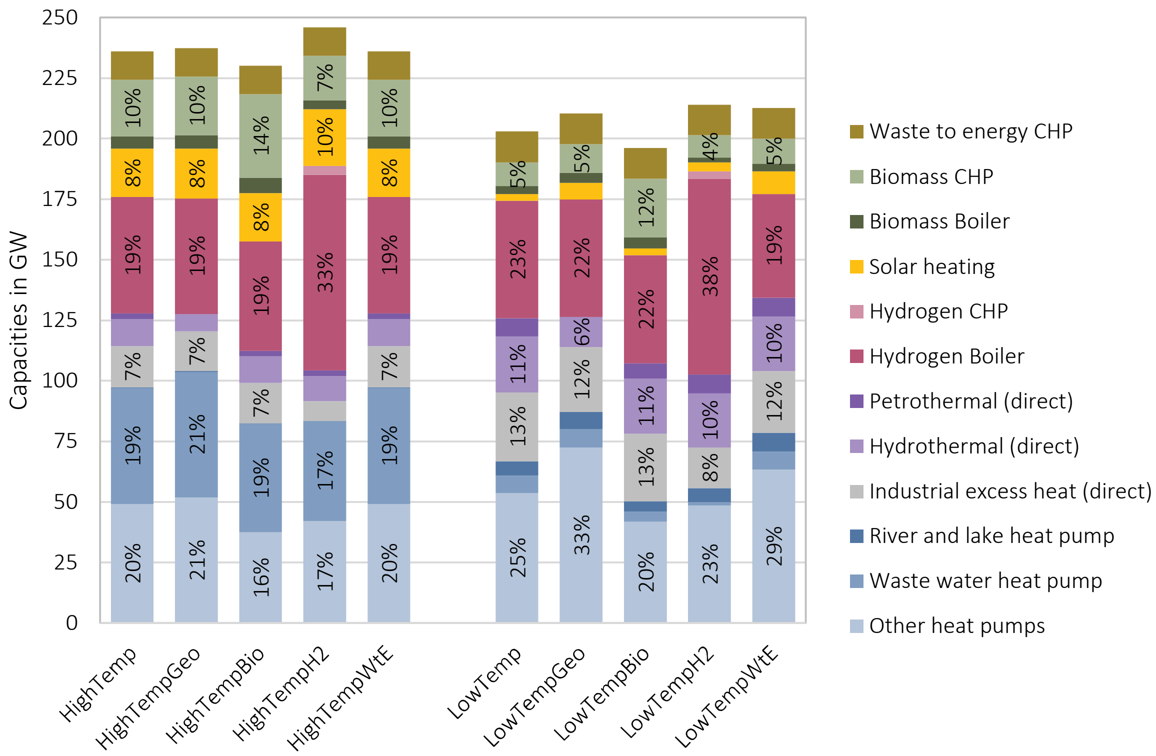

Figure 6.4: DH installed capacities in the EU in 2050

On the other hand, geothermal energy technologies and WtE plants show an opposite trend. Despite their lower installed capacities, these technologies comprise a considerable portion of the DH supply mix. The reason for this disparity lies in their role as base-load suppliers, attributed to their stable heat supply and low operational costs. However, their deployment is constrained by higher investment costs.

6.3.3 Exploitation of RES and EH potentials

In this section, we analyse the exploitation rate of the RES and EH potentials, represented as the share of the utilised potential in the total potential for respective RES and EH sources. Figure 6.5 visualises the exploitation rates in two heat maps for high-temperature and low-temperature scenario variants. While 100% exploitation means that all the available potential of the respective RES or EH source is exploited, any share less than 100% means there is still unused potential left.

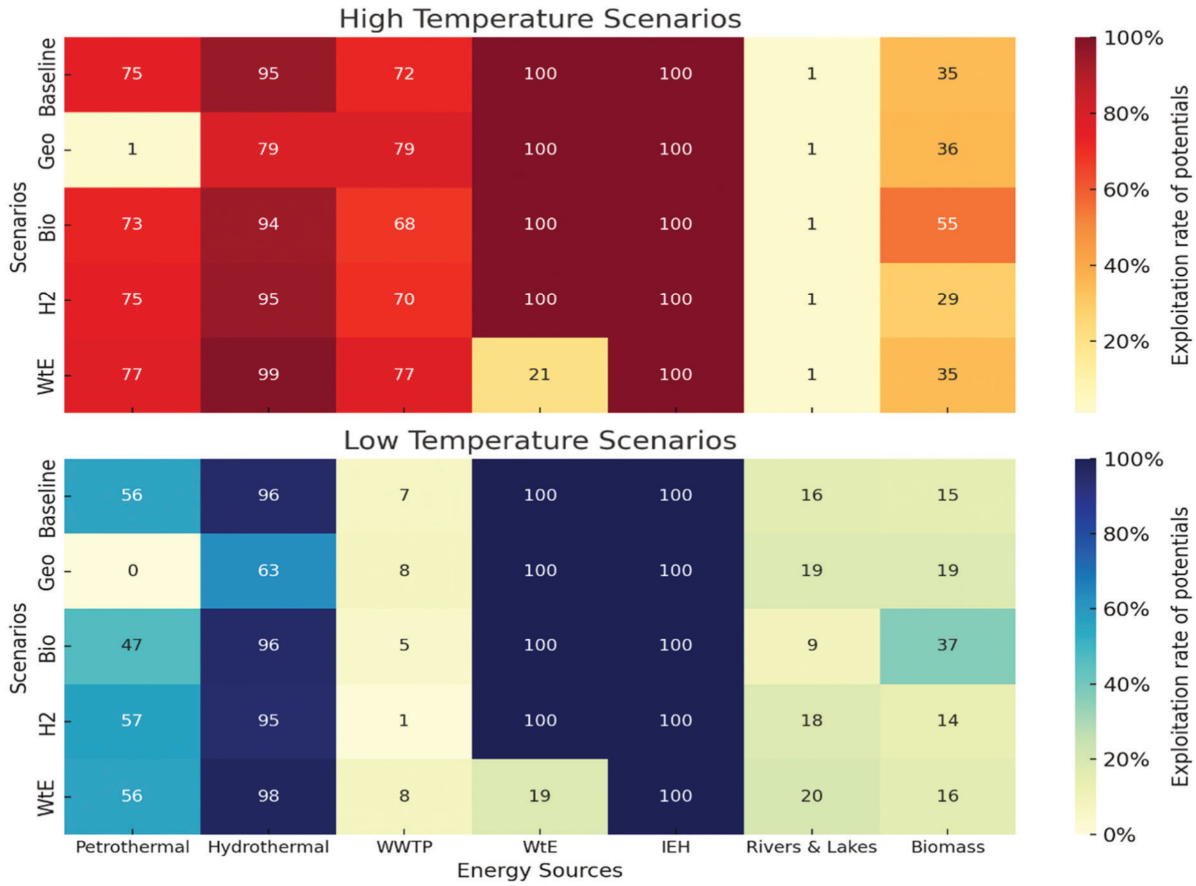

Figure 6.5: Heat map of the exploitation of RES and EH potentials for high-temperature (top) and low-temperature (bottom) scenarios

The high-temperature scenarios reveal a substantial potential for hydrothermal and WtE, consistently reaching near-full or full exploitation across different economic conditions, underlying their robustness and critical role in high-temperature DH systems. This is mainly due to their ability to supply heat at high temperatures and the absence of other RES and EH potentials. Petrothermal energy, while significantly exploited in the *HighTemp* scenario, shows a marked decrease in scenarios with increased geothermal investment costs, indicating its sensitivity to economic factors.

Conversely, low-temperature scenarios exhibit a diverse exploitation pattern, which can be attributed as an advantage contributing to the security of supply through diverse local heat sources. Notably, there is a significant decrease in the use of wastewater treatment and petrothermal energies compared to high-temperature scenarios, suggesting lower competitiveness at reduced temperatures. In high-temperature scenarios, wastewater treatment plants are preferred due to their relatively high and stable source temperatures, resulting in a high COP, and a lack of other RES and EH sources. On the other hand, in low-temperature scenarios, the availability of hydrothermal energy increases significantly. Hydrothermal energy replaces wastewater treatment plants as a cheaper heat source due to its constant availability and low operational costs.

IEH shows a consistent 100% exploitation across all scenarios and temperatures, emphasising its significance and constant demand in DH systems. The notably higher exploitation of rivers and lakes in low-temperature scenarios shows that temperature reduction can unlock its potential.

The sensitivity scenarios introduce distinct shifts in the exploitation patterns. A notable increase in geothermal investment costs leads to a drastic reduction in petrothermal source utilisation, emphasising its economic sensitivity. The biomass price reduction and the hydrogen price decrease show an uptick in their respective resource exploitation, highlighting price as a significant driver for their adoption. The implementation of a CO_2 price for WtE plants resulted in a diversification of the supply mix, showcasing the potential for policy measures to influence sustainable energy exploitation.

6.4 Discussion and limitations

Our main results, the DH supply mix, are determined through the optimization of capacity and operations. They rely on various techno-economic factors, including investment and operational costs, efficiencies, energy prices, operational flexibilities, and the RES and EH potentials. The available potentials ultimately determine the maximum amount of heat that can be generated by each heat source. Therefore, their competitiveness also depends on how much of the available potential is utilized. Section 6.3.3 and Figure 6.5 give this perspective. Geographical constraints play a significant role in determining the potential of each heat source. This was calculated in the RES potentials by Ref. [319].The authors match the available RES and EH potentials for DH with the DH areas defined by the DH expansion modelling. Geographical constraints have a notable impact on the availability of renewable heat sources. However, the DH regions do not differ within the two temperature scenarios in our study. What changes is the amount of available heat from a heat source as a result of temperature reduction. For example, geothermal energy becomes more cost-effective as a higher amount of geothermal energy becomes available at lower temperatures, which can be used as a base-load supply.

A key limitation lies in the greenfield optimisation assumption in our modelling. It is a simplification required mainly due to the lack of data (as explained in Section 6.2.3) not accounting for existing DH plants. This approach overlooks the influence of these existing infrastructures on the transition to newer systems. Even though there are 26 years until 2050 and most DH plants will complete their lifetimes, existing DH plants could still influence the future DH systems through lifetime extensions and the know-how and qualified workforce developed through them. On the other hand, the existing DH supply of EU-27 highly relies on fossil fuels, and these plants, anyway, need to be replaced by 2050. Furthermore, the political context within each country can significantly impact the pace and direction of DH development. Future research could address this limitation by incorporating more detailed data on the current DH infrastructure, including installed capacities, plant lifetimes, and retrofit potential, to provide a more nuanced transition pathway.

In our DH supply technologies, we do not have electric boilers. This is for several reasons: first, Ref. [51], where we get the electricity and hydrogen prices, models the generation and distribution of these energy carriers explicitly in an integrated energy system model; however, it does not consider electric boilers as an option. Hence, the interaction between electricity generation and the use of electric boilers is not captured. Since, we rely on the electricity and hydrogen prices from this study, introducing electric boilers would cause inconsistency. The use of electric boilers would require a system-wide perspective to determine whether it is more efficient to use cheap or excess renewable electricity directly with electric boilers, or to store it as heat in thermal storage (possibly much more efficiently via large-scale heat pumps), or to use it for hydrogen production (again another type of energy storage) for peak-time usage. Further research should investigate this question from a system perspective on the European level.

Another limitation is the conservative assumption in modelling low-temperature geothermal, excess heat, and data centre heat pumps as heat pumps with the same COP as air source heat pumps. The COP of heat pumps utilising sources other than air is likely to be higher, potentially underestimating their efficiency. This conservative approach may not fully capture the potential benefits of these technologies. To overcome this limitation, future research should focus on generating high-resolution spatial data for low-temperature geothermal and excess heat sources. Such data could make the modelling of these low-temperature heat pumps possible.

In addition, the excess heat sources included in our input data by Ref. [319] involve IEH and excess heat from waste incineration plants. However, the excess heat that can be utilized by DH is not limited to these potentials. Future research should explore the excess heat potentials from emerging technologies such as Power-to-X (e.g., hydrogen production, methanation) and data centres, given that the market for these technologies is growing rapidly. These potentials could significantly enhance the DH supply mix, particularly considering the full utilization of IEH across all the scenarios in our study.

In preparation of the RES potentials, Ref. [319] employs conservative assumptions regarding biomass availability and costs, focusing on high prices and only the local availability of secondary biomass resources. This approach might not accurately reflect the dynamic market conditions and the potential availability of more affordable biomass sources. If cheaper biomass becomes available for the DH sector, it could significantly alter the supply mix and the overall economics of DH systems. Future research should explore a wider range of biomass price scenarios and availability, including potential advances in biomass technology and supply chains, to better reflect future market conditions.

The imposition of a CO_2 price on WtE plants could make them economically infeasible and could reduce the emissions they are causing. However, this raises a further question on what happens to the no longer incinerated waste. Even though circular economy practices could reduce the amount of waste, this question requires further research. The economic pressure through CO_2 price could also incentivise WtE companies to invest in carbon capture and storage. Future research could explore alternative waste management strategies and the role of carbon capture technologies, offering a broader range of solutions for managing emissions from WtE plants.

The methodology employed in this study is highly replicable for other regions and contexts, as we use open datasets on renewable energy sources, and excess heat potentials with the open-source Hotmaps DH GEN model. Researchers can also adapt our approach to different geographic areas.

6.5 Conclusions

Our findings reveal that large-scale heat pumps and geothermal energy technologies could play a pivotal role in decarbonizing the European DH sector. These technologies are particularly effective in low-temperature scenarios, as they can operate with greater efficiency and ease of integration with renewable sources. Lower system temperatures thus pave the way for integrating more geothermal energy and various types of heat pumps, ultimately reducing the LCOHG up to 20% compared to the case with high system temperature levels.

Second, changes in system temperature levels significantly influence the choice of energy sources in DH systems. For instance, wastewater heat pumps are more prominently featured in high-temperature scenarios, while the river and lake heat pumps and biomass are generally more favourable for low-temperature scenarios.

Third, geothermal technologies show considerable potential, specifically in low-temperature scenarios, where they can potentially replace or complement heat pumps depending on factors such as investment costs. This spotlights the significance of geothermal energy as EU MS strive to decarbonise their heating sector, especially considering the benefits of geothermal energy, such as low environmental impact (minimal land coverage, low noise levels), a stable and reliable energy supply, and low operational costs over the long term. However, it is critical to address the high initial capital costs associated with their deployment for geothermal technologies to become viable.

Fourth, our scenarios indicate that hydrogen technologies only play a marginal role in the future DH supply, even under reduced hydrogen prices. Therefore, their contribution to DH remains limited as of now.

Fifth, the role of biomass in the DH supply is found to be highly sensitive to price, where it competes with large-scale heat pumps. The role of biomass also depends on policy interventions like biomass allocation within the different sectors. The low share of biomass in the baseline scenarios does not mean that it does not have an essential role in the decarbonization of DH. Biomass could serve as a vital transitional fuel as it constitutes a considerable share of renewable DH supply today.

From a policy perspective, these findings point to several actionable steps. Targeted investments in geothermal and heat pump technologies should be prioritised, especially for low-temperature DH systems. Regulations might also need to encourage the transition from high to low system temperatures, such as building renovation, as lower temperatures enable the incorporation of more renewable and efficient technologies into the energy mix. Furthermore, considering the urgency of meeting the EU’s 2050 carbon neutrality targets, implementing higher carbon prices on fossil fuel-based systems and WtE could accelerate the shift towards cleaner, more sustainable energy sources.

In summary, our study provides insights into how system temperatures, the integration of RES and EH, and the economic viability of various technologies interplay to shape the future of sustainable heating. The insights gained offer a roadmap for policymakers and industry stakeholders, emphasising the need for technological innovations and robust policy frameworks to support the transition towards more sustainable and efficient DH systems.

Acknowledgement

The analysis is partially based on work conducted within the project “Renewable Heating and Cooling Pathways, Measures and Milestones for the Implementation of the Recast Renewable Energy Directive and Full Decarbonisation by 2050” with the project reference number N° ENER C1 2019-482 but did not receive direct funding.

A.8 RES and EH potentials of individual MS

The figure below shows the DH demand and RES potentials for each MS by Ref. [319].

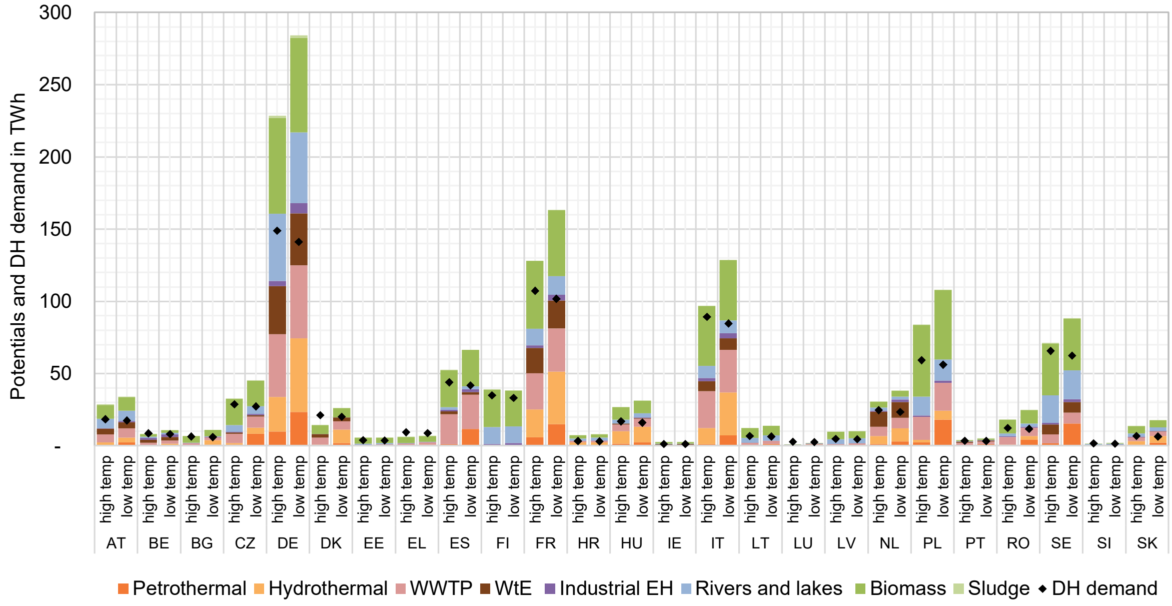

FigureAnnex 4: DH demand and RES potentials for each MS [319]

A.9 DH shares

The table below shows the DH shares in each MS as a result of the DH expansion modelling by Ref. [7]. The details on the DH expansion model are available in Refs. [58,319].

TableAnnex 23: Share of DH in the total heat demand [58,317]

Country	Demand in DH areas in GWh		Heat demand covered by DH in %		Heat demand covered by DH in GWh		Average distribution costs in €/MWh
	2020	2050	2020	2050	2020	2050	
AT	38,763	19,890	25.3%	33.2%	21,319	15,912	28.1
BE	26,027	10,636	3.4%	14.1%	3904	7445	32.8
BG	10,160	7382	26.7%	34.9%	6503	5536	28.7
CZ	51,729	30,994	24.7%	43.0%	22,761	24,795	28.1
DE	375,321	171,208	14.9%	32.4%	120,103	128,406	33.0
DK	35,273	20,287	52.8%	46.7%	31,040	18,259	32.6
EE	9105	4293	42.1%	52.2%	5281	3434	14.3
EL	14,346	11,582	10.8%	24.8%	4160	8107	29.4
ES	65,881	54,311	1.4%	30.8%	1976	38,018	33.3
FI	57,870	33,453	47.6%	63.0%	36,458	30,108	30.5
FR	203,160	123,460	6.3%	27.5%	30,474	92,595	33.7
HR	7702	3614	11.3%	25.7%	2850	2892	31.9
HU	32,249	18,281	13.3%	32.5%	10,642	14,625	28.2
IE	1760	1630	0.0%	4.7%	0	1141	33.1
IT	178,312	109,970	7.9%	31.0%	30,313	76,979	33.8
LT	10,987	6625	49.2%	59.2%	8570	5962	15.9
LU	5266	3066	19.5%	51.7%	1527	2453	29.0
LV	11,195	5253	41.5%	59.9%	6381	4203	15.9
NL	46,759	28,372	9.0%	26.5%	12,157	21,279	35.7
PL	130,002	63,942	27.2%	38.0%	66,301	51,153	29.6
PT	5437	4390	6.4%	13.9%	1794	3073	40.5
RO	29,236	14,314	15.0%	26.0%	12,571	10,735	29.8
SE	66,416	62,989	66.3%	65.5%	57,118	56,690	30.7
SI	3192	1809	13.6%	19.2%	1660	1447	30.7
SK	13,582	6,614	32.7%	36.9%	10,051	5952	29.4
EU	1,429,732	818,367	16.2%	33.2%	505,916	631,202	31.4

A.10 DH generation technologies

The table below shows the list of DH generation technologies modelled by the Hotmaps DH Gen model in this paper and if and how they are affected by the reduction in system temperatures. While direct impacts mean the effect of temperature reduction is explicitly modelled in the DH generation modelling, indirect impact means the effect is reflected in the RES potential data.

TableAnnex 24: List of DH generation technologies and the impact of temperature levels on them

Technology	Impacted by temperature reduction	Type of impact
Natural gas boiler	No	-
Natural gas CHP	No	-
Biomass boiler	No	-
Biomass CHP	Yes	Indirect through an **increase in potential**
WtE CHP	Yes	Indirect through an **increase in potential**
River and lake heat pump	Yes	Direct through an **increase in COP** of the heat pump
Wastewater heat pump	Yes	Direct through an **increase in COP** of the heat pump
Other heat pumps	Yes	Direct through an **increase in COP** of the heat pump
Solar thermal	No	-
Industrial excess heat (direct)	Yes	Indirect through an **increase in potential**
Geothermal direct (hydrothermal)	Yes	Indirect through an **increase in potential**
Geothermal direct (petrothermal)	Yes	Indirect through an **increase in potential**
Hydrogen boiler	No	-
Hydrogen CHP	No	-
Biomethane boiler	Yes	Indirect through an **increase in potential**
Heat storage	No	-

A.11 DH generation mix of MS

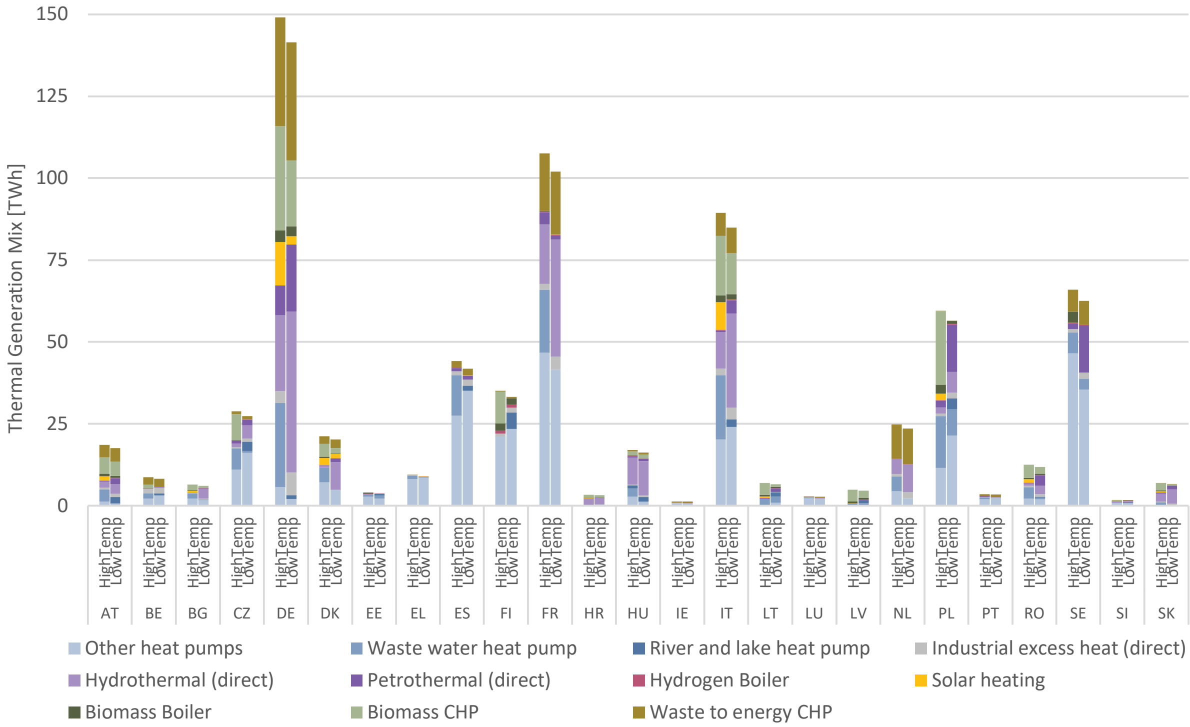

FigureAnnex 5: DH generation mix of MS for the main temperature scenarios

7 Integrating district heating potentials into European energy system modelling: An assessment of cost advantages of renewable and excess heat

Anna Billerbeck, Christiane Bernath, Pia Manz, Gerda Deac, Anne Held, Jenny Winkler, Ali Kök, Mario Ragwitz: Integrating district heating potentials into European energy system modelling: An assessment of cost advantages of renewable and excess heat. In: Smart Energy 15 1000150, 2024. DOI: 10.1016/j.segy.2024.100150.

7.1 Introduction

Achieving the European Union's (EU) target of climate-neutrality by 2050 [325] requires rapid progress in decarbonizing the energy sector and in making energy demand and supply more efficient and more closely interlinked. To this end, several studies have modelled different scenarios or pathways for future energy systems and discussed in detail the feasibility of achieving this target (see overview in [326]). The existing literature shows that an integrated, holistic perspective is required, which takes into account several sectors, as discussed within the concept of smart energy systems [298,327–329].

The key to reaching a climate-neutral energy system is to phase out fossil fuels, rapidly expand renewable electricity generation and electrify the other sectors (e.g. heating, transport) as far as possible [326,330]. Moreover, reducing energy demand and supplying energy more efficiently play an important role in line with the "energy efficiency first" principle (EE1st) [331]. As the heating and cooling sector accounts for about 50% of European energy demand [332], energy savings in this sector are vital. Efficiency measures in buildings can reduce fuel demand, running costs and investments in (new) heating systems [52]. In the case of district heating, heat savings in buildings allow operators to reduce the temperature level of their grid, making it easier to integrate (low temperature) renewables and excess heat sources (i.e. 4th generation district heating as defined by [21], studied by [86,275,333] or 5th generation district heating as described by [233]). Thereby, the compatibility of district heating with building refurbishment as a competing or synergetic strategy is still being explored [59]. Even if heat savings in buildings are achieved, the remaining district heating demand still needs to be climate-neutral and efficient. As mentioned above, electrification via heat pumps appears to be a promising option (cf. overview in [326] or project reports [33,51,73]).

However, renewables such as the direct use of geothermal and solar thermal energy, as well as waste or excess heat from industrial processes, can also make a significant contribution to a climate-neutral and efficient district heating supply. District heating networks are very heterogeneous also because renewable and excess heat potentials are unevenly distributed [319,334]. Given the difficulty of representing these local differences, district heating is usually modelled in a spatially simplified way in integrated energy system models covering Europe. There are several projects, such as Heat Roadmap Europe, Hotmaps, ReUseHeat, ReInvest or sEEnergies that have made substantial contributions to energy modelling and provided detailed results for future district heating demand and generation. Moreover, there are scientific publications analysing district heating as part of an integrated energy system (e.g. using the model BALMOREL [61,75] or ENERGYPLAN [41,335]). To the best of our knowledge, the existing European energy system analyses model district heating based on different temperature levels, network sizes or technologies. In contrast to the existing approaches, we use a differentiation of district heating networks based on available renewable and excess heat potentials.

Hence, this paper contributes to the existing literature by exploring a modelling approach for district heating technology mixes based on high spatial resolution generation potentials. Our novel approach integrates differences in district heating generation potentials between and within EU countries into the existing high temporal resolution energy system model ENERTILE (i.e. optimisation of investment and dispatch for district heating, electricity and hydrogen for all hours of the year). The new modelling approach allows a detailed analysis of the impact of district heating technology mixes on system and district heating costs. On this basis, we aim to answer the following research question: Can a high direct use of geothermal, solar thermal and industrial excess heat provide cost advantages for district heating and the overall European energy system in 2050 compared to a high use of heat pumps based on air and water sources?

To address this question, 10 scenarios are modelled for the EU and the year 2050. The analysis builds on preliminary work by Manz et al. [319], which provides the high spatial resolution renewable and excess heat potentials for district heating. A model extension integrates these potentials into the optimisation problem of ENERTILE. Subsequently, each modelled scenario sets a different rate of potential utilisation to account for differences in the exploitation of renewable and excess heat potentials. Two scenario groups are analysed: focusing on (1) high and (2) low temperatures in district heating. Lowering the temperature in district heating networks recognises that improvements in energy efficiency can make a significant contribution to achieving climate-neutrality (i.e. EE1st).

The paper is structured as follows: Section 7.2 describes the methodology and data. Section 7.3 presents the main results, i.e. the modelling output for district heating and electricity generation as well as the overall system costs and costs for district heating generation. Section 7.4 discusses the key results, and section 7.5 draws conclusions.

7.2 Methodology and data

7.2.1 Overview of the modelling approach

Regionally heterogeneous resource availability substantially influences the prospects for different technologies in district heating. For example, the availability of geothermal energy depends on the geological situation [319] and industrial excess heat is only available in some areas [266,336]. This means that an approach that assesses the contribution of renewable and excess heat technologies based on high spatial resolution data is necessary. Besides a high level of detail with regard to district heating, interaction with the remaining energy system, e.g. through large-scale heat pumps, also needs to be considered. Therefore, this paper takes a novel approach in order to model the technology mix in district heating based on high spatial resolution heat potentials in an integrated energy system model.

The analysis uses heat potentials for district heating generation from [319], aggregated into four so-called district heating types. The heat potentials in [319] are calculated using a spatial matching algorithm that maps the heat demand in a given district heating area to the heat generation potentials of different sources. The district heating areas with different heat potentials are then clustered into four district heating types. The district heating types represent multivalent district heating networks, in which specific resources are abundantly available [319]. For example, in *DH type 2: Geothermal*, a significant part of the demand could be covered by geothermal energy due to its favourable geological situation.

The types are integrated into the existing energy system model ENERTILE as separate regions. Subsequently, we carry out a scenario-based analysis for the year 2050 using a greenfield approach. The greenfield approach is a solution to overcome data limitations, as data on existing district heating networks and the capacity of different heat plants is lacking in most European countries. Investments in new generation capacity is required in any case by 2050 in order to phase out fossil fuels, as they still represented 59% of the district heating supply [334]. Existing climate-neutral heat generation plants will also need to invest in maintenance, further arguing in favour of a greenfield approach.

Figure 7.1 provides an overview of the modelling approach. FigureAnnex 6 in the annex visualises the modelling chain and the connection with the preliminary work of [319]. Section 7.2.2 provides a general overview of the model ENERTILE and section 7.2.3 describes the model extension with the district heating types.

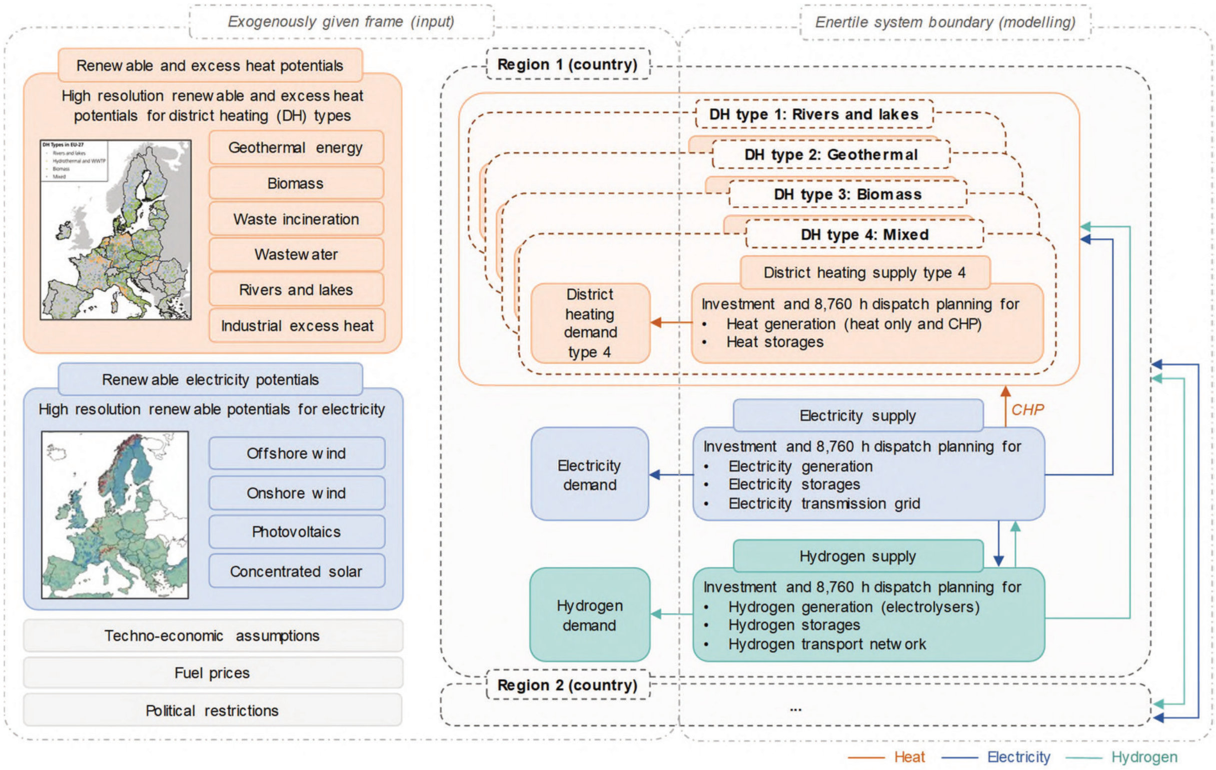

Figure 7.1: Schematic representation of the quantities, interactions, and boundary conditions in the model ENERTILE

7.2.2 The energy system model ENERTILE

ENERTILE is a detailed techno-economic linear optimisation model for energy systems, which minimises the costs of energy supply, transmission and storage (cf. Figure 7.1 and [62]). The model has been continuously developed for more than 15 years and has been used in several publications (e.g. [24,64,67,317]). A complete documentation of ENERTILE can be found in [63,67,337,338].

The model covers the supply of electricity, district heating, and hydrogen. It simultaneously optimises capacity expansion and hourly generation of all system components based on the exogenously specified demand for electricity, district heating and hydrogen. It covers conventional and renewable power plants, combined heat and power (CHP) plants, conventional and renewable heating technologies in district heating networks, cross-border electricity transmission capacities, energy storage technologies, hydrogen generation technologies and infrastructures. Furthermore, the model considers demand-side flexibility from decentralised heat pumps in buildings and electric mobility in the transport sector. The key constraints of the model ensure that the demand for electricity, district heat and hydrogen is met in every region and at every hour of the day. Political decisions and restrictions, such as a CO_2 price and a phase out of fossil fuels, are included to ensure that a climate-neutral energy system is achieved (cf. Figure 7.1).

The objective function minimises all costs associated with the vectors of the decision variables for installed capacity $\vec{X}$ and generation $\vec{x}$. For reasons of space and clearness, only an excerpt and simplified version of the objective function of the linear optimisation model is presented (cf. formula 1). Detailed descriptions of ENERTILE and all equations can be found in [63,337–339].

$$\min_{\vec{x}\vec{X}} \left[\mathrm{cost}_{\mathrm{el}}^{\mathrm{fix}}(\vec{X}) + \mathrm{cost}_{\mathrm{el}}^{\mathrm{var}}(\vec{x}) + \mathrm{cost}_{\mathrm{heat}}^{\mathrm{fix}}(\vec{X}) + \mathrm{cost}_{\mathrm{heat}}^{\mathrm{var}}(\vec{x}) + \mathrm{cost}_{\mathrm{el,chp}}^{\mathrm{var}}(\vec{x}) + \mathrm{cost}_{\mathrm{hydrogen}}^{\mathrm{fix}}(\vec{X}) + \mathrm{cost}_{\mathrm{hydrogen}}^{\mathrm{var}}(\vec{x}) \right] \quad (16)$$

with

$\mathrm{cost}_{\mathrm{el}}^{\mathrm{fix}}$:	fixed costs of electricity capacity expansion in €
$\mathrm{cost}_{\mathrm{el}}^{\mathrm{var}}$:	variable costs of electricity generation in €
$\mathrm{cost}_{\mathrm{heat}}^{\mathrm{fix}}$:	fixed costs of capacity expansion in heat grids in €
$\mathrm{cost}_{\mathrm{heat}}^{\mathrm{var}}$	variable costs of heat generation in heat grids in €
$\mathrm{cost}_{\mathrm{el,chp}}^{\mathrm{var}}$:	variable costs of electricity generation from CHP plants in heating grids in €
$\mathrm{cost}_{\mathrm{hydrogen}}^{\mathrm{fix}}$:	fixed costs of hydrogen capacity expansion in €
$\mathrm{cost}_{\mathrm{hydrogen}}^{\mathrm{var}}$:	variable costs of hydrogen generation in €

In this paper, ENERTILE's geographical coverage comprises the 25 Member States (MS) of the EU[20]. ENERTILE can model several years in a row and has a high temporal resolution with the ability to analyse 8760 hours per year. However, in this paper, we use a greenfield approach and only model the year 2050, as the research question in the paper relates to the cost advantages in the year 2050 (cf. section 7.1 and 7.2.1).

The heat supply in district heating and the associated capacity expansion of generation technologies is modelled endogenously in ENERTILE based on the predetermined exogenously heat demand for each region (i.e. district heating types per country). ENERTILE scales the annual demand down to hourly demand, using daily district heating time series that incorporate the average daily outdoor temperatures. Different technologies are available, including electric boilers, large-scale heat pumps, geothermal energy and solar thermal plants, biomass boilers and CHP, waste CHP, hydrogen boilers and CHP, and heat storage. A description of the modelling of the heat generation technologies is provided in the following section 7.2.3.

[20] Malta and Cyprus do not have a district heating infrastructure and it is assumed that they will not start investing.

7.2.3 District heating types and heating technologies in ENERTILE

As stated in section 7.2.1, data on heat potentials, aggregated into so-called district heating types, is used and integrated into ENERTILE. The four types are based on a clustering analysis where 5815 district heating areas in Europe in 2050 are clustered according to the available climate-neutral heat potentials [319]. Thereby, the cluster analysis has shown that these four district heating types adequately represent the diversity and heterogeneity of the potentials [319].

The types represent multivalent district heating networks which have several sources: (1) ambient heat from rivers and lakes used with heat pumps, (2) ambient heat from wastewater treatment plants used with heat pumps, (3) industrial excess heat used directly[21], (4) (deep) geothermal energy (hydrothermal and petrothermal) used directly, (5) biomass and biogas and (6) waste incineration. The district heating types are named based on the heat source with the highest potential, i.e. in *DH type 1: Rivers and lakes*, large-scale heat pumps using rivers or lakes as a heat source could meet about 50% of the demand. All of the potentials are integrated into the model, except petrothermal potentials due to the low probability of their exploitation, the high costs and the lower specific potentials. Furthermore, solar thermal potentials are not provided by [319], as the spatial availability of technical potentials exceeds the economic potentials. Potentials for other types of heat pumps, e.g. air source heat pumps, are not considered for similar reasons in [319]. Solar thermal energy and air source heat pumps are, however, included in the modelling of this paper as available technologies (cf. below and section 7.2.4).

Following [319], two different temperature settings for district heating grids are analysed: Higher grid temperatures (flow around 80 °C) and lower grid temperatures (flow around 65 °C).[22] With the lower temperatures, a higher share of heat potentials can be utilised. Both temperature settings are used in this paper, leading to two scenario groups: Group (1) includes the potentials for high grid temperatures and group (2) the potentials for low grid temperatures. Figure 7.2 illustrates the four district heating types on the European level by showing the aggregated mix of potentials for the two scenario groups.

[21] The industrial excess heat provided by Ref. [319] corresponds to climate-neutral heat, i.e. a transformation of the industry is already taken into account.

[22] For simplicity, we assume constant flow temperatures in the modelling and have taken the average temperature of each of the two temperature scenarios from [319].

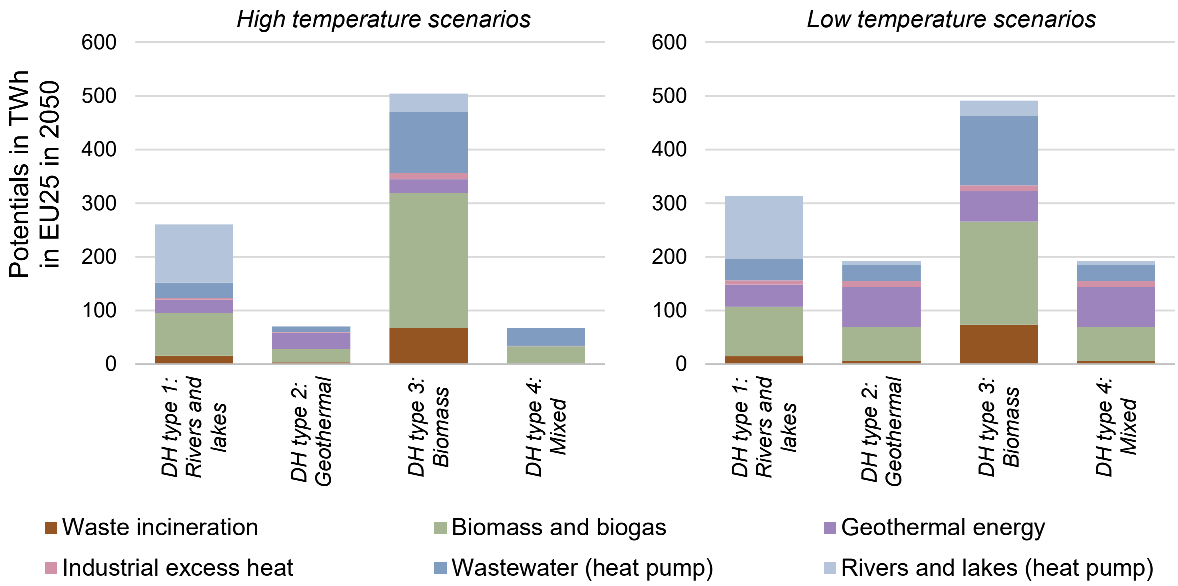

Figure 7.2: **Potentials per district heating types (own illustration, based on data from [319])[23]**

The four types are integrated into ENERTILE on the MS level, i.e. for each MS, four types of district heating grids are implemented, with the sum of the available renewable and excess heat potentials per type and MS (cf. Figure 7.1). As stated, the types represent future district heating areas with the spatially matched heat generation potentials. Thus, the high spatial resolution of the analysis of available potentials is represented with these types (cf. [319]). Even though it is a simplification, this approach makes it possible to represent the available potential for district heating in an aggregated way. Previously, district heating was modelled in ENERTILE with only one grid for each MS. Therefore, the extension of the model strongly improves its representation of district heating.

Furthermore, several technologies have been updated or added to ENERTILE in order to reflect the technological diversity associated with the wide variety of potentials.

(i) Geothermal and solar thermal plants

The use of deep geothermal and solar thermal energy for heat generation in district heating is associated with comparatively high investment and is often also influenced by political preferences. Therefore, the generation of district heating with deep geothermal and solar thermal energy is not subject to the cost optimisation procedure in ENERTILE but is included as an exogenous assumption (cf. [63]). Heat generation from these sources is predefined per district heating type in each MS (in this paper e.g. based

[23] The difference in potential between the two scenario groups is due to the fact that the potentials are limited to a fixed district heating demand, i.e. 732 TWh in the high temperature scenario and 695 TWh in the low temperature scenario. The district heating demand is lower in the low temperature scenarios because lower heat losses were assumed in [319].

on [319], cf. section 7.2.4). However, different utilisation rates and the related costs of the two technologies are explored within the scenario design by varying the share of the predefined heat generation from these sources (see section 7.2.4). Since these renewable heat sources are quasi-inexhaustible, it is assumed that the predefined annual values directly correspond to the heat production in the heat grids. To achieve the required heat production, only the heat flow taken from the water reservoir or the solar collector area and the overall configuration of the system must be adjusted accordingly. Furthermore, a geothermal plant is usually operated as a base load so that constant hourly production is assumed during the year. In contrast, solar thermal generation varies considerably due to the diurnal and seasonal variation of solar radiation. Therefore, an hourly solar irradiance profile is used to derive hourly generation profiles.

(ii) Direct use of industrial excess heat

For this paper, the use of industrial excess heat in district heating is integrated into ENERTILE. The modelling method used for this technology is analogous to geothermal energy. Consequently, the annual heat generation quantities are predefined and converted into a constant hourly generation profile. Again, different utilisation rates and their related costs are explored within the scenario design (cf. section 7.2.4).

(iii) Large-scale heat pumps

Usually, all large-scale heat pumps in ENERTILE are simplified and modelled as air-source heat pumps. For this paper, the representation of large-scale heat pumps is amplified by integrating additional heat sources like water from rivers and lakes or wastewater. A methodological challenge in modelling heat pumps is how to represent the variable efficiency as realistically as possible. Since the coefficient of performance (COP) of heat pumps strongly depends on the variable temperature of the heat source, the COP is determined in the model in hourly resolution using a piecewise linear approximation function depending on the temperature of the heat source. Based on the assumptions of the inlet and outlet temperatures of the heat source and sink, respectively, and the use of the estimated Lorenz efficiencies of large heat pumps in district heating in Denmark [340], different linear approximation functions for the COP of the heat pumps are derived. Furthermore, two versions of linear functions are used in this analysis to reflect the two different temperature flow settings for district heating grids (high temperature vs. low temperature scenarios). As a result, heat pumps achieve a higher efficiency in the low temperature scenario. For air as the heat source, hourly average temperatures per country are used. Similarly, hourly average water temperatures per country based on [319] are used for rivers and lakes. Furthermore, it is assumed that rivers and lakes can only be used at a water temperature of 3°C and higher. For wastewater heat pumps, a constant COP is assumed to simplify the calculation. This assumption can be reasoned by the fact that the wastewater temperature is relatively stable and remains around 10°C even in winter. To incorporate the upper limit of potentials for heat pumps with wastewater and rivers or lakes, additional capacity restrictions for these technologies are included in the linear optimisation with ENERTILE.

(iv) Biomass and waste

The use of biomass for district heating is limited according to the derived potential for each district heating type (cf. [319]). Therefore, maximum generation restrictions limit the possible use of biomass for district heating. The same applies to heat from waste incineration.

7.2.4 Scenario design

The objective of this paper is to analyse whether local renewable and excess heat sources can provide cost advantages for district heating and the overall energy system (cf. section 7.1). Therefore, an explorative scenario-based approach is chosen which scans a broad solution space and includes different scenarios for Europe for the year 2050. In line, 10 scenarios are designed by varying the share of specific renewable and excess heat sources in district heating. In particular, in each scenario, the utilisation of geothermal energy, industrial excess heat and solar thermal energy is set at different levels using equal restrictions in the optimisation problem. Thus, a certain share of the district heating generation mix is fixed, and only the remaining supply to meet the demand is freely optimised with the remaining climate-neutral technologies (i.e. heat pumps, biomass and hydrogen boilers and CHP, and waste CHP). This approach makes it possible to analyse the impact of different technology shares on the system and district heating costs.

In order to specify the levels of geothermal energy, industrial excess heat and solar thermal energy, the potential data provided for each district heating type given in [319] are used (cf. section 7.2.3). In the scenarios, the utilisation rates of the technically available geothermal and industrial excess heat potentials vary from 50% to 100%. As previously stated, solar thermal potentials are not provided in [319]. However, solar thermal plants can be utilised (almost) everywhere, as solar radiation is high enough in all European countries [293]. Therefore, solar thermal energy is included with a share expressed as coverage of the demand. In line with the literature [293], this share ranges from 5% to 10% in the different scenarios. In contrast, the potentials of rivers and lakes, wastewater, biomass and waste incineration provided by [319] are used as upper limits, and the contribution of these technologies is freely optimised.

Table 7.1 provides an overview of the scenarios. The first scenario *RES* focuses on an overall high use of renewables and excess heat. Thus, the utilisation rates of geothermal and industrial excess heat potentials are set to 100%. Solar thermal is set to a maximal contribution of 10% of the district heating demand. In the second scenario *Geo*, geothermal potentials are set to 100% utilisation of the technical potentials, while industrial excess heat and solar thermal are reduced to half of their maximal contribution. Similarly, in the scenario *Solar,* a focus lies on solar thermal energy. Thus, solar is set to its maximal contribution of 10% of the demand, and the other potentials are reduced to 50%. In line with this, in the *IEH* scenario, industrial excess heat is set to 100% utilisation of the potentials and the two other sources are reduced to half of their contribution. Finally, the scenario *HP* focuses on a (potentially) high share of large-scale heat pumps. Therefore, geothermal, solar and industrial excess heat are reduced to half of their maximal contribution in order to have a high residual demand that is optimised. This overall scenario design is used for the high temperature (*HT*) scenario group and the low temperature (*LT*) scenario group, resulting in 10 different scenarios. Figure 7.3 provides a graphical illustration of the 10 scenarios.

Table 7.1: Overview of the modelled scenarios

Scenario name	Utilisation rate of geothermal potential	Utilisation rate of industrial excess heat potential	Contribution of solar thermal as a share of demand
RES	100%	100%	10%
Geo	100%	50%	5%
Solar	50%	50%	10%
IEH	50%	100%	5%
HP	50%	50%	5%

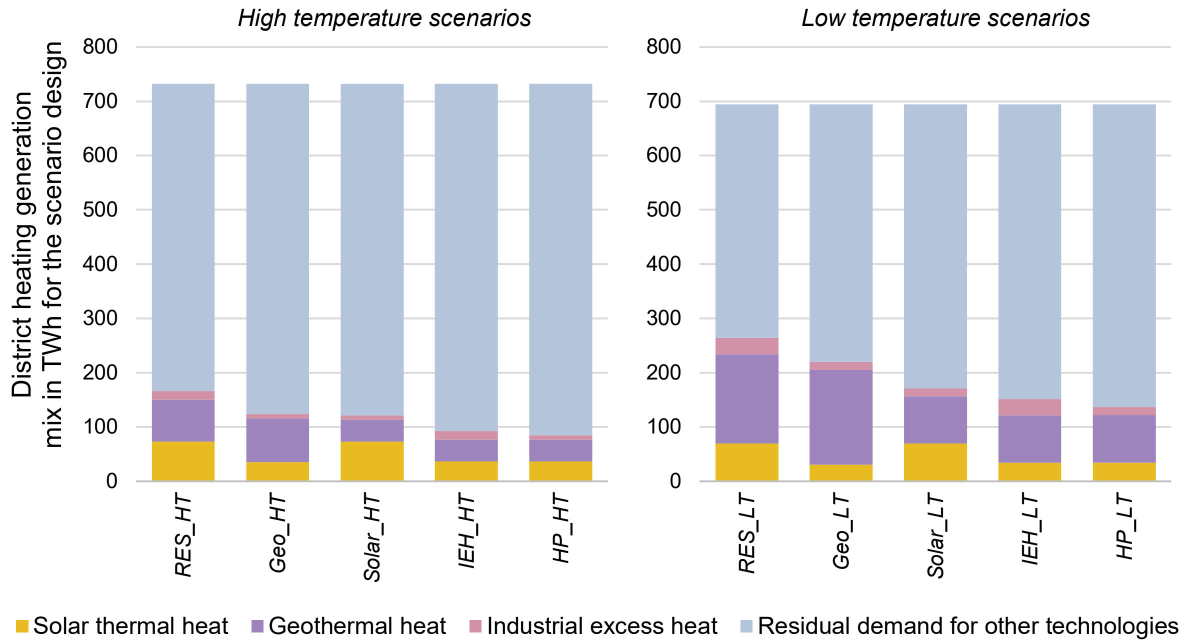

Figure 7.3: Overview of renewable and excess heat contributions in the scenarios

All of the modelled scenarios achieve climate-neutrality in 2050. Assumptions in the other sectors, i.e. all sectors except the district heating supply mix, remain constant in the scenarios (e.g. assumptions for transport or industry). This means that effects caused by changes in the district heating supply mix can be identified, quantified and interpreted.

The scenarios all involve fundamental changes in the district heating technology mix, as district heating in Europe is still dominated by fossil fuels (in 2018: 30% natural gas, 29% coal and oil, 7% non-renewable waste, 27% biomass, 1% geothermal, 1% heat pumps, 2% industrial excess heat and 2% others according to [334]).

7.2.5 Data and assumptions

The future district heating demand in 2050 and heat potentials to cover this demand form the basis of the modelling analysis. The district heating demand for 2050 is based on [319] (building on [58]). Thereby, the future district heating areas are calculated based on future heat demand, distribution costs, and an assumed future district heating market share in the countries (cf. [58]). The resulting district heating demand is kept constant in the scenarios. It represents an increase of current district heating demand to 732 TWh in the *HT* scenarios and 695 TWh in the *LT* scenarios. Compared to current levels of around 445 TWh [334], this means an increase of at least 250 TWh (+50%).[24] This ambitious deployment of district heating is overall in line with other energy system scenarios that foresee 400 to 800 TWh for district heating in Europe in 2050 (cf. e.g. [52,53,73,326]).

The district heating demand is used together with heat generation potential data, representing the technical renewable and excess heat potentials with high spatial resolution that are spatially matched to the identified district heating areas (provided by [319]). The spatial matching assumes maximum distances between the different heat sources and district heating areas. The results of the spatial matching are then used in a clustering algorithm to define so-called district heating types, which represent all areas with a similar potential pattern (cf. section 7.2.3). A detailed description of the methodology, including all assumptions, is given in [319]. The final results are presented and described in [319] and datasets related to [319] can be found in an online data repository.[25] The geographical distribution of the district heating types in Europe is shown in FigureAnnex 7 in the annex.

[24] In the input data for district heating demand (based on [58,319]), it is assumed that the annual useful heat demand decreases due to renovation activities from 3,129 TWh in 2020 to 1,900 TWh in 2050. This significant decrease of the heat demand leads to a decreased economic competitiveness of district heating, which is compensated with high connection rates between 70% and 90%. For the identification of the district heating areas, two conditions are set in [37]: The annual heat demand supplied in a district heating area must be greater than 5 GWh/a and the average distribution cost must not exceed the pre-defined distribution cost ceiling. Furthermore, the demand projections are based on climate data, i.e. the demand is also influenced by the number of heating degree days. Due to the reduction based on renovation and heating degree days, the increase of the district heating demand is even higher than 50%.

[25] Fordatis - Research Data Repository of Fraunhofer-Gesellschaft; http://doi.org/10.24406/fordatis/280.2 [294].

In addition to the district heating demand, the scenario runs require demand data for all the other sectors (e.g. electricity demand for appliances in households, electric vehicles or processes in the industry). The primary source for this demand data set is the project '*Potentials and levels for the electrification of space heating in buildings*' (ENER C1 2019-481) and, thereby, the *Elec_60* scenario. This project provides model-based scenarios of the space and water heating sector up to 2050, combining several highly detailed models. In the project, demand data of buildings is provided by the INVERT model, which is then used as input to ENERTILE. Details on the model INVERT can be found in [53,73]. The energy demand is kept constant in all scenarios to ensure that the differences between the scenarios can be compared and interpreted. TableAnnex 25 in the annex presents the input demand data. Losses incurred within energy distribution grids are also accounted for (5.5% for electricity, and 10% to 16% for district heating, depending on the temperature level).

Renewable electricity generation is endogenously optimised in ENERTILE (cf. Figure 7.1). Thereby, lower limits are defined based on the current electricity generation in the countries [341]. In addition, upper limits for wind and solar are defined on the basis of the calculated generation potential (see methodology in [24,62]). For electricity generation from hydro and geothermal energy, it is assumed that their current production remains constant until 2050 [341].

Lastly, the optimal investment and operation of different technologies (in heating and electricity) depend strongly on the assumed energy carrier prices and techno-economic parameters of the technologies. In all scenarios, a very high CO_2 price of 500 €/t in 2050 is assumed in order to achieve a climate-neutral energy system and to be in line with the input data [51]. Furthermore, an interest rate of 2% is assumed for all technologies in all scenarios. The techno-economic parameters of the technologies comprise specific investments, variable and fixed operating and maintenance costs, efficiency, lifetime, etc., and are presented in TableAnnex 26 in the annex.

7.3 Results

7.3.1 District heating generation

The generation of district heating to meet the given demand is one of the main outputs of ENERTILE. In line with the input demand data, the district heating generation is, in general, higher in the *HT* scenarios than in the *LT* scenarios (cf. demand data in section 7.2.5). Furthermore, the scenario groups and the scenarios have different technology mixes. Figure 7.4 shows the modelled district heating technology mixes at the European level in 2050 for the different scenarios.

The technology mixes in the different scenarios show that heat pumps (air, rivers and lakes, wastewater) provide the majority of the heat in all the scenarios. In line with the scenario design, the highest contribution of heat pumps occurs in the *HP_HT* scenario

(459 TWh) and the *HP_LT* scenario (468 TWh). In terms of capacities, this relates to 209 GW in the *HP_HT* scenario and 219 GW of capacities for heat pumps in the *HP_LT* scenario. The lowest contribution of heat pumps occurs in the *RES_HT* scenario (420 TWh) and the *RES_LT* scenario (399 TWh).

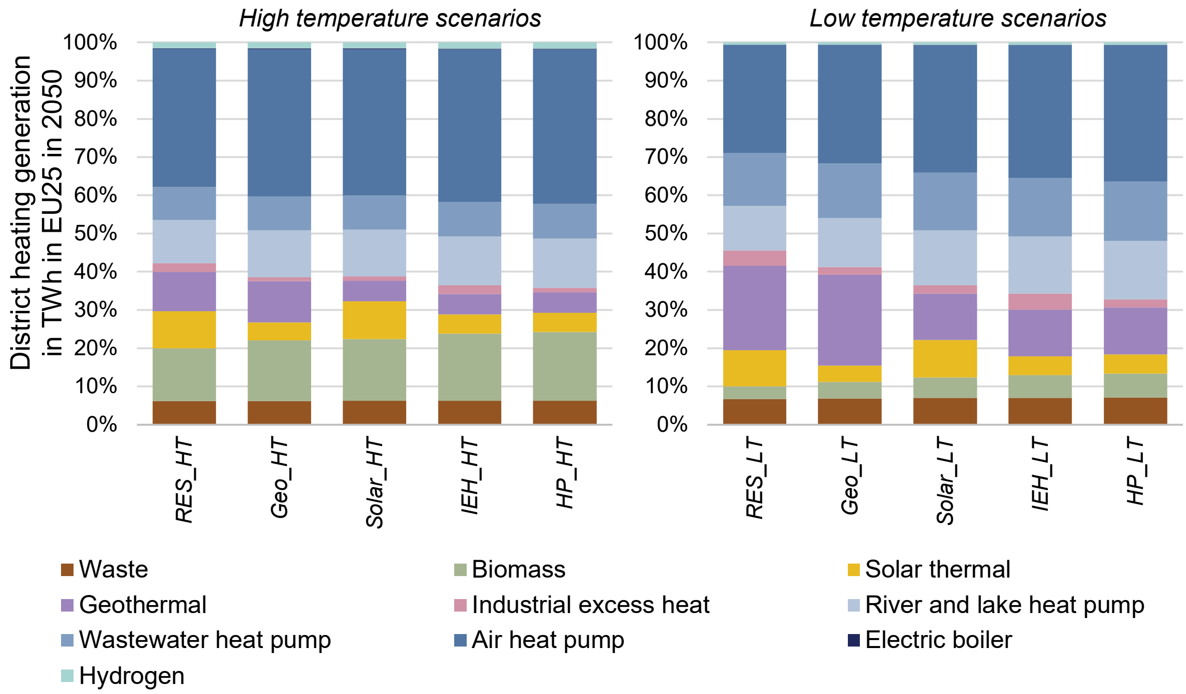

Figure 7.4: District heating generation mix in the scenarios in Europe in 2050

The results in Figure 7.4 show further that river and lake heat pumps and wastewater heat pumps significantly contribute to the share provided by heat pumps overall (9% to 15% each). Both technologies are optimised with an upper limit according to their potential (cf. section 7.2). The results show that river and lake heat pumps are on average utilised to around half of their limit, i.e. almost 60% of the potential is exploited. However, in several district heating types, the river and lake potentials are exploited to 100%. Wastewater heat pumps are on average utilised to their upper limit, i.e. around 95% to 99% of their potential is exploited.

As with scenario design, geothermal heat generation is highest in the *Geo* and *RES* scenarios. Similarly, solar thermal and industrial excess heat enter the mix in line with the assumptions and the scenario design (cf. section 7.2.4). In contrast, biomass is optimised in the scenarios with an upper limit. However, biomass shows only slight variations in the scenario groups. Overall, the biomass results show that less biomass is needed in the *LT* scenarios due to higher potentials in general and higher heat pump efficiencies. Furthermore, in both scenario groups, the biomass shares are slightly higher in the *HP* scenarios compared to the other scenarios, as less renewable and excess heat potentials are available.

The heat from waste incineration is more or less constant in the scenario groups, with around 6% to 7%. Electric heaters account for only a very low share of the generation mix in both scenario groups, mainly because of their lower efficiency compared to heat pumps. Lastly, hydrogen-based heat generation technologies contribute only a small amount, around 2% in the *HT* scenarios and 1% in the *LT* scenarios. Hydrogen-based technologies show low generation but higher capacities. They have a backup role for district heating in times of electricity shortages as well as shortages of renewable and excess heat.

Figure 7.5 shows the district heating generation mix in 2050 in the scenarios per district heating type. In line with the definition of the types, Figure 7.5 displays multivalent district heating networks where one or two sources cover a large part of the demand.

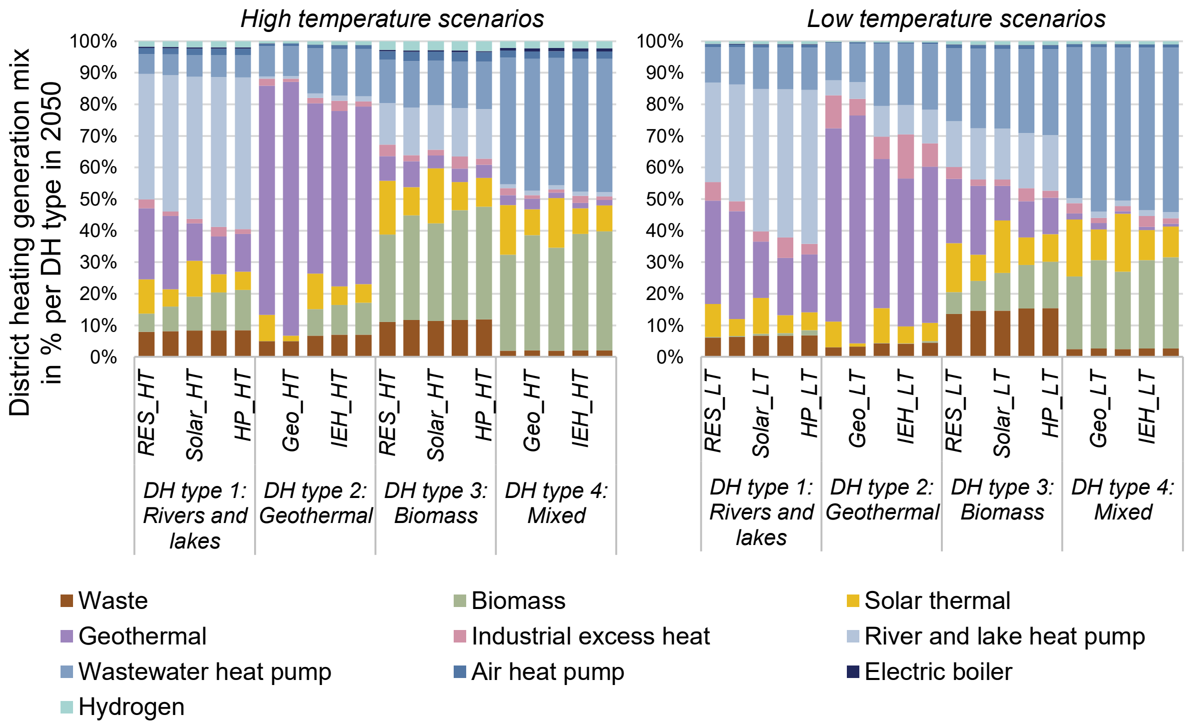

Figure 7.5: District heating generation mix in the scenarios per DH type in 2050

The technology mixes in Figure 7.5 show that in the *HT* scenarios, in *DH type 1*, river and lake heat pumps provide up to 50% (48 TWh) of the generation. *DH type 2* shows a very high share of geothermal energy, up to 80% (30 TWh). In *DH type 3*, up to 36% (54 TWh) is covered by biomass. Finally, *DH type 4* shows a generation profile with up to 38% (10 TWh) biomass and up to 42% (11 TWh) wastewater heat pumps. Similarly, in the *LT* scenarios, in *DH type 1*, river and lake heat pumps can provide up to 49% (55 TWh) of the generation. In line, *DH type 2* shows a very high share of up to 72% (75 TWh) of geothermal energy. In *DH type 3*, around 15% (36 TWh) is covered by biomass. Again, *DH type 4* shows a generation profile with up to 29% (6 TWh) biomass and up to 52% (11 TWh) wastewater heat pumps. Notably, there are district heating types without the need for biomass, because other sources are available. In particular, in the *LT* scenarios, *DH type 1* and *DH type 2* have (almost) no biomass.

Overall, the results for the district heating types underline the diversity and heterogeneity of the potentials, as all types are multivalent networks using several potentials. The resolution of district heating generation is greatly increased and the heterogeneous resource availability affecting the technology mix in district heating is more adequately reflected by the ENERTILE model extension.

7.3.2 Electricity generation

This section focuses on electricity generation to assess further differences between the scenarios. Figure 7.6 shows the modelled electricity generation mix in the scenarios in Europe in 2050.

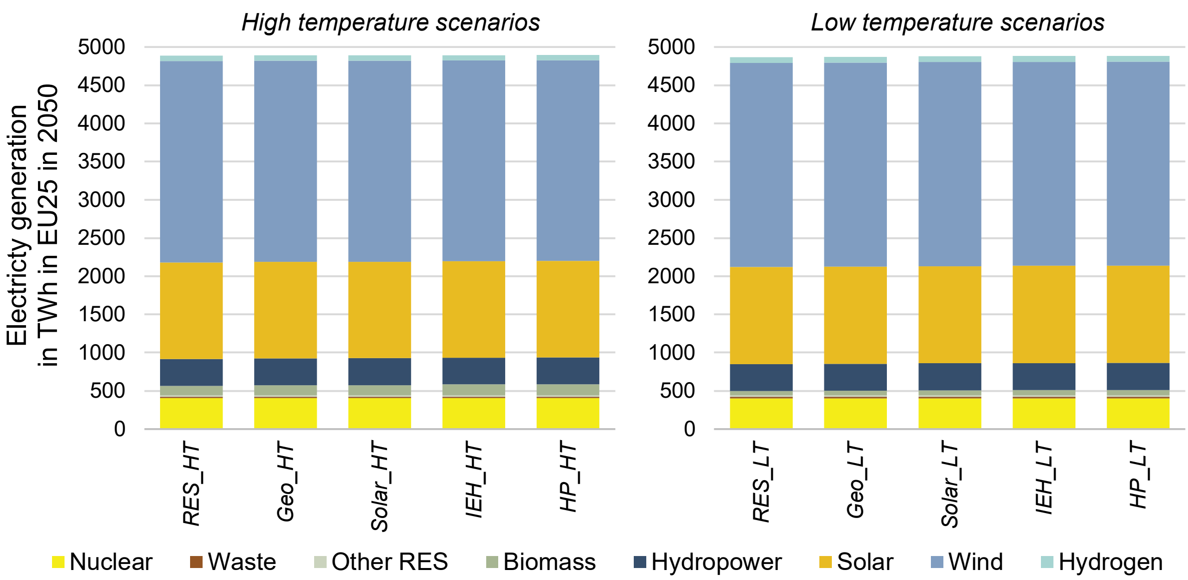

Figure 7.6: Electricity generation mix in the scenarios in Europe in 2050

One might assume that a higher share of heat pumps in district heating would lead to higher electricity generation, however, the differences between the scenarios are negligible. Overall, in the *HT* scenarios, electricity generation ranges from 4,895 TWh in the *RES_HT* scenario to 4,885 TWh in the *HP_HT* scenario. Thus, the difference is only 0.19%. Similarly, in the *LT* scenarios, generation ranges from 4,883 TWh in the *RES_LT* to 4,866 TWh in the *HP_LT* scenario, i.e. 0.35% difference.

The maximal generation difference of heat pumps reaches 70 TWh heat (difference between *HP_LT* and *RES_LT*). This relates to a 20 TWh difference in electricity needs, which illustrates why the differences in electricity generation are not visible (i.e. very low electricity demand for district heating compared to other sectors).

Also, regarding the technology mix, there are no relevant differences. In all the scenarios, electricity generation is greatly dominated by wind and solar power. The need for flexibility in order to balance the energy system increases because of the high share of fluctuating renewable electricity. Energy storage, international trading and demand-side flexibility, electric mobility as well as hydrogen production provide the necessary flexibility in this electricity system of the future.

7.3.3 System and district heating costs

This last result section focuses on (i) overall system costs and (ii) district heating costs. The objective is to identify the lowest cost scenario, i.e. to analyse whether direct renewables and industrial excess heat in district heating provide cost advantages. Thereby it is important to emphasise that the costs between the *HT* and *LT* scenarios should not be compared. For the *LT* scenarios, additional investments (e.g. in infrastructure and on the building side) and, therefore, capital costs would be necessary in order to reduce grid temperatures. District heating grid costs (e.g. for pipes) and costs on the building side are not in the scope of the ENERTILE modelling. Hence, a comparison of the costs between the scenario groups is not reasonable.

(i) System costs

The system costs (in billion (bn) €) are an output of ENERTILE. They represent the annualised cost of the energy system, covering all fixed and variable costs of the supply side as a whole. Figure 7.7 shows the differences between the system costs in the scenarios in Europe in 2050. Thereby the average of the system costs per scenario group serves as a baseline for the comparison. Thus, only the differences to this baseline are displayed. For example, the system costs in the *RES_HT* scenario are € 1.22 bn higher than the average costs of all *HT* scenarios. The defined baseline reflects the average performance of the scenarios and therefore provides a clear and fair basis for comparison.

Comparing the system costs of the scenarios per scenario group shows a similar picture. In both groups, the *HP* scenario is the cheapest scenario, closely followed by the *Geo* scenario. Furthermore, in both groups, the *IEH* scenario shows lower system costs than the average of the scenarios. In contrast, the *RES* and the *Solar* scenarios show higher than average costs. Thus, independent of temperature levels, higher shares of heat pumps, geothermal and industrial excess heat in district heating seem to be cost-efficient for the energy system.

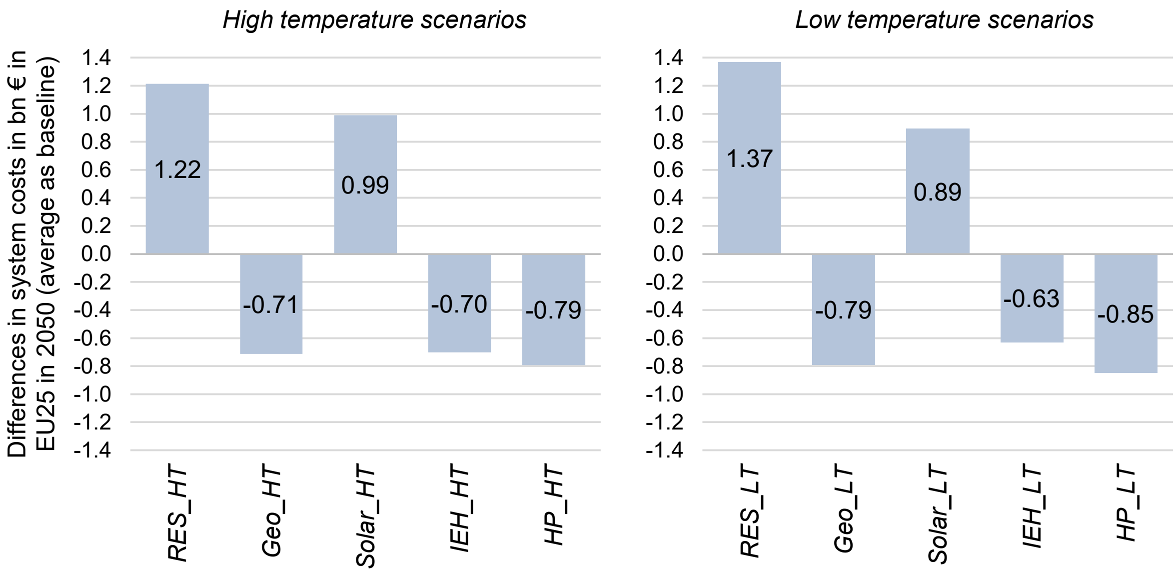

Figure 7.7: Difference in system costs between the scenarios in Europe in 2050 (average of the system costs per scenario group serves as a baseline for the comparison)

The system cost comparison shows, however, that the differences between the scenarios are very small. In the *HT* scenarios, the differences are € 2.0 bn, which relates to only 0.7% of the total system costs (which are around € 280 bn). Similarly, in the *LT* scenarios, the differences are € 2.2 bn, i.e. 0.8% of the total system costs. Hence, the district heating generation mix has only a minimal impact on the overall European energy system costs. District heating generation reaches up to 770 TWh in the scenarios, while electricity generation reaches almost 4900 TWh (cf. sections 7.3.1 and 7.3.2). The relatively low generation of district heating compared to electricity explains the small differences in system costs.

Moreover, sensitivity calculations show that the system costs are very sensitive to the underlying cost assumptions. At the same time, costs for renewable and industrial excess heat projects are still little explored. Geothermal investment, in particular, is highly uncertain. In the scenarios, the investment for geothermal is set to 1300 €/kW [340] (cf. TableAnnex 26 in the annex). If the investment could be reduced by more than 15%, the overall picture would change, and the *Geo* scenarios would become the cheapest scenarios as shown in Figure 7.8.

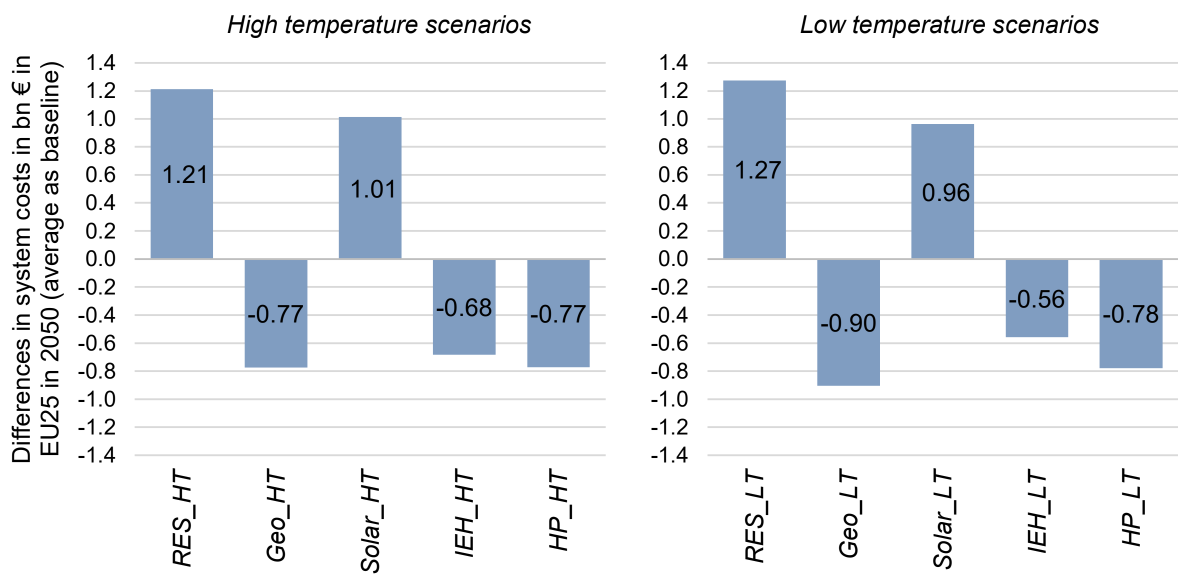

Figure 7.8: **Difference in system costs between scenarios in Europe in 2050 with 15% reduced investment in geothermal energy (sensitivity calculation; average of the system costs per scenario group serves as a baseline for the comparison)**

(ii) District heating generation costs

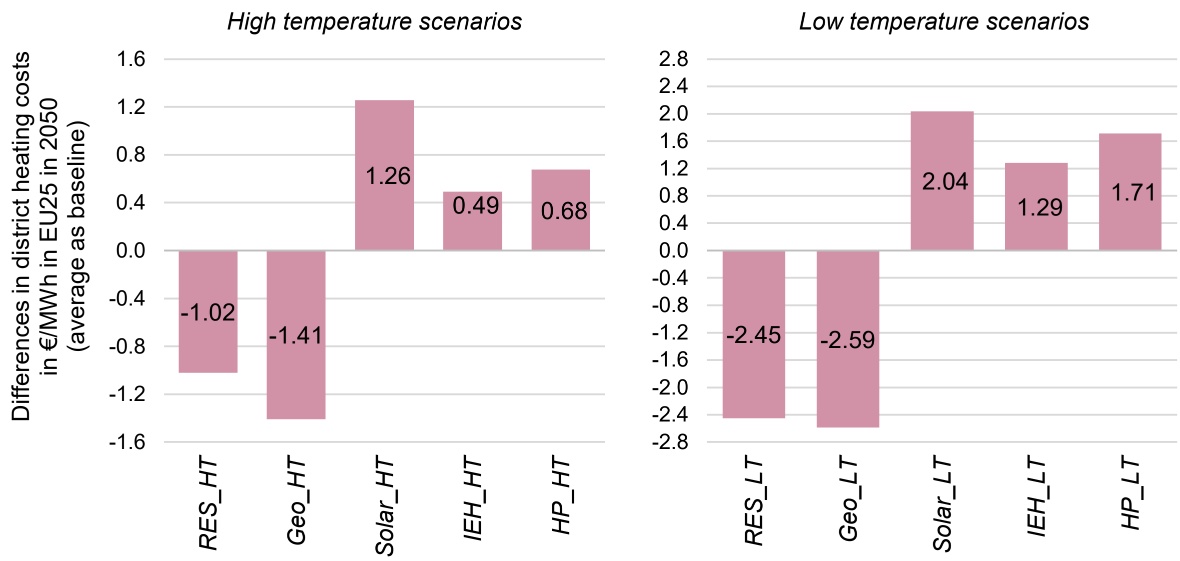

Figure 7.9: **Difference in the district heating costs between the scenarios in Europe in 2050 (average of the costs per scenario group serves as a baseline for the comparison)**

The district heating costs (in €/MWh) represent the cost of district heating generation (in €) divided by the district heating generation (in MWh). Thus, these costs reflect the fixed and variable costs of the total district heating generation (without pipes, substations etc.). Figure 7.9 shows the differences between the district heating generation costs in the scenarios in Europe in 2050. Again, the average of the costs per scenario group serves as a baseline for the comparison. Thus, only the differences to this baseline are displayed.

The comparison of the district heating costs between the different scenarios shows that in both scenario groups, the *RES* and the *Geo* scenarios are below average, while the other scenarios are above average. Thus, high shares of renewable heat, in particular geothermal heat, seem to offer cost advantages for district heating. Overall, the district heating generation mix has a greater impact on district heating generation costs than on total energy system costs. The differences range from up to 2.66 €/MWh (4% of total district heating generation costs of 66 €/MWh) in the *HT* scenarios and even up to 4.62 €/MWh (7%) in the *LT* scenarios. Particularly for low-income households, which already spend a high proportion of their income on energy, a cost difference of 4.62 €/MWh is a significant amount.

7.4 Discussion

The optimisation results show that in all the scenarios heat pumps achieve a high share in the district heating generation mix in Europe in 2050. Even in the scenarios focussing more on direct renewable and industrial excess heat, heat pumps cover more than half of the demand. The main reason for this is the cost efficiency of heat pumps compared to alternative technologies (i.e. biomass or hydrogen boilers and CHP etc.). In addition to their economic advantage, our results show that heat pumps also provide valuable flexibility to the electricity system (in line with a more detailed analysis of the flexibility of heat pumps in [24]).

The high share which heat pumps account for is in line with the results from other scenario analyses [51,73,326,342]. Compared to these existing studies, our results provide more technological detail and a more differentiated view, showing that river and lake heat pumps and wastewater heat pumps can make a significant contribution to the district heating generation mix in 2050 (up to 15% each). These heat pumps are more efficient than air-source heat pumps, and their deployment should be the focus of further research. Furthermore, additional sources for heat pumps (e.g. near-surface geothermal energy and excess heat from data centres, shopping malls, metro stations and electrolysers) should be explored in future research.

According to the results, other generation technologies also have relevant contributions to a climate-neutral and efficient district heating generation mix. Geothermal, solar thermal, and industrial excess heat enter the mix in line with the scenario design and assumptions. Biomass shows a higher generation share in the high temperature (*HT)* scenarios than in the low temperature (*LT)* scenarios. This is mainly because of lower geothermal and industrial excess heat potentials and lower efficiencies of heat pumps in the *HT* scenarios. However, sensitivity analyses show that biomass heat generation is very sensitive to the assumed price. With a higher price (i.e. more than 13 €/MWh), even less biomass would be used. An existing study also demonstrates that district heating can reduce biomass dependency more than individual solutions [323]. Overall, the role of (sustainable) biomass and the various uncertainties regarding biomass prices should be analysed in future research. Regarding the power sector, the results show only negligible variation in electricity generation between the scenarios. The electricity demand increase in scenarios with a higher share of heat pumps is less than 1%. This is mainly attributed to the high efficiency of heat pumps.

Similarly, the differences in the overall system costs between the scenarios are very low with less than 0.8%. Thus, the developments in the district heating mix seem to have only a very limited impact on the overall system costs. Nevertheless, the results show that higher shares of heat pumps, geothermal and industrial excess heat in district heating are cost-efficient for the energy system. In particular, the scenarios with the higher shares of heat pumps achieve the lowest system costs. This can be explained by their comparatively low (levelised) costs of heating and by their flexible contribution to the power system, helping to integrate a high share of fluctuating renewable electricity.

However, our results and in particular the system cost comparison is very sensitive to the techno-economic assumptions. Thereby it should be noted that in the modelled scenarios, relatively high, conservative cost assumptions are made for geothermal energy. With 15% lower investment costs for geothermal plants, the scenario with higher geothermal contribution could become the most cost-efficient one. Higher shares of geothermal energy would lead to accordingly lower shares of heat pumps. Hence, further research should focus on the costs of direct renewables and industrial excess heat and their impact on the district heating mix and the energy system. Analyses with multiple cost sensitivities that comprehensively cover uncertainty ranges can thereby build on the methodological approach and initial findings of this paper.

In contrast, there are greater differences in district heating costs between the scenarios reaching 4% in the *HT* and 7% in the *LT* scenarios. Thereby, higher shares of geothermal energy seem to offer cost advantages for district heating. Higher shares of solar thermal energy cannot provide cost advantages for district heating according to our modelling results. This is most likely reasoned by the fact that the profile of solar thermal energy is less suited to the demand curve. However, it is important to note that the modelling analysis does not include seasonal storage[26], which could overcome this disadvantage. Further research with seasonal storage should be carried out to analyse the optimal contribution of solar thermal energy optimally with several cost sensitivities.

Overall, our modelling approach uses cost assumptions per technology that do not vary by country or region. In reality, however, investment in the technologies modelled may be more expensive in some regions than in others due to geological and financing

[26] In the district heating networks, water storage tanks that can store heat for several days are modelled, but no seasonal storages have been included so far.

conditions or labour costs. Therefore, analyses with further cost sensitivities and possibly regional cost variations to the extent possible are crucial for future research to complement and extend our findings.

In addition, it is important to stress that the results are obtained for a fixed district heating demand in 2050 (732 TWh in the *HT* and 695 TWh in the *LT* scenarios; cf. section 7.2.5). Different trends in district heating demand can have a large impact on potentials and costs. Hence, further research could explore how different paths of district heating demand would affect the results of the scenarios analysed in this paper. In this context, it would also be interesting to investigate whether different technology options for district heating supply could change the competitiveness of district heating compared to other heat supply options (e.g. individual heat pumps).

Lastly, it is important to emphasise that the results are highly dependent on the input data and assumptions and are subject to a wide range of uncertainties. In order to reflect these uncertainties, further analyses are needed that cover both the whole system perspective to capture cross-sectoral and international dependencies, and regional analyses that can take into account more granularity and variation. Our results show that, in particular, large-scale heat pumps are cost-effective for the energy system and geothermal energy offers cost advantages for district heating. However, as the cost differences are relatively small, no climate-neutral technology should be excluded in future research and especially in practical implementation projects of district heating networks. For each district heating network, all possible potentials should be considered and their suitability analysed from different perspectives at the local level.

7.5 Conclusions

This paper takes a novel approach and models different technology mixes in district heating for 2050 in Europe taking into account interaction with and the impacts on the power sector while simultaneously using high spatial resolution renewable and excess heat potentials for district heating generation. For this, the analysis uses heat potentials, aggregated into four district heating types, and integrates them into the existing energy system model ENERTILE. Consequently, the representation of district heating in ENERTILE is significantly improved.

A set of 10 scenarios is used to analyse different rates of potential exploitation and the impact on the overall system and district heating costs. In the process, one set of scenarios focuses on high temperatures and one on low temperatures in district heating networks. The regionally heterogeneous resource availability which affects the technology mix in district heating is more accurately reflected by this novel modelling approach. Nevertheless, future research is needed on the required resolution of district heating in integrated energy system models.

The optimisation results show that at the European level, heat pumps achieve high shares in the district heating generation mix in all the scenarios. Besides air-source heat pumps, river and lake and wastewater heat pumps can significantly contribute to the future generation mix (with up to 15% each). The advantages of lower grid temperatures are an increase in heat generation potentials, improved efficiencies for heat pumps and a reduced need for biomass. Nevertheless, (some) disadvantages, such as the need for investment in infrastructure and buildings in order to heat homes at lower temperatures, must be considered. Future research should focus on optimal grid temperature levels, e.g. with different temperature type networks.

With regard to system costs, the results indicate that the developments in the technology mix in district heating networks in the analysed scenarios only have a very limited impact on the total European energy system costs. It might be expected that higher shares of heat pumps in district heating could lead to higher electricity generation and thus higher system costs, but the differences between the scenarios are negligible, mainly due to the high efficiency of heat pumps. Nevertheless, higher shares of heat pumps, geothermal energy and industrial excess heat in district heating are cost-efficient for the overall energy system. Scenarios with the highest share of heat pumps are the cheapest, probably due to low generation costs and their role in providing flexibility in the power sector. However, system costs are very sensitive to the cost assumptions, which makes further research a necessity.

When looking at district heating costs, the results show that a higher share of geothermal energy is cost-efficient for district heating. Hence, the research question of the paper can be answered to the extent that a high direct use of geothermal can offer cost advantages for district heating, but does not have a relevant impact on the costs of the overall energy system. Future research should focus on the deployment of renewable and excess heat in district heating to achieve a rapid market uptake and a climate-neutral energy system in 2050.

Acknowledgements

This work was supported by the Fraunhofer Cluster of Excellence Integrated Energy Systems (CINES). Anna Billerbeck would like to thank Barbara Koch, Chair of Remote Sensing and Landscape Information Systems at the University of Freiburg, and Barbara Breitschopf, Fraunhofer ISI, for their support and guidance.

A.12 Detailed description of model approach and input data

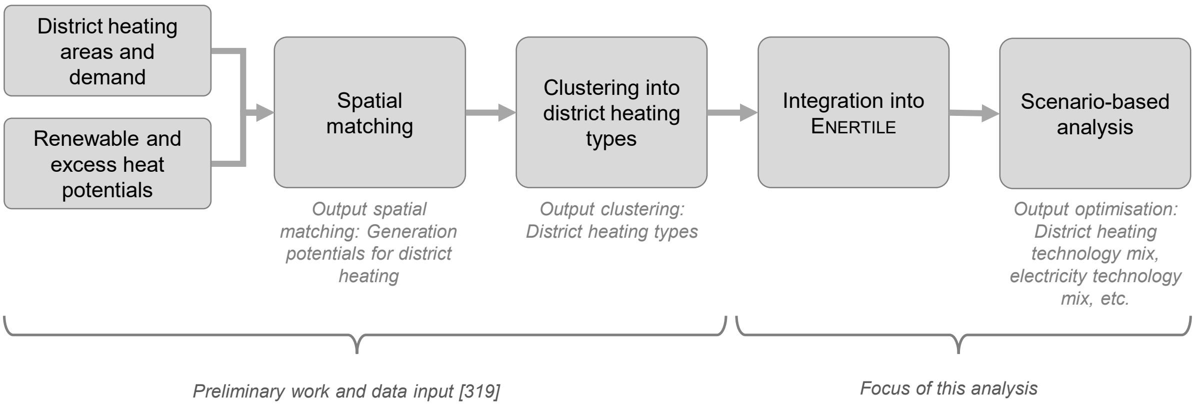

FigureAnnex 6: Overview of the modelling chain and connection to the preliminary work of [319]

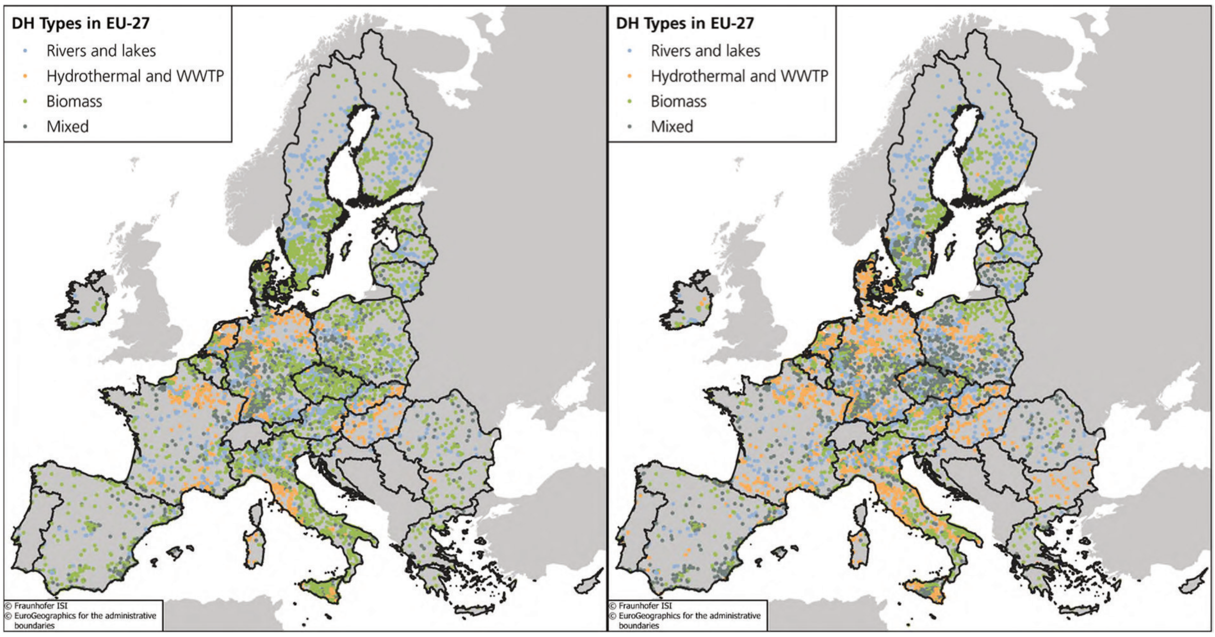

FigureAnnex 7: Location of the DH types in the HT scenario (left) and LT scenario (right) (based on [319])

TableAnnex 25: Energy demands per country used as input in Enertile in 2050

Country / Demand in TWh	District heating demand [319]		Demand other sectors ([51] building on [71,343])		
	HT scenario	LT scenario	Heat demand de-centralised heat pumps in build-ings	Electricity de-mand	Hydrogen de-mand
Austria	18.5	17.5	19.3	89.9	27.0
Belgium	8.6	8.2	26.3	121.8	74.5
Bulgaria	6.4	6.1	6.3	37.7	7.8
Cyprus	0.0	0.0	0.3	5.0	0.2
Czech Republic	28.8	27.3	27.8	81.5	14.2
Germany	148.9	141.2	120.1	734.4	143.6
Denmark	21.2	20.1	11.2	53.2	0.3
Estonia	4.0	3.8	2.7	9.4	0.5
Spain	44.1	41.8	29.0	308.5	29.2
Finland	34.9	33.1	14.5	98.1	6.6
France	107.3	101.8	149.7	586.3	148.0
Greece	9.4	8.9	4.9	59.1	6.5
Croatia	3.4	3.2	3.6	17.0	0.8
Hungary	17.0	16.1	25.4	52.3	11.8
Ireland	1.3	1.3	11.2	32.8	2.4
Italy	89.3	84.7	74.7	372.3	50.4
Lithuania	6.9	6.6	3.6	13.9	5.5
Luxembourg	2.9	2.7	2.4	9.8	0.0
Latvia	4.9	4.6	3.0	10.0	0.0
Malta	0.0	0.0	0.0	2.5	0.1
Netherlands	24.7	23.4	40.9	172.7	56.7
Poland	59.3	56.3	40.5	223.5	23.4
Portugal	3.6	3.4	5.2	67.2	7.4
Romania	12.5	11.8	14.6	77.4	22.7
Sweden	65.8	62.4	25.1	169.9	11.4
Slovenia	1.7	1.6	19.3	18.0	0.0
Slovakia	6.9	6.5	26.3	39.4	9.2
Total	732	694	708	3463	660

Note: The data publicly available from the 1.5TECH is limited to overall values for Europe in 2050 [71]. Thus, the demand distribution between countries were based on the SET-Nav project (diversification pathway) [343].

TableAnnex 26: Techno-economic parameters of investment options in Enertile in 2050 [340,344]

Technology		Lifetime	Investment in €/kW	Fixed O&M in €/kW	Variable O&M in €/MWh	Efficiency el (chp)	Efficiency heat
Electricity	Battery storage	10	204	5.5	0.0	95%	
	Combined cycle hydrogen turbine	30	750	11.3	3.0	61%	
	Hydrogen turbine	30	400	7.5	1.5	41%	
CHP	Biomass CHP	25	2900	103	2.1	30% (71%)	
	Waste to energy CHP	25	6460	148	23.6	24% (80%)	
	Hydrogen CHP	30	950	30	3	48% (88%)	
District heating	Biomass boiler	25	750	42.9	0.7		103%
	Electric boiler	20	60	0.9	0.4		99%
	Air source heat pump	25	760	2.0	1.7		variable
	River and lake heat pump	25	380	4.0	1.7		variable
	Wastewater heat pump	25	570	2.0	1.7		variable
	Geothermal	30	1300	18.8	2		-
	Solar thermal	30	310	60	0		-
	Industrial excess heat	25	1500	80	5.6		-
	Heat storage	20	22	0.0	0.0		99%
	Hydrogen boiler	25	50	1.7	0.9		104%

8 Conclusion

District heating (DH), once decarbonized, can play a significant role in the transition to climate-neutral heating. To achieve this, DH systems need to be expanded, utilise climate-neutral heat sources and improve efficiency. Identifying the potential for climate-neutral DH is essential for designing optimal pathways to transform the EU's energy system and building stock. DH relies on infrastructure development, making high-spatial-resolution modelling essential for demonstrating future scenarios. This requires extensive and detailed data sets. Existing models have not yet quantified the potential for climate-neutral DH in the EU using empirical data and available heat sources.

This thesis aims to identify potential DH areas based on future heat demand in residential and non-residential buildings and to explore possible climate-neutral heat sources for DH. This final chapter provides an overview of the main results addressing the research questions, demonstrates methodological advancements and draws conclusions. Finally, an outlook and recommendations for future research is presented.

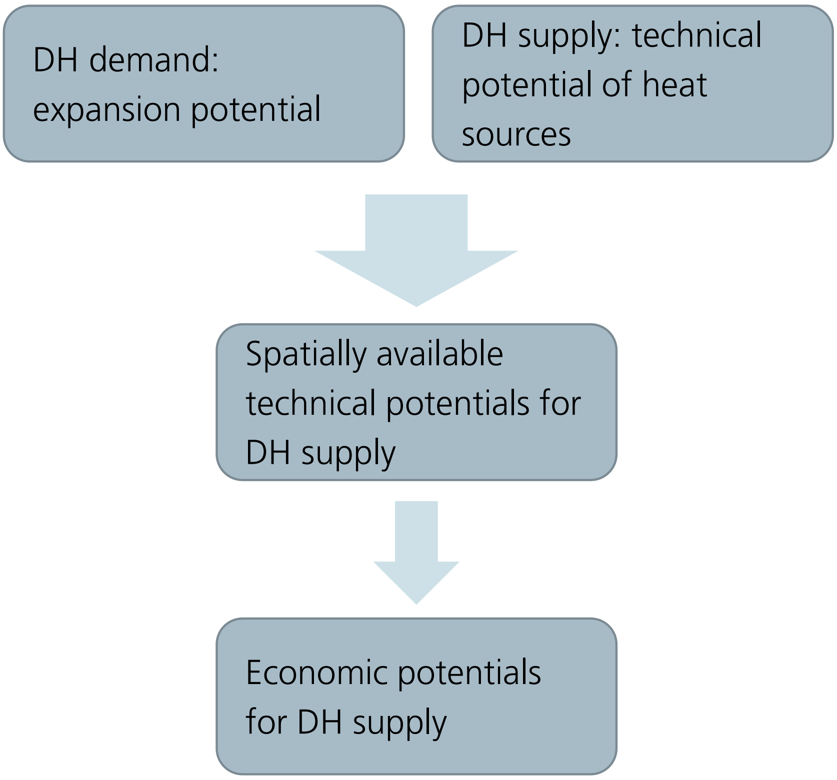

Figure 8.1: Data flow and analyses in this thesis

The thesis is structured into six main chapters (Chapter 2 to 7), each addressing a specific sub-question of the main research question. The chapters were published in several journals, each with its own focus and audience, demonstrating the need for multiple methods to answer the main research question. These chapters investigate key elements of the DH sector, construct detailed data sets and develop quantitative modelling approaches. Figure 8.1 depicts the stepwise data flow and analyses of the thesis.

The first part of the thesis focuses on DH demand modelling. Chapter 2 explored the expansion potential and resulting DH demand based on threshold values, which formed the base for Chapters 3 to 7 to identify available heat sources. The results reveal correlations between the building sector and the DH expansion potential, enabling the identification and mapping of potential future DH areas.

The second part identified and mapped the technical potential of renewable and excess heat sources for future DH supply. Chapters 3, 4 and 5 constructed data sets with high spatial resolution, with a focus of Chapter 4 and 4 on industrial excess heat. The aim was to include detailed technical parameters for the future industrial excess heat potential in the data sets and map industrial sites with coordinates. Chapter 5 extended the analysis to other available renewable and excess heat sources. In each of the chapters, spatial matching of the demand and heat sources quantified the available technical potential for DH. To explore future developments, several spatial matchings were conducted, varying the expansion of DH areas, maximum distances between supply and demand, the possible level of exploitation of supply potential as well as the efficiency increase of DH system. The expansion of DH areas was modelled by co-authors or taken from open data sets, and was validated in Chapter 2.

Chapters 6 and 7 quantified the economic potential for DH, based on the technical potential identified in Chapter 5, using two different energy system models, each with a different focus. The identified available technical potential was integrated into these optimisation models, together with cost assumption for generation technologies, hourly profiles e.g. for electricity prices and heat source temperatures, as well as further technical specifications. The main contribution of this thesis to the optimisation models is providing the identified technical potential along with the technical specification and assumptions in a suitable spatial resolution and aggregation.

Open data strategy

The main results of this thesis were published as open data sets under a CC-BY-4.0 license where possible. This allows them to be assessed, reviewed and further utilised and improved by the scientific community and stakeholders. Table 8.1 lists the data sets published in this thesis.

Table 8.1: Overview of published open data sets

Origin	Name of data set	Link to online resource	Type of data
Chapter 3	sEEnergies Open Data Hub: D5.1 Industrial excess heat potentials, 2021.	https://s-eenergies-open-data-euf.hub.arcgis.com [150]	Tabular data of georeferenced industrial excess heat sources (coordinates) and outlines of possible DH areas (.csv/.shp)
	Visualised in the D5.1 Data set WebApp	https://tinyurl.com/sEEnergies-D5-1 [151]	
	Included in Peta 5.2	https://www.arcgis.com/apps/webappviewer/index.html?ii=8d51f3708ea54fb9b732ba0c94409133 [89]	
	Included in Hotmaps toolbox	https://www.hotmaps.eu/map [48]	
Chapter 4	Manz, P.; Fleiter, T.; Eichhammer, W.: The effect of low-carbon processes on industrial excess heat potentials for district heating in the EU: a GIS-based analysis, 2023.	http://dx.doi.org/10.24406/fordatis/252.2 [345]	Tabular data on georeferenced future industrial excess heat sources and results of spatial matching (.xlsx)
Chapter 5	Manz, P.; Billerbeck, A.; Fallahnejad, M.: Spatial analysis of renewable and excess heat potentials for climate-neutral district heating in Europe, 2023.	http://dx.doi.org/10.24406/fofordat/280.3 [294]	Geographic data on renewable and excess heat sources (.gpkg) Tabular data on results of spatial matching and clustering (.xlsx)

8.1 Summary of achievements

The key contributions of this thesis to establishing the role of DH in a future decarbonized energy system are highlighted and briefly summarised in the following.

Modelling district heating and the energy system at high spatial resolution on a large geographical extent

This thesis has achieved detailed results through high spatial resolution modelling covering a large geographical extent. The modelling of DH in the EU covered different sectors, including demand, supply and infrastructure. Consequently, multiple methodological approaches were required to assess the DH potential, by linking building stock modelling, spatial matching and scenario analyses. This comprehensive approach has enhanced the spatial perspective in evaluating future DH potential, leading to more realistic methods and data for energy system modelling across a vast geographic extent.

Providing empirical evidence for identifying potential district heating areas

Existing literature has modelled future DH areas by assuming thresholds for heat density or distribution costs. This thesis provides empirical evidence to support this approach and offers deeper insights into the correlation involved. By combining and analysing several high-resolution databases and data sources, a correlation between the presence of DH and heat density was demonstrated, leading to an empirically derived threshold for acceptable heat distribution costs. The data confirm that most assumed thresholds in the literature are comparable to currently accepted distribution costs, thereby validating the existing modelling approaches for identifying potential district heating areas.

Creation and publication of a database for georeferenced industrial excess heat in the future

The potential contribution of industrial excess heat to district heating supply in the context of a transformation to a climate-neutral industry was quantified in detail. A site-specific database was established, providing detailed process information and annual production quantities. This database was used for scenario-based approaches to quantify the impact of the transformation of industry to low-carbon processes on the available excess heat for DH.

8.1.1 Key findings

In this thesis, the sub-questions are answered by the individual dedicated chapters, each closing the research gaps identified in Chapter 1 and contributing to the overall conclusions on the future potential of DH and its role in the heating transition. The following sections summarise the contributions of each chapter, draw conclusions and ultimately answer the main research question, leading to a main conclusion.

How does decreasing heat demand affect the future expansion of DH areas, based on empirical data?

DH faces several future challenges, including reduced heat demand, notably due to thermal renovation of buildings. DH infrastructure is more economical in densely populated areas with high heat demand. Literature identifies future potential DH areas by heat density thresholds. In Chapter 2, these thresholds and the normative approach were mostly confirmed through empirical data analysis on a hectare-level in Germany. This analysis correlated heat demand and DH connections, enabling to identify feasible future DH share in two scenarios varying the ambition of thermal renovation.

Ambitious DH market shares of up to 50% of the heating and sanitary hot water demand of residential and non-residential buildings demand by 2050 could be feasible in Germany, which implies a significant increase compared to 9.2% today. This high market share can be achieved if nearly all buildings within DH areas are connected and heat demand decreases by no more than 30% compared to current levels. However, with high renovation rates and thus strong decrease of heat demand, and no further improvements in the DH connection rate, it is possible to at least double the DH market share with constant heat distribution costs of 6 €/GJ. Generally, the results show a large variance and a plateau of possible future market share with similar costs.

In conclusion, the future market share primarily depends on the connection rate and, to a lesser degree, on the level of thermal renovations. A reduced heat demand in buildings can therefore be compensated for by a higher connection rate. Generally, an expansion to higher market shares of at least 20% is cost-effective, and DH can play a key role in the heating transition in Germany. Doubling the DH market share to 20% means that DH will be deployed in all big and large cities, possibly replacing the gas infrastructure if it exists.

How much excess heat from energy-intensive industrial processes is technically available for DH at the regional level?

In the future, DH must be supplied by renewables and excess heat sources to achieve decarbonization, as fossil fuels are still widely used for DH production today. It is essential to analyse possible climate-neutral heat sources to supply the future DH demand. Chapter 3 focused on the significant potential of utilising excess heat from high-temperature industrial processes by developing a georeferenced database.

The total excess heat potential from 1608 industrial sites in the EU ranges from 53 to 267 TWh/a, largely depending on the DH temperature level to which the available excess heat can be cooled down to. Lowering DH temperatures by 40 K doubles the usable amount from industrial processes. Another parameter is the efficiency of the industrial processes, including internal heat recovery. More than 80% of all industrial sites are within 2 km of possible DH areas, representing more than 90% of the total annual excess heat. This leads to the conclusion that a high share of available excess heat potential from energy-intensive industrial processes could be utilised with low transport costs if DH will expand. Overall, industrial excess heat is expected to contribute 8% to 14% of future DH demand. Despite this low EU-wide contribution, industrial plants can locally cover a significant share of the heat supply in individual DH networks. These conclusions are based on the assumption that today's processes will not undergo major changes towards a low-carbon industry, which is the focus of the next section.

How does the transformation to a climate-neutral industry affect the excess heat that is available for DH?

Industrial processes will not only become more energy efficient but will also need to be transformed, replacing fossil-based processes to achieve climate-neutrality. Most studies expect that existing processes will be replaced with electrified or hydrogen-based alternatives, like hydrogen-based steel making or using alternative routes in the chemical sector with green hydrogen as feedstock. Chapter 4 analysed the impact of the transformation of industry to low-carbon processes on the available excess heat.

The available excess heat from industrial processes will reduce by 63% to 90% due to higher efficiency in new installations and the process design. Electrification of former fossil-based processes, such as in the steel or paper production, substantially reduces heat losses and thus excess heat. In total, industrial excess heat could contribute between 1% and 8% to future DH demand in the EU, compared to an 8% to 14% contribution if only process efficiency improves. Main sources of excess heat are cement, glass, chemicals and steel production. This leads to the conclusion that the available excess heat from industrial processes will likely decrease due to new processes in a climate-neutral energy system. With growing DH demand, industrial excess heat will not be a main heat source. Thus, other renewable and excess heat sources will have to play a much larger role in future DH supply, replacing the fossil fuels that currently dominate DH supply, which is quantified in the next section.

What is the technical potential for renewable and excess heat sources to supply DH demand in a climate-neutral energy system?

To supply a growing DH demand in a climate-neutral energy system, several possibilities are available. Renewable and excess heat sources can either be used directly or as sources for heat pumps, increasing the efficiency compared to air-source heat pumps. High-resolution spatial data is needed to map and quantify these sources in the EU, and their usable potential is determined by matching them spatially with future DH demand. Chapter 5 used a spatial approach to map and quantify the technical potential from geothermal, waste incineration, and heat from wastewater treatment plants, rivers and lakes combined with heat pumps.

The technical potential of sources available within an economic distance to future DH areas can supply over 80% of the future DH demand (around 700 TWh). Decreasing DH system temperatures by 20 K increases the renewable and excess heat potential, up to the factor of two for geothermal resources. Thereby, the necessary utilisation of biomass or air-source heat pumps for DH supply can be reduced in the future. In conclusion, even with increased DH demand, many renewable and excess heat sources can supply heat with low electricity demand. The dependency on biomass as a scarce resource in the future can be reduced by increasing the geothermal potential due a reduced DH system temperature.

The resulting DH areas were clustered based on their share of each available renewable and excess heat source, forming four clusters in the EU. These clusters enable the integration of detailed spatial data into energy system models with lower spatial resolution, maintaining the details about potential heat sources for individual DH systems.

What is the economic potential of climate-neutral supply options and what is the influence of the supply temperature in DH grids?

The availability of renewable and excess heat sources for DH depends not only on spatial availability but also on temporal availability and technology costs. Investment and operation costs influence the capacity of the technology and their dispatch. These parameters are included in energy system models with hourly resolution, however often with low spatial resolution. Therefore, the clustered results of the renewable and excess heat potential for DH supply, derived in Chapter 5 with high spatial resolution, are used in Chapter 6. An optimisation model covering the DH supply was improved and utilised to identify installing cost-optimal capacities based on a greenfield approach and analyse the impact of reducing temperature in DH grids.

The technical potential of geothermal resources as well as excess heat from waste incineration and industrial processes is exploited almost completely in most scenarios. The high potential of geothermal can cover a large share of DH supply (up to 25%). Even with these high available technical renewable and excess heat potentials, air-source heat pumps will play a significant role. Solar thermal potential plays a minor role, and the heat from rivers and lakes is not used to the full technical potential. Wastewater treatment plants and biomass are more favourable in DH system with high temperatures. Low system temperatures of around 60°C increase especially the efficiency of geothermal utilisation due to higher potential and efficiency, reducing the overall levelised costs of heat by 20%. The role of biomass in future DH systems is sensitive to the biomass price, while geothermal technologies are sensitive to the relatively high investment costs. Concluding, a climate-neutral DH supply based on a mix based on mainly geothermal resources (hydrothermal) and heat pumps is cost-optimal, together with biomass combined heat and power (CHP) and excess heat from waste incineration and industry, and temperatures should be reduced in DH grids to increase the utilisation of renewable sources and reduce costs.

How do different renewable and excess heat sources for DH interact with the electricity sector?

In the future, large heat pumps interact with the rest of the energy system and potentially provide flexibility options for the electricity grid. To assess these interactions, an integrated energy system model that optimises all sectors is extended to include the heterogeneous DH types and used for different scenarios in Chapter 7.

In all scenarios, large-scale heat pumps cover most of the DH demand. Besides air-source heat pumps, water-source heat pumps utilising heat from rivers, lakes and wastewater treatment plants significantly contribute to the DH supply. They provide additional system benefits, particularly flexibility. However, the cost-benefits of this flexibility play only a minor role compared to the overall system costs, as these heat pumps increase the overall electricity demand in 2050 by only 1%. Heat pumps and geothermal technologies are particularly effective in low-temperature DH systems. In DH systems with high geothermal potentials, up to 70% of DH generation can be supplied by geothermal resources, demonstrating the substantial contribution of this resource where available. Generally, a higher share of geothermal energy is more cost-effective than utilising industrial excess heat or solar thermal energy for the DH sector.

In conclusion, renewable sources like geothermal can provide a cost advantage for DH generation with negligible impact on the overall energy system costs, while a high share of air-source heat pumps offers cost advantages to the energy system.

The answers and conclusion from the individual sub-questions and chapters enable to answer the main research question in this thesis:

What is the potential for a climate-neutral district heating in the EU, taking into account the spatial diversity of heat demand and supply?

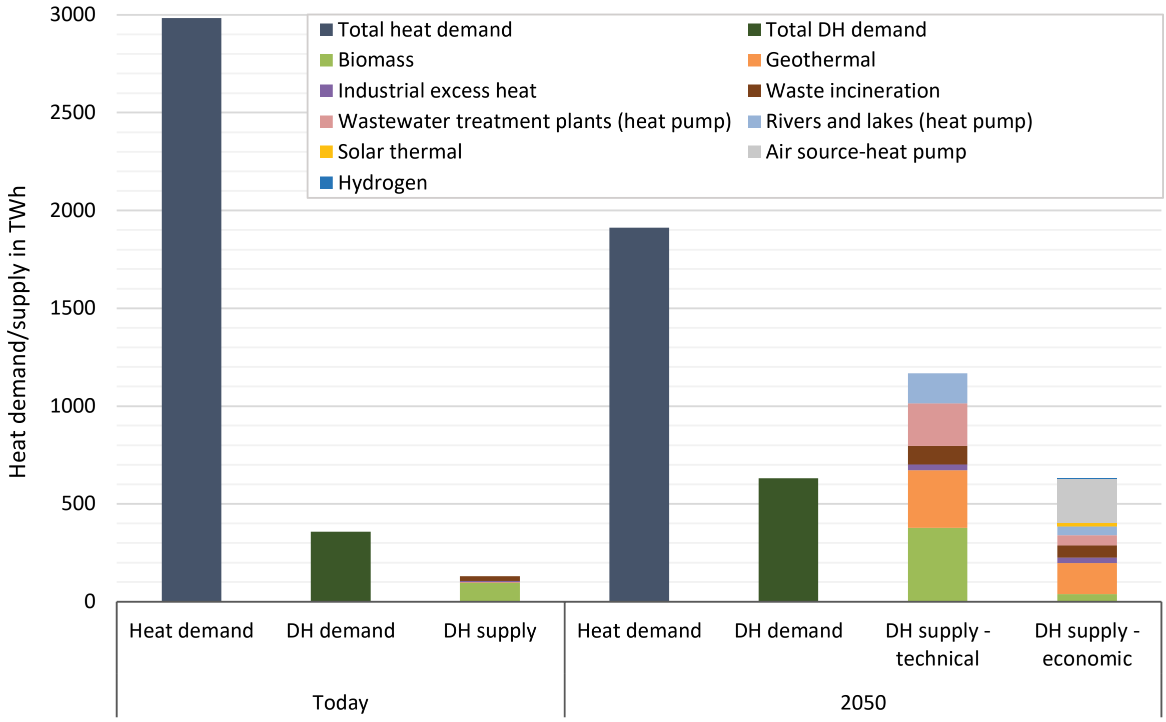

Figure 8.2: Current and future heat demand, DH demand and DH supply from renewable and excess heat in the EU. Own illustration based on the findings of this thesis and data from European Commission, 2022 [9]

District heating can play a significant role in transitioning to climate-neutrality in the EU, which is summarised in Figure 8.2. Substantially more households than today could potentially be connected to DH in the future, as investigated empirically in Chapter 2 and further assumed in Chapters 3 to 7. The DH demand could be technically (Chapter 5) and economically (Chapter 6 and 7) supplied by several climate-neutral sources, such as geothermal resources, biomass, heat pumps utilising heat from wastewater treatment plants, rivers and lakes as well as excess heat from waste incineration. Industrial excess heat will only play a minor future role (Chapter 3 and 4). Considering the slow progress in transitioning to sustainable heating and the need for a climate-neutral building sector, DH offers an economical heating solution with significant potential in the EU.

The identification of future **DH demand** and areas demonstrates significant expansion potential, possibly connecting more than twice the number of households to DH compared to today. High DH market shares are possible without significantly increasing infrastructure costs, as shown in Chapter 2. The case study of Germany shows that large DH market shares of 50% could be possible, if almost all buildings within a DH area are connected and thermal renovation of buildings does not drastically decrease heat demand. The results of this thesis support the ambitious 45% DH market share outcome proposed by the Heat Roadmap Europe study [38], representing the upper limit of the DH expansion potential, assuming all households within a DH area connect and barriers are overcome. Otherwise, a low connection rate combined with ambitious thermal renovation of buildings could lead to a DH market share of around 20%. Even at this lower end, DH remains an important pillar for providing climate-neutral heat to buildings. This highlights the trade-off between building thermal renovation and the extension of an efficient DH network. Thus, an optimal balance should be found to minimise societal costs in line with the Energy Efficiency First (EE1st) Principle [346]. DH has the greatest economic advantages in city centres and densely populated areas, mainly for multi-family houses. These houses are often heated with natural gas and are less suitable for heat pumps compared to single-family houses in rural areas, due to higher heat demands, older buildings and noise from the outside unit. Thermal renovation of buildings in the future decreases the heat demand and makes DH less economical, which could be compensated by increasing the connection rate within a DH area by 10 to 25 percentage points. Spatial modelling in a scenario-based approach resulted in a broad range of possible DH expansion in Chapter 2, validating existing modelling approaches that have not been using empirical parameters for cost thresholds. Chapters 3 to 7 use future DH areas and demand that were derived by co-authors with the existing method and thresholds, resulting in DH market shares and demands that are in the range of the values found in the empirical analysis in Chapter 2. Chapters 3 and 4 employed two scenarios for DH development to show the possible range of DH demands from 165 to 1949 TWh per year in the EU. Chapter 5 used scenario-based results of future DH areas and demands, similar to the Chapter 2 regarding the results and the method, which have an outcome of an average connection rate of 77%, a DH market share of 33% and a DH demand of 631 TWh (Figure 8.2). This number represents nearly double the current absolute DH demand of 358 TWh, and a tripling of the current market share [9]. This leads to distribution costs of 8.7 €/GJ on average, comparable to the upper limit of the values found for Germany in Chapter 2.

This thesis shows that a future DH demand of 631 TWh (representing 33% market share) can be supplied with **climate-neutral sources** in the EU, which is also depicted in Figure 8.2. The spatial analysis and matching of demand and supply enables the quantification of potential renewable and excess heat sources. **Industrial excess heat** is a very interesting source where it is available. Industrial plants are point sources often with high amounts of excess heat as it comes from energy-intensive processes. This potential can supply a large share of the demand locally. An industrial database with locations of energy-intensive industrial plants was developed, showing that most of these locations are close to potential DH areas. However, the impact of the introduction of low-carbon processes in industries was estimated, leading to the results that the majority of current industrial excess heat potential could be not available in the future due to changes in industrial processes. Therefore, industrial excess heat should be included as an option for supplying DH locally, however, its contribution should not be overestimated as it amounts to 1-8%. The major share will need to come from other sources. Various renewable and excess heat sources were mapped, resulting in a large **geothermal** potential from aquifers (hydrothermal), but also from hot-dry-rock (petrothermal) that can be used directly without heat pumps. The geothermal potential is large (107 to 294 TWh depending on the temperatures in the DH networks), which can cover 15%, and up to 42% of the DH demand, if temperatures are decreased. This emphasises the large potential of geothermal resources and the need for efficiency measures in the DH grids. However, this technology is bound to exploration risks, which means that field drillings all over the EU are needed to confirm or contradict the modelling results. This leads to the conclusion that more research should be going to this technology. Furthermore, **wastewater treatment plants** show a high potential to provide heat pumps with ambient heat around 8°C to 15°C from the wastewater. The temperatures are quite stable in winter months leading to technical advantages compared to air-source heat pumps, which was proven in several realised projects. Heat from **waste incineration plants** and from heat pumps with the source from **rivers and lakes** can contribute also considerable amount of energy for DH supply. **Biomass**, even though a resource with high competition for both energy and non-energy use from other sectors, is a viable option for supplying DH when other sources are scarce, or during periods of low availability of renewables, serving as a peak load heat source. The thesis showed that the potential of secondary biomass (agricultural or industrial residues) is sufficient to meet the demand.

In the **supply mix**, the integration of prices and costs of the supply technologies highlights the substantial contribution of air-source heat pumps. Despite the high investment required, geothermal resources also play a pivotal role in a cost-efficient DH supply across the EU, almost realising their full technical potential. Lowering DH grid temperatures reduces dependence on biomass, as alternative renewable and excess heat sources, particularly geothermal resources and heat from rivers and lakes, can be utilised more efficiently and at lower costs. In a climate-neutral energy system, during periods of low electricity prices and high renewable electricity generation, large-scale heat pumps within the DH sector can efficiently produce heat. These have positive effects on the electricity market by offering flexibility, making them more cost-competitive and providing minor cost advantages to the overall energy system. Exploiting the technical geothermal potential mitigates costs for the DH sector, given its comparatively low operation costs and high seasonal availability.

Summarised, this thesis demonstrates the potential for DH to become a major supplier of heat for buildings in the future. The market share can be increased while maintaining similar distribution costs to those seen today. To achieve this, nearly all buildings within DH areas must be connected. DH demand can be met with climate-neutral heat from various sources, notably geothermal and air-source heat pumps, offering economic advantages, as well as providing flexibility to the electricity sector, with high spatial and seasonal availability. These findings emphasise the significant role of DH in the heating transition, potentially replacing the gas infrastructure in cities and densely populated areas. Achieving climate-neutrality within the next 25 years could be supported by the central decarbonization of the building sector, phasing out fossil-based heating sources such as oil, gas, and coal. However, realising this potential necessitates the refurbishment and densification of existing networks as well as new construction of an extensive DH infrastructure. This includes both transport pipes connecting heat sources such as industrial plants, geothermal or wastewater treatment facilities, as well as distribution grids connecting the buildings within urban areas.

An ambitious goal is to achieve a DH market share of 20% to 50% of the heating and sanitary hot water demand in the EU by 2050. It is worth noting that the current gas infrastructure, with half of the buildings supplied with natural gas [8], demonstrates that widespread heating infrastructure is feasible. Significant DH market shares of 50% have already been achieved in countries like Sweden and Denmark. Furthermore, reducing temperatures in the DH grid offers several advantages, including lower heat losses, more efficient utilisation of renewable and excess heat sources, improved performance factors for heat pumps resulting in lower electricity demand, and reduced reliance on biomass. These measures contribute to overall lower system costs and are essential steps towards achieving a climate-neutral DH system.

With these individual studies focusing each on several aspects of the demand and supply potential, the research questions about the future potential of DH in the EU could be answered, emphasising the key influencing parameters, and highlighting DH's significant role in the heating transition.

8.1.2 Methodological development

DH as a technology imposes inherent challenges on modelling and scenario design, as it depends on the evolution of local heat demand, the supply possibilities, and the need for regional infrastructure. These parameters are interdependent; for example, infrastructure costs decrease as more buildings within an area connect to the DH system, which in turn facilitates the connection of even more buildings. Furthermore, it necessitates spatial approaches due to the highly regional character of the systems, i.e. the local building stock and its heat density, the available renewable and excess heat potential and the regional costs for the infrastructure. Thus, to answer the research questions of this thesis, several models were established with high spatial resolution, linked together and applied with the existing and well-established models FORECAST [47], ENERTILE [62] and Hotmaps DH GEN Model [50]. This thesis extended the model frameworks and increased the spatial and technological detail of them by developing and integrating spatial algorithms and models. In general, simplification in models enables a large geographical context, which was conducted in the models of this thesis by empirical parameters or clustering. The software QGIS, alongside with the Python plugin PyQGIS, was utilised to automate and streamline spatial analyses and models.

DH demand: Empirical evidence derived for accepted distribution costs of DH

The potential future of the building sector and regional heat density was examined using the newly developed DISCO model in Chapter 2, which operates with a spatial resolution of one hectare. It was linked via a common database to the building stock model of FORECAST that calculates and stores the results of the evolution of specific heat demands of several building categories. In DISCO, current DH networks in Germany were mapped using data on DH connections at the hectare level. By combining these data with the local heat density, empirical parameters for distribution costs were identified. These parameters were used in scenarios to quantify the future DH demand potential. In the regional approach, a statistical method was used to distribute the building categories regionally as data are not available on this resolution. Census data of a resolution of 100 m x 100 m were used to derive parameters for a normal distribution of existing DH connections with the heat density. This has closed a research gap, providing empirical evidence for threshold values, based on the census data for DH connection at the hectare level, that are used in literature for the identification of suitable DH areas. The empirics confirm the suitability of modelling approaches that use a threshold for the identification of potential DH areas. With this contribution, the simplification of using a threshold in modelling suitable DH areas proves as suitable. The derived values for Germany are in the range of assumptions used in existing literature and in the Chapters 3 to 7 of this thesis. In these chapters, the future DH demand potential in the EU was modelled by co-authors, Urban Persson and Mostafa Fallahnejad.

DH supply: Extensive databases established for renewable and excess heat potential

The supply of a future potentially higher DH demand in extended areas needs to be studied with high spatial resolution. Therefore, a database of regional renewable and excess heat sources with various input data and technical assumptions is needed. For that, numerous data sources were collected, processed, combined and further developed in this thesis (Chapter 3). The focus lies on the collection of energy-intensive industrial sites that use process heat on a high temperature level. These sites are often suitable for external utilisation of excess heat. For that purpose, databases for the EU

Emission Trading Scheme (EU ETS), the European Pollutant Release and Transfer Register (E-PRTR), and several sectoral databases with over 5000 sites were compared, matched and validated. Additionally, the future transformation of industrial processes based on existing scenarios was taken into account and combined in the Industrial Database (Chapter 4). Further heat sources for DH were identified and mapped (Chapter 5). In particular, the technical geothermal potential was derived from underground temperatures and designated areas with water basins, by an algorithm developed in QGIS. Further potential heat sources, collected in the database, are heat from waste incineration facilities (Waste-to-Energy), biomass, rivers and lakes, wastewater treatment plants. They were published as open data in high spatial resolution as GeoPackage (.gpkg, which is an open, standards-based, platform-independent format for transferring geospatial information), as well as in an online GIS web-app, as listed in Table 8.1. The data sets can be used by the scientific community and stakeholders.

DH supply and demand: Spatial matching algorithm developed

The renewable and excess heat potential for the supply of DH was quantified with a spatial matching algorithm established for this thesis. With that, the proximity of demand and supply is incorporated, by defining categories of the technical potential, depending on the spatial parameter: supply and utilisation potentials. As an input, the location and demand of identified DH areas and the database of renewable and excess heat potential is used. The algorithm was developed in the programming language Python and uses the Python environment in QGIS, enabling the utilisation of the GDAL library and tools for spatial calculations. The algorithm calculates the potential of the sources that could supply the DH areas within certain distances, by using a prioritisation approach for large sources and DH areas. The calculation time is about three to six hours, depending on the geographical extent and number of DH areas. The output is the renewable and excess heat potential for each DH area within a certain distance. This allowed the clustering of these areas for simplified representation in further modelling with a large geographical extent, yet maintaining the diversity of the heat supply potential of each DH network (Chapter 5). The preparation of the data and choice of parameters for the clustering was part of this thesis, the actual clustering was conducted by a co-author, Anna Billerbeck.

In this thesis, the results of the clustering were integrated into two optimisation models, one with the focus on the interaction with the power sector (Chapter 6), and the second with the focus on temperature profiles and hourly load (Chapter 7). The preparation of the technical data, simplification of dependencies as well as providing hourly profiles of renewable sources was part of this thesis, the application of the optimisation models was conducted by co-authors, Ali Kök, Anna Billerbeck and Christiane Bernath.

In general, the stepwise approach taken in this thesis, first the demand, then the supply and last the matching between these two, allows to model and represent the most important aspects of the future potential of DH in the EU. Different methods were used, developed and adapted, as well as several extensive databases closing significant research gaps were published in this thesis. Thus, this thesis offers a broad contribution to the quantitative modelling of DH.

8.2 Limitations

The necessary simplifications for modelling the DH sector in the EU come with limitations. Additionally, this thesis does not thoroughly investigate all aspects of the transformation towards a climate-neutral heating. While the quantitative modelling highlights technical and economic potential of DH, however, it does not address political implications from these results in detail. The following sections first outline the most important limitations in the modelling and quantification of the potential of the demand, the supply and by the spatial matching, followed by a presentation of other factors that may influence the identified potential in the future.

Identification of future DH areas based on threshold values of today's costs structure

For quantifying future DH demand and mapping DH areas, a commonly adopted approach in the literature, using a threshold value for a heat demands, was used. Although this approach was validated with current data in the thesis, it does not account for future developments or country-specific differences like climate and price differences e.g. due to taxes. It assumes that the currently accepted infrastructure costs will remain applicable in the future and can be used as a threshold. This is an approach from the macroeconomic perspective, calculating with an interest rate of 3% and an investment lifetime of 30 years for DH infrastructure. However, from a microeconomic perspective for the consumers, the competition between the heating options will look differently. To incorporate the microeconomic perspective, an integrated modelling approach that considers the costs for consumers for all heating technologies is needed. This approach should be iterative, as specific distribution costs for consumers depend on the share of consumer who choose to connect, which in turn partially depends on these distribution costs. Additionally, the consumer price for DH will include the generation costs, necessitating an integrated modelling approach with high computational demands, spatial and temporal resolution, and different approaches and perspectives like optimisation and simulation. The costs and prices of heating options significantly impact consumer choices, but not all consumers will behave rationally or anticipate future price trends. Factors such as independence or ease of access to a certain technology also play a substantial role. If DH becomes less attractive than decentral options like heat pumps or biomass, fewer households may connect to DH than identified by modelling, increasing specific infrastructure costs for the remaining consumers. In general, using a threshold value is a transparent and viable approach. In the future, as the costs of heat generation for DH and decentral options change, the threshold could change and should be adjusted accordingly. Moreover, this thesis does not address the industrial demand for DH, as industrial demand profiles and locations differ significantly from those of buildings. Typically, industrial DH networks are separate networks and have higher specific demands. However, with extensive DH networks in the future, connecting industrial plants could reduce specific distribution costs due to their high heat demands and uniform demand profile over the year.

Quantification of high potential contribution of geothermal sources based on modelling data and assumptions

The spatial modelling and matching of technical potential indicate that geothermal energy could potentially cover over 40% of future DH demand. This quantification is based on temperature data and potential aquifers modelled on the EU-level from individual drillings. However, the success of geothermal projects depends on site-specific test drillings. To address this, risk factors reflecting typical geothermal project success rates were incorporated into the modelling. Additional limitations in geothermal modelling include the uniform assumptions for flow rates, exploration depths and full load hours across the EU. These are based on hydrothermal projects that have been successfully realised for CHP or heat generation for DH. In the EU, 261 plants for DH are in operation with a capacity of 4457 MW_{th} in 2022, with even more under investigation. Most of the plants for heat generation are installed in Italy, and in Germany a capacity of 50 MW_{e} as CHP plants was installed in 2022 [347]. The exploitation of the identified potential in this thesis of about 40 GW_{th} each for hydrothermal and petrothermal projects represents a twentyfold increase over the current number of plants. An EU-wide database of field drilling data and geothermal resources mapping, publicly available, is a crucial first step for a European strategy. Additionally, financial support and risk mitigation measures, such as insurance or direct support, are necessary, as advocated in a resolution by the European Parliament in 2024 [348].

The future potential from geothermal projects needs to be reflected according to the large uncertainties in the modelling. The main uncertainties are the quantification of the technical potential as detailed on-site test drillings are needed to estimate achievable flow rates, and the cost assumptions for 2050 that are dependent on technical progress. As upfront costs and risks are high, the technical progress due to upscaling, standardising and learning may need to be supported by politics. However, this analysis is the first to quantify the potential for deep geothermal plants based on detailed assumptions and incorporating the risks with conservative parameters and high risk factors, i.e. assuming that 50% to 75% of the projects are successful.

Another way to utilise heat from the underground is through shallow geothermal plants combined with heat pumps. This increases spatial availability across the EU and alters the cost structure by lowering drilling costs and adding investment and operation costs for the heat pump.

Quantification of future renewable and excess heat potential based on assumptions for future development

Similar to the geothermal potential, the quantification of other identified renewable and excess heat potential also has limitations. The potential of industrial excess heat depends on the location of industrial plants, and it was assumed that all current sites will remain at their location and transform to low-carbon processes. Additionally, the excess heat factors from low-carbon processes were mostly estimated by comparing them to current processes or based on modelling results, as most low-carbon processes have not yet been built, and efficiency advancement and process design are not fully determined. For utilising heat from rivers and lakes with heat pumps, typical project sizes were assumed based on river flow rates. However, actual project designs will depend on various parameters such as temperature profiles and regulations and will differ from the simplified assumptions in this thesis. The regional availability of biomass was conservatively estimated, assuming limited transport distances. If biomass were transported over longer distances, the potential for DH generation could be increased. Waste incineration plants represent a substantial heat potential, often located near cities, and current sites will potentially continue to operate in the future. The impact of circular economy policies, which may reduce the amount of waste incinerated in the EU, was assumed to be offset by the additional incineration of waste that is currently landfilled, particularly in Eastern EU countries, as well as by higher recovery efficiencies [268].

Fixed maximum distances for DH heat sources to the DH area

The spatial matching of the demand and supply assumes typical transport distances via transport pipes that are considered economic for the typical size of the source. The greater the amount of excess heat, the longer the transport infrastructure remains economic, as calculated by Bertelsen et al, 2021 [224]. In this thesis, different maximum distances were chosen for the considered heat supply potential, prioritising the supply of larger DH areas. For instance, industrial excess heat is assumed to have a higher feasible transport distance compared to heat from wastewater treatment plants, given the typically larger amount of energy available. However, the validity of these distances depends on individual projects. For example, the maximum distance in this thesis is the same for all industrial plants, but a larger cement plant generates more excess heat than a small paper factory and thus the transport pipe could be longer. This simplification is made to save calculation time and enhance the transparency of the results. In comparison, the approach of the Heat Roadmap Europe project uses an optimisation model [17] for 14 EU studies to minimise transport costs, which prioritises larger quantities of heat. The actual acceptable distance primarily depends on the size of the specific realised project, as well as on other factors such as available subsidies and the assumed lifetime of the project. Furthermore, to quantify the supply and utilisation potential of all heat sources, annual demand and supply data were used. Seasonal mismatches were simplified using typical full load hours. In the optimisation modelling step, a temporal resolution of one hour is used, while the spatial resolution was reduced through a clustering approach. This stepwise approach allowed the modelling of the geographical extent of the EU while maintaining the computational feasibility.

Barriers for implementation of identified strategies

In the modelling and identification of DH demand and supply potentials, possible barriers were not integrated and therefore their impact on realising this potential is not part of this thesis. They can be grouped into policy and regulation barriers (e.g. the lack of clear targets and incentives, numerous laws and improperly regulated prices), market barriers (e.g. high investments costs for infrastructures), financial barriers (e.g. high investments, split incentives for building owners and tenants or unsecure market conditions for investors) and capacity barriers (e.g. lack of skilled workers or knowledge) [330]. In general, acceptance is an important aspect for DH, as it is a natural monopoly which makes the consumers dependent on one supplier. This could represent a barrier for consumers, especially with low income, and decrease the utilisation of the technical potential. A solution to such natural local monopolies can be socio-economic cost-benefit analyses for evaluating heating projects as required in Denmark, ensuring that projects that have the most net benefit to society are realised [349]. These various barriers require a range of adequate policy instruments, working together within a consistent policy framework, incorporating regulatory, economic, and other supporting policies.

Interaction with political framework

The policies that can be derived from the results of this thesis to pave the path for a climate-neutral DH sector are not part of this thesis. Nevertheless, existing policies could significantly influence the DH potential, as implicit assumptions about the political framework are inherent in the modelling. Key policies include the EU's Energy Performance of Buildings Directive (EPBD revised EU/2024/1275) [11,183], which regulates thermal renovation of buildings and consequently affects future heat density; the EU Emissions Trading System (EU ETS) [350], which prices emissions from industrial processes and thus facilitates the shift to low-carbon processes; and policy measures aimed at increasing renewable energy generation, such as the Renewable Energy Directive (RED III EU/2023/2413) [12], the Energy Efficiency Directive (EED III EU/2023/1791) [20] and the EU Heating and Cooling Strategy (2016) [123], which promote phasing out fossil fuels in heat generation. Changes or updates to these frameworks will impact the transformation pathway and its speed.

8.3 Outlook

The main contribution of this thesis is the quantification of the potential of DH demand areas and available heat sources for DH in models with high spatial resolution, and the identification of the most important parameters. This fills a major data gap in many energy system models as this had not been integrated, often resulting in lower DH demand and higher electricity or hydrogen demand for DH supply.

Previous estimates of DH demand potential were often based on expert guesses, with a wide range of possible DH market shares in the literature, as shown in Ref. [85] and in Figure 8.3. In this publication, no relation between the assumed renovation rate or focus of the scenario and the resulting DH market share can be found. The results for the EU and Germany differ, with no obvious reason, with the highest DH market share resulting from models that have a detailed representation of the DH sector. Generally, the results from this thesis demonstrate that the wide range of a DH market share from 4% to 45% in the EU is justified by a large plateau of distribution costs. Additionally, it was found that the DH market share primarily depends on the connection rate within the DH areas, a parameter often not published in the studies, as well as to a lower extent on the renovation rate of buildings. The expansion potential identified by the modelling in this thesis is in the upper range of the scenario outcomes in the literature. This work shows that future potential DH areas can more widespread and demand for DH could be higher than most studies assume, even if overall heat demand decreases.

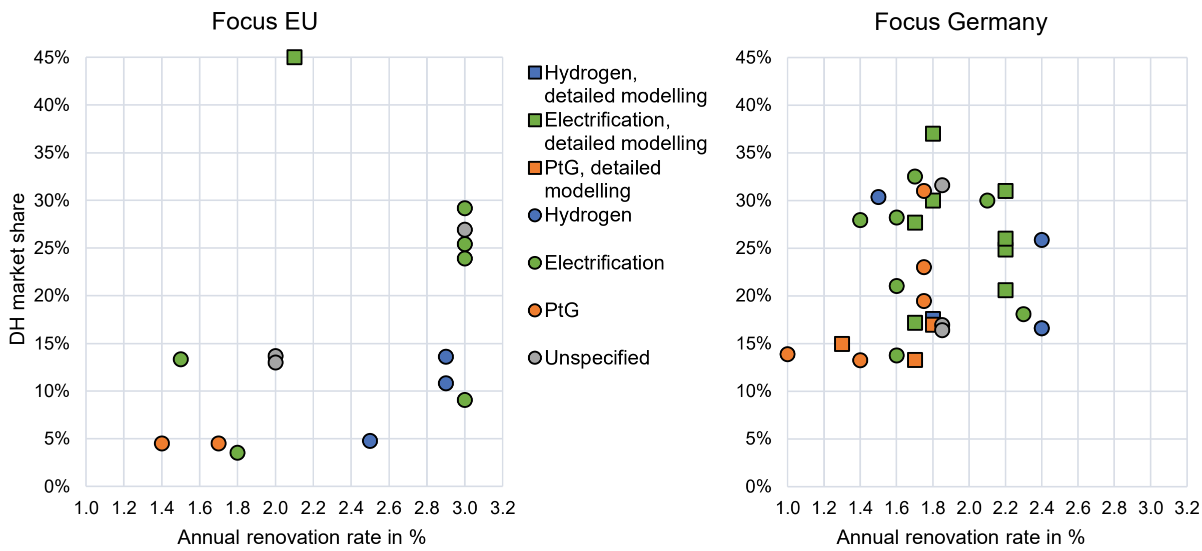

Figure 8.3: Scenario results of DH market shares in 2050 from different studies. Figure from Manz et al., 2022 [85]

The results of this thesis are not intended for direct use in regional and local planning, such as communal heat planning. Despite the high spatial resolution, the data sets were derived by statistical approaches and the quality is not sufficient for local planning and needs on-site verification and collection. Instead, the results are valuable to illustrate possible scenarios and quantify the future role of DH in the EU energy system, aiding national and EU policy makers in the identification of necessary policies. Additionally, the published data sets can be used by the scientific community and local stakeholders for coordinated planning to refine and further develop modelling approaches and transformation strategies.

The following recommendations for further research can be made. Emerging heating options, such as the so-called 5th generation district heating (i.e. cold networks combined with individual heat pumps for the building), should be explored. This alters the technical parameters for utilising renewable and excess heat sources, as well as the cost structure for the consumers. It also presents an opportunity for southern countries with warmer climates, where cooling could be provided in city centres by the same infrastructure. This significantly increases the efficiency compared to individual air conditioners, especially as average temperatures rise in the future. However, the economic advantages of this technology have not yet been proven on larger scale [236,351]. Additionally, the transport of available heat could be based on technologies other than traditional pipe infrastructure, such as phase-change materials [352]. Further research should also focus on integrated modelling of the demand and supply sectors with high spatial resolution to find the optimum in line with the EE1st-Principle while maintaining computational feasibility, e.g. as conducted for heating on local scale in Ref. [346]. This could help to partially overcome the limitations of the stepwise modelling approaches shown above. Using optimisation models can reveal cost-optimal pathways for demand and supply. Future studies should focus on understanding human behaviour in the transformation, exploring how individuals interact with and respond to future challenges, as demonstrated in the survey referenced in [353]. Investigating factors that influence acceptance and adaptability will be crucial for driving the transition.

Modelling is a tool to investigate scenarios and quantify potentials to achieve climate-neutrality. The technical and economic potential of DH identified in this thesis forms the basis for developing pathways and an adequate political framework in the EU. The significant potential for DH requires supportive policies exploit it and overcome barriers. Combining technical, economic and behavioural insights enables the creation of comprehensive strategies that ensure the successful implementation of DH and other sustainable energy solutions towards a climate-neutral future.

References

[1] M. Crippa, D. Guizzardi, F. Pagani, M. Banja, M. Muntean, Schaaf E., W. Becker, F. Monforti-Ferrario, R. Quadrelli, A. Risquez Martin, P. Taghavi-Moharamli, J. Köykkä, G. Grassi, S. Rossi, J. Brandao De Melo, D. Oom, A. Branco, J. San-Miguel, E. Vignati, GHG emissions of all world countries – 2023, Luxembourg, 2023.

[2] European Commission, 'Fit for 55': delivering the EU's 2030 Climate Target on the way to climate neutrality: Communication from the Commission to the European Parliament, the Council, the European economic and social committee and the committee of the regions. COM(2021) 550 final, 2021.

[3] European Commission, The European Green Deal: Communication from the Commission to the European Parliament, the European Council, the European Economic and Social Committee and the Committee of the Regions. COM(2019) 640 final, 2019.

[4] European Union, Regulation (EU) 2021/1119 of the European Parliament and of the Council of 30 June 2021 establishing the framework for achieving climate neutrality and amending Regulations (EC) No 401/2009 and (EU) 2018/1999 ('European Climate Law'). Official Journal of the European Union, Luxembourg, 2021.

[5] European Environment Agency, Decarbonising heating and cooling — a climate imperative: Briefing no. 27/2022, 2023.

[6] T. Fleiter, R. Elsland, M. Rehfeldt, J. Steinbach, U. Reiter, G. Catenazzi, M. Jakob, C. Rutten, R. Harmsen, F. Dittmand, P. Riviére, P. Stabat, Profile of heating and cooling demand in 2015. Deliverable 3.1 Heat Roadmap Europe - A low-carbon heating and cooling strategy, 2017.

[7] Öko-Institut, Fraunhofer ISI, TU Wien, e-think Energy Research, Halmstad University, Renewable Heating and Cooling Pathways – Towards full decarbonisation by 2050: ENER C1 2019-482 Final report, Luxembourg, 2023.

[8] Agora Energiewende, Transitioning to a climate-neutral EU buildings sector: Benchmarks for the success of the European Green Deal. Impulse, 2021.

[9] European Commission, District Heating and Cooling in the European Union: Overview of District Heating and Cooling Markets and Regulatory Frameworks under the Revised Renewable Energy Directive. Main report, Luxembourg, 2022.

[10] eurostat, Production of electricity and derived heat by type of fuel (nrg_bal_peh), 2023.

[11] European Union, Directive (EU) 2024/1275 of the European Parliament and of the Council of 24 April 2024 on the energy performance of buildings (recast). Official Journal of the European Union, Luxembourg, 2024.

[12] European Union, Directive (EU) 2023/2413 of the European Parliament and of the Council of 18 October 2023 amending Directive (EU) 2018/2001, Regulation (EU) 2018/1999 and Directive 98/70/EC as regards the promotion of energy from renewable sources, and repealing Council Directive (EU) 2015/652. Official Journal of the European Union, Luxembourg, 2023.

[13] International Energy Agency (IEA), Renewable Heat Policies: Delivering clean heat solutions for the energy transition, 2018.

[14] S. Braungardt, K. Hennenberg, I. Ganal, B. Köhler, V. Bürger, C. Winger, The role of biomass in the decarbonisation of the heating sector: Study on behalf of the European Climate Foundation, 2022.

[15] eurostat, Population on 1 January by broad age group, sex and other typologies (urt_pjanaggr3), 2024.

[16] B.V. Mathiesen, N. Bertelsen, N.C.A. Schneider, L.S. García, S. Paardekooper, J.Z. Thellufsen, S.R. Djørup, Towards a decarbonised heating and cooling sector in Europe: Unlocking the potential of energy efficiency and district energy, 2019.

[17] B. Möller, E. Wiechers, U. Persson, L. Grundahl, R.S. Lund, B.V. Mathiesen, Heat Roadmap Europe: Towards EU-Wide, local heat supply strategies, Energy 177 (2019) 554–564. https://doi.org/10.1016/j.energy.2019.04.098.

[18] U. Persson, E. Wiechers, B. Möller, S. Werner, Heat Roadmap Europe: Heat distribution costs, Energy 176 (2019) 604–622. https://doi.org/10.1016/j.energy.2019.03.189.

[19] U. Persson, District heating in future Europe: Modelling expansion potentials and mapping heat synergy regions. Zugl.: Göteborg, Univ., Diss., 2015, Chalmers Univ. of Technology, Göteborg, 2015.

[20] European Union, Directive (EU) 2023/1791 of the European Parliament and of the Council of 13 September 2023 on energy efficiency and amending Regulation (EU) 2023/955 (recast). Official Journal of the European Union, Luxembourg, 2023.

[21] H. Lund, S. Werner, R. Wiltshire, S. Svendsen, J.E. Thorsen, F. Hvelplund, B.V. Mathiesen, 4th Generation District Heating (4GDH), Energy 68 (2014) 1–11. https://doi.org/10.1016/j.energy.2014.02.089.

[22] International Renewable Energy Agency (IRENA), Renewable Energy in District Heating and Cooling, A sector roadmap for REmap, 2017.

[23] U. Persson, H. Averfalk, Accessible urban waste heat. Deliverable 1.4 ReUseHeat - Recovery of Urban Excess Heat, 2018.

[24] C. Bernath, G. Deac, F. Sensfuß, Influence of heat pumps on renewable electricity integration: Germany in a European context, Energy Strategy Reviews 26 (2019) 100389. https://doi.org/10.1016/j.esr.2019.100389.

[25] M. Gumhalter, The value of flexibility for large-scale heat pumps in district heating systems: A survey on technical constraints and economic opportunities. Diploma Thesis, 2019.

[26] M. Köfinger, R.R. Schmidt, D. Basciotti, O. Terreros, I. Baldvinsson, J. Mayrhofer, S. Moser, R. Tichler, H. Pauli, Simulation based evaluation of large scale waste heat utilization in urban district heating networks: Optimized integration and operation of a seasonal storage, Energy 159 (2018) 1161–1174. https://doi.org/10.1016/j.energy.2018.06.192.

[27] F. Ochs, A. Dahash, A. Tosatto, M. Bianchi Janetti, Techno-economic planning and construction of cost-effective large-scale hot water thermal energy storage for Renewable District heating systems, Renewable Energy 150 (2020) 1165–1177. https://doi.org/10.1016/j.renene.2019.11.017.

[28] H. Averfalk, S. Werner, Economic benefits of fourth generation district heating, Energy 193 (2020) 116727. https://doi.org/10.1016/j.energy.2019.116727.

[29] S. Boesten, W. Ivens, S.C. Dekker, H. Eijdems, 5th generation district heating and cooling systems as a solution for renewable urban thermal energy supply, Adv. Geosci. 49 (2019) 129–136. https://doi.org/10.5194/adgeo-49-129-2019.

[30] U. Persson, S. Werner, Heat distribution and the future competitiveness of district heating, Applied Energy 88 (2011) 568–576. https://doi.org/10.1016/j.apenergy.2010.09.020.

[31] Imperial College London, Sustainable biomass availability in the EU, to 2050: Ref: RED II Annex IX A/B, 2021.

[32] M. Wissner, Regulation of district-heating systems, Utilities Policy 31 (2014) 63–73. https://doi.org/10.1016/j.jup.2014.09.001.

[33] Agora Energiewende, Breaking free from fossil gas: A new path to a climate-neutral Europe, 2023.

[34] Deutsche Energie-Agentur (dena), dena-Leitstudie Aufbruch Klimaneutralität: Eine gesamtgesellschaftliche Aufgabe. Abschlussbericht, 2021.

[35] European Commission, EU Reference Scenario 2020: Energy, transport and GHG emissions - Trends to 2050, 2021.

[36] European Network of Transmission System Operators for Electricity (ENTSO-E), High-Level Report TYNDP 2022: July 2022 – version for public consultation, 2022.

[37] Fraunhofer ISI, consentec, TU Berlin, ifeu Institut, Langfristszenarien für die Transformation des Energiesystems in Deutschland 3: Treibhausgasneutrale Hauptszenarien - Modul Energieangebot, Karlsruhe, 2021.

[38] S. Paardekooper, R.S. Lund, B.V. Mathiesen, M. Chang, U.R. Petersen, L. Grundahl, A. David, J. Dahlbaek, J. Kapetanakis, H. Lund, N. Bertelsen, K. Hansen, D. Drysdale, U. Persson, Heat Roadmap Europe 4: Quantifying the Impact of Low-Carbon Heating and Cooling Roadmaps. Aalborg Universitetsforlag, 2018.

[39] D. Connolly, H. Lund, B.V. Mathiesen, S. Werner, B. Möller, U. Persson, T. Boermans, D. Trier, P.A. Østergaard, S. Nielsen, Heat Roadmap Europe, Energy Policy 65 (2014) 475–489. https://doi.org/10.1016/j.enpol.2013.10.035.

[40] H. Lund, J.Z. Thellufsen, P.A. Østergaard, P. Sorknæs, I.R. Skov, B.V. Mathiesen, EnergyPLAN – Advanced analysis of smart energy systems, Smart Energy 1 (2021) 100007. https://doi.org/10.1016/j.segy.2021.100007.

[41] M. Yuan, J.Z. Thellufsen, P. Sorknæs, H. Lund, Y. Liang, District heating in 100% renewable energy systems: Combining industrial excess heat and heat pumps, Energy Conversion and Management 244 (2021) 114527. https://doi.org/10.1016/j.enconman.2021.114527.

[42] D. Maya-Drysdale, H. Abid, A.D. Korberg, I.R. Skov, B.V. Mathiesen, L.S. Illeva, F.D. Nielsen, Energy Efficiency 2050 Roadmap for Europe: A cost-effective and energy-efficient strategy for decarbonising. Deliverable 6.3 sEEnergies - Quantification of Synergies between Energy Efficiency First Principle and Renewable Energy Systems, 2022.

[43] Europa-Universität Flensburg, Pan-European Thermal Atlas 4.3 (Peta 4.3): Heat Roadmap Europe - A low-carbon heating and cooling strategy for Europe, 2018, https://heatroadmap.eu/peta4, accessed 22 November 2018.

[44] Europa-Universität Flensburg, Halmstad University, Aalborg University, Pan-European Thermal Atlas 5.1 (Peta 5.1): sEEnergies - Quantification of synergies between Energy Efficiency first principle and renewable energy systems, 2021, https://www.arcgis.com/apps/webappviewer/index.html?id=8d51f3708ea54fb9b732ba0c94409133, accessed 19 August 2021.

[45] L. Sánchez-García, H. Averfalk, E. Möllerström, U. Persson, Understanding effective width for district heating, Energy 277 (2023) 127427. https://doi.org/10.1016/j.energy.2023.127427.

[46] L. Sánchez-García, Modelling District Heating Network Costs. Dissertation, Lund, 2023.

[47] T. Fleiter, M. Rehfeldt, A. Herbst, R. Elsland, A.-L. Klingler, P. Manz, S. Eidelloth, A methodology for bottom-up modelling of energy transitions in the industry sector: The FORECAST model, Energy Strategy Reviews 22 (2018) 237–254. https://doi.org/10.1016/j.esr.2018.09.005.

[48] HotMaps, Hotmaps Toolbox: The open source mapping and planning tool for heating and cooling, 2020, https://www.hotmaps.eu, accessed 19 August 2021.

[49] L. Kranzl, M. Hartner, A. Müller, G. Resch, S. Fritz, T. Fleiter, A. Herbst, M. Rehfeldt, P. Manz, A. Zubaryeva, J.G. Vilchez, Heating & Cooling outlook until 2050, EU-28: Report Hotmaps - Heating and Cooling Open Source Tool for Mapping and Planning of Energy Systems, 2018.

[50] HotMaps, Hotmaps Dispatch: Model description, 2020, https://tuw-eeg.github.io/hotmapsDispatch/Hotmaps%20Dispatch%20-%20Description.html, accessed 1 June 2024.

[51] T. Dröscher, A. Ladermann, C. Maurer, B. Tersteegen, S. Willemsen, A. Billerbeck, C. Kiefer, J. Winkler, C. Bernath, F. Sensfuß, L. Kranzl, A. Müller, P. Kotek, B. Tóth, Potentials and levels for the electrification of space heating in buildings: Final report, 2023.

[52] T. Mandel, L. Kranzl, E. Popovski, F. Sensfuß, A. Müller, W. Eichhammer, Investigating pathways to a net-zero emissions building sector in the European Union: what role for the energy efficiency first principle?, Energy Efficiency 16 (2023). https://doi.org/10.1007/s12053-023-10100-0.

[53] M. Hummel, A. Müller, S. Forthuber, L. Kranzl, B. Mayr, R. Haas, How cost-efficient is energy efficiency in buildings? A comparison of building shell efficiency and heating system change in the European building stock, Energy Efficiency 16 (2023). https://doi.org/10.1007/s12053-023-10097-6.

[54] M. Hartner, S. Forthuber, L. Kranzl, S. Fritz, A. Müller, C. Bernath, F. Sensfuß, H. Maranon-Ledesma, Issue paper on heating and cooling demand and supply in buildings and the role for RES market integration. Deliverable 5.2 SET-Nav - Navigating the Roadmap for clean, secure and efficient energy innovation, 2018.

[55] A. Müller, M. Hummel, L. Kranzl, M. Fallahnejad, R. Büchele, Open Source Data for Gross Floor Area and Heat Demand Density on the Hectare Level for EU 28, Energies 12 (2019) 4789. https://doi.org/10.3390/en12244789.

[56] M. Fallahnejad, L. Kranzl, M. Hummel, District heating distribution grid costs: a comparison of two approaches, IJSEPM 34 (2022) 79–90. https://doi.org/10.54337/ijsepm.7013.

[57] M. Fallahnejad, M. Hartner, L. Kranzl, S. Fritz, Impact of distribution and transmission investment costs of district heating systems on district heating potential, Energy Procedia 149 (2018) 141–150. https://doi.org/10.1016/j.egypro.2018.08.178.

[58] M. Fallahnejad, L. Kranzl, R. Haas, M. Hummel, A. Müller, L.S. García, U. Persson, District heating potential in the EU-27: Evaluating the impacts of heat demand reduction and market share growth, Applied Energy 353 (2024) 122154. https://doi.org/10.1016/j.apenergy.2023.122154.

[59] E. Popovski, M. Ragwitz, H. Brugger, Decarbonization of district heating and deep retrofits of buildings as competing or synergetic strategies for the implementation of the efficiency first principle, Smart Energy 10 (2023) 100096. https://doi.org/10.1016/j.segy.2023.100096.

[60] F. Wiese, R. Bramstoft, H. Koduvere, A. Pizarro Alonso, O. Balyk, J.G. Kirkerud, Å.G. Tveten, T.F. Bolkesjø, M. Münster, H. Ravn, Balmorel open source energy system model, Energy Strategy Reviews 20 (2018) 26–34. https://doi.org/10.1016/j.esr.2018.01.003.

[61] M.B. Siddique, P.S. Nielsen, M.B. Rosendal, I.G. Jensen, D. Keles, Impacts of earlier natural gas phase-out & heat-saving policies on district heating and the energy system, Energy Policy 174 (2023) 113441. https://doi.org/10.1016/j.enpol.2023.113441.

[62] Fraunhofer ISI, Enertile: Website, https://www.enertile.eu.

[63] C. Bernath, Auswirkungen der Sektorkopplung von Strom und Wärme durch Wärmenetze auf das europäische Stromerzeugungssystem: Eine modellbasierte Szenarioanalyse. Dissertation, Karlsruhe, 2023.

[64] C. Bernath, G. Deac, F. Sensfuß, Impact of sector coupling on the market value of renewable energies – A model-based scenario analysis, Applied Energy 281 (2021) 115985. https://doi.org/10.1016/j.apenergy.2020.115985.

[65] B. Lux, N. Schneck, B. Pfluger, W. Männer, F. Sensfuß, Potentials of direct air capture and storage in a greenhouse gas-neutral European energy system, Energy Strategy Reviews 45 (2023) 101012. https://doi.org/10.1016/j.esr.2022.101012.

[66] K. Franke, J.F. Garcia, C. Kleinschmitt, F. Sensfuß, Assessing worldwide future potentials of renewable electricity generation: Installable capacity, full load hours and costs, Renewable Energy 226 (2024) 120376. https://doi.org/10.1016/j.renene.2024.120376.

[67] B. Lux, G. Deac, C.P. Kiefer, C. Kleinschmitt, C. Bernath, K. Franke, B. Pfluger, S. Willemsen, F. Sensfuß, The role of hydrogen in a greenhouse gas-neutral energy supply system in Germany, Energy Conversion and Management 270 (2022) 116188. https://doi.org/10.1016/j.enconman.2022.116188.

[68] T. Brown, M. Victoria, L. Zeyen, F. Neumann, PyPSA-Eur-Sec: Documentation on the PyPSA-Eur Version 0.7.0 and Technology Data Version 0.5.0, 2024, https://pypsa-eur-sec.readthedocs.io/en/latest/supply_demand.html, accessed 15 June 2024.

[69] K. Keramidas, S. Tchung-Ming, A. Diaz Vazquez, M. Weitzel, T. Vandyck, J. Després, A. Schmitz, L. Rey Los Santos, K. Wójtowicz, B. Schade, B. Saveyn, A. Soria-Ramirez, Global Energy and Climate Outlook 2018: Sectoral mitigation options towards a low-emissions economy. Global context to the EU strategy for long-term greenhouse gas emissions reduction, Publications Office of the European Union, Luxembourg, 2018.

[70] P. Korkmaz, R. Cunha Montenegro, D. Schmid, M. Blesl, U. Fahl, On the Way to a Sustainable European Energy System: Setting Up an Integrated Assessment Toolbox with TIMES PanEU as the Key Component, Energies 13 (2020) 707. https://doi.org/10.3390/en13030707.

[71] European Commission, A Clean Planet for all. A European long-term strategic vision for a prosperous, modern, competitive and climate neutral economy: In-Depth analysis in support of the Commission Communication COM(2018) 773, 2018.

[72] International Energy Agency (IEA), World Energy Outlook 2023, 2023.

[73] L. Kranzl, S. Forthuber, M. Fallahnejad, R. Büchele, A. Müller, M. Hummel, T. Fleiter, T. Mandel, M. Bagheri, G. Deac, C. Bernath, J. Miosga, C. Kiefer, J. Fragoso, S. Braungardt, V. Bürger, D. Spasova, J. Viegand, R. Naeraa, ENER/C1/2018-494 - Renewable Space Heating under the Revised Renewable Energy Directive: Final report, Luxembourg, 2021.

[74] Cambridge Econometrics, Element Energy, Towards fossil-free energy in 2050, 2019.

[75] J. Gea-Bermúdez, I.G. Jensen, M. Münster, M. Koivisto, J.G. Kirkerud, Y. Chen, H. Ravn, The role of sector coupling in the green transition: A least-cost energy system development in Northern-central Europe towards 2050, Applied Energy 289 (2021) 116685. https://doi.org/10.1016/j.apenergy.2021.116685.

[76] G. Bianchi, G.P. Panayiotou, L. Aresti, S.A. Kalogirou, G.A. Florides, K. Tsamos, S.A. Tassou, P. Christodoulides, Estimating the waste heat recovery in the European Union Industry, Energ. Ecol. Environ. 4 (2019) 211–221. https://doi.org/10.1007/s40974-019-00132-7.

[77] S. Brückner, L. Miró, L.F. Cabeza, M. Pehnt, E. Laevemann, Methods to estimate the industrial waste heat potential of regions – A categorization and literature review, Renewable and Sustainable Energy Reviews 38 (2014) 164–171. https://doi.org/10.1016/j.rser.2014.04.078.

[78] F. Bühler, S. Petrović, K. Karlsson, B. Elmegaard, Industrial excess heat for district heating in Denmark, Applied Energy 205 (2017) 991–1001. https://doi.org/10.1016/j.apenergy.2017.08.032.

[79] C. Forman, I.K. Muritala, R. Pardemann, B. Meyer, Estimating the global waste heat potential, Renewable and Sustainable Energy Reviews 57 (2016) 1568–1579. https://doi.org/10.1016/j.rser.2015.12.192.

[80] Industrial Thermal Energy Recovery conversion and Management (I-TheRM), D 2.1 Literature review of energy use and potential for heat recovery in the EU28 Report (2016).

[81] R.C. McKenna, J.B. Norman, Spatial modelling of industrial heat loads and recovery potentials in the UK, Energy Policy 38 (2010) 5878–5891. https://doi.org/10.1016/j.enpol.2010.05.042.

[82] M. Papapetrou, G. Kosmadakis, A. Cipollina, U. La Commare, G. Micale, Industrial waste heat: Estimation of the technically available resource in the EU per industrial sector, temperature level and country, Applied Thermal Engineering 138 (2018) 207–216. https://doi.org/10.1016/j.applthermaleng.2018.04.043.

[83] U. Persson, B. Möller, S. Werner, Heat Roadmap Europe: Identifying strategic heat synergy regions, Energy Policy 74 (2014) 663–681. https://doi.org/10.1016/j.enpol.2014.07.015.

[84] E. Svensson, M. Morandin, S. Harvey, Characterization and visualization of industrial excess heat for different levels of on-site process heat recovery, Int J Energy Res 43 (2019) 7988–8003. https://doi.org/10.1002/er.4787.

[85] P. Manz, T. Fleiter, S. Alibas, A. Billerbeck, Finding an optimal district heating market share in 2050 for EU-27: Comparison of modelling approaches, eceee Summer Study Proceedings (2022) 177–186.

[86] H. Lund, N. Duic, P.A. Østergaard, B.V. Mathiesen, Future district heating systems and technologies: On the role of smart energy systems and 4th generation district heating, Energy 165 (2018) 614–619. https://doi.org/10.1016/j.energy.2018.09.115.

[87] M.S. Triebs, E. Papadis, H. Cramer, G. Tsatsaronis, Landscape of district heating systems in Germany – Status quo and categorization, Energy Conversion and Management: X 9 (2021) 100068. https://doi.org/10.1016/j.ecmx.2020.100068.

[88] J.M. Weinand, R. McKenna, K. Mainzer, Spatial high-resolution socio-energetic data for municipal energy system analyses, Scientific data 6 (2019) 243. https://doi.org/10.1038/s41597-019-0233-0.

[89] Europa-Universität Flensburg, Halmstad University, Aalborg University, Pan-European Thermal Atlas 5.2 (Peta 5.2): sEEnergies - Quantification of synergies between Energy Efficiency first principle and renewable energy systems, 2022, https://euf.maps.arcgis.com/apps/webappviewer/index.html?id=8d51f3708ea54fb9b732ba0c94409133, accessed 30 November 2022.

[90] P. Manz, K. Kermeli, U. Persson, M. Neuwirth, T. Fleiter, W. Crijns-Graus, Decarbonizing District Heating in EU-27 + UK: How Much Excess Heat Is Available from Industrial Sites?, Sustainability 13 (2021) 1439. https://doi.org/10.3390/su13031439.

[91] J. Pelda, S. Holler, U. Persson, District heating atlas - Analysis of the German district heating sector, Energy 233 (2021) 121018. https://doi.org/10.1016/j.energy.2021.121018.

[92] Dekade-F-Waerme, Der Fernwärmeatlas: Dekarbonisierung der Fernwärmeversorgung durch die Sektorenkopplung von Strom und Wärme und die Einbindung erneuerbarer Energien, HAWK University of Applied Sciences and Art Hildesheim/Holzminden/Göttingen, Germany, 2022.

[93] U. Persson, B. Möller, L. Sánchez-García, E. Wiechers, District heating investment costs and allocation of local resources for EU28 in 2030 and 2050. Deliverable 4.5 sEEnergies - Quantification of Synergies between Energy Efficiency First Principle and Renewable Energy Systems, 2021.

[94] U. Persson, B. Möller, E. Wiechers, Methodologies and assumptions used in the mapping. Deliverable 2.3 Heat Roadmap Europe - A low-carbon heating and cooling strategy, 2017.

[95] M. Leurent, Analysis of the district heating potential in French regions using a geographic information system, Applied Energy 252 (2019) 113460. https://doi.org/10.1016/j.apenergy.2019.113460.

[96] I. Dochev, I. Peters, H. Seller, G.K. Schuchardt, Analysing district heating potential with linear heat density. A case study from Hamburg, Energy Procedia 149 (2018) 410–419. https://doi.org/10.1016/j.egypro.2018.08.205.

[97] S. Blömer, C. Götz, M. Pehnt, D. Hering, S. Ochse, S. Hespeler, S. Richter, P. Thomassen, G. Grytsch, C. Zopff, S. Jäger, B. Huber, EnEff:Wärme - netzgebundene Nutzung industrieller Abwärme (NENIA): Kombinierte räumlich-zeitliche Modellierung von Wärmebedarf und Abwärmeangebot in Deutschland. Schlussbericht im Auftrag des Bundesministeriums für Wirtschaft und Energie, 2019.

[98] zensus 2011, Ergebnisse des Zensus 2011 zum Download - erweitert: Gitterzellenbasierte Ergebnisse. Wohnungen im 100 Meter-Gitter, 2017, https://www.zensus2011.de/DE/Home/Aktuelles/DemografischeGrunddaten.html, accessed 25 March 2024.

[99] Kreditanstalt für Wiederaufbau (KfW), Förderreport KfW Bankengruppe 2020: Stichtag 31.Dezember 2020, 2021, https://www.kfw.de/Presse-Newsroom/Pressematerial/F%C3%B6rderreport/KfW-F%C3%B6rderreport_2020.pdf, accessed 15 July 2021.

[100] Kreditanstalt für Wiederaufbau (KfW), Förderreport KfW Bankengruppe 2019: Stichtag 31.Dezember 2019, 2020, https://www.kfw.de/Presse-Newsroom/Pressematerial/F%C3%B6rderreport/KfW-F%C3%B6rderreport_2019.pdf, accessed 15 July 2021.

[101] Kreditanstalt für Wiederaufbau (KfW), Förderreport KfW Bankengruppe 2018: Stichtag 31.Dezember 2018, 2019, https://www.kfw.de/Presse-Newsroom/Pressematerial/F%C3%B6rderreport/KfW-F%C3%B6rderreport_2018.pdf, accessed 15 July 2021.

[102] Kreditanstalt für Wiederaufbau (KfW), Förderreport KfW Bankengruppe 2017: Stichtag 31.Dezember 2017, 2018, https://www.kfw.de/Presse-Newsroom/Pressematerial/F%C3%B6rderreport/KfW-F%C3%B6rderreport_2017.pdf, accessed 15 July 2021.

[103] Kreditanstalt für Wiederaufbau (KfW), Förderreport KfW Bankengruppe 2016: Stichtag 31.Dezember 2016, 2017, https://www.kfw.de/Presse-Newsroom/Pressematerial/F%C3%B6rderreport/KfW-F%C3%B6rderreport_2016.pdf, accessed 15 July 2021.

[104] Kreditanstalt für Wiederaufbau (KfW), Förderreport KfW Bankengruppe 2015: Stichtag 31.Dezember 2015, 2016, https://www.kfw.de/Presse-Newsroom/Pressematerial/F%C3%B6rderreport/KfW-F%C3%B6rderreport_2015.pdf, accessed 15 July 2021.

[105] R. Elsland, T. Boßmann, I. Peksen, M. Wietschel, Auswirkungen von Nutzerverhalten und Klimawandel auf den Heizwärmebedarf im europäischen Haushaltssektor bis 2050, 8. Internationale Energiewirtschaftstagung (IEWT) (2013).

[106] T. Fleiter, R. Elsland, A. Herbst, P. Manz, E. Popovski, M. Rehfeldt, U. Reiter, G. Catenazzi, M. Jakob, R. Harmsen, C. Rutten, F. Dittmann, P. Riviére, P. Stabat, Baseline scenario of the heating and cooling demand in buildings and industry in the 14 MSs until 2050. Deliverable 3.3 and 3.4 Heat Roadmap Europe - A low carbon heating and cooling strategy, 2017.

[107] R. Elsland, Long-term Energy Demand in the German Residential Sector: Development of an Integrated Modelling Concept to Capture Technological Myopia. Dissertation, Karlsruhe, 2015.

[108] L. Greif, Modelling of district heating potentials in Germany. Master's Thesis, Karlsruhe, 2021.

[109] QGIS Documentation, PyQGIS Developer Cookbook: v.3.22, 2022, https://docs.qgis.org/3.22/en/docs/pyqgis_developer_cookbook/index.html, accessed 18 August 2022.

[110] H. Lund, P.A. Østergaard, T.B. Nielsen, S. Werner, J.E. Thorsen, O. Gudmundsson, A. Arabkoohsar, B.V. Mathiesen, Perspectives on fourth and fifth generation district heating, Energy 227 (2021) 120520. https://doi.org/10.1016/j.energy.2021.120520.

[111] D.-J. van de Ven, S. Mittal, B. Boitier, A. Sorman, E. Galende, A. Nikas, Report on the reference and policy scenario modelling results. Deliverable 7.6 Paris Reinforce - Delivering on the Paris Agreement: A demand-driven, integrated assessment modelling approach, 2022.

[112] Stadtwerke Karlsruhe, Fernwärme Online-Netzplan: Geoportal Karlsruhe: Stadtplan: Fernwärmeleitungsnetz, 2021, https://geoportal.karlsruhe.de/stadtplan/index.html?webmap=616597c654ea41d19f4002c5e8af1897, accessed 17 August 2023.

[113] Arbeitsgemeinschaft Energiebilanzen (AGEB), Energiebilanz der Bundesrepublik Deutschland 2014, https://ag-energiebilanzen.de/daten-und-fakten/bilanzen-1990-bis-2030, accessed 7 October 2024.

[114] Arbeitsgemeinschaft Energiebilanzen (AGEB), Anwendungsbilanzen zur Energiebilanz Deutschland: Endenergieverbrauch nach Energieträgern und Anwendungszwecken, https://ag-energiebilanzen.de/wp-content/uploads/2023/01/AGEB_21p2_V3_20221222.pdf, accessed 8 October 2023.

[115] eurostat, Population and housing censuses: Census rounds 2021 and 2011, 2021, https://ec.europa.eu/eurostat/web/population-demography/population-housing-censuses, accessed 14 August 2023.

[116] T. Mandel, E. Worrell, Ş. Alibaş, Balancing heat saving and supply in local energy planning: Insights from 1970-1989 buildings in three European countries, Smart Energy 12 (2023) 100121. https://doi.org/10.1016/j.segy.2023.100121.

[117] H. Lund, N. Duic, P.A. Østergaard, B.V. Mathiesen, Smart energy systems and 4th generation district heating, Energy 110 (2016) 1–4. https://doi.org/10.1016/j.energy.2016.07.105.

[118] eurostat, Complete energy balances (nrg_bal_c), 2023.

[119] M. Rehfeldt, T. Fleiter, F. Toro, A bottom-up estimation of the heating and cooling demand in European industry, Energy Efficiency 11 (2017) 1057–1082. https://doi.org/10.1007/s12053-017-9571-y.

[120] European Commission, Energy prices and costs in Europe: Report from the Commission to the European Parliament, the Council, the European Economic and Social Committee and the Committee of Regions. COM (2019) I final, Brussels, 2019.

[121] W. Eichhammer, R. Walz, Industrial energy efficiency and competitiveness. Development policy, statistics and research branch working paper 05/2011, 2011.

[122] A. Aydemir, C. Rohde, What about heat integration? Quantifying energy saving potentials for Germany, eceee Summer Study Proceedings (2018) 197–205.

[123] European Commission, An EU Strategy on Heating and Cooling: Communication from the Commission to the European Parliament, the Council, the European Economic and Social Committee and the Committee of the Regions, Brussels, 2016.

[124] Odyssee-Mure, Odyssee database, 2023, www.odyssee-mure.eu, accessed 9 January 2023.

[125] A. Colmenar-Santos, D. Borge-Díez, E. Rosales-Asensio, District Heating and Cooling Networks in the European Union, Springer International Publishing, Cham, 2017.

[126] U. Persson, S. Werner, District heating in sequential energy supply, Applied Energy 95 (2012) 123–131. https://doi.org/10.1016/j.apenergy.2012.02.021.

[127] S. Werner, International review of district heating and cooling, Energy 137 (2017) 617–631. https://doi.org/10.1016/j.energy.2017.04.045.

[128] S. Nielsen, B. Möller, GIS based analysis of future district heating potential in Denmark, Energy 57 (2013) 458–468. https://doi.org/10.1016/j.energy.2013.05.041.

[129] Euroheat & Power, Country by Country District Heating and Cooling, 2019, https://www.euroheat.org/knowledge-hub/country-profiles/, accessed 1 September 2020.

[130] European Commission, EU Reference Scenario 2016: Energy, transport and GHG emissions - Trends to 2050, 2016.

[131] International Energy Agency (IEA), World Energy Outlook 2019, IEA Publications, 2019.

[132] S. Pezzutto, S. Zambotti, S. Croce, P. Zambelli, G. Garegnani, C. Scaramuzzino, R.P. Pascuas, F. Haas, D. Exner, E. Lucchi, N. Della Valle, A. Zubaryeva, A. Müller, M. Hartner, T. Fleiter, A.-L. Klingler, M. Kühnbach, P. Manz, S. Marwitz, M. Rehfeldt, J. Steinbach, E. Popovski, Open Data Set for the EU28. Deliverable 2.3 WP 2 Report Hotmaps - Heating and Cooling Open Source Tool for Mapping and Planning of Energy Systems, 2019.

[133] L. Miró, S. Brückner, L.F. Cabeza, Mapping and discussing Industrial Waste Heat (IWH) potentials for different countries, Renewable and Sustainable Energy Reviews 51 (2015) 847–855. https://doi.org/10.1016/j.rser.2015.06.035.

[134] BCS Inc, Waste Heat Recovery: Technology and Opportunities in U.S. Industry, 2008.

[135] G.P. Hammond, J.B. Norman, Heat recovery opportunities in UK industry, Applied Energy 116 (2014) 387–397. https://doi.org/10.1016/j.apenergy.2013.11.008.

[136] European Environment Agency, European Union Emissions Trading System (EU ETS) data from EUTL (EU Transaction Log), 2020.

[137] P. Manz, T. Fleiter, A. Aydemir, Developing a georeferenced database of energy-intensive industry plants for estimation of excess heat potentials, eceee Summer Study Proceedings (2018) 239–247.

[138] A. Aydemir, T. Fleiter, D. Schilling, M. Fallahnejad, Industrial excess heat and district heating: potentials and costs for the EU-28 on the basis of network analysis, eceee Summer Study Proceedings (2020) 285–294.

[139] F. Bühler, T.-V. Nguyen, B. Elmegaard, Energy and exergy analyses of the Danish industry sector, Applied Energy 184 (2016) 1447–1459. https://doi.org/10.1016/j.apenergy.2016.02.072.

[140] F. Bühler, S. Petrović, F.M. Holm, K. Karlsson, B. Elmegaard, Spatiotemporal and economic analysis of industrial excess heat as a resource for district heating, Energy 151 (2018) 715–728. https://doi.org/10.1016/j.energy.2018.03.059.

[141] S. Brückner, Industrielle Abwärme: Bestimmung von gesichertem Aufkommen und technischer bzw. wirtschaftlicher Nutzbarkeit. Dissertation, München, 2016.

[142] European Environment Agency, The European Pollutant Release and Transfer Register (EPRTR), Member States reporting under Article 7 of Regulation (EC) No 166/2006, 2020.

[143] S. Brückner, R. Arbter, M. Pehnt, E. Laevemann, Industrial waste heat potential in Germany—a bottom-up analysis, Energy Efficiency 10 (2017) 513–525. https://doi.org/10.1007/s12053-016-9463-6.

[144] M. Pehnt, J. Bödeker, M. Arens, E. Jochem, F. Idrissova, Die Nutzung industrieller Abwärme: technisch-wirtschaftliche Potenziale und energiepolitische Umsetzung. Wissenschaftliche Begleitforschung zu übergreifenden technischen, ökologischen, ökonomischen und strategischen Aspekten des nationalen Teils der Klimaschutzinitiative, 2010.

[145] Energetics, E3M, Energy Use, Loss and Opportunities Analysis: U.S. Manufacturing & Mining. Prepared for the U.S. Department of Energy - Energy Efficiency and Renewable Energy Industrial Technologies Program, 2004.

[146] G. Sollesnes, H.E. Helgerud, Utnyttelse av spillvarme fra norsk industri: En potensialstudie, 2009.

[147] G.P. Panayiotou, G. Bianchi, G. Georgiou, L. Aresti, M. Argyrou, R. Agathokleous, K.M. Tsamos, S.A. Tassou, G. Florides, S. Kalogirou, P. Christodoulides, Preliminary assessment of waste heat potential in major European industries, Energy Procedia 123 (2017) 335–345. https://doi.org/10.1016/j.egypro.2017.07.263.

[148] L. Miró, R. McKenna, T. Jäger, L.F. Cabeza, Estimating the industrial waste heat recovery potential based on CO_2 emissions in the European non-metallic mineral industry, Energy Efficiency 11 (2018) 427–443. https://doi.org/10.1007/s12053-017-9575-7.

[149] A. Aydemir, M. Fritz, Estimating excess heat from exhaust gases: why corrosion matters, Energ. Ecol. Environ. 5 (2020) 330–343. https://doi.org/10.1007/s40974-020-00171-5.

[150] T. Fleiter, P. Manz, M. Neuwirth, F. Mildner, U. Persson, K. Kermeli, W. Crijns-Graus, C. Rutten, D5.1 Industry Dataset: sEEnergies Open Data, 2020, https://s-eenergies-open-data-euf.hub.arcgis.com/, accessed 10 August 2020.

[151] T. Fleiter, P. Manz, M. Neuwirth, F. Mildner, U. Persson, K. Kermeli, W. Crijns-Graus, C. Rutten, sEEnergies D5.1 Dataset Web-App, 2020, https://tinyurl.com/sEEnergies-D5-1, accessed 24 February 2020.

[152] T. Fleiter, P. Manz, M. Neuwirth, F. Mildner, U. Persson, K. Kermeli, W. Crijns-Graus, C. Rutten, Documentation on excess heat potentials of industrial sites including open data file with selected potentials. Deliverable 5.1 sEEnergies - Quantification of synergies between Energy Efficiency first principle and renewable energy systems, 2020.

[153] International Energy Agency (IEA), Tracking Industrial Energy Efficiency and CO_2 Emissions. In support of the G8 Plan of Action, 2007.

[154] European Commission, Best available techniques (BAT) Reference Document for Iron and Steel production: Industrial emissions directive 2010/75/EU (integrated pollution prevention and control), 2013.

[155] H.S. Ray, B.P. Singh, S. Bhattacharjee, V.N. Misra, Energy in minerals and metallurgical industries, Allied Publishers, India, 2005.

[156] European Commission, Best Available Techniques (BAT) Reference Document for the Production of Cement, Lime and Magnesium Oxide: Industrial Emissions Directive 2010/75/EU (Integrated Pollution Prevention and Control), 2013.

[157] European Commission, Best available techniques (BAT) Reference document for the Manufacture of Glass: Industrial Emissions Directive 2010/75/EU (Integrated Pollution Prevention and Control), 2013.

[158] G. Hough (Ed.), Chemical Recovery in the alkaline pulping processes, TAPPI Pr, Atlanta, Ga., 1985.

[159] P. Lundqvist, Mass and energy balances over the lime kiln in a kraft pulp mill. Master's Thesis, Uppsala, 2009.

[160] T. Hendricks, W.T. Choate, Engineering Scoping Study of Thermoelectric Generator Systems for Industrial Waste Heat Recovery, 2006.

[161] European Commission, Energy efficiency and GHG emissions: Prospective Scenarios for the Chemical and Petrochemical Industry, 2017.

[162] United States Department of Energy, Steam System Opportunity Assessment for the Pulp and Paper, Chemical Manufacturing, and Petroleum Refining Industries: Main Report. Office of Energy Efficiency and Renewable Energy, 2002.

[163] J. Jörissen, T. Turek, R. Weber, Chlorherstellung mit Sauerstoffverzehrkathoden. Energieeinsparung bei der Elektrolyse, Chemie in unserer Zeit 45 (2011) 172–183. https://doi.org/10.1002/ciuz.201100545.

[164] Halmstad University, Halmstad University District Heating and Cooling Database_version 5 (2016 update by date 2019-09-30), 2019.

[165] E. Wiechers, B. Möller, U. Persson, D5.2 Urban Area Dataset: sEEnergies Open Data, 2020, https://s-eenergies-open-data-euf.hub.arcgis.com/, accessed 11 August 2020.

[166] K.C. Kavvadias, S. Quoilin, Exploiting waste heat potential by long distance heat transmission: Design considerations and techno-economic assessment, Applied Energy 216 (2018) 452–465. https://doi.org/10.1016/j.apenergy.2018.02.080.

[167] M. Pehnt, M. Arens, E. Jochem, J. Bödeker, F. Idrissova, Industrial waste heat - tapping into a neglected efficiency potential, eceee Summer Study Proceedings (2011) 691-700.

[168] eurostat, Statistics on the production of manufactured goods: Total production by PRODCOM list (NACE Rev. 2) - annual data (DS-066342), 2020.

[169] D. Brough, H. Jouhara, The aluminium industry: A review on state-of-the-art technologies, environmental impacts and possibilities for waste heat recovery, International Journal of Thermofluids 1-2 (2020) 100007. https://doi.org/10.1016/j.ijft.2019.100007.

[170] K. Kermeli, E. Worrel, W. Graus, M. Corsten, Energy Efficiency and Cost Saving Opportunities for Ammonia and Nitrogenous Fertilizer Production: An ENERGY STAR® Guide for Energy and Plant Managers, 2017.

[171] European Council, European Council meeting (12 December 2019) - Conclusions. EUCO 29/19, 2019.

[172] European Parliament, The European Green Deal: European Parliament resolution of 15 January 2020 on the European Green Deal (2019/2956 (RSP)). P9TA(2020)0005, 2020.

[173] European Environment Agency, EU's 2020 GHG inventory submission under the UNFCCC: Data Viewer, 2022, https://www.eea.europa.eu/data-and-maps/data/data-viewers/greenhouse-gases-viewer, accessed 28 November 2022.

[174] M. Rehfeldt, Fuel Switching as Contribution to the Decarbonisation of the Industry Sector: Integration in a Bottom-up Energy System Model. Dissertation, Utrecht, 2020.

[175] T. Fleiter, A. Herbst, M. Rehfeldt, M. Arens, Industrial Innovation: Pathways to deep decarbonisation of Industry: Part 2: Scenario analysis and pathways to deep decarbonisation. A report submitted by ICF Consulting Services Limited and Fraunhofer ISI to the European Commission, DG Climate Action, 2019.

[176] T. Wyns, G. Khandekar, I. Robson, A Bridge Towards a Carbon Neutral Europe: Industrial Value Chain. Europe's Energy Intensive Industries contribution to the EU Strategy for long-term EU greenhouse gas emission reductions, Institute for European Studies (IES), 2018.

[177] Ramboll, Fraunhofer ISI, Quantification methodology for, and analysis of, the decarbonisation benefits of sectoral circular economy actions: Final report for the European Environmental Agency, 2020.

[178] I. Bonilla-Campos, N. Nieto, L. Del Portillo-Valdes, B. Egilegor, J. Manzanedo, H. Gaztañaga, Energy efficiency assessment: Process modelling and waste heat recovery analysis, Energy Conversion and Management 196 (2019) 1180–1192. https://doi.org/10.1016/j.enconman.2019.06.074.

[179] J. Haraldsson, M.T. Johansson, Barriers to and Drivers for Improved Energy Efficiency in the Swedish Aluminium Industry and Aluminium Casting Foundries, Sustainability 11 (2019) 2043. https://doi.org/10.3390/su11072043.

[180] M.J.S. Zuberi, M.K. Patel, Cost-effectiveness analysis of energy efficiency measures in the Swiss chemical and pharmaceutical industry, Int J Energy Res 43 (2019) 313–336. https://doi.org/10.1002/er.4267.

[181] A. Levesque, R.C. Pietzcker, L. Baumstark, G. Luderer, Deep decarbonisation of buildings energy services through demand and supply transformations in a 1.5°C scenario, Environ. Res. Lett. 16 (2021) 54071. https://doi.org/10.1088/1748-9326/abdf07.

[182] European Commission, Proposal for a Directive of the European Parliament and of the Council on the energy performance of buildings (recast). COM(2021) 802 final 2021/0426 (COD), 2021.

[183] European Union, Directive (EU) 2018/844 of the European Parliament and of the Council of 30 May 2018 amending Directive 2010/31/EU on the energy performance of buildings and Directive 2012/27/EU on energy efficiency (revised in 2023). Official Journal of the European Union, Luxembourg, 2018.

[184] eurostat, Production of electricity and derived heat by type of fuel (nrg_bal_peh), 2022.

[185] A. Dénarié, F. Fattori, G. Spirito, S. Macchi, V.F. Cirillo, M. Motta, U. Persson, Assessment of waste and renewable heat recovery in DH through GIS mapping: The national potential in Italy, Smart Energy 1 (2021) 100008. https://doi.org/10.1016/j.segy.2021.100008.

[186] I. Pakere, A. Gravelsins, D. Lauka, D. Blumberga, Will there be the waste heat and boiler house competition in Latvia? Assessment of industrial waste heat, Smart Energy 3 (2021) 100023. https://doi.org/10.1016/j.segy.2021.100023.

[187] J. Knies, A spatial approach for future-oriented heat planning in urban areas, International Journal of Sustainable Energy Planning and Management (2018) 3–30. https://doi.org/10.5278/ijsepm.2018.16.2.

[188] T. Novosel, T. Pukšec, N. Duić, J. Domac, Heat demand mapping and district heating assessment in data-pour areas, Renewable and Sustainable Energy Reviews 131 (2020) 109987. https://doi.org/10.1016/j.rser.2020.109987.

[189] J. Chambers, K. Narula, M. Sulzer, M.K. Patel, Mapping district heating potential under evolving thermal demand scenarios and technologies: A case study for Switzerland, Energy 176 (2019) 682–692. https://doi.org/10.1016/j.energy.2019.04.044.

[190] G. Spirito, A. Dénarié, F. Fattori, M. Motta, S. Macchi, U. Persson, Potential Diffusion of Renewables-Based DH Assessment through Clustering and Mapping: A Case Study in Milano, Energies 14 (2021) 2627. https://doi.org/10.3390/en14092627.

[191] B. Möller, E. Wiechers, L. Sánchez-García, U. Persson, Spatial models and spatial analytics results. Deliverable 5.7 sEEnergies - Quantification of Synergies between Energy Efficiency First Principle and Renewable Energy Systems, 2022.

[192] R. Geyer, J. Krail, B. Leitner, R.-R. Schmidt, P. Leoni, Energy-economic assessment of reduced district heating system temperatures, Smart Energy 2 (2021) 100011. https://doi.org/10.1016/j.segy.2021.100011.

[193] Y. Chan, L. Petithuguenin, T. Fleiter, A. Herbst, M. Arens, P. Stevenson, Industrial Innovation: Pathways to deep decarbonisation of Industry: Part 1: Technology Analysis. A report submitted by ICF Consulting Services Limited and Fraunhofer ISI to the European Commission, DG Climate Action, 2019.

[194] M. Neuwirth, T. Fleiter, P. Manz, R. Hofmann, The future potential hydrogen demand in energy-intensive industries - a site-specific approach applied to Germany, Energy Conversion and Management 252 (2022) 115052. https://doi.org/10.1016/j.enconman.2021.115052.

[195] A. Bhaskar, M. Assadi, H. Nikpey Somehsaraei, Decarbonization of the Iron and Steel Industry with Direct Reduction of Iron Ore with Green Hydrogen, Energies 13 (2020) 758. https://doi.org/10.3390/en13030758.

[196] R. Stormont, Electric Melting And Boosting for Glass Quality Improvement, Glass Woldwide 2010-09 (2010) 1–4.

[197] R. Ireson, A. Fuller, J. Woods, R. Simon, G. Andrews, P. Bingham, S. Hakes, M. Davies, Alternative Fuel Switching Technologies for the Glass Sector: Final Report. BEIS Industrial Fuel Switching Phase 2, 2019.

[198] M. Antunes, R.L. Santos, J. Pereira, P. Rocha, R.B. Horta, R. Colaço, Alternative Clinker Technologies for Reducing Carbon Emissions in Cement Industry: A Critical Review, Materials (Basel, Switzerland) 15 (2021). https://doi.org/10.3390/ma15010209.

[199] C. Smith, A.K. Hill, L. Torrente-Murciano, Current and future role of Haber–Bosch ammonia in a carbon-free energy landscape, Energy Environ. Sci. 13 (2020) 331–344. https://doi.org/10.1039/C9EE02873K.

[200] N. Thonemann, S. Stießel, D. Maga, M. Hiebel, B. Dresen, B. Hunstock, G. Deerberg, E. Weidner, Standortplanung für die Herstellung CO_2-basierter Chemikalien am Beispiel der Olefinproduktion, Chemie Ingenieur Technik 91 (2019) 1238–1250. https://doi.org/10.1002/cite.201800147.

[201] M. Fritz, A. Aydemir, The energy of exergy – analysis of different olefin production routes, eceee Summer Study Proceedings (2020) 49-57.

[202] M. Arens, E. Worrell, W. Eichhammer, Drivers and barriers to the diffusion of energy-efficient technologies—a plant-level analysis of the German steel industry, Energy Efficiency 10 (2017) 441–457. https://doi.org/10.1007/s12053-016-9465-4.

[203] M. Arens, E. Worrell, W. Eichhammer, A. Hasanbeigi, Q. Zhang, Pathways to a low-carbon iron and steel industry in the medium-term – the case of Germany, Journal of Cleaner Production 163 (2017) 84–98. https://doi.org/10.1016/j.jclepro.2015.12.097.

[204] K. Rechberger, A. Spanlang, A. Sasiain Conde, H. Wolfmeir, C. Harris, Green Hydrogen-Based Direct Reduction for Low-Carbon Steelmaking, steel research int. 91 (2020) 2000110. https://doi.org/10.1002/srin.202000110.

[205] A. Toktarova, I. Karlsson, J. Rootzén, L. Göransson, M. Odenberger, F. Johnsson, Pathways for Low-Carbon Transition of the Steel Industry—A Swedish Case Study, Energies 13 (2020) 3840. https://doi.org/10.3390/en13153840.

[206] V. Vogl, M. Åhman, L.J. Nilsson, Rethinking steelmaking: Zero-emissions and flexibility with hydrogen direct reduction. Presentation eceee Industrial Summer Study Proceedings, Berlin, 2018.

[207] HYBRIT, Fossil free steel, 2020, https://www.hybritdevelopment.se/en/, accessed 23 February 2021.

[208] Dillinger, Sustainable steel production at the Saar: Press release, 2019, https://www.dillinger.de/d/en/news/press-releases/sustainable-steel-production-at-the-saar-88575.shtml, accessed 24 February 2021.

[209] Tenova, First Hydrogen based ENERGIRON DRI Plant for Tenova in China, 2020, https://www.tenova.com/news/press-media/press-releases/detail/first-hydrogen-based-energiron-dri-plant-for-tenova-in-china/, accessed 1 March 2021.

[210] Thyssenkrupp-Steel, Climate strategy of thyssenkrupp Steel, 2020, https://www.thyssenkrupp-steel.com/en/company/sustainability/climate-strategy/, accessed 26 February 2021.

[211] SALCOS, Salzgitter Low CO_2 Steel Making, 2020, https://salcos.salzgitter-ag.com/en/index.html?no_cache=1, accessed 26 February 2021.

[212] H2 Green Steel, Introducing H2 Green Steel, 2021, https://www.h2greensteel.com/green-steel, accessed 1 March 2021.

[213] ArcerlorMittal, Hydrogen-based steelmaking to begin in Hamburg, 2020, https://corporate.arcelormittal.com/media/case-studies/hydrogen-based-steelmaking-to-begin-in-hamburg, accessed 26 February 2021.

[214] F. Patisson, O. Mirgaux, Hydrogen Ironmaking: How It Works, Metals 10 (2020) 922. https://doi.org/10.3390/met10070922.

[215] V. Vogl, M. Åhman, L.J. Nilsson, Assessment of hydrogen direct reduction for fossil-free steelmaking, Journal of Cleaner Production 203 (2018) 736–745. https://doi.org/10.1016/j.jclepro.2018.08.279.

[216] M. Zier, P. Stenzel, L. Kotzur, D. Stolten, A review of decarbonization options for the glass industry, Energy Conversion and Management: X 10 (2021) 100083. https://doi.org/10.1016/j.ecmx.2021.100083.

[217] A. Reynolds, Electric Boosting and Melting Technology: Overview of developments and current work programs at FSL. Presentation Glassman Latin America 2018, 2018.

[218] A. Giese, J. Leicher, T. Nowakowski, B. Fleischmann, N.-H. Löber, B. Stranzinger, S. Bialek, P. Hemmann, C. Treu, Gemeinsamer Abschlussbericht des Forschungsvorhabens Gasbeschaffenheitsschwankungen - Erarbeitung von Kompensationsstrategien für die Glasindustrie zur Optimierung der Energieeffizienz: GasQualitätGlas, 2019.

[219] B. Fleischmann, K. Arnold, D. Schüwer, R.-U. Dietrich, S. Estelmann, Kapital 3: Behälterglasherstellung, in: Flexibilitätsoptionen in der Grundstoffindustrie: Methodik | Potenziale | Hemmnisse. Bericht des AP V.6 „Flexibilitätsoptionen und Perspektiven in der Grundstoffindustrie" im Kopernikus-Projekt „SynErgie – Synchronisierte und energieadaptive Produktionstechnik zur flexiblen Ausrichtung von Industrieprozessen auf eine fluktuierende Energieversorgung", 2019.

[220] B. Wilhelmsson, C. Kollberg, J. Larsson, J. Eriksson, M. Eriksson, Cemzero: A feasibility study evaluating ways to reach sustainable cement production via the use of electricity. Vattenfall und Cementa, 2018.

[221] J. Rogers, Paper making in a low carbon economy, AIMS Energy 6 (2018) 187–202. https://doi.org/10.3934/energy.2018.1.187.

[222] H. Zhang, U. Desideri, Techno-economic optimization of power-to-methanol with co-electrolysis of CO_2 and H_2O in solid-oxide electrolyzers, Energy 199 (2020) 117498. https://doi.org/10.1016/j.energy.2020.117498.

[223] S. Alibas, T. Fleiter, P. Manz, R. Elsland, On the way to low-emission European buildings: investigating the role of non-ETS CO2 pricing in the residential and tertiary sectors, 12. Internationale Energiewirtschaftstagung an der TU Wien (IEWT 2021) (2021).

[224] N. Bertelsen, B.V. Mathiesen, S.R. Djørup, N.C.A. Schneider, S. Paardekooper, L. Sánchez-García, J.Z. Thellufsen, J. Kapetanakis, L. Angelino, J. Kiruja, Integrating low-temperature renewables in district energy systems: Guidelines for policy makers. International Renewable Energy Agency, 2021.

[225] A. Billerbeck, B. Breitschopf, J. Winkler, V. Bürger, B. Köhler, A. Bacquet, E. Popovski, M. Fallahnejad, L. Kranzl, M. Ragwitz, Policy frameworks for district heating: A comprehensive overview and analysis of regulations and support measures across Europe, Energy Policy 173 (2023) 113377. https://doi.org/10.1016/j.enpol.2022.113377.

[226] European Commission, RePowerEU Plan: Communication from the Commission to the European Parliament, the Council, the European economic and social committee and the committee of the regions. COM(2022) 230 final, 2022.

[227] European Commission, A hydrogen strategy for a climate-neutral Europe: Communication from the Commission to the European Parliament, the European Council, the European Economic and Social Committee and the Committee of the Regions. COM(2020) 301 final, 2020.

[228] A. Wang, K. van der Leun, D. Peters, M. Buseman, European Hydrogen Backbone: How a dedicated hydrogen infrastructure can be created. Enagás, Energinet, Fluxys Belgium, Gasunie, GRTgaz, NET4GAS, OGE, ONTRAS, Snam, Swedegas, Teréga, 2020.

[229] W.J. Tiktak, Heat Management of PEM Electrolysis: A study on the potential of excess heat from medium-- to large-scale PEM electrolyisis and the performance analysis of a dedicated cooling system. Master's Thesis, Delft, 2019.

[230] H. Böhm, S. Moser, S. Puschnigg, A. Zauner, Power-to-hydrogen & district heating: Technology-based and infrastructure-oriented analysis of (future) sector coupling potentials, International Journal of Hydrogen Energy (2021) 31938–31951. https://doi.org/10.1016/j.ijhydene.2021.06.233.

[231] S. Reuter, R.-R. Schmidt, Assessment of the Future Waste Heat Potential from Electrolysers and its Utilization in District Heating, Proceeding of the 2nd NEFI Conference (2022) 41-51.

[232] M. Hummel, A. Müller, M. Fallahnejad, L. Kranzl, The economic value of existing district heating grid infrastructure for the transition towards a carbon neutral heating system. Presentation IEWT 2021, 2021.

[233] S. Buffa, M. Cozzini, M. D'Antoni, M. Baratieri, R. Fedrizzi, 5th generation district heating and cooling systems: A review of existing cases in Europe, Renewable and Sustainable Energy Reviews 104 (2019) 504–522. https://doi.org/10.1016/j.rser.2018.12.059.

[234] A. Volkova, I. Pakere, L. Murauskaite, P. Huang, K. Lepiksaar, X. Zhang, 5th generation district heating and cooling (5GDHC) implementation potential in urban areas with existing district heating systems, Energy Reports 8 (2022) 10037–10047. https://doi.org/10.1016/j.egyr.2022.07.162.

[235] A.M. Jodeiri, M.J. Goldsworthy, S. Buffa, M. Cozzini, Role of sustainable heat sources in transition towards fourth generation district heating – A review, Renewable and Sustainable Energy Reviews 158 (2022) 112156. https://doi.org/10.1016/j.rser.2022.112156.

[236] H. Averfalk, T. Benakopoulos, I. Best, F. Dammel, C. Engel, R. Geyer, O. Gudmundsson, K. Lygnerud, N. Nord, J. Oltmanns, K. Ponweiser, D. Schmidt, H. Schrammel, D.S. Østergaard, S. Svendsen, M. Tunzi, S. Werner, Low-Temperature District Heating Implementation Guidebook. Annex TS2 IEA DHC Report, 2021.

[237] L. Pompei, F. Nardecchia, B. Mattoni, L. Gugliermetti, F. Bisegna, Combining the exergy and energy analysis for the assessment of district heating powered by renewable sources, IEEE, Piscataway, NJ, 2019.

[238] N. Nord, D. Schmidt, A.M.D. Kallert, Necessary Measures to Include more Distributed Renewable Energy Sources into District Heating System, Energy Procedia 116 (2017) 48–57. https://doi.org/10.1016/j.egypro.2017.05.054.

[239] M. Rämä, M. Wahlroos, Introduction of new decentralised renewable heat supply in an existing district heating system, Energy 154 (2018) 68–79. https://doi.org/10.1016/j.energy.2018.03.105.

[240] I. Sarbu, M. Mirza, D. Muntean, Integration of Renewable Energy Sources into Low-Temperature District Heating Systems: A Review, Energies 15 (2022) 6523. https://doi.org/10.3390/en15186523.

[241] H. Lund, P.A. Østergaard, M. Chang, S. Werner, S. Svendsen, P. Sorknæs, J.E. Thorsen, F. Hvelplund, B.O.G. Mortensen, B.V. Mathiesen, C. Bojesen, N. Duic, X. Zhang, B. Möller, The status of 4th generation district heating: Research and results, Energy 164 (2018) 147–159. https://doi.org/10.1016/j.energy.2018.08.206.

[242] J.C. Santamarta, A. García-Gil, M.C. Del Expósito, E. Casañas, N. Cruz-Pérez, J. Rodríguez-Martín, M. Mejías-Moreno, G. Götzl, V. Gemeni, The clean energy transition of heating and cooling in touristic infrastructures using shallow geothermal energy in the Canary Islands, Renewable Energy 171 (2021) 505–515. https://doi.org/10.1016/j.renene.2021.02.105.

[243] A. Walch, N. Mohajeri, A. Gudmundsson, J.-L. Scartezzini, Quantifying the technical geothermal potential from shallow borehole heat exchangers at regional scale, Renewable Energy 165 (2021) 369–380. https://doi.org/10.1016/j.renene.2020.11.019.

[244] C. Tissen, K. Menberg, S.A. Benz, P. Bayer, C. Steiner, G. Götzl, P. Blum, Identifying key locations for shallow geothermal use in Vienna, Renewable Energy 167 (2021) 1–19. https://doi.org/10.1016/j.renene.2020.11.024.

[245] A.S. Pratiwi, E. Trutnevyte, Decision paths to reduce costs and increase economic impact of geothermal district heating in Geneva, Switzerland, Applied Energy 322 (2022) 119431. https://doi.org/10.1016/j.apenergy.2022.119431.

[246] S. Kaur, J.S. Yadav, R. Bhambri, K. Sain, S.K. Tiwari, Assessment of geothermal potential of Kumaun Himalaya: A perspective for harnessing green energy, Renewable Energy 212 (2023) 940–952. https://doi.org/10.1016/j.renene.2023.05.112.

[247] V.M. Soltero, R. Chacartegui, C. Ortiz, R. Velázquez, Potential of biomass district heating systems in rural areas, Energy 156 (2018) 132–143. https://doi.org/10.1016/j.energy.2018.05.051.

[248] J. Idsø, T. Årethun, Water-Thermal Energy Production System: A Case Study from Norway, Sustainability 9 (2017) 1665. https://doi.org/10.3390/su9091665.

[249] Y.-J. Baik, M. Kim, K.-C. Chang, Y.-S. Lee, H.-S. Ra, Potential to enhance performance of seawater-source heat pump by series operation, Renewable Energy 65 (2014) 236–244. https://doi.org/10.1016/j.renene.2013.09.021.

[250] Y. Jung, J. Kim, H. Kim, R. Yun, C. Park, Y. Nam, H. Cho, H. Lee, Comprehensive feasibility investigation of river source heat pump systems in terms of life cycle, Applied Thermal Engineering 188 (2021) 116655. https://doi.org/10.1016/j.applthermaleng.2021.116655.

[251] E. Mäki, L. Kannari, I. Hannula, J. Shemeikka, Decarbonization of a district heating system with a combination of solar heat and bioenergy: A techno-economic case study in the Northern European context, Renewable Energy 175 (2021) 1174–1199. https://doi.org/10.1016/j.renene.2021.04.116.

[252] A. Aliana, M. Chang, P.A. Østergaard, M. Victoria, A.N. Andersen, Performance assessment of using various solar radiation data in modelling large-scale solar thermal systems integrated in district heating networks, Renewable Energy 190 (2022) 699–712. https://doi.org/10.1016/j.renene.2022.03.163.

[253] P. Manz, M. Fallahnejad, A. Billerbeck, Potentials for district heating generation in a climate-neutral energy system, 12. Internationale Energiewirtschaftstagung an der TU Wien (IEWT 2021) (2021).

[254] J. Pelda, F. Stelter, S. Holler, Potential of integrating industrial waste heat and solar thermal energy into district heating networks in Germany, Energy 203 (2020) 117812. https://doi.org/10.1016/j.energy.2020.117812.

[255] M. Jakob, U. Reiter, G. Catenazzi, B. Sunarjo, L. Lienhard, A. Müller, S. Steinmann, A. Herbst, C. Nägeli, Erneuerbare- und CO_2-freie Wärmeversorgung Schweiz: Eine Studie zur Evaluation von Erfordernissen und Auswirkungen, 2020.

[256] R. Bracke, E. Huenges, Roadmap Tiefe Geothermie für Deutschland: Handlungsempfehlungen für Politik, Wirtschaft und Wissenschaft für eine erfolgreiche Wärmewende. Strategiepapier von sechs Einrichtungen der Fraunhofer-Gesellschaft und der Helmholtz-Gesellschaft, Fraunhofer-Gesellschaft, 2021.

[257] J. Limberger, P. Calcagno, A. Manzella, E. Trumpy, T. Boxem, M.P.D. Pluymaekers, J.-D. van Wees, Assessing the prospective resource base for enhanced geothermal systems in Europe, Geoth. Energ. Sci. 2 (2014) 55–71. https://doi.org/10.5194/gtes-2-55-2014.

[258] F. Dalla Longa, L.P. Nogueira, J. Limberger, J.-D. van Wees, B. van der Zwaan, Scenarios for geothermal energy deployment in Europe, Energy 206 (2020) 118060. https://doi.org/10.1016/j.energy.2020.118060.

[259] Büro für Technikfolgen-Abschätzung beim Deutschen Bundestag (TAB), Möglichkeiten geothermischer Stromerzeugung in Deutschland.: Sachstandsbericht. Arbeitsbericht Nr. 84, 2003.

[260] K. Könighofer, G. Domberger, S. Gunzy, M. Hingsamer, J. Pucker, M. Schreilechner, J. Amtmann, J. Goldbrunner, H.P. Heiss, J. Füreder, G. Burgstaller, U. Pölzl, Potenzial der Tiefengeothermie für die Fernwärme- und Stromproduktion in Österreich: Endbericht GeoEnergie2050, 2014.

[261] UK Department of Energy & Climate Change, National Heat Map: Water source heat map layer, 2015.

[262] A. Gaudard, M. Schmid, A. Wüest, Thermische Nutzung von Seen und Flüssen, AQUA & GAS N°2 (2018) 26-33.

[263] V. Somogyi, V. Sebestyén, E. Domokos, Assessment of wastewater heat potential for district heating in Hungary, Energy 163 (2018) 712–721. https://doi.org/10.1016/j.energy.2018.07.157.

[264] K. Münch, S. Blömer, L. Lütkes, M. Pehnt, B. Schoor, C. Schmidt, W. Schuler, Abwasserwärmenutzung aus dem Auslauf von Kläranlagen: Lokalisierung von Standorten in Baden-Württemberg, 2022.

[265] S. Nielsen, K. Hansen, R. Lund, D. Moreno, Unconventional Excess Heat Sources for District Heating in a National Energy System Context, Energies 13 (2020) 5068. https://doi.org/10.3390/en13195068.

[266] P. Manz, T. Fleiter, W. Eichhammer, The effect of low-carbon processes on industrial excess heat potentials for district heating in the EU: A GIS-based analysis, Smart Energy 10 (2023) 100103. https://doi.org/10.1016/j.segy.2023.100103.

[267] S. Stark, F. Uthoff, J.A. Miller, Leitfaden zur Erschließung von Abwärmequellen für die Fernwärmeversorgung: Ein Leitfaden des AGFW, 2020.

[268] U. Persson, M. Münster, Current and future prospects for heat recovery from waste in European district heating systems: A literature and data review, Energy 110 (2016) 116–128. https://doi.org/10.1016/j.energy.2015.12.074.

[269] K. Weber, P. Quicker, J. Hanewinkel, S. Flamme, Status of waste-to-energy in Germany, Part I - Waste treatment facilities, Waste management & research the journal of the International Solid Wastes and Public Cleansing Association, ISWA 38 (2020) 23–44. https://doi.org/10.1177/0734242X19894632.

[270] D. Moreno, S. Nielsen, U. Persson, The European Waste Heat Map: ReUseHeat project - Recovery of Urban Excess Heat, ReUseHeat project - Recovery of Urban Excess Heat, 2022.

[271] J. Unternährer, S. Moret, S. Joost, F. Maréchal, Spatial clustering for district heating integration in urban energy systems: Application to geothermal energy, Applied Energy 190 (2017) 749–763. https://doi.org/10.1016/j.apenergy.2016.12.136.

[272] X. Li, A. Walch, S. Yilmaz, M. Patel, J. Chambers, Optimal spatial resource allocation in networks: Application to district heating and cooling, Computers & Industrial Engineering 171 (2022) 108448. https://doi.org/10.1016/j.cie.2022.108448.

[273] C. Scaramuzzino, G. Garegnani, P. Zambelli, Integrated approach for the identification of spatial patterns related to renewable energy potential in European territories, Renewable and Sustainable Energy Reviews 101 (2019) 1–13. https://doi.org/10.1016/j.rser.2018.10.024.

[274] J.F. Marquant, L.A. Bollinger, R. Evins, J. Carmeliet, A new combined clustering method to Analyse the potential of district heating networks at large-scale, Energy 156 (2018) 73–83. https://doi.org/10.1016/j.energy.2018.05.027.

[275] P. Sorknæs, P.A. Østergaard, J.Z. Thellufsen, H. Lund, S. Nielsen, S. Djørup, K. Sperling, The benefits of 4th generation district heating in a 100% renewable energy system, Energy 213 (2020) 119030. https://doi.org/10.1016/j.energy.2020.119030.

[276] European Commission, Joint Research Centre (JRC), ENSPRESO - BIOMASS: [dataset], 2019, http://data.europa.eu/89h/74ed5a04-7d74-4807-9eab-b94774309d9f, accessed 15 January 2023.

[277] European Commission, Atlas of Geothermal Resources in Europe, 2002.

[278] GeoDH European Geothermal Energy Council, Geographic Information System (map), 2014, https://map.mbfsz.gov.hu/geo_DH/, accessed 9 March 2023.

[279] Copernicus Climate Change Service (C3S) Climate Data Store (CDS), Hydrology-related climate impact indicators from 1970 to 2100 derived from bias adjusted European climate projections, ECMWF, 2021.

[280] P. Ruiz, W. Nijs, D. Tarvydas, A. Sgobbi, A. Zucker, R. Pilli, R. Jonsson, A. Camia, C. Thiel, C. Hoyer-Klick, F. Dalla Longa, T. Kober, J. Badger, P. Volker, B.S. Elbersen, A. Brosowski, D. Thrän, ENSPRESO - an open, EU-28 wide, transparent and coherent database of wind, solar and biomass energy potentials, Energy Strategy Reviews 26 (2019) 100379. https://doi.org/10.1016/j.esr.2019.100379.

[281] European Geothermal Energy Council, 2020 EGEC Geothermal Market Report: Key Findings, 2021.

[282] GeoDH European Geothermal Energy Council, Developing Geothermal District Heating in Europe: Final Report, 2014.

[283] Umweltbundesamt, Kommunaler Klimaschutz durch Verbesserung der Effizienz in der Fernwärmeversorgung mittels Nutzung von Niedertemperaturwärmequellen am Beispiel tiefengeothermischer Ressourcen: Abschlussbericht, 2020.

[284] G. Yu, H. Li, C. Liu, W. Cheng, H. Xu, Thermal and hydraulic characteristics of a new proposed flyover-crossing fracture configuration for the enhanced geothermal system, Renewable Energy 211 (2023) 859–873. https://doi.org/10.1016/j.renene.2023.04.148.

[285] European Commission, Potential impacts of solar, geothermal and ocean energy on habitats and species protected under the birds and habitats directives: Final report, 2020.

[286] R. Schulz, E. Suchi, J. Dittmann, S. Knopf, Geothermie-Atlas zur Darstellung möglicher Nutzungskonkurrenzen zwischen CCS und Tiefer Geothermie: Endbericht, 2013.

[287] M. Douziech, I. Blanc, L. Damen, K. Dillman, V. Eggertsson, N. Farrara, S.R. Gudjonsdottir, V. Harcouet-Menou, M.L. Parisi, P. Perez-Lopez, G. Ravier, H. Sigurjonson, L. Tosti, Generation of simplified parametrised models for a selection of GEOENVI geothermal installations categories. Deliverable 3.4 GEONEVI, 2020.

[288] V. Wilk, B. Windholz, M. Hartl, T. Fleckl, Techno-ökonomische Analyse der Integration von flusswassergespeisten Großwärmepumpen in FW-Netzen. Austrian Institute of Technology (AIT), 2015.

[289] Gewässerkundlicher Dienst Bayern, Wassertemperatur Bayern, 2022, https://www.gkd.bayern.de/de/fluesse/wassertemperatur, accessed 14 June 2022.

[290] A. Lyden, Viability of river source heat pumps for district heating. Master's Thesis, Strathclyde, 2015.

[291] J. Jung, J. Nam, J. Kim, Y.H. Bae, H.S. Kim, Estimation of Temperature Recovery Distance and the Influence of Heat Pump Discharge on Fluvial Ecosystems, Water 12 (2020) 949. https://doi.org/10.3390/w12040949.

[292] L. Tobiasen, B. Kamuk, Waste to energy (WTE) systems for district heating, in: N.B. Klinghoffer, M.J. Castaldi (Eds.), Waste to Energy Conversion Technology, Woodhead Publishing, 2013, pp. 120–145.

[293] D. Trier, C.K. Skov, S.S. Sørensen, F. Bava, Solar District Heating Trends and Possibilities: Characteristics of Ground-Mounted Systems for Screening of Land Use Requirements and Feasibility. Subtask B report in the IEA SHC Task 52 Programme, 2018.

[294] P. Manz, A. Billerbeck, M. Fallahnejad, Spatial analysis of renewable and excess heat potentials for climate-neutral district heating in Europe: Supplementary Material, 2023, https://dx.doi.org/10.24406/fordatis/280.3, accessed 15 June 2024.

[295] S. Coss, V. Verda, O. Le-Corre, Multi-objective optimization of district heating network model and assessment of demand side measures using the load deviation index, Journal of Cleaner Production 182 (2018) 338–351. https://doi.org/10.1016/j.jclepro.2018.02.083.

[296] D.M. Sneum, E. Sandberg, Economic incentives for flexible district heating in the Nordic countries, International Journal of Sustainable Energy Planning and Management (2018) 27–44. https://doi.org/10.5278/ijsepm.2018.16.3.

[297] Y. Zhang, P. Johansson, A. Sasic Kalagasidis, Assessment of district heating and cooling systems transition with respect to future changes in demand profiles and renewable energy supplies, Energy Conversion and Management 268 (2022) 116038. https://doi.org/10.1016/j.enconman.2022.116038.

[298] H. Lund, Renewable heating strategies and their consequences for storage and grid infrastructures comparing a smart grid to a smart energy systems approach, Energy 151 (2018) 94–102. https://doi.org/10.1016/j.energy.2018.03.010.

[299] D. Fiaschi, G. Manfrida, B. Mendecka, L. Tosti, M.L. Parisi, A Comparison of Different Approaches for Assessing Energy Outputs of Combined Heat and Power Geothermal Plants, Sustainability 13 (2021) 4527. https://doi.org/10.3390/su13084527.

[300] European Commission, Background Report on EU-27 District Heating and Cooling Potentials, Barriers, Best Practice and Measures of Promotion: Report EUR 25289 EN, Luxembourg, 2012.

[301] J. Chambers, S. Zuberi, M. Jibran, K. Narula, M.K. Patel, Spatiotemporal analysis of industrial excess heat supply for district heat networks in Switzerland, Energy 192 (2020) 116705. https://doi.org/10.1016/j.energy.2019.116705.

[302] P. Huang, B. Copertaro, X. Zhang, J. Shen, I. Löfgren, M. Rönnelid, J. Fahlen, D. Andersson, M. Svanfeldt, A review of data centers as prosumers in district energy systems: Renewable energy integration and waste heat reuse for district heating, Applied Energy 258 (2020) 114109. https://doi.org/10.1016/j.apenergy.2019.114109.

[303] M. Fallahnejad, District heating economic assessment (v1.0). Zenodo, 2022, https://doi.org/10.5281/zenodo.7455372, accessed 15 August 2023.

[304] P. Stein, S. Vollnhals, Grundlagen clusteranalytischer Verfahren, Institut für Soziologie - Universität Duisburg-Essen (2011) 74 pp.

[305] European Commission, Heating and Cooling: Heating and cooling constitute around half of the EU energy consumption, 2023, https://energy.ec.europa.eu/topics/energy-efficiency/heating-and-cooling_en, accessed 13 December 2023.

[306] International Energy Agency (IEA), District Heating - Energy Systems, 2023, https://www.iea.org/energy-system/buildings/district-heating, accessed 13 December 2023.

[307] P. Leoni, R. Geyer, R.-R. Schmidt, Developing innovative business models for reducing return temperatures in district heating systems: Approach and first results, Energy 195 (2020) 116963. https://doi.org/10.1016/j.energy.2020.116963.

[308] H.İ. Topal, H.İ. Tol, M. Kopaç, A. Arabkoohsar, Energy, exergy and economic investigation of operating temperature impacts on district heating systems: Transition from high to low-temperature networks, Energy 251 (2022) 123845. https://doi.org/10.1016/j.energy.2022.123845.

[309] P. Lorenzen, C. Alvarez-Bel, Variable cost evaluation of heating plants in district heating systems considering the temperature impact, Applied Energy 305 (2022) 117909. https://doi.org/10.1016/j.apenergy.2021.117909.

[310] S. Werner, Network configurations for implemented low-temperature district heating, Energy 254 (2022) 124091. https://doi.org/10.1016/j.energy.2022.124091.

[311] Y. Merlet, R. Baviere, N. Vasset, Optimal retrofit of district heating network to lower temperature levels, Energy 282 (2023) 128386. https://doi.org/10.1016/j.energy.2023.128386.

[312] M. Capone, E. Guelpa, V. Verda, Potential for supply temperature reduction of existing district heating substations, Energy 285 (2023) 128597. https://doi.org/10.1016/j.energy.2023.128597.

[313] R. Lund, D.S. Østergaard, X. Yang, B.V. Mathiesen, Comparison of Low-temperature District Heating Concepts in a Long-Term Energy System Perspective. https://doi.org/10.5278/IJSEPM.2017.12.2.

[314] E. Guelpa, M. Capone, A. Sciacovelli, N. Vasset, R. Baviere, V. Verda, Reduction of supply temperature in existing district heating: A review of strategies and implementations, Energy 262 (2023) 125363. https://doi.org/10.1016/j.energy.2022.125363.

[315] P. Caputo, G. Ferla, M. Belliardi, N. Cereghetti, District thermal systems: State of the art and promising evolutive scenarios. A focus on Italy and Switzerland, Sustainable Cities and Society 65 (2021) 102579. https://doi.org/10.1016/j.scs.2020.102579.

[316] M. Belliardi, P. Caputo, G. Ferla, N. Cereghetti, B. Antonioli Mantegazzini, An innovative application of 5GDHC: A techno-economic assessment of shallow geothermal systems potential in different European climates, Energy 280 (2023) 128104. https://doi.org/10.1016/j.energy.2023.128104.

[317] A. Billerbeck, C.P. Kiefer, J. Winkler, C. Bernath, F. Sensfuß, L. Kranzl, A. Müller, M. Ragwitz, The race between hydrogen and heat pumps for space and water heating: A model-based scenario analysis, Energy Conversion and Management 299 (2024) 117850. https://doi.org/10.1016/j.enconman.2023.117850.

[318] TU Wien, e-think Energy Research, Invert/EE-Lab: Modelling the energy demand for space heating and cooling in building stocks, https://www.invert.at/index.php, accessed 3 January 2024.

[319] P. Manz, A. Billerbeck, A. Kök, M. Fallahnejad, T. Fleiter, L. Kranzl, S. Braungardt, W. Eichhammer, Spatial analysis of renewable and excess heat potentials for climate-neutral district heating in Europe, Renewable Energy 224 (2024) 120111. https://doi.org/10.1016/j.renene.2024.120111.

[320] Github, tuw-eeg/hotmapsDispatch at reshc_pathways, 2019, https://github.com/tuw-eeg/hotmapsDispatch/tree/reshc_pathways, accessed 4 January 2024.

[321] European Commission, Long term (2050) projections of large-scale heating and cooling in the EU: External study performed by ILF Consulting Engineers Austria GmbH, and AIT Austrian Institute of Technology GmbH for the Joint Research Centre, Luxembourg, 2017.

[322] M. Sulzer, S. Werner, S. Mennel, M. Wetter, Vocabulary for the fourth generation of district heating and cooling, Smart Energy 1 (2021) 100003. https://doi.org/10.1016/j.segy.2021.100003.

[323] B.V. Mathiesen, H. Lund, D. Connolly, Limiting biomass consumption for heating in 100% renewable energy systems, Energy 48 (2012) 160–168. https://doi.org/10.1016/j.energy.2012.07.063.

[324] European Union, Directive (EU) 2023/959 of the European Parliament and of the Council of 10 May 2023 amending Directive 2003/87/EC establishing a system for greenhouse gas emission allowance trading within the Union and Decision (EU) 2015/1814 concerning the establishment and operation of a market stability reserve for the Union greenhouse gas emission trading system. Official Journal of the European Union, Luxembourg, 2023.

[325] European Commission, 2050 long-term strategy, 2020, https://ec.europa.eu/clima/policies/strategies/2050_en.

[326] I. Tsiropoulos, Nijs. W., D. Tarvydas, P. Ruiz Castello, Towards net-zero emissions in the EU energy system by 2050: Insights from scenarios in line with the 2030 and 2050 ambitions of the European Green Deal, Luxembourg, 2020.

[327] D. Connolly, H. Lund, B.V. Mathiesen, Smart Energy Europe: The technical and economic impact of one potential 100% renewable energy scenario for the European Union, Renewable and Sustainable Energy Reviews 60 (2016) 1634–1653. https://doi.org/10.1016/j.rser.2016.02.025.

[328] H. Lund, P.A. Østergaard, D. Connolly, B.V. Mathiesen, Smart energy and smart energy systems, Energy 137 (2017) 556–565. https://doi.org/10.1016/j.energy.2017.05.123.

[329] B.V. Mathiesen, H. Lund, D. Connolly, H. Wenzel, P.A. Østergaard, B. Möller, S. Nielsen, I. Ridjan, P. Karnøe, K. Sperling, F.K. Hvelplund, Smart Energy Systems for coherent 100% renewable energy and transport solutions, Applied Energy 145 (2015) 139–154. https://doi.org/10.1016/j.apenergy.2015.01.075.

[330] F. Gerard, L.G. Opinska, T. Smit, K. Rademaekers, S. Braungardt, M.E.M. Montagud, Policy Support for Heating and Cooling Decarbonisation: Roadmap, 2021.

[331] European Commission, Energy efficiency first principle, 2023, https://energy.ec.europa.eu/topics/energy-efficiency/energy-efficiency-targets-directive-and-rules/energy-efficiency-first-principle_en, accessed 14 November 2023.

[332] Heat Roadmap Europe, Heating and Cooling: Facts and Figures. The transformation towards a low-carbon Heating & Cooling sector, 2017.

[333] H. Li, N. Nord, Transition to the 4th generation district heating - possibilities, bottlenecks, and challenges, Energy Procedia 149 (2018) 483–498. https://doi.org/10.1016/j.egypro.2018.08.213.

[334] European Commission, District Heating and Cooling in the European Union: Overview of Markets and Regulatory Frameworks under the Revised Renewable Energy Directive. DHC Trend (ENER/C1/2018-496), 2022.

[335] K. Askeland, K.N. Bozhkova, P. Sorknæs, Balancing Europe: Can district heating affect the flexibility potential of Norwegian hydropower resources?, Renewable Energy 141 (2019) 646–656. https://doi.org/10.1016/j.renene.2019.03.137.

[336] R.M. Johannsen, B.V. Mathiesen, K. Kermeli, W. Crijns-Graus, P.A. Østergaard, Exploring pathways to 100% renewable energy in European industry, Energy 268 (2023) 126687. https://doi.org/10.1016/j.energy.2023.126687.

[337] G. Deac, Auswirkung der Kopplung von Strom- und Wärmemarkt auf die künftige Integration der erneurbaren Energien und die CO_2-Emissionen in Deutschland. Dissertation, 10th ed., Dresden, 2019.

[338] B. Pfluger, Assessment of least-cost pathways for decarbonising Europe's power supply: A model-based long-term scenario analysis accounting for the characteristics of renewable energies. Dissertation, Karlsruhe, 2013.

[339] B. Lux, Supplying Europe with Hydrogen and Negative Emissions: A Model-Based Assessment. Dissertation, Karlsruhe, 2023.

[340] Danish Energy Agency, Technology Data for Generation of Electricity and District Heating, 2020, https://ens.dk/en/our-services/projections-and-models/technology-data/technology-data-generation-electricity-and, accessed 17 August 2023.

[341] EurObserv'ER, The state of renewable energies in Europe: Edition 2019. 19th EurObserv'ER Report, 2019.

[342] Fraunhofer ISI, consentec, ifeu Institut, Langfristszenarien für die Transformation des Energiesystems in Deutschland: Modul 1: Hintergrund, Szenarioarchitektur und übergeordnete Rahmenparameter. Studie im Auftrag des Bundesministeriums für Wirtschaft und Energie, 2017.

[343] C. Karakosta, K. Papapostolou, P. Del Crespo Granado, R. Egging, M. Welisch, et al., Final Report on SET-Nav Policy Briefs: Deliverable 11.14 Set-Nav Navigating the Roadmap for Clean, Secure and Efficient Energy Innovation, 2019.

[344] A. de Vita, I. Kielichowska, P. Mandatowa, Technology pathways in decarbonisation scenarios: Asset Advanced System Studies for Energy Transistion, 2018.

[345] P. Manz, T. Fleiter, W. Eichhammer, The effect of low-carbon processes on industrial excess heat potentials for district heating in the EU: A GIS-based analysis: Supplementary Material, 2023, http://dx.doi.org/10.24406/fordatis/252.2, accessed 15 April 2024.

[346] T.D. Mandel, The energy efficiency first principle in European energy and climate policy: Bridging the gap between conceptual foundations and practical policy implementation. Dissertation, Utrecht, 2024.

[347] European Geothermal Energy Council, 2022 EGEC Geothermal Market Report: Key Findings, 2023.

[348] European Parliament, Geothermal energy: European Parliament resolution of 18 January 2024 on geothermal energy. P9TA(2024)0049, 2024.

[349] Danish Energy Agency, Regulation and planning of district heating in Denmark, 2015.

[350] European Union, Directive 2003/87/EC of the European Parliament and of the Council of 13 October 2003 establishing a system for greenhouse gas emission allowance trading within the Union and amending Council Directive 96/61/EC. Official Journal of the European Union, Luxembourg, 2023.

[351] L. Sánchez-García, H. Averfalk, U. Persson, N. Hermoso-Martínez, P. Hernández-Iñarra, Viability of district heating networks in temperate climates: Benefits and barriers of cold and warm temperature networks. 9th International Conference on Smart Energy Systems (SES), Copenhagen, 2023.

[352] M. Fritz, Industrial excess heat utilisation for residential heating. Dissertation, Darmstadt, 2022.

[353] A. Billerbeck, B. Breitschopf, S. Preuß, J. Winkler, M. Ragwitz, D. Keles, Perception of district heating in Europe: A deep dive into influencing factors and the role of regulation, Energy Policy 184 (2024) 113860. https://doi.org/10.1016/j.enpol.2023.113860.

Summary

District heating is a possibility to supply heat to buildings centrally. Unlike individual, decentralised heating systems, which rely on boilers or furnaces within each building, district heating systems utilise a network of pipes to distribute heat generated from one or several central sources. This offers significant advantages, such as the ability to utilise various heat sources that are often not available or cost-effective for individual heating systems. These sources include combined heat and power plants (using fossil fuels, biomass or hydrogen), heat pumps, geothermal energy, solar thermal energy as well as excess heat from industrial processes and waste incineration. This versatility makes district heating systems highly adaptable to local conditions, enhancing their overall efficiency and sustainability.

To achieve a climate-neutral heating sector in the European Union, district heating can play a substantial role, alongside thermal renovation of buildings and climate-neutral individual heating solutions. However, district heating systems face several challenges in the future and must undergo significant transformations. Currently, heat generation in a district heating system is primarily based on fossil fuels, from one or two large combined heat and power plants and boilers. To decarbonize the heat supply, it is essential to utilise multiple typically smaller climate-neutral sources. Integrating these typically low-temperature heat sources can be more efficient if the temperatures in district heating systems are reduced. Additionally, as thermal renovations decrease the heat demand of buildings and thus the heat density, specific costs for district heating possibly increase. To address this, district heating grids should connect more households within a supply area, thereby increasing the heat sold for a pipe length. All these factors contribute to the uncertainty regarding the future potential and transformation pathways of district heating. Adding to the complexity, district heating grids are highly heterogeneous and estimates of future potentials must account for specific regional conditions, such as available heat sources and the future heat demand of the building stock.

Modelling plays a crucial role in understanding the future role of district heating within the energy system. By assessing the complex interactions between various factors such as heat demand, supply sources and infrastructure design, specific sector models and integrated energy system models can provide valuable insights. By exploring different scenarios, the technical and economic potentials can be quantified as well as the impact of important factors. High spatial resolution is essential for identifying possible heat sources, future heat demands and suitable district areas based on heat density. The result assessment from these models informs decision-making processes and guides stakeholders involved in district heating policies and planning. Additionally, modelling

supports researchers identifying opportunities and challenges in district heating implementation, such as determining suitable locations for new district heating networks, optimising energy storage solutions, and integrating district heating systems with other energy infrastructures.

The thesis explores the role of district heating systems in achieving climate-neutrality in the building sector within the European Union. It investigates the potential for district heating demand and climate-neutral supply, using several modelling approaches and methodological steps. By developing comprehensive data sets with high spatial resolution and integrating them into the models, the potential of district heating in a climate-neutral system was quantified, contributing to the transition towards more sustainable and resilient energy systems. This research addresses several gaps in the literature and existing models, particularly regarding the spatial resolution and technical detail of demand and supply data for district heating as well as the integration of these data into sector models and energy system model.

The main contributions of this thesis are:

1. *Modelling district heating and the energy system at high spatial resolution on a large geographical extent:* Detailed results were achieved by increasing the spatial resolution (coordinates or hectare-level) in the modelling across a vast geographical extent. The modelling covered various aspects of district heating, including demand (coupling building stock model with spatial analysis), supply (establishing extensive databases for renewable and excess heat potential) and infrastructure (spatially matching demand and source). Consequently, multiple methodological approaches were employed to assess the potential, including building stock modelling, spatial assessments and scenario analyses. This comprehensive approach enhanced the spatial perspective in evaluating the future district heating potential, leading to more realistic methods and data for energy system modelling covering the European Union. The results indicate that district heating can be expanded, with possibly achieving a market share of 33% in the heating sector. This potential could be even higher if barriers are overcome and all buildings within a district heating area are connected. Furthermore, the potentially high district heating demand could be met with renewable and excess heat sources in the future, at feasible costs and with manageable impacts on the electricity sector. The main heat sources in the future are possibly geothermal, biomass and water-source heat pumps, with industrial excess heat playing a minor role. In summary, this lays the foundation for identifying possible pathways and policies to support the expansion and transformation of district heating systems.
2. *Providing empirical evidence for identifying potential district heating areas:* Existing literature often has modelled future district heating areas by assuming a threshold for heat density or distribution costs. This thesis provides empirical

evidence to support this approach and offers deeper insights into the correlation involved. By combining and analysing several databases and data sources with high spatial resolution, a clear correlation between the presence of district heating and heat density was demonstrated, leading to an empirically derived threshold for acceptable distribution costs. The data have confirmed that most assumed thresholds in the literature are comparable to the currently accepted distribution costs, thereby validating the existing modelling approaches used for identifying potential district heating areas.

3. *Creating and publishing a database for georeferenced industrial excess heat in the future:* The potential contribution of industrial excess heat to district heating supply, in the context of a transformation to a climate-neutral industry, was quantified in detail. A site-specific database was established by matching, validating and comparing several databases, providing detailed information on the industrial processes located at the industrial sites. This database was utilised for scenario-based approaches to quantify the impact of industry transformation to low-carbon processes on the available excess heat for district heating. The results indicate that industrial excess heat, particularly from the cement, glass, chemical and steel industry, can be large point sources of heat and contribute a large share to supply district heating locally. However, the transformation of industry will significantly reduce the available potentials due to the implementation of more efficient or electrified processes.

The modelling results lead to the conclusion, that district heating demand could increase by a factor of 2 – 5 compared to current levels and that even an ambitious expansion could be supplied by climate-neutral sources. District heating will therefore play a decisive role in the heating transition in the European Union towards a climate-neutral energy system. The research fills important gaps in the existing research and identifies district heating as a promising solution for climate-neutral heating, due to its ability to efficiently access diverse energy sources. However, it also highlights challenges, such as decreasing heat demand from building renovation and the need to replace fossil fuels for district heating supply. Overall, the thesis underscores the significance of district heating in the transition to climate-neutrality.

Samenvatting

Stadsverwarming is een mogelijkheid om gebouwen centraal van warmte te voorzien. In tegenstelling tot individuele, gedecentraliseerde verwarmingssystemen, die afhankelijk zijn van ketels of ovens in elk gebouw, maken stadsverwarmingssystemen gebruik van een netwerk van leidingen om warmte te distribueren die wordt opgewekt uit één of meerdere centrale bronnen. Dit biedt aanzienlijke voordelen, zoals het gebruik van diverse warmtebronnen die vaak niet beschikbaar of kosteneffectief zijn voor individuele verwarmingssystemen. Deze bronnen omvatten warmtekrachtkoppeling (op basis van fossiele brandstoffen, biomassa of waterstof), warmtepompen, geothermische energie, zonthermische energie en restwarmte van industriële processen en afvalverbranding. Deze veelzijdigheid maakt stadsverwarmingssystemen zeer aanpasbaar aan lokale omstandigheden, wat hun algehele efficiëntie en duurzaamheid verhoogt.

Om een klimaatneutrale verwarmingssector in de Europese Unie te bereiken, kan stadsverwarming een belangrijke rol spelen, naast thermische renovatie van gebouwen en klimaatneutrale individuele verwarmingsoplossingen. Echter, stadsverwarmingssystemen staan voor verschillende uitdagingen in de toekomst en moeten aanzienlijke transformaties ondergaan. Momenteel is de warmteopwekking in een stadsverwarmingssysteem voornamelijk gebaseerd op fossiele brandstoffen, afkomstig van één of twee grote warmtekrachtcentrales en ketels. Om de warmtevoorziening te decarboniseren, is het essentieel om meerdere, meestal kleinere, klimaatneutrale bronnen te benutten. Het integreren van deze doorgaans lage-temperatuur warmtebronnen kan efficiënter zijn als de temperaturen in stadsverwarmingssystemen worden verlaagd. Bovendien, naarmate thermische renovaties de warmtevraag van gebouwen en dus de warmte-dichtheid verminderen, kunnen de specifieke kosten voor stadsverwarming mogelijk toenemen. Om dit aan te pakken, moeten stadsverwarmingsnetwerken meer huishoudens binnen een voorzieningsgebied aansluiten, waardoor de verkochte warmte per leidinglengte toeneemt. Al deze factoren dragen bij aan de onzekerheid over het toekomstige potentieel en de transformatie trajecten van stadsverwarming. Daar komt nog bij dat stadsverwarmingsnetwerken zeer heterogeen zijn en dat schattingen van toekomstige potentiëlen rekening moeten houden met specifieke regionale omstandigheden, zoals beschikbare warmtebronnen en de toekomstige warmtevraag van de gebouwenvoorraad.

Modellering speelt een cruciale rol bij het begrijpen van de toekomstige rol van stadsverwarming binnen het energiesysteem. Door de complexe interacties tussen verschillende factoren zoals warmtevraag, bronnen en infrastructuurontwerp te beoordelen, kunnen specifieke sectormodellen en geïntegreerde energiesysteemmodellen waardevolle inzichten bieden. Door verschillende scenario's te verkennen,

kunnen de technische en economische potentiëlen, evenals de impact van belangrijke factoren, worden gekwantificeerd. Een hoge ruimtelijke resolutie is essentieel om mogelijke warmtebronnen, toekomstige warmtevraag en geschikte gebieden voor stadsverwarming op basis van warmte-dichtheid te identificeren. De resultaat-beoordeling van deze modellen informeert besluitvormingsprocessen en begeleidt belanghebbenden bij stadsverwarmingsbeleid en planning. Daarnaast ondersteunt modellering onderzoekers bij het identificeren van kansen en uitdagingen bij de implementatie van stadsverwarming, zoals het bepalen van geschikte locaties voor nieuwe stadsverwarmingsnetwerken, het optimaliseren van energieoplossingen voor opslag en het integreren van stadsverwarmingssystemen met andere energie-infrastructuren.

De thesis onderzoekt de rol van stadsverwarmingssystemen bij het bereiken van klimaatneutraliteit in de gebouwensector binnen de Europese Unie. Het onderzoekt het potentieel voor stadsverwarmingsvraag en klimaatneutrale levering, met behulp van verschillende modelleringsbenaderingen en methodologische stappen. Door uitgebreide datasets met hoge ruimtelijke resolutie te ontwikkelen en in de modellen te integreren, werd het potentieel van stadsverwarming in een klimaatneutraal systeem gekwantificeerd, wat bijdraagt aan de transitie naar duurzamere en veerkrachtigere energiesystemen. Dit onderzoek adresseert verschillende hiaten in de literatuur en bestaande modellen, met name wat betreft de ruimtelijke resolutie en technische details van vraag- en aanbodgegevens voor stadsverwarming, evenals de integratie van deze gegevens in sectormodellen en energiesysteemmodellen.

De belangrijkste bijdragen van deze thesis zijn:

1. *Modellering van stadsverwarming en het energiesysteem met hoge ruimtelijke resolutie op grote geografische schaal:* Gedetailleerde resultaten werden bereikt door de ruimtelijke resolutie (coördinaten of hectare-niveau) in de modellering te verhogen over een groot geografisch gebied. De modellering besloeg verschillende aspecten van stadsverwarming, waaronder vraag (koppeling van gebouwenvoorraadmodel met ruimtelijke analyse), aanbod (opzetten van uitgebreide databases voor hernieuwbare en restwarmtepotentieel) en infrastructuur (ruimtelijk matchen van vraag en bron). Hierdoor werden meerdere methodologische benaderingen toegepast om het potentieel te beoordelen, waaronder gebouwvoorraadmodellering, ruimtelijke beoordelingen en scenarioanalyses. Deze uitgebreide benadering verbeterde het ruimtelijke perspectief bij het evalueren van het toekomstige potentieel van stadsverwarming, wat leidde tot realistischere methoden en gegevens voor energiesysteemmodellering in de Europese Unie. De resultaten geven aan dat stadsverwarming kan worden uitgebreid, met mogelijk een marktaandeel van 33% in de verwarmingssector. Dit potentieel kan zelfs hoger zijn als barrières worden overwonnen en alle gebouwen binnen een stadsverwarmingsgebied

worden aangesloten. Bovendien kan de potentieel hoge vraag naar stadsverwarming in de toekomst worden vervuld met hernieuwbare en restwarmtebronnen, tegen haalbare kosten en met beheersbare gevolgen voor de elektriciteitssector. De belangrijkste warmtebronnen in de toekomst zijn mogelijk geothermische energie, biomassa en waterbron-warmtepompen, waarbij industriële restwarmte een kleinere rol speelt. Samengevat legt dit de basis voor het identificeren van mogelijke trajecten en beleidsmaatregelen ter ondersteuning van de uitbreiding en transformatie van stadsverwarmings-systemen.

2. *Het leveren van empirisch bewijs voor het identificeren van potentiële stadsverwarmingsgebieden:* Bestaande literatuur heeft vaak toekomstige stadsverwarmingsgebieden gemodelleerd door een drempelwaarde voor warmte-dichtheid of distributiekosten aan te nemen. Deze thesis biedt empirisch bewijs ter ondersteuning van deze benadering en biedt diepere inzichten in de betrokken correlatie. Door meerdere databases en gegevens-bronnen met hoge ruimtelijke resolutie te combineren en te analyseren, werd een duidelijke correlatie aangetoond tussen de aanwezigheid van stadsverwarming en warmte-dichtheid, wat leidde tot een empirisch afgeleide drempelwaarde voor acceptabele distributiekosten. De gegevens hebben bevestigd dat de meeste aangenomen drempelwaarden in de literatuur vergelijkbaar zijn met de momenteel geaccepteerde distributiekosten, waardoor de bestaande modelleringsbenaderingen voor het identificeren van potentiële stadsverwarmingsgebieden worden gevalideerd.
3. *Het creëren en publiceren van een database voor gegeorefereerde industriële restwarmte in de toekomst:* De potentiële bijdrage van industriële restwarmte aan de levering van stadsverwarming, in de context van een transformatie naar een klimaatneutrale industrie, werd gedetailleerd gekwantificeerd. Een sitespecifieke database werd opgezet door meerdere databases te matchen, te valideren en te vergelijken, waardoor gedetailleerde informatie over de industriële processen op de industriële locaties werd verstrekt. Deze database werd gebruikt voor scenario-gebaseerde benaderingen om de impact van industriële transformatie naar koolstofarme processen op de beschikbare restwarmte voor stadsverwarming te kwantificeren. De resultaten geven aan dat industriële restwarmte, met name uit de cement-, glas-, chemische en staalindustrie, grote puntbronnen van warmte kunnen zijn en lokaal een groot aandeel kunnen bijdragen aan de levering van stadsverwarming. Echter, de transformatie van de industrie zal de beschikbare potentiëlen aanzienlijk verminderen door de implementatie van efficiëntere of geëlektrificeerde processen.

De modelleringsresultaten leiden tot de conclusie dat de vraag naar stadsverwarming kan toenemen met een factor 2 tot 5 vergeleken met de huidige niveaus en dat zelfs een ambitieuze uitbreiding kan worden geleverd door klimaatneutrale bronnen. Stadsverwarming zal daarom een beslissende rol spelen in de verwarmings transitie in de Europese Unie naar een klimaatneutraal energiesysteem. Het onderzoek vult belangrijke hiaten in het bestaande onderzoek en identificeert stadsverwarming als een veelbelovende oplossing voor klimaatneutrale verwarming, dankzij het vermogen om efficiënt toegang te krijgen tot diverse energiebronnen. Het benadrukt echter ook uitdagingen, zoals de afnemende warmtevraag door gebouwrenovatie en de noodzaak om fossiele brandstoffen voor stadsverwarming te vervangen. Over het geheel genomen onderstreept de thesis het belang van stadsverwarming in de transitie naar klimaatneutraliteit.

AI assistance

During the preparation of this thesis, AI assistance was utilized. Specifically, *ChatGPT-4*, a language model developed by OpenAI, and *DeepL Write* was employed for improving readability and language checking. Additionally, *DALL·E 2*, an image generator model developed by OpenAI, was used to generate the title figure and parts of Figure 1.1. The author reviewed and edited the content as necessary and takes full responsibility for the content of this thesis.

Acknowledgments

This thesis finally comes to an end. With its completion, I would like to express my gratitude to the following people, without whom this thesis would have not been possible.

First and foremost, I would like to thank my PhD supervisor, Wolfgang Eichhammer, for his continuous support, patience, and expertise. His encouragement and guidance have been pivotal in the successful completion of this thesis.

I wish to acknowledge my PhD supervisor at Utrecht University, Gert Jan Kramer, for his feedback and suggestions, which have enhanced the storyline of this work.

The support and mentorship of Tobias Fleiter were critical in completing this thesis. His profound knowledge, constructive feedback on numerous paper drafts, and guidance through several projects have been invaluable. These various interesting projects eventually inspired me to shift the focus of my dissertation.

Furthermore, I would like to thank my mentor during difficult times from the Reiner Lemoine-Foundation, Guido Pleßmann, whose academic and moral guidance helped me persevere with this project.

I am grateful to my fellow researchers and friends at Fraunhofer ISI (… and IEG/ISE/IAO) for creating such a supportive working environment. Special thanks to Andrea, Anna, Thurid, Şirin, Khaled and Tim for needed distraction and inspiring discussions during coffee breaks or long walks, as well as my former colleagues Matthias, Vasili and Anna-Lena for their always up-to-date rumours during long coffee breaks, which are painfully missed. You all made this journey less arduous. I would like to particularly thank Katja, Judith, Stella, Christiane, Alex and Mahsa, for your regular, long-term moral support. Thank you, Judith, for your creativity in naming the newly developed model, and our long Teams focus sessions.

A special mention to my co-authors and project partners, especially Ali Kök and Urban Persson, for the many discussions and knowledge exchanges that helped clarify my ideas. Working together in such an open atmosphere was invaluable.

I would also like to thank Viktor Wesselak and Sebastian Voswinckel from in.RET for guiding me through the first steps of my journey in research on renewable energy systems, and for creating an enjoyable working atmosphere.

My heartfelt gratitude goes to my family and friends, whose emotional support and encouragement have been invaluable. I am especially grateful to Hannes for being my companion on the highway of life, and to Amelie and Maya for keeping me grounded.

Curriculum Vitae

Pia Manz completed the Bachelor's programme in Renewable Energy Technology and the Master's programme in Systems Engineering at the University of Applied Sciences Nordhausen and spent one semester abroad at the University of Dundee in Scotland. During her studies, she was working as a researcher at the Institute for Renewable Energies (in.RET) at the University of Applied Sciences Nordhausen, focusing on the aging of PV modules. Since 2017, she has been a researcher at the Competence Center Energy Technology and Energy Systems at Fraunhofer ISI in Karlsruhe, specialising in the modelling of energy systems and district heating, as well as regional analyses for industry and buildings. She has contributed to several national and EU-wide research and consulting projects.

While working at Fraunhofer ISI, she pursued her PhD at the Copernicus Institute of Sustainable Development at Utrecht University and received a PhD-scholarship from the Reiner Lemoine-Foundation.

Achieving the target of a climate-neutral energy system in the European Union necessitates the transition to heating solutions in buildings eliminating the use of fossil fuels. District heating is potentially an important component in this transition.

This thesis explores the role of district heating systems in a climate-neutral energy system, addressing challenges such as reduced heat demand due to thermal renovations of buildings and the phasing out of fossil fuels in district heating generation. Detailed empirical data analysis, spatial analysis and scenario-based methods with high-resolution data sets were utilised to quantify the potential demand and supply of district heating in the future. The results indicate that the demand could increase significantly compared to current levels. Large supply potentials can be expected from geothermal and biomass resources as well as from heat pumps at wastewater treatment plants or surface water. Excess heat from industrial processes will play a minor role as its potential decreases due to industrial transformation to low-carbon processes. Overall, district heating systems could be expanded and decarbonized in the future.

ISBN 978-3-8396-2029-8

9 783839 620298

Fraunhofer
VERLAG